

A study on links between the tropical Atlantic and Indian summer monsoon on interannual timescales

A thesis submitted to the University of Hyderabad

in partial fulfilment of

the requirements for the degree of

Doctor of Philosophy

in

Earth Sciences

by

Pottapinjara Vijay

(Reg. No.14ESPE06)

under the guidance of

Prof. Karumuri Ashok

and

Dr. M. Ravichandran



Centre for Earth, Ocean and Atmospheric Sciences

School of Physics

University of Hyderabad

Hyderabad - 500 046, India

2020

Declaration

I, *Pottapinjara Vijay*, certify that the work embodied in this Ph.D. thesis entitled **A study on links between the tropical Atlantic and Indian summer monsoon on interannual timescales** is my own bona fide work carried out by me under the supervision of Prof. Karumuri Ashok and Dr. M. Ravichandran during January 2015–March 2020. The matter embodied in this Ph.D. thesis has not been submitted either in part or in full for the award of any other degree/diploma.

I declare that I have faithfully acknowledged, given credit to and referred to the research works wherever they have been cited in the thesis. I further certify that I have not willfully lifted up some other's work, paragraph, text, data, results, et cetera reported in the journals, books, magazines, reports, dissertations, theses, et cetera or material available at websites and included them in this Ph.D. thesis and cited as my own work.

Date:
Hyderabad

(Pottapinjara Vijay)
Reg. No. 14ESPE06



University of Hyderabad
Gachibowli, Hyderabad 500046
Telangana, India
Website: www.uohyd.ac.in

CERTIFICATE

This is to certify that the thesis entitled **A study on links between the tropical Atlantic and Indian summer monsoon on interannual timescales** by **Pottapinjara Vijay** bearing the Registration Number **14ESPE06** in partial fulfillment of the requirements for award of Doctor of Philosophy in the Centre for Earth, Ocean and Atmospheric Sciences, School of Physics is a bona fide work carried out by him under our supervision and guidance. This thesis is free from plagiarism and has not been submitted previously in part or in full to this or any other University or Institution for award of any degree or diploma. Further, the student has the following publication(s) before submission of the thesis for adjudication and has produced evidence for the same in the form of reprints in the relevant area of his research (Note: At least one publication in a refereed journal is required)

1. **Pottapinjara, V.**, M. S. Girishkumar, S. Sivareddy, M. Ravichandran, and R. Murtugudde, 2016: Relation between the upper ocean heat content in the equatorial Atlantic during boreal spring and the Indian monsoon rainfall during June–September. *International Journal of Climatology*, **36**, 2469–2480
2. **Pottapinjara, V.**, M. S. Girishkumar, R. Murtugudde, K. Ashok, and M. Ravichandran, 2019: On the Relation between the Boreal Spring Position of the Atlantic Intertropical Convergence Zone and Atlantic Zonal Mode. *Journal of Climate*, **32**, 4767–4781

and has made presentations in the following conferences:

1. WMO's 6th International Workshop on Monsoon during 13–17 September 2017 at Singapore
2. National Oceanography Workshop during 14–16 November 2018 at INCOIS, Hyderabad

Further, the student has passed the following courses towards fulfillment of the coursework requirement for Ph.D.

Course No.	Course Title	Credits	Pass/Fail
ES-801	Earth System Sciences	4	Pass
ES-805	Research Methodology	3	Pass
ES-806	Mathematics for Earth Sciences	4	Pass
ES-807	Interdisciplinary Course	3	Pass
AP-811-830	Special Paper on Specified Research Topic	2	Pass

(Dr. M. Ravichandran)
Co-supervisor
Indian National Centre for Ocean
Information Services (INCOIS)

(Prof. Karumuri Ashok)
Supervisor
Centre for Earth, Ocean, and
Atmospheric Sciences (CEOAS)

Head, CEOAS

Dean, School of Physics

Dedicated To

My parents, sisters, maternal grand parents, and teachers

*And to all the great souls who paved my path
to the land of light and freedom*

Contents

Declaration	i
Certificate	ii
Dedication	iii
Acknowledgements	viii
Synopsis	xi
List of Abbreviations	xvi
List of Figures	xviii
List of Tables	xxx
List of Publications	xxxi
1 Introduction	1
1.1 The Indian Summer Monsoon	1
1.2 El Niño-Southern Oscillation, Indian Ocean Dipole and their influence on ISM	8
1.3 The Atlantic Zonal Mode and its relation to the ISM	13

1.4	Modulation of the frequency of monsoon depressions in the Bay of Bengal by the AZM	21
1.5	Scope of the work	25
1.6	Summary	25
2	Description of Datasets and Statistical Methods	27
2.1	Datasets used	27
2.1.1	Sea Surface Temperature	28
2.1.2	Rainfall	28
2.1.3	Winds	29
2.1.4	Ocean Temperature	29
2.2	Statistical Methods	30
2.2.1	Composite Analysis	30
2.2.2	Linear Correlation	31
2.2.3	Linear Regression	32
2.2.4	Determination of statistical significance	33
3	Exploring clues of predictability of the Indian Summer Monsoon Rainfall in the tropical Atlantic	36
3.1	Introduction	37
3.2	Relationship between the AZM and ISMR	39
3.3	Evolution of the zonal wind, heat content and SST in the equatorial Atlantic associated with AZM	44
3.4	Relationship between the ISMR, and the variability of heat content and winds in the equatorial Atlantic in boreal spring	48

3.5	Summary and Discussion	51
4	Asymmetric relation between boreal spring position of Atlantic Inter-tropical Convergence Zone and Atlantic Zonal Mode	54
4.1	Introduction	55
4.2	The relevance of AMM and spring ITCZ to the AZM	59
4.3	Asymmetry in the relationship between the Atlantic spring ITCZ position and AZM	61
4.4	Relationship between the meridional migration of spring ITCZ and strong canonical AZM events	70
4.5	Diversity of causative mechanisms of cold and warm AZM events	72
4.6	The peculiar AZM events	76
4.7	Summary and Discussion	82
5	Simulation of interannual relationship between the Atlantic Zonal Mode and the Indian Summer Monsoon in CFSv2	87
5.1	Introduction	87
5.2	The model, observed data and design of the sensitivity experiment	89
5.3	The mean state of the tropical Atlantic in CFSv2	91
5.4	Simulation of the AZM and its links with the Indian summer monsoon in CFSv2 free-run	94
5.5	Response of the ISM to the imposed warm AZM SST anomalies	98
5.6	Summary and Discussion	106
6	Conclusion and scope for future work	109
	Appendix A	114

Acknowledgements

The journey of my PhD has been exciting and enlightening, and I have to thank many people for making it possible. Undoubtedly, the foremost of them are my research supervisor and co-supervisor.

I consider myself fortunate to have worked for my PhD under the supervision of Prof. Karumuri Ashok who set a great example through his monumental achievements in the field of climate science. He is down to earth, approachable and patient. He is uncompromising on quality and novelty of the research work, and always pushes the goalpost. His constructive criticism of my work pushed me to do deliver my best. Extending his support beyond academics, he helped me with several administrative matters. I sincerely thank him for his great guidance and constant support throughout my PhD tenure.

I would like to express my sincere gratitude to my research co-supervisor Dr. M. Ravichandran who was also the Head of my division in the organization I am working. Under his tutelage, I have grown from being a novice to a confident researcher. He is open to new ideas, and encouraged me to collaborate with other researchers whenever necessary. He has been my source of strength and motivation. Besides training me in research, he has also taught me how to be a good human being, by his example.

I take this opportunity to thank Dr. M. S. Girishkumar, a research collaborator and a scientist in my organization. He walked me through my initial steps in my research career. Since then, he has been my go-to scientist and I thoroughly enjoy working with him.

I am greatly indebted to Prof. Raghu Murtugudde, another research collaborator, who taught me how to think out-of-the-box with his deep understanding and broad view of the field of Oceanic and Atmospheric Sciences. He has also helped me in improving my writing skills. I truly cherish my association with him.

I wish to thank Dr. Roxy Mathew Koll who set up a coupled model experiment for me, to validate a key hypothesis of my study. Despite his busy schedule, he has been patient with my queries with regards to the model.

I would like to pay my special regards to the members of my Research Advisory Committee: Drs. S. Srilakshmi, Maqbool Ahmed and Vijay Kanawade for their constant encourage-

ment and valuable feedback on the progress of my research work. I thank Dr. Srilakshmi also for the clarifications regarding the administrative procedures.

I must thank several people for helping me with the administrative procedures. Foremost of them is Dr. S. S. C. Sheno, Director, Indian National Centre for Ocean Information Services (INCOIS), the organization where I am working. I sincerely thank Dr. Sheno for his encouragement, and support to my research work through advancing the funding for journal page charges. Further, I wish to show my gratitude to Dr. Sudhir Joseph who presently heads my division at the organization for giving me enough time to complete my PhD. I also thank Dr. Francis Pavanathara for his support.

I must thank Prof. K. S. Krishna, Head, Centre for Earth, Ocean and Atmospheric Sciences (CEOAS) for his encouragement and administrative support. I express my gratitude to Profs. V. Chakravarthy and M. Jayananda who headed the CEOAS earlier during my PhD tenure, for extending the same support. I also thank the office staff at the CEOAS, library and administration for their help.

I am greatly obliged to Prof. B. N. Goswami, former Director of Indian Institute of Tropical Meteorology (IITM), Pune who introduced me to this exciting field of Oceanic and Atmospheric Sciences through a special training program which gave me a tenured position. If not for this program which was a brainchild of his, I would never have moved to this interesting field.

I would like to take this opportunity to thank my wonderful teachers from elementary school through university, who encouraged my curiosity and inquisitive nature, and contributed to my pursuing a career in research. I specially thank Mr. K. V. L. Narasimha Rao, my Physics lecturer at my junior college, who made the study of Physics quite interesting and enjoyable. His influence is significant on my decision to pursue higher studies in Physical Sciences. During my Master's at the university, I got an opportunity to learn from some of the best teachers in the country, who inspired me to pursue a career in research. Profs. A. K. Kapoor, S. Chaturvedi, S. R. Sheno, K. P. N. Murthy and Nirmal Viswanathan are just a few to name. Some of my teachers have been great guides in my life and of particular mention are Mr. S. Shadrak and Mr. P. V. N. Papparao.

This list would be incomplete without the mention of my friends and fellow trainee

scientists from my IITM days: U Srinivasu, Suyash Bire, Sayanti Bardhan, Amit Verma, Prajish A. G. and Latika N. P. who kept me going all these years with their encouragement. I share some of the best days of my life with them. Particularly, U Srinivasu, who is also a colleague presently, has been very supportive emotionally since my initial days at IITM till date. He has been my solace at difficult times.

In this journey, I have made good friends with the other PhD students of Prof. Ashok: Feba Francis, Charan Tejavath, Govardhan D, Boyaj Alugula, Bidya Soraisam, Hemadri Amath and Vikas Kushwaha. They have supported me in many ways and I thank each of them. I particularly thank Feba for reading my draft thesis and giving me a critical feedback on the same. I should also thank my friends and juniors from my Master's days Gurram Ashok, Medi Chaitanya and Naresh Shyaga, who are also currently the students of the university, for their friendship and emotional support all these years.

Finally, I end this list with the people who give me the essential life energy: my family. I have a great family who love me unconditionally. My sisters are quite affectionate and my niece has made my days in the recent years, happier. I owe a lot to my maternal grand parents. I believe that my primary school days' life at their house, which had its own library, taught me the joy of learning at an early age. The aspirations and sacrifice of my parents strongly motivated me to pursue PhD, the highest university degree. They continue to motivate me to do the best in whatever I do. No words or deeds of mine can thank them enough. I remain indebted to them throughout my life.

Pottapinjara Vijay

Synopsis

The Indian Summer Monsoon (ISM) is a large scale land-ocean-atmosphere coupled system dominating the climate of the Indian Ocean region (e.g., Webster et al., 1998). Among other things, it is manifest in the winds blowing across the Indian Ocean over to the Indian subcontinent and the associated distribution of precipitation during boreal summer (e.g., Wang, 2006a). It is the lifeline of millions of people of the Indian subcontinent, and critical for the food production, economy, etc. of the subcontinent (Gadgil et al., 1999; Gadgil and Gadgil, 2006). Although great strides have been made in understanding the ISM and its variability, and predicting the monsoon over the past decades, there is a great need for improvements (e.g., Nanjundiah, 2009; Rao et al., 2019).

Although the Indian Summer Monsoon Rainfall (ISMR) exhibits variability on a spectrum of timescales, its year-to-year variations are of particular interest as they are associated with droughts and floods over India (e.g., Parthasarathy and Mooley, 1978; Webster et al., 1998; Gadgil, 2003). The interannual variability of ISMR is a result of both internal dynamics and the influence of external factors (e.g., Webster et al., 1998). The part of variability that is driven by external factors forms the basis for the seasonal prediction, given the decent lead prediction skills of the tropical ocean drivers of the monsoon such as the El Niño-Southern Oscillation (ENSO). The ENSO is a coupled ocean-atmosphere phenomenon operating in the tropical Pacific (e.g., Philander, 1989; Wang and Picaut, 2004). It is a major driver of the ISM as well as the global climate (e.g., Keshavamurty, 1982; Ashok and Saji, 2007; Yeh et al., 2018). While a warm phase of ENSO (or an El Niño) tends to reduce the monsoon rainfall over India, a cold phase of ENSO (or a La Niña) favors the enhancement of the rainfall (e.g., Sikka, 1980; Keshavamurty, 1982; Ashok et al., 2019, for the detailed literature). Although the ENSO is a major external driver of ISM, it does not explain all the droughts or floods over India. Hence it is imperative to study the impacts of other external factors on the ISM, especially that of the tropical modes of interannual variability. Another coupled ocean-atmosphere mode existing in the tropical Indian Ocean called the Indian Ocean Dipole (IOD; e.g., Saji et al., 1999; Webster et al., 1999; Murtugudde et al., 2000) is also shown to affect the ISM. A strong positive (negative) IOD event can contribute to an enhancement (a reduction) of ISMR, and even reduce the impacts of a strong concurrent El Niño (La Niña) event (e.g., Behera et al., 1999; Ashok et al., 2004b; Ashok and Saji, 2007). The remaining tropical ocean, i.e., the tropical Atlantic hosts its

own coupled phenomenon called the Atlantic Zonal Mode (AZM) but studies on the impacts of AZM on the interannual variability of the ISM are all recent and relatively less in number (e.g., Kucharski et al., 2008; Lübbecke et al., 2018).

The AZM, a phenomenon similar to but weaker than ENSO, is active during boreal summer (Zebiak, 1993). Recent studies showed that a warm (cold) AZM induces a reduction (an enhancement) of rainfall over India (e.g., Kucharski et al., 2008; Wang et al., 2009; Yadav, 2017). Based on sensitivity tests using an atmospheric general circulation model, Kucharski et al. (2009) proposed a physical mechanism in which a warm AZM tends to reduce the ISMR on interannual time scales by inducing a quadrupole response in upper level stream function and sinking motion over India. Further, in a recent related study Pottapinjara et al. (2014), we have shown that the AZM influences the ISMR not only on interannual timescales but also the monsoon transients such as depressions which significantly contribute to the ISMR. A warm (cold) AZM favors the formation of anomalously less (more) depressions in the Bay of Bengal resulting in reduced (enhanced) rainfall over core monsoon region. Furthermore, a thermodynamic manifestation of the response of the ISM to AZM is outlined. The AZM also affects the primary productivity in the Arabian Sea via the changes in the strength of the low level monsoon circulation and associated changes in upwelling (Barimalala et al., 2013a). The relation between the AZM and ISM is shown to be strengthening in recent decades (Sabeerali et al., 2019a). In addition, the misrepresentation of AZM in a coupled model is shown to leading to the loss of predictive skill of the ISM in the model (Sabeerali et al., 2019b). These previous studies touch upon some important aspects of the relationship between the AZM and ISM but obviously, there is a need for greater understanding of the relationship. Importantly, studies by Keenlyside and Latif (2007) and Ding et al. (2010) show that winds, heat content, and Sea Surface Temperature (SST) in the equatorial Atlantic during boreal spring are significantly related to the AZM during boreal summer. Further, Servain et al. (1999) and Murtugudde et al. (2001) demonstrated that the meridional migration of the Inter-tropical convergence zone during spring also is closely related to the AZM. That is, precursors to the summer AZM are available during boreal spring. However, it is not yet known if the evolution of cold and warm AZM events is symmetric as in the case of ENSO. Addressing this issue is of course important and eventually leads to a better predictability of the impacts of cold and warm AZMs on global climate, including the ISM.

In this background, the objectives of this thesis are set as follows.

- (i) To explore the lead association of the known precursors of the AZM in boreal spring to the following ISM
- (ii) To investigate if the evolution of warm and cold AZM in the boreal spring is symmetric, which would enhance our understanding of the AZM
- (iii) To explore the capability of a current day seasonal forecast model in simulating the relationship between the AZM and ISM

The thesis is organized into 6 chapters whose contents are summarized in the following.

Chapter 1: This chapter provides a general introduction of some important concepts which are relevant to the thesis. It introduces the features of mean ISM, its variability on interannual timescales, and the external drivers of its interannual variability, such as ENSO and the IOD. The AZM operating in the tropical Atlantic, a coupled ocean-atmosphere phenomenon similar to ENSO, is discussed in detail. A survey of literature on the relation between the AZM and ISM is conducted, which brings out the gaps in the understanding of the relationship. Based on the gaps identified, a few specific objectives are set, which the thesis aims to achieve.

Chapter 2: In this chapter, the common observational and reanalysis datasets, and statistical techniques used in the thesis are discussed. Nevertheless, the data products used in each following chapter are also of course briefly mentioned in the respective chapters. Any datasets that are specific only to a particular chapter, such as the details of outputs from the simulations of a coupled model, are discussed in the relevant chapter.

Chapter 3: Both the AZM and ISM are active during boreal summer, and the relation between the two as such lacks any predictive value for the ISM. It is known that a great part of the variability of the AZM can be explained by ENSO-like dynamics (Zebiak, 1993; Keenlyside and Latif, 2007). In this chapter, the goal is to extend this process-understanding to develop a basis for an eventual lead relationship between the tropical Atlantic and the ISMR, potentially inclusive of the AZM teleconnections to the ISM. Various composite analyses of the monthly zonal surface winds, heat content, and SST in the equatorial Atlantic carried out in this chapter, suggest that signatures of a warm or cold AZM event begin to emerge in the early spring of that year. We found significant correlations between the ISMR, and the low level zonal winds in the western equatorial Atlantic and heat content in the eastern equatorial Atlantic in the boreal spring. These coherent changes in the winds and heat content in the deep tropical Atlantic in

boreal spring associated with the AZM events may facilitate more skillful predictions of the ensuing summer monsoon anomalies, especially during non-ENSO years when the predictability of ISMR tends to be low. This chapter addresses Objective (i).

Chapter 4: This chapter delves deep into the details of precursors and causative mechanisms of an AZM event, with the expectation that it enhances our understanding of the AZM (addresses Objective ii). This would potentially contribute to an improved prediction of the Indian summer monsoon, through the links between the two as discussed in the earlier studies. It is known that, apart from the AZM, the interannual variability of the tropical Atlantic is dominated by the Atlantic Meridional Mode (AMM; Nobre and Shukla, 1996; Xie and Carton, 2004), which is active in boreal spring. Previous studies have talked about the existence of a relationship between the AMM and AZM via the meridional displacement of the Inter-tropical Convergence Zone (ITCZ) in the Atlantic during boreal spring and the resulting cross-equatorial zonal winds (e.g., Servain et al., 1999; Murtugudde et al., 2001). However, the strong relationship between the ITCZ (or AMM) and zonal winds does not translate into a strong relationship between the ITCZ and AZM. Importantly, the lack of such a strong relationship has not been explained in any of the previous studies. This question is addressed here using observational and reanalysis data sets. The results indicate that there is an asymmetry in the relationship between ITCZ and AZM: while a northward migration of ITCZ during spring, in general, leads to a cold AZM event in the ensuing summer, the southward migration of the ITCZ is less likely to lead to a warm event. It implies that the evolution of cold and warm AZM events with respect to the meridional position of Atlantic ITCZ during boreal spring is asymmetric. This asymmetry is in contradiction with what the previous studies imply. The asymmetry is attributed to the Atlantic seasonal cycle and the strong seasonality of the AZM. It is also found that all those cold AZM events preceded by a northward ITCZ movement during spring strictly adhere to typical timings and evolution of different components of the Bjerknes feedback involved. Based on the results, it is conjectured that the causative mechanisms of warm events are more diverse than those of the cold events. It could imply that the AZM cold events are inherently more predictable compared to the warm events.

Chapter 5: In this chapter, we use a state-of-the-art coupled ocean-atmospheric general circulation model (the NCEP's Coupled Forecast System version 2), a major and modern operational dynamical model utilized for monsoon forecasts in India, to investigate whether

the model simulates the observed relationship between the AZM and ISM. The simulation of different manifestations of response of the ISM to AZM in the model are also examined. In a previous study, Kucharski et al. (2009), using an atmospheric general circulation model, showed that a warm (cold) AZM can induce a quadrupole response in the upper level stream function and a sinking (rising) motion over India which tends to reduce (enhance) the ISMR. In addition, the physical mechanism connecting the tropical Atlantic and Indian Oceans via the mid-tropospheric temperature is proposed in our recent study Pottapinjara et al. (2014), which entails a thermodynamic manifestation of the response. From an analysis of the model free-run, it is found that the model simulates the relationship between the AZM and ISM rainfall reasonably well. In a complementary sensitivity experiment we carried out, a warm AZM SST anomaly is imposed in the tropical Atlantic during boreal summer and the response of the ISM is studied. It is found that while the model simulates the important aspects of both dynamical and thermodynamical manifestations of the response of ISM to the AZM, some details of the mechanism are not simulated due to mean state biases in the model. This chapter highlights the need for the improvement of the simulated mean state of the tropical Atlantic in the model to better capture the relationship between AZM and ISM, which will potentially improve the monsoon forecasts issued using this model. This chapter addresses Objective (iii).

Chapter 6: In this chapter, a summary of important findings of the thesis, and a brief discussion on the scope for further research are presented.

List of Abbreviations

AGCM	Atmospheric General Circulation Model
AMJ	April-May-June
AMM	Atlantic Meridional Mode
Atl 3	Atlantic 3
AZM	Atlantic Zonal Mode
BoB	Bay of Bengal
CC	Correlation Coefficient
CFS	Coupled Forecast System
CI	Central India
CMIP 5	Coupled Model Intercomparison Project 5
DJF	December-January-February
ECMWF	European Centre for Medium Range Weather Forecasting
EEA	Eastern Equatorial Atlantic
ENSO	El Niño-Southern Oscillation
ERA	ECMWF's Re-analysis
HadISST	Hadley Centre Sea Ice and Sea Surface Temperature
HC	Heat Content
IMD	India Meteorological Department
IO	Indian Ocean
IOD	Indian Ocean Dipole
ISM	Indian Summer Monsoon
ISMR	Indian Summer Monsoon Rainfall
ISO	Intra-seasonal Oscillation
ITCZ	Inter-tropical Convergence Zone
JJA	June-July-August
JJAS	June-July-August-September
LPS	Low Pressure System
MAM	March-April-May
MJJ	May-June-July
NCEP	National Centers for Environmental Prediction
Obs	Observations
ONI	Oceanic Niño Index

SAA	South Atlantic Anticyclone
SE	Standard Error
SODA	Simple Ocean Data Analysis
SST	Sea Surface Temperature
SSTA	Sea Surface Temperature Anomaly
TNA	Tropical North Atlantic
TT	Tropospheric Temperature
WG	Western Ghats
WEA	Western Equatorial Atlantic

List of Figures

1.1	The seasonal mean tropospheric temperature ($^{\circ}\text{C}$) averaged between 500 and 200 hPa in JJA (top) and DJF (bottom). The air temperature is obtained from ERA-Interim Reanalysis (Dee et al., 2011).	2
1.2	Monthly means of rainfall over India using All India Summer Monsoon Rainfall datasets obtained from www.tropmet.res.in/DataArchival-51-Page .	3
1.3	The important components of the Indian summer monsoon (Krishnamurti and Bhalme, 1976).	4
1.4	Seasonal (JJAS) mean SST based on HadISST (Rayner et al., 2003) and low level winds (850 hPa) based on ERA-Interim Reanalysis (Dee et al., 2011) in the Indian Ocean during summer monsoon.	5
1.5	The mean (left) and standard deviation (right) of JJAS mean monsoon rainfall over India using the high resolution ($0.25^{\circ} \times 0.25^{\circ}$) gridded rainfall provided by the India Meteorological Department (IMD; Pai et al., 2014) over the period 1979–2013. The mean is scaled by 4 to have a common scale. Units mm/day.	6
1.6	The interannual variations of JJAS rainfall over India during 1871–2016, using the All India Rainfall time series obtained from www.tropmet.res.in . The time series is normalized by its own standard deviation.	7
1.7	A schematic diagram depicting a) the normal conditions and b) anomalous conditions in the tropical Pacific. This image is obtained from Ashok and Yamagata (2009) ©Springer Nature. Reproduced with permission.	9

1.8	A schematic showing the positive (upper panel) and negative (lower panel) phases of the Indian Ocean Dipole. Source: Woods Hole Oceanography Institute (https://www.whoi.edu)	12
1.9	The monthly evolution of climatological SST (°C) based on HadISST (Rayner et al., 2003) and surface winds (m/s) from ERA-Interim Reanalysis (Dee et al., 2011), in the tropical Atlantic. A contour of 25.5°C is shown to demonstrate the development of seasonal cold tongue. The position of oceanic ITCZ is marked in thick blue (See Chapter 5 for the details of how the position of ITCZ is identified).	14
1.10	Monthly evolution of anomalies of SST and low level winds at 850 hPa associated with the cold (left) and warm (right) phases of AZM. The SST and winds are taken from HadISST (Rayner et al., 2003) and ERA-Interim Reanalysis (Dee et al., 2011), respectively. The period of analysis is 1979–2013.	15
1.11	The locations of genesis (brown circles), and tracks (blue lines) of monsoon (June-July-August) depressions in the BoB that occurred during a) cold and b) warm phases of AZM. The AZM events that co-occur with ENSO events are omitted in the analysis to highlight the intrinsic influence of AZM on the depressions. The period of analysis is 1975–2012. The depressions data provided by the IMD is available at http://www.imdchennai.gov.in/cyclone_atlas.htm . The AZM and ENSO events are identified using the June-July-August Atlantic 3 and ONI indices, respectively. The indices are prepared from the HadISST (Rayner et al., 2003). The identification of AZM and ENSO events, and their respective lists are the same as in Chapter 3.	22

- 1.12 The differences of seasonal (June-July-August) composites of anomalies of a) vertically integrated moisture transport b) vorticity (10^{-7} s^{-1}) overlaid by winds at 850 hPa, and c) vertical wind shear (m s^{-1}) between levels 850 and 200 hPa. The composites of anomalies of each variable are first computed during the cold and warm phases of AZM separately, and the difference of cold and warm (cold–warm) composites, is presented here. The contours in pink and white (in b and c) indicate the significance levels of 20% and 10%, respectively as per Student's *t*-test. The variables are taken from NCEP's Reanalysis–2 (Kanamitsu et al., 2002). The period of analysis is 1979–2012. The list of AZM events used in this analysis is a subset of that in Chapter 3. See Chapter 2 for details on how to compute the composites and determine the level of statistical significance. 24
- 1.13 The simultaneous correlation between monthly time series of tropospheric temperature (TT) anomalies averaged over 1000 through 200 hPa, and the Atlantic 3 index. The influence of ENSO is regressed out from these variables before computing the correlation to highlight the impact of AZM on the TT anomalies. All the shaded values are statistically significant at the 10% level as per Student's *t*-test. The tropospheric temperature is taken from NCEP's Reanalysis-2 (Kanamitsu et al., 2002). The period of analysis is 1979–2012. See Chapter 3 for details on why and how to regress out the influence of ENSO on the target variable. See Pottapinjara et al. (2014) for further details such as development and decay of this response with time. 24
- 3.1 Differences of composites of rainfall (mm) between the cold and warm events of (a) AZM, (b) AZM only (excluding those co-occurring with ENSO), (c) ENSO and (d) ENSO only (excluding ENSO events co-occurring with AZM). The two regions selected for the analysis, i.e., Central India (15°N – 26°N and 76°E – 85°E ; black box) and the Western Ghats (10°N – 23°N and 72.5°E – 75.5°E ; pink box) are shown in (b). The contours in black color indicate 10% significance level. 40

3.2	The lead-lag correlations between ONI index, and rainfall over Central India (blue) and the Western Ghats (red) before (thick line) and after (dashed) removing the effect of ENSO over the respective regional rainfall. The dashed straight lines indicate the 10% significance level for the correlations using the two-tailed Student's t-test.	41
3.3	a) The time series of JJA Atl3 (blue line) and JJAS rainfall over the Western Ghats and Central India before (line) and after (dashed line) removing the influence of ENSO on the rainfall. While the rainfall over the Western Ghats is marked in black, that over Central India is marked in red. All time series are normalized by their respective standard deviation.	43
3.4	Spatial correlations between the anomalies of (a) SST in the Atl3 region and zonal winds, (b) western equatorial Atlantic (3°S–3°N and 40°W–20°W; WEA) zonal winds and heat content, (c) eastern equatorial Atlantic (3°S–3°N and 5°W–10°E; EEA) heat content and SST, and d) monthly lead-lag correlations between anomalies of SST in the Atl3 region and WEA zonal wind (black), WEA zonal wind and EEA heat content (red) and EEA heat content and Atl3 (blue). The zonal winds are taken at 850 hPa level. In spatial correlation plots (a, b and c), contours of 20% and 10% significance are indicated in pink and black colors respectively and in (d), the level of 10% significance is indicated by a pink dashed line. The correlations over land are masked in (a) to highlight the same over the ocean. The black box in (c) indicates the Atl3 region.	45
3.5	Evolution of composites of anomalies of western equatorial zonal wind (red), eastern equatorial zonal wind (pink), eastern equatorial heat content (black) and SST in the Atl3 region (blue) during the warm (a) and cold (b) events of AZM. All the fields are normalized before compositing. The zonal winds are taken at 850 hPa level. The peaks of different fields plotted are marked as vertical lines in their respective colors. The statistical significance of the composites at the 10% is indicated by circles in their respective colors.	47

3.6	Monthly correlations, during January–May, between anomalies of heat content and JJAS rainfall anomalies over Central India (a and b), and the Western Ghats (c and d), before (a and c) and after (b and d) removing the effect of ENSO on the respective regional rainfall during the monsoon season. Correlations above 10% significance level around the equator are shown in black contours. This figure is consistent with Fig. A.1 which is repeated using a different dataset to demonstrate the robustness of the results across datasets.	49
3.7	Monthly correlations, during January–May, between anomalies of low level winds, and JJAS rainfall anomalies over Central India (a and b), and the Western Ghats (c and d), before (a and b) and after (b and d) removing the effect of the ENSO on the respective regional rainfall during the monsoon season. The contours of 20% and 10% significance levels are indicated in pink and white colors, respectively. Correlations over land are masked to highlight the same over the ocean. This figure is consistent with Fig. A.2 which is repeated using a different dataset to demonstrate the robustness of the results across datasets.	50
4.1	Regressions of the Atlantic Meridional Mode (AMM) index onto March–May anomalies of SST ($^{\circ}\text{C}$) and winds (ms^{-1}). See Section 4.2 for the definition of AMM index.	57
4.2	Interannual variations of anomalous meridional position of ITCZ in March–May (black). The time series is normalized by its standard deviation and standard deviation is indicated by a black dashed line. Whenever the central to western equatorial zonal wind in March–May is sufficiently strong crossing $+0.9$ (-0.9) of its respective standard deviation, i.e., westerly (easterly), it is indicated by blue (red) circles. Whenever the Atl3 SST in June–August crosses $+1$ (-1) of its respective standard deviation, i.e., when there is a warm (cold) AZM event, it is indicated by red (blue) stars.	60

- 4.3 Monthly (February–August) evolution of composites of (a) ITCZ position (lines) and zonal wind anomalies (shading; ms^{-1}); (b) anomalies of winds (vector) and heat content (shading; 10^{10}Jm^{-2}) and (c) SST (shading; $^{\circ}\text{C}$) when the spring Atlantic ITCZ is anomalously northwards and gave rise to a cold AZM event. In (a), red line (dot inside a black circle) indicates the ITCZ position at respective longitudes (along 28°W) whereas the blue lines (circle) indicate the envelope of ITCZ variability, i.e., middle blue line (circle) indicates the climatological ITCZ position in that month, and the top and bottom blue lines (circles) indicate ± 1 standard deviation of the position from the mean in the same month. The calendar month is indicated on each subpanel. Only those zonal winds in (a) and vectors in (b) that are significant at the 5% level are shown. The significance of heat content anomalies in (b) and SST anomalies in (c) are indicated by line contours. The rectangular boxes in black [in (a); April], red [in (b); May], and blue [in (b); June] and thick black [in (c); July] indicate the regions over which anomalies of winds, eastern equatorial Atlantic heat content, western equatorial Atlantic heat content and SST are averaged respectively, for use in other analyses. 63
- 4.4 Scatter plot between the normalized indices of MAM western equatorial Atlantic (WEA) zonal winds (averaged over 3°S – 3°N and 40°W – 10°W) and MAM ITCZ position. The black dashed horizontal (vertical) lines indicate the ± 1 standard deviation of ordinate (abscissa). The points surrounded by blue (red) circles indicate the years in which cold (warm) AZM events occurred in the following summer. 64
- 4.5 Same as Fig. 4.3 but the composites of different fields presented here are of events when the spring ITCZ is anomalously in the south. As discussed in Section 4.3, except in the year 1995, no southward movement of spring ITCZ led to a warm AZM event in the ensuing summer. This singular event is excluded while computing the composite to ensure its homogeneity as well as to highlight the predominantly westerly nature of winds in the western equatorial Atlantic in all events included. The composite of ITCZ position in (a) is shown in green for better visibility. In (b), even the non-significant wind anomalies are also shown to highlight the variation of their strength across the equator. 65

4.6	Monthly evolution of the mean position of the ITCZ in the Atlantic (black line; along 28°W; °N) with the shading indicating the ± 1 standard deviation about the mean in the respective months.	66
4.7	(a),(b): Hovmöller diagram of the composite of anomalies of thermocline depth (shading) overlaid by zonal winds (contours) over the equator in the Atlantic when the MAM ITCZ is anomalously north (south) and zonal wind anomalies over WEA are easterly (westerly). (c) Hovmöller diagram obtained by adding the anomalies shown in (a) and (b) [= anomalies in (a) – negative of anomalies in (b)], intended to show the dominance of anomalies in (a) over that in (b). In (a) and (b), only the wind anomalies that are significant at the 5% level are shown. In (c), the significant wind anomalies are indicated by the contour lines in red. Significance contour lines become discontinuous if the zonal winds between the two ends of a contour are not significant.	66
4.8	Monthly evolution of composites of anomalies of (top) zonal winds (ms^{-1}) in the western equatorial Atlantic and position of ITCZ (° latitude) and (bottom) SST averaged over Atl3 region (°C), heat content (10^{10} J m^{-2}) averaged in the western/eastern equatorial Atlantic, composited in the years when MAM ITCZ is north and leads to the development of a cold AZM event in the subsequent summer. The circles on each line indicate when the respective composite means become significant at the 5% level.	69
4.9	Interannual variations of anomalies of western equatorial Atlantic zonal winds in March–May (red; ms^{-1}), eastern equatorial Atlantic heat content in April–June (purple; 10^{10} J m^{-2}), western equatorial Atlantic heat content in May–July (green; 10^{10} J m^{-2}) and SST in the characteristic Atl3 region in June–August (blue; °C). Strong canonical cold (warm) events are indicated with black dashed line in upper (lower) portion. All the time series are normalized by their respective standard deviation. Whenever the spring ITCZ crosses +1 (–1) standard deviation, i.e., north (south), it is indicated with blue (red) thick circles.	71

4.10	Evolution of different Bjerknes components during March–July of each AZM event in the phase space of zonal winds averaged over central to western equatorial Atlantic (abscissa; m s^{-1}) and heat content in the western equatorial Atlantic (ordinate; 10^{10} J m^{-2}) with the color of each point/symbol representing the SST in the Atl3 region ($^{\circ}\text{C}$). Different symbols are used to mark different AZM events and the red (blue) dashed lines connecting them indicate a warm (cold) AZM event. The starting point of each year, i.e., March, is indicated by a black circle. The gray line connects the one standard deviation points in the phase space during March–July and the March point is indicated with a bigger gray circle. This line serves as a reference against which the strength of a particular event can be compared. All the Bjerknes components plotted are smoothed by a 3-month running mean for better appearance. For the Bjerknes feedback to be considered active all three elements of (Keenlyside and Latif, 2007) have to be present. While the heat content and zonal wind anomalies are used as the axes, SST in the Atl3 region is shown filling different symbols used to differentiate between the events and is easy to miss. Since only the AZM events which we already know have an SST response (AZM definition is based on Atl3 SST index) are plotted, this representation is adequate to tell us whether or not an AZM event can be explained by the Bjerknes feedback.	73
4.11	Same as Fig. 4.10 except that in case of the cold event in 1994, the zonal winds are averaged in the region centered around 5°S (7°S – 3°S and 20°W – 10°E) and the heat content is negative of that averaged in the eastern Atlantic centered around 5°S (7°S – 3°S and 0°E – 15°E). In the case of warm event in 1998, the zonal winds are averaged over 3°S – 3°N and 5°W – 15°E	75
4.12	Same as Fig. 4.3 but the anomalies of corresponding variables in the year 1981 are presented instead of the composites.	77
4.13	Same as Fig. 4.12 but for the year 2012.	78
4.14	Same as Fig. 4.12 but for the year 1982	79
4.15	Same as Fig. 4.12 but for the year 1994.	80
4.16	Same as Fig. 4.12 but for the year 1998.	81

4.17	A schematic diagram summarizing the most likely scenario when the Atlantic ITCZ in spring is anomalously (a) north and (b) south. When the Atlantic ITCZ in spring is anomalously north as shown in (a) at point 1, it leads to concurrent anomalous winds that have strong easterly component over the WEA (point 2), which in turn shoals the equatorial thermocline in the east and deepens the same in the west with a delay of 1 or 2 months (point 3; dashed line: mean thermocline; thick line: shifted thermocline), finally resulting in a cold AZM event in the following summer (point 4). On the contrary, when the ITCZ in spring is anomalously south as shown in (b) at point 1, it leads to concurrent anomalous winds that are predominantly northerly in the vicinity of the equator but develop a strong westerly component upon crossing into the south but away from the equator (point 2). The westerly component of the winds in the WEA is so weak that they cause insufficient deepening of equatorial thermocline in the east (point 3) inducing weak warm SST anomalies and thus no warm AZM event (point 4). In summary, while the anomalous northward spring ITCZ leads to a cold AZM event in the following summer most of the times, the converse is less likely and hence the skewness in the relation between spring ITCZ position and AZM. Atl3 region is marked with a rectangular box. The above is only for representative purposes and not to scale.	83
4.18	Monthly (February–August) evolution of SST anomalies in the years a) 1983, b) 1992, c) 1997 and d) 2005 when the anomalous spring ITCZ in the north leads to a cold AZM event in the following summer. These are the SST anomalies used to compute the respective monthly composite shown in Fig. 4.3c	85
5.1	The observed monthly climatology of SST (°C; shaded) overlaid by surface winds (vectors), and position of the oceanic ITCZ (thick blue line) in the tropical Atlantic. The SST contour of 25.5°C is overlaid (blue) to show the development of the seasonal cold tongue in the southern tropical Atlantic during boreal spring–summer. The corresponding month is indicated on each subpanel. This figure is the same as Fig. 1.9.	92

5.2	Monthly evolution of the bias (CFSv2 _{REF} – Observations) in the annual cycle of SST (shaded; °C) and surface winds (vectors; ms ⁻¹) when the reference run is compared against the observations.	93
5.3	The monthly climatological position of the ITCZ (degree north) in the Atlantic in the model reference run (CFSv2 _{REF} ; solid line) and in the observations (dashed line).	94
5.4	Monthly composites of anomalies of SST (shaded; °C) and low level winds at 850 hPa (vectors; ms ⁻¹) of cold and warm AZM events in a) observations and b) in the reference run during June–September. a) is the same as Fig. 1.10 . . .	95
5.5	The monthly lead-lag correlations between the Atl3 index and Tropospheric Temperature (TT) integrated over 600 hPa to 200 hPa after removing the effect of ENSO on both TT and Atl3 index in a) Observations and b) Model. The lead of TT in months is indicated on each subpanel. The effect of ENSO is removed to elicit the signal clearly (as discussed in Section 3.2). The removal also takes care of the wrong AZM-ENSO relation in the model, albeit partially. The correlations are statistically significant at the 10% level.	97
5.6	The correlation between the JJA Atl3 index and the JJAS precipitation over India in the a) observations and b) model reference run (CFSv2 _{REF}), after removing the effect of ENSO over precipitation. The correlations are significant at the 20% level.	98
5.7	Composite of observed JJA SST anomalies (shaded; °C) of warm AZM events that is imposed in the sensitivity experiment. The composite is statistically significant at 10% level. The construction of the composite is described in Section 5.2.	99

5.8	Influence of the AZM on the seasonal mean precipitation and low level circulation in the Indian Ocean in the a) observations and b) model sensitivity experiment (CFSv2 _{SST}). a) Regression of JJA Atl3 index onto anomalies of JJAS precipitation (shading; mm day ⁻¹) and low level winds (850 hPa; vectors; m s ⁻¹) after removing the influence of ENSO b) JJAS mean response in precipitation (shading; mm day ⁻¹) overlaid by winds (vectors; m s ⁻¹). In (a), the statistically significant regressions at 20% in precipitation (winds) are shown in red contours (blue vectors).	100
5.9	Monthly mean response of precipitation (shading; mm day ⁻¹) overlaid by low level winds (vectors) in each month during June–September (a: June; b: July; c: August; d: September).	101
5.10	The response in vorticity at 850 hPa (shading; 10 ⁻⁶ s ⁻¹) overlaid by vectors of shear between at 850 hPa and 200 hPa (winds at 850 hPa – winds at 200 hPa; ms ⁻¹) in August.	103
5.11	The response and analyses of different fields covering the tropical Atlantic and Indian oceans: a) low level wind vectors at 850 hPa (m s ⁻¹); b) precipitation (mm day ⁻¹); c) SST (°C; multiplied by 0.25); d) mid-tropospheric temperature averaged between 600 and 200 hPa (0.1 K) e) upper level velocity potential at 200 hPa (shading; 10 ⁶ m ² s ⁻¹) and low level stream function at 850 hPa (contours; 10 ⁶ m ² s ⁻¹). The specified fields are scaled to have a common color scale. In c), the SST response in the tropical Atlantic is masked because that is where we impose the warm AZM SST anomalies. In (d), the positive (negative) contours of stream function are shown in blue (red) colors to highlight the quadrupole structure of Kucharski et al. (2009).	104
5.12	Vertical cross sections of the response in mid-tropospheric temperature (TT; K) in August, a) after averaging over the latitudinal band of 5°S–5°N to show the TT teleconnection between the Atlantic and Indian oceans and b) after averaging over the longitudinal band of 60°E–120°E to show the gradient in TT between over the Indian subcontinent and Indian Ocean.	105

- A.1 Same as Fig. 3.6 but using EN4 subsurface analysis version 4.2.0 of the UK Met Office (Good et al., 2013) for the computation of heatcontent. 114
- A.2 Same as Fig. 3.7 but using the wind data from the ERA-Interim (Dee et al., 2011).115

List of Tables

- 3.1 Correlation coefficients between JJA Atl3 index and JJAS rainfall anomalies over Central India (15° – 26° N and 76° – 85° E) and Western Ghats (10° – 23° N and 72.5° – 75.5° E) before and after removing the effect of ENSO on the respective rainfall series. The coefficients marked in bold are significant at the 10% level. 43
- 4.1 Correlation Coefficients (CC) between different parameters averaged over different months (MAM: March–May; AMJ: April–June; MJJ: May–July; JJA: June–August). AMM: Atlantic Meridional Mode; AZM: Atlantic Zonal Mode; zonal wind: central to western equatorial Atlantic zonal winds; EEA HC: Eastern Equatorial Atlantic Heat Content; WEA HC: Western Equatorial Atlantic Heat Content; ITCZ: Inter-tropical Convergence Zone. See Section 4.3 and Fig. 4.3 for the regions over which different parameters are averaged. 58
- 4.2 Correlations between different factors representing a chain of processes with respect to relation between AMM, ITCZ and AZM. The abbreviations are the same as in Table 4.1. Additionally, the first three lettered string of each factor represents the season in which the factor is averaged (e.g., MAM: March-April-May; AMJ: April-May-June). The cross-correlations among the factors MAM ITCZ, MAM zonal wind, AMJ EEA HC, MJJ EEA HC, JJA Atl3 are the highest and are shown in blue color. These factors are used in further analysis in 4.9. 68

List of Publications

1. **Pottapinjara, V.**, M. S. Girishkumar, M. Ravichandran, and R. Murtugudde, 2014: Influence of the Atlantic zonal mode on monsoon depressions in the Bay of Bengal during boreal summer. *Journal of Geophysical Research: Atmospheres*, **119** (11), 6456–6469 (earlier study which is the basis of the thesis)
2. **Pottapinjara, V.**, M. S. Girishkumar, S. Sivareddy, M. Ravichandran, and R. Murtugudde, 2016: Relation between the upper ocean heat content in the equatorial Atlantic during boreal spring and the Indian monsoon rainfall during June–September. *International Journal of Climatology*, **36**, 2469–2480
3. **Pottapinjara, V.**, M. S. Girishkumar, R. Murtugudde, K. Ashok, and M. Ravichandran, 2019: On the Relation between the Boreal Spring Position of the Atlantic Intertropical Convergence Zone and Atlantic Zonal Mode. *Journal of Climate*, **32**, 4767–4781
4. **Pottapinjara, V.**, Roxy M. K., M. S. Girishkumar, K. Ashok, M. Ravichandran, and R. Murtugudde, 2020: Simulation of the relationship between the Atlantic Zonal Mode and Indian summer monsoon in CFSv2 (to be communicated)

Other Publications

1. Girishkumar, M. S., J. Joseph, V. P. Thangaprakash, **V. Pottapinjara**, M. J. McPhaden, 2017: Mixed Layer Temperature Budget for the Northward Propagating Summer Monsoon Intraseasonal Oscillation (MISO) in the Central Bay of Bengal. *Journal of Geophysical Research: Oceans*, **122**, 8841–8854

Chapter 1

Introduction

This chapter introduces some important basic concepts relevant to the Indian summer monsoon and the Atlantic zonal mode, and sets the stage for problems in the context of the research carried out so far, which will be addressed in the following chapters of the thesis.

1.1 The Indian Summer Monsoon

The ‘monsoon’, derived from an Arabic word ‘mausam’ for season, is traditionally defined as a seasonal reversal of surface winds (Ramage, 1971). The major regions that satisfy the strict criteria of steady and sustained wind regime of Ramage (1971) are India and Southeast Asia, northern Australia, and West and central Africa. However, monsoon is now broadly used to refer to seasonal changes in the atmospheric circulation and rainfall associated with asymmetric heating of land and sea (e.g., Webster et al., 1998). All these regions with a monsoon are mainly located in the tropics.

A thermal contrast between the land and ocean is necessary for a monsoon to be established. The land responds to seasonal cycle in solar heating rapidly compared to the ocean. When the land is hot, it draws in air carrying moisture from over surrounding oceans. When this air rises after reaching the land (lifted mechanically or otherwise), the moisture condenses and rains. In this traditional description, the existence of monsoon is explained as a gigantic land-sea breeze (Halley, 1753). However, the difference in surface temperatures cannot maintain the monsoon as the land surface tends to cool after initial rains. The latent heat released by

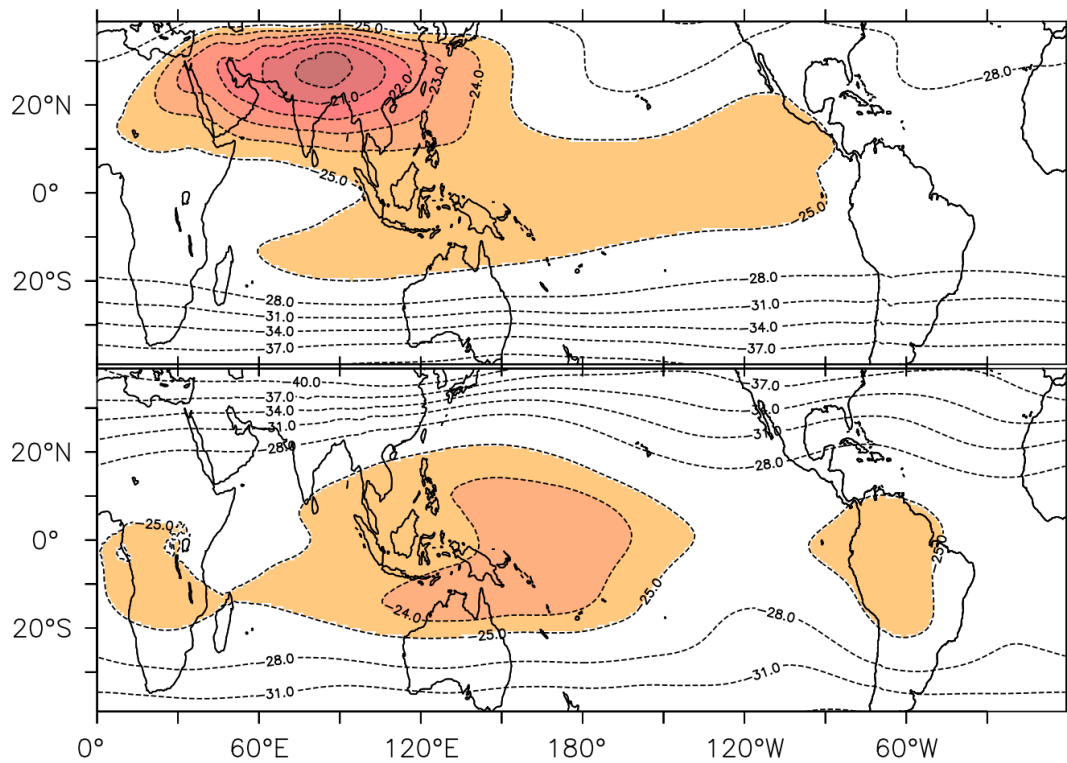


Figure 1.1: The seasonal mean tropospheric temperature ($^{\circ}\text{C}$) averaged between 500 and 200 hPa in JJA (top) and DJF (bottom). The air temperature is obtained from ERA-Interim Reanalysis (Dee et al., 2011).

condensing water vapor maintains the low pressure over land and continues to drive the monsoon (e.g., Webster et al., 1998; Slingo, 2003; Goswami and Xavier, 2005; Gadgil, 2018). As an alternative to the traditional explanation of monsoon as a gigantic land-sea breeze and with a particular reference to the monsoon in the north Indian Ocean region, Gadgil (2018) proposes that the monsoon should be seen as a seasonal migration of the Inter-tropical Convergence Zone (ITCZ), the zone where the trade winds from either hemisphere meet.

A monsoon is more complex than the simplistic picture presented above and several factors such as orography, shape of continents and ocean temperatures give a regional character to the monsoon (Webster et al., 2003). Of all the monsoons mentioned earlier, the monsoon over south Asia is the strongest and has the largest variation between seasons, for the reasons stated in the following. The geographical orientation of oceans and land in the north-south direction, and the presence of Tibetan plateau which acts as an elevated heat source distinguish the monsoon over Indian subcontinent from the rest. The north-south distribution of land and ocean

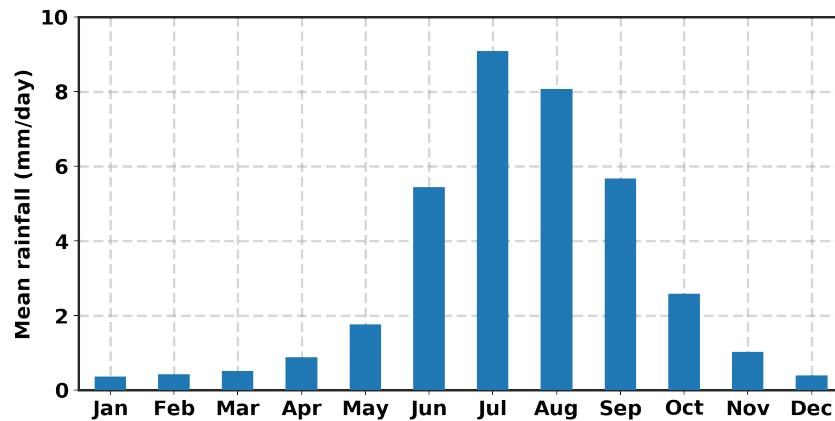


Figure 1.2: Monthly means of rainfall over India using All India Summer Monsoon Rainfall datasets obtained from www.tropmet.res.in/DataArchival-51-Page.

takes the advantage of meridional movement of solar heating seasonal cycle (Slingo, 2003). The seasonal heating of the plateau causes reversal of meridional temperature gradient which penetrates deep into the troposphere and sets up large-scale circulation over south Asia (e.g., Webster et al., 1998; Slingo, 2003; Wang, 2006a). During boreal summer, the mid troposphere over the plateau is at a higher temperature compared to the equatorial Indian Ocean establishing a thermal gradient between land and ocean. This gradient reverses its direction in boreal winter (Fig. 1.1).

The monsoon in the north Indian Ocean region can be divided into two parts depending on the direction from where surface winds blow or the season in which it occurs, viz., the southwest monsoon or the summer monsoon occurring during June–September, and the northeast monsoon or the winter monsoon occurring during October–December. However, in this thesis, we focus on the summer monsoon as it is stronger than the winter monsoon and contributes to about 80% of the annual total rainfall over India (Fig. 1.2; Parthasarathy et al., 1994; Kothawale and Rajeevan, 2017). For people inhabiting the region, the seasonal variation of rainfall is so much more important than the reversal of winds that the lives, customs, agriculture and economy are tied to variations of rainfall (e.g., Gadgil et al., 1999; Gadgil, 2003; Gadgil and Gadgil, 2006; Amat and Ashok, 2018). Unsurprisingly, the word monsoon came to mean rainfall in the colloquial use. Therefore, in the remainder of the thesis, the words summer monsoon and monsoon refer to the monsoon over the Indian subcontinent during summer or the Indian Summer Monsoon (ISM), unless otherwise mentioned.

During the summer monsoon, strong winds blowing away from a subtropical region of

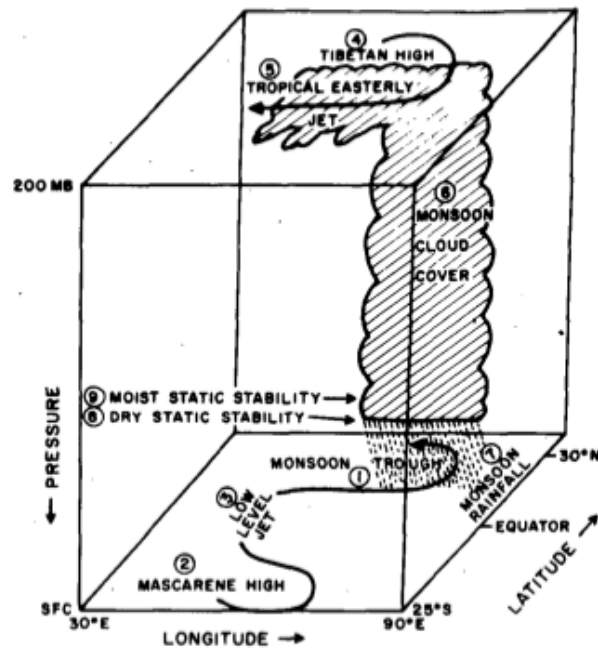


Figure 1.3: The important components of the Indian summer monsoon (Krishnamurti and Bhalme, 1976).

high pressure called the ‘Mascarene High’ cross the equator via the southern tropical Indian Ocean and flow over to the Indian subcontinent (Fig. 1.3). The Mascarene High, together with an upper level anticyclone over the Tibetan Plateau, drives a large scale cross equatorial atmospheric circulation (Fig. 1.3; Krishnamurti and Bhalme, 1976). The surface southwesterlies are intense in the vicinity of Somali coast and form the Low Level Jet (Joseph and Raman, 1966) or the Findlater Jet (Findlater, 1969) which has speeds as high as 20 ms^{-1} at the core of the jet (Fig. 1.3). This jet stream drives a strong cross-equatorial ocean current along the coast of Somalia called the Somali Current. As a result, a strong upwelling takes place and cools the Sea Surface Temperature (SST) in the Arabian sea (Fig. 1.4).

The southwesterlies of summer monsoon flow in two branches (Fig. 1.4). One branch directly blows over to the Indian subcontinent hitting the Western Ghats, and the other branch enters the Bay of Bengal and goes over to central parts of India featuring the monsoon trough (e.g., Rao, 1976; Gadgil, 2018). The monsoon trough, a region of low pressure, extends in the northwest direction from the head Bay of Bengal to the northwestern India. Complementing the large scale southwesterlies in the lower levels, a jet of easterlies in the upper levels forms an important feature of the southwest monsoon and is called the Tropical Easterly Jet (Fig. 1.3; Koteswaram, 1958). The first rains of the southwest monsoon occur over the state of Kerala

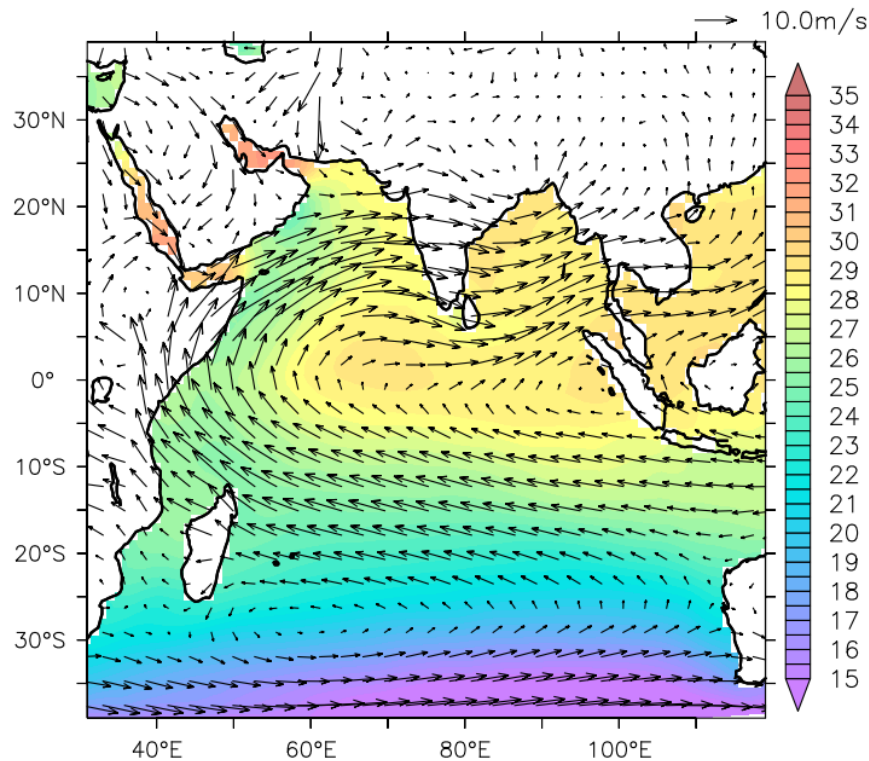


Figure 1.4: Seasonal (JJAS) mean SST based on HadISST (Rayner et al., 2003) and low level winds (850 hPa) based on ERA-Interim Reanalysis (Dee et al., 2011) in the Indian Ocean during summer monsoon.

in India sometime between late May to early June, and when they do, the ‘onset’ of monsoon is said to have occurred. These rains last for one season and withdraw from the subcontinent towards the end of September. Given the importance of summer monsoon rainfall, it is important to understand its space-time variations and any contribution to predicting the same is of immense value.

The rainfall over India is not uniformly distributed and varies both in space and time. It rains heavily along the Western Ghats and over the northeastern parts of India (Fig. 1.5). Though not as high, another rainfall maximum occurs over central part of India along the monsoon trough region, mainly confined between the latitudes of 17°N and 27°N . It is called the monsoon zone. The monsoon rainfall varies on a spectrum of time scales ranging from daily to decadal and more (e.g., Webster et al., 1998). The seasonal mean rainfall over all-India is about 7 mm/day (e.g., Krishnamurthy and Shukla, 2000; Kothawale and Rajeevan, 2017). However, it does not rain continuously and is marked with variations within the season on different timescales including synoptic (5–7 days period) and intra-seasonal (10–90 day period)

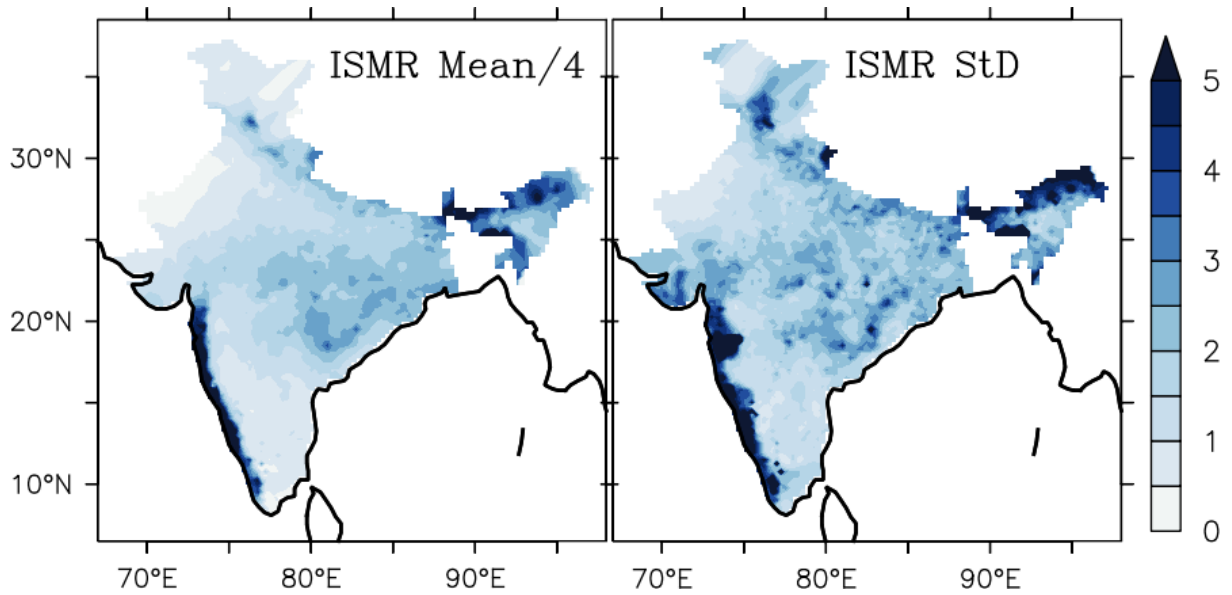


Figure 1.5: The mean (left) and standard deviation (right) of JJAS mean monsoon rainfall over India using the high resolution ($0.25^\circ \times 0.25^\circ$) gridded rainfall provided by the India Meteorological Department (IMD; Pai et al., 2014) over the period 1979–2013. The mean is scaled by 4 to have a common scale. Units mm/day.

timescales (e.g., Goswami and Xavier, 2005). Synoptic scale disturbances or Low Pressure Systems (LPS) occurring during monsoon contribute to about 50% of the rainfall over the monsoon trough region (Krishnamurthy and Ajayamohan, 2010; Praveen et al., 2015). An LPS is called a low, depression, or cyclone depending on its cyclonic wind speeds. For example, an LPS with associated cyclonic wind speeds between 17–33 knot (1 knot is 8.52 km per hour) and two closed isobars with an interval of 2 hPa on the synoptic weather charts, is called a depression (India Meteorological Department’s Terminology and Glossary available at <http://imd.gov.in/section/nhac/termglossary.pdf>). Most LPS during monsoon form over the northern Bay of Bengal where the SST is warm enough to support convection, although some monsoon depressions can form in the eastern Arabian sea and in the monsoon trough region over land. The LPS forming in the Bay of Bengal generally move north-west along the monsoon trough axis and last for 3–6 days (e.g., Krishnamurthy and Ajayamohan, 2010; Hunt et al., 2016). In general, these systems do not grow to become a tropical cyclone (wind speeds greater than 33 knot) during the summer monsoon due to strong vertical wind shear, among others. As mentioned earlier, apart from the synoptic scales, the rainfall varies on intraseasonal timescales as well. It is associated with prolonged relatively wet or dry conditions called ‘active’ or ‘break’ spells lasting for 2–3 weeks (e.g., Rajeevan et al., 2010). The Intra-seasonal Oscillations (ISO) of rainfall have two particularly important periodicities,

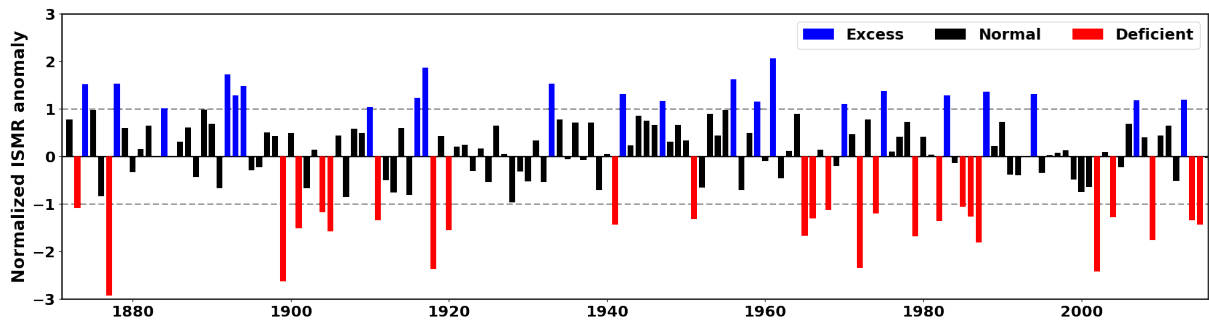


Figure 1.6: The interannual variations of JJAS rainfall over India during 1871–2016, using the All India Rainfall time series obtained from www.tropmet.res.in. The time series is normalized by its own standard deviation.

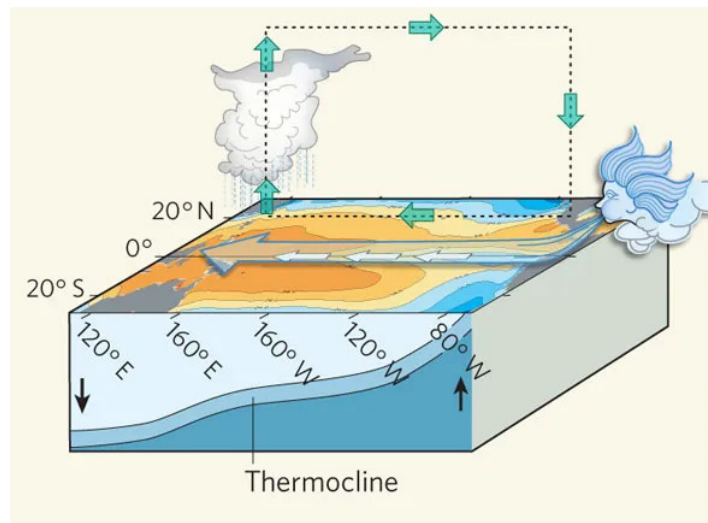
viz., 10–20 days and 30–60 days. While the 10–20 day ISO is a westward propagating mode, the 30–60 day ISO is a northward propagating mode. The spatial scale of 30–60 day ISO is larger than that of 10–20 day ISO and dominates the intraseasonal variability of the monsoon (Goswami and Xavier, 2005).

In the above, we have briefly discussed the variations of Indian summer monsoon rainfall within the season but it varies on longer timescales as well (e.g., Parthasarathy and Moolley, 1978; Parthasarathy et al., 1994; Webster et al., 1998; Krishnamurthy and Shukla, 2000; Goswami and Chakravorty, 2017; Gadgil, 2018), with the interannual variability being a dominant component of the monsoon variability. The spatial map of standard deviation of JJAS rainfall over India is shown in Fig. 1.5. Interestingly, the regions of high mean rainfall are also the regions of high interannual variability. The standard deviation of year-to-year variations of the seasonal mean rainfall averaged over India is only 10% of the mean, which is not large (seasonal mean rainfall 852.3 mm and standard deviation 84.3 mm; Parthasarathy et al., 1994; Kothawale and Rajeevan, 2017). However, such small changes in the seasonal mean rainfall can cause ‘droughts’ and ‘floods’ over India (Fig. 1.6). Hence, it is important to understand the interannual variability of ISM rainfall which is what we will focus on, in this thesis.

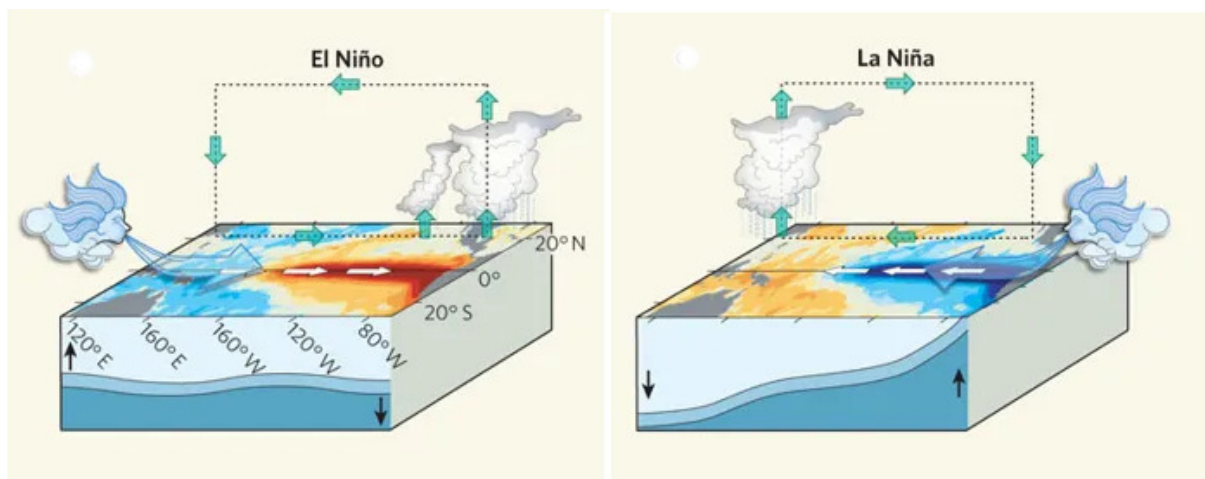
1.2 El Niño-Southern Oscillation, Indian Ocean Dipole and their influence on ISM

The interannual variability of Indian Summer Monsoon Rainfall (ISM_R) is governed by both internal dynamics and external factors (e.g., Webster et al., 1998). Although there are several external factors that influence the ISM_R, we concentrate here on the modes of climate variability operating in the tropical oceans. Particularly, the El Niño-Southern Oscillation (e.g., Sikka, 1980; Keshavamurty, 1982; Mooley and Parthasarathy, 1984; Webster et al., 1998) and Indian Ocean Dipole (e.g., Behera et al., 1999; Saji et al., 1999; Ashok et al., 2001; Slingo and Annamalai, 2000; Ashok et al., 2004b; Ashok and Saji, 2007) are the two dominant coupled ocean-atmosphere phenomena housed in the tropical oceans that are known to influence the ISM_R. Before discussing their relation with the ISM_R, we describe these modes briefly in the following.

The El Niño-Southern Oscillation (ENSO) is a quasi-periodic natural coupled ocean-atmosphere phenomenon involving variations in ocean surface and sub-surface temperatures, thermocline, and corresponding changes in the atmosphere in the tropical Pacific (e.g., Rasmusson and Carpenter, 1982; Neelin et al., 1998; Wang and Picaut, 2004). While an El Niño (or a La Niña) is the oceanic component, the Southern Oscillation (Walker and Bliss, 1932) is the atmospheric component of the same phenomenon and thus the name El Niño-Southern Oscillation (Bjerknes, 1969). The normal conditions in the tropical Pacific are: the trade winds from either hemisphere converge in the vicinity of the equator and blow from east to west (Fig. 1.7a). They accompany a shallow thermocline, cool SST and high sea level pressure in the eastern equatorial Pacific, and a deep thermocline, warm SST and low sea level pressure in the western equatorial Pacific (Philander, 1989; Kump et al., 2004). The gradient between the permanent warm surface waters in the western equatorial Pacific and cold surface waters in the eastern equatorial Pacific drives and sustains the surface easterlies. The upper branch of these surface easterlies is formed by an ascent over the western equatorial Pacific where there is a permanent warm pool and descent over the eastern equatorial Pacific completing a circulation loop known as the Walker circulation. The persistent easterlies drive a westward flowing ocean current which piles up warm waters in the western equatorial Pacific, resulting in a deep thermocline in the west and a shallow thermocline in the east. The atmospheric and oceanic circulation



(a) Normal conditions



(b) Anomalous conditions (El Niño and La Niña)

Figure 1.7: A schematic diagram depicting a) the normal conditions and b) anomalous conditions in the tropical Pacific. This image is obtained from Ashok and Yamagata (2009) ©Springer Nature. Reproduced with permission.

described so far can be regarded as the norm, but there can be deviations from this norm in a given year (Fig. 1.7a). An intensified Walker circulation can cause the increased east-west SST gradient, enhanced convection over the western Pacific, shallower (deeper) thermocline in the eastern (western) equatorial Pacific which in turn results in the strengthened equatorial easterlies and vice versa. This positive feedback between the winds, SST, convection and thermocline depth is known as the Bjerknes feedback (Bjerknes, 1969) and is primarily responsible for the growth of an ENSO event. The Bjerknes feedback operates even if the Walker circulation anomalously weakens but it does so in an opposite direction. The two extreme anomalous conditions of ENSO are El Niño and La Niña. A La Niña is simply an enhancement of normal

conditions described above but an El Niño is a negative deviation from the normal conditions (Fig. 1.7b). An El Niño is associated with a warmer SST and deeper thermocline than normal in the eastern to central equatorial Pacific and anomalous cold SST in the western equatorial Pacific (Fig. 1.7b). These changes in ocean surface temperatures are accompanied by enhanced convection over eastern equatorial Pacific and suppressed precipitation over the western Pacific. While the Bjerknes feedback helps an ENSO event grow, theories such as Delayed Oscillator (Suarez and Schopf, 1988), Recharge-Discharge Oscillator (Jin, 1997a,c), the Western Pacific Oscillator (Weisberg and Wang, 1997; Wang et al., 1999) and the Advective-Reflective Oscillator (Picaut et al., 1997) explain how an ENSO event could be terminated but we will not discuss those details in this thesis. An ENSO event usually starts to develop in the early northern hemispheric summer, peaks in the boreal winter (December–February) and decays later. Often, these events can span a few years. A widely used index of ENSO is the Oceanic Niño Index (ONI) which is the average of SST anomalies over the region 5°S – 5°N and 170°W – 120°W . ENSO is an irregular low frequency oscillation with a periodicity of 3–7 years and it has a dominant interannual variability. In the recent past, an El Niño occurred in 2015–16 and a La Niña in 2011–12. Recently, a different type of El Niño, called the El Niño-Modoki, has been discovered. It has its characteristic warm SST anomalies concentrated in the equatorial central Pacific as opposed to the typical El Niño described above which has its warm SST anomalies concentrated in the eastern Pacific (Ashok et al., 2007). Further, the El Niño-Modoki has cool SST anomalies in the eastern and western equatorial Pacific. The ENSO, irrespective of its types, has far reaching implications for the global climate (e.g., Klein et al., 1999; Dai and Wigley, 2000; Chiodi and Harrison, 2015) although the teleconnections of these different types of El Niño are shown to be different (e.g., Ashok et al., 2007, 2009; Ashok and Yamagata, 2009; Jeong et al., 2012; Preethi et al., 2015; Marathe et al., 2015; Yeh et al., 2018). For the sake of simplicity, in this thesis, we will not discuss ENSO-Modoki and restrict ourselves only to the typical ENSO described above.

With a particular reference to the impact of ENSO on ISMR, whereas an El Niño tends to reduce the ISMR, a La Niña event is likely to enhance the same (e.g., Sikka, 1980; Keshavamurty, 1982; Soman and Slingo, 1997; Webster et al., 1998; Ashok et al., 2019), although the strength of this relation waxes and wanes (e.g., Rasmusson and Carpenter, 1982; Kumar et al., 1999, 2006). Note that although an ENSO event generally peaks during boreal winter, a developing ENSO event in the boreal summer can still influence the ISMR. During an El Niño,

the Walker circulation moves eastward and has its descending branch over maritime continent and equatorial western Pacific (e.g., Wang, 2002). This subsidence generates an atmospheric Rossby wave response to the northwest and southwest of the heat sink. The low level anticyclonic circulation over south Asia and east Asia opposes the mean monsoon southwesterlies in the Indian Ocean and reduces summer monsoon rainfall over India (Keshavamurty, 1982; Lau and Nath, 2003; Wang, 2006a). The accompanying anomalous low level convergence over the tropical Indian Ocean also contributes to low level divergence over the monsoon region via the adjustment of monsoon Hadley circulation (e.g., Ashok et al., 2004a). In addition, Goswami and Xavier (2005) suggest an upper atmospheric pathway for the ENSO to influence the Indian summer monsoon. Through the modulation of surface latent and radiative fluxes, and ocean currents, an El Niño causes weak warm SST anomalies in the Indian Ocean. These warm SST anomalies become more pronounced with the peaking of El Niño in the following boreal winter and, when the El Niño is strong enough, they survive into the boreal spring and early summer of the next year. Through the air-sea coupled feedbacks in the Indian Ocean, the stronger monsoonal southwesterlies blow toward these warm SST sites and result in an enhanced precipitation over India. Thus, while a developing El Niño in boreal summer tends to reduce ISM rainfall, it can enhance the ISMR in the following year (Wang, 2006a).

The Indian Ocean (IO), for a long time, was thought to be a passive ocean simply responding to ENSO described above and other modes of climate variability (e.g., Cadet, 1985; Alexander et al., 2002; Lau and Nath, 2003). However, it has been shown recently that the Indian Ocean hosts its own mode of climate variability, called the Indian Ocean Dipole (IOD; e.g., Saji et al., 1999; Behera et al., 1999; Webster et al., 1999; Murtugudde et al., 2000; Ashok et al., 2001; Slingo and Annamalai, 2000). Strong positive IOD events such as in 1961, 1963, 1994, 1997, (and the recent positive IOD in 2019) are shown to influence the ISMR (e.g., Ashok et al., 2001, 2004a). The IOD is a coupled-ocean atmosphere phenomenon operating in the tropical Indian Ocean strongly phase locked to the seasonal cycle (e.g., Saji and Yamagata, 2003; Ashok et al., 2003; Yamagata et al., 2003; Vinayachandran et al., 2009). An IOD event usually starts to develop in boreal summer and peaks during September–October and decays thereafter. During September–October, the mean state of the Indian Ocean is that the southeasterly trade winds are constrained mostly to the south of equator from the eastern to central equatorial Indian Ocean but they cross the equator in the western IO. The westerlies are present in the central to eastern IO between the equator up to the southern tip of India. A positive IOD is characterized

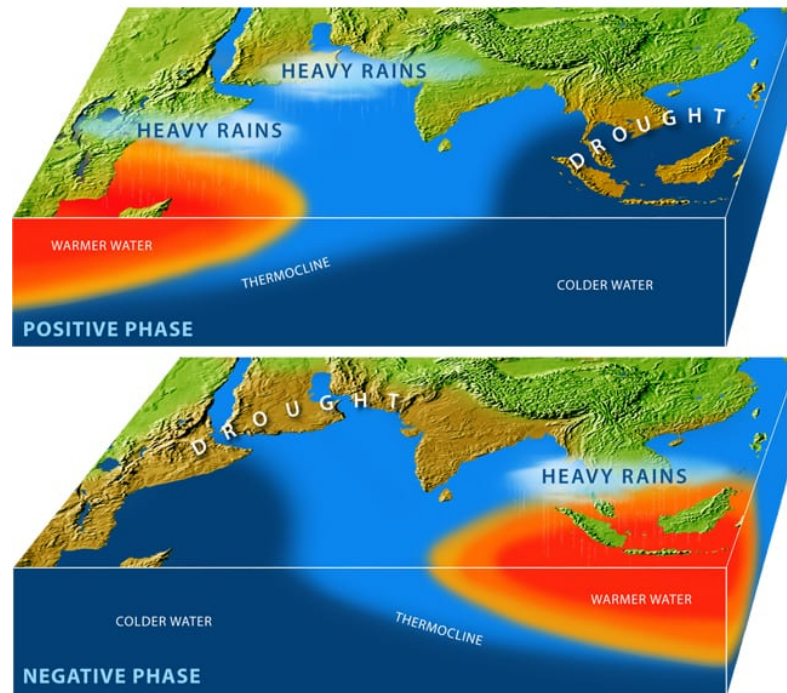


Figure 1.8: A schematic showing the positive (upper panel) and negative (lower panel) phases of the Indian Ocean Dipole. Source: Woods Hole Oceanography Institute (<https://www.whoi.edu>)

by anomalously cool SST, shallow thermocline, and suppressed convection in the southeastern equatorial IO off the western coast of Sumatra (Fig. 1.8). Further, it is associated with anomalously warm SST, deep thermocline and enhanced convection in the western equatorial IO. A negative IOD event is an intensification of the climatological conditions and has the anomalies opposite to that of a positive IOD. The recent notable positive (negative) IOD events are 2012, 2015 and 2019 (2010, 2014 and 2016; <http://www.bom.gov.au/climate/iod/>). Although, the IOD can be generated by processes inherent to the Indian Ocean, it can sometimes be triggered by an ENSO event, among others (e.g., Iizuka et al., 2000; Murtugudde et al., 2000; Annamalai et al., 2002, 2003; Gualdi et al., 2003). Normally, a positive (negative) IOD event co-occurs with an El Niño (a La Niña). For instance, during boreal winter of 1997–98, a strong positive IOD was accompanied by a strong El Niño event.

The strong IOD events impact ISMR by modulating the monsoon meridional and zonal circulation (e.g., Behera et al., 1999; Ashok et al., 2001; RAO et al., 2004). A strong positive (negative) IOD induces an upper level convergence (divergence) over the southeastern equatorial Indian Ocean and an upper level divergence (convergence) over the Bay of Bengal strengthening (weakening) the monsoon trough and leads to enhanced (reduced) rainfall over

India (Fig. 1.8). The western pole of the IOD is also suggested to impact the northwestern regions of monsoon trough (Ashok et al., 2004a). As already mentioned, many a time, a positive (negative) IOD co-occurs with an El Niño (a La Niña) and when it does, the strong IOD can counter the effect of ENSO on ISMR (e.g., Ashok et al., 2001, 2004b). As discussed earlier, an El Niño induces subsidence over the Bay of Bengal region and tends to reduce the rainfall over India. However, when it co-occurs with a strong positive IOD event, the subsidence induced by an El Niño over the Bay of Bengal is weakened by the lower level convergence caused by the positive IOD through the modulation of the monsoon Hadley circulation. For instance, the ISMR in the year 1997 was near normal despite a strong El Niño due to the counteracting effect of a strong positive IOD event in the same year (Ashok et al., 2001). The Equatorial Indian Ocean Oscillation (EQUINOO), the atmospheric component of the IOD, seems to have a stronger correlation with the ISMR (Gadgil et al., 2003, 2007) but we will not discuss those details here.

1.3 The Atlantic Zonal Mode and its relation to the ISM

As may be noted, ENSO and IOD are two phenomena operating in the tropical Pacific and Indian oceans, respectively. It is interesting to inquire if there is a similar mode of climate variability in the other and only remaining tropical ocean, i.e., the tropical Atlantic. If there is, does it have any influence on the ISMR? A similar mode indeed exists in the tropical Atlantic and it is called the Atlantic Zonal Mode (AZM), details of which are discussed shortly after. While much can be found about the influence of ENSO and IOD on the ISM in the literature as discussed above, the studies on the relation between the AZM and the ISM are recent and relatively less in number (Kucharski et al., 2008, 2009; Wang et al., 2009; Barimalala et al., 2012, 2013a; Yadav, 2017; Lübbecke et al., 2018). This motivated us to investigate the relation between the AZM and ISM in more detail in this thesis.

Before describing the AZM, it is worthwhile to look at the geography and climatology of the tropical Atlantic where the AZM occurs. The tropical Atlantic is the smallest of the three tropical ocean basins in size, with a horizontal extent of around 65° longitude at the equator. It is surrounded by the continents of Africa to the east and South America to the west, and is open in the north-south direction at an angle due to the geometry of the continents (Fig. 1.9). Its small

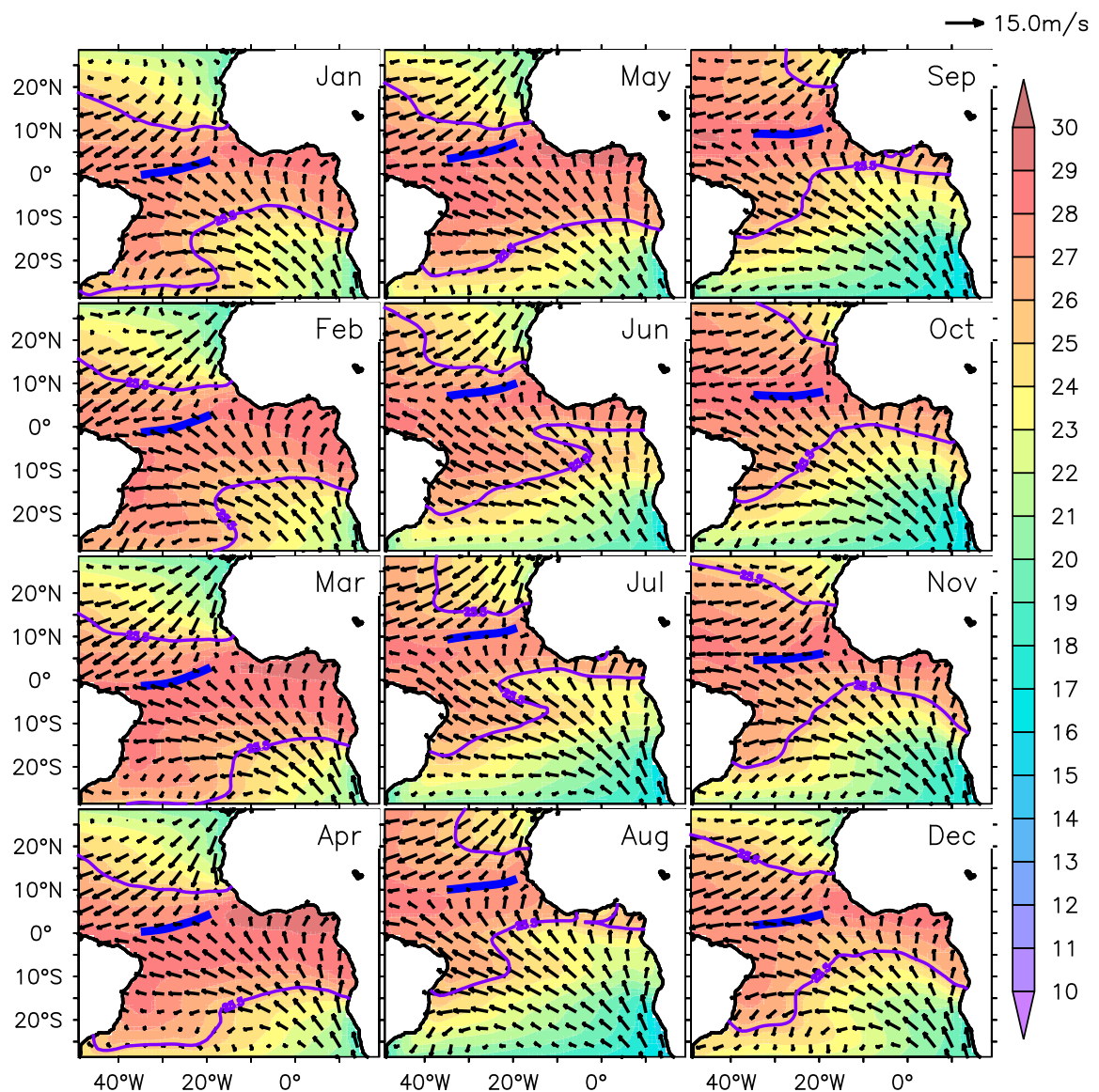


Figure 1.9: The monthly evolution of climatological SST ($^{\circ}\text{C}$) based on HadISST (Rayner et al., 2003) and surface winds (m/s) from ERA-Interim Reanalysis (Dee et al., 2011), in the tropical Atlantic. A contour of 25.5°C is shown to demonstrate the development of seasonal cold tongue. The position of oceanic ITCZ is marked in thick blue (See Chapter 5 for the details of how the position of ITCZ is identified).

basin size and the proximity of land makes the role of continents important in determining the climatology of this ocean (e.g., Xie and Carton, 2004). The variability of SST in the tropical Atlantic is dominated by the seasonal cycle (e.g., Ding et al., 2010). The band of high SST exceeding 27°C moves from slightly south of equator in boreal winter to over the equator in spring and reaches its northern most extent in summer (Fig. 1.9). Tightly coupled with the band of high SSTs, the ITCZ where the trade winds from either hemisphere meet, follows the

high SST band with a lag of one month owing to the large heat capacity of ocean (e.g., Xie and Carton, 2004). The trades are weak over the equator in boreal spring and as the ITCZ moves north in the summer, the southeasterlies intensify over and south of equator, causing strong upwelling along the African coast resulting in a shallow thermocline in the east and deep thermocline in the west. This upwelling cools the SST and a distinct SST cold tongue develops in the east slightly south of equator in the boreal summer (Fig. 1.9). The eastern equatorial Atlantic thermocline is the shallowest in boreal summer allowing for the strongest surface-subsurface coupling compared to other seasons (e.g., Keenlyside and Latif, 2007).

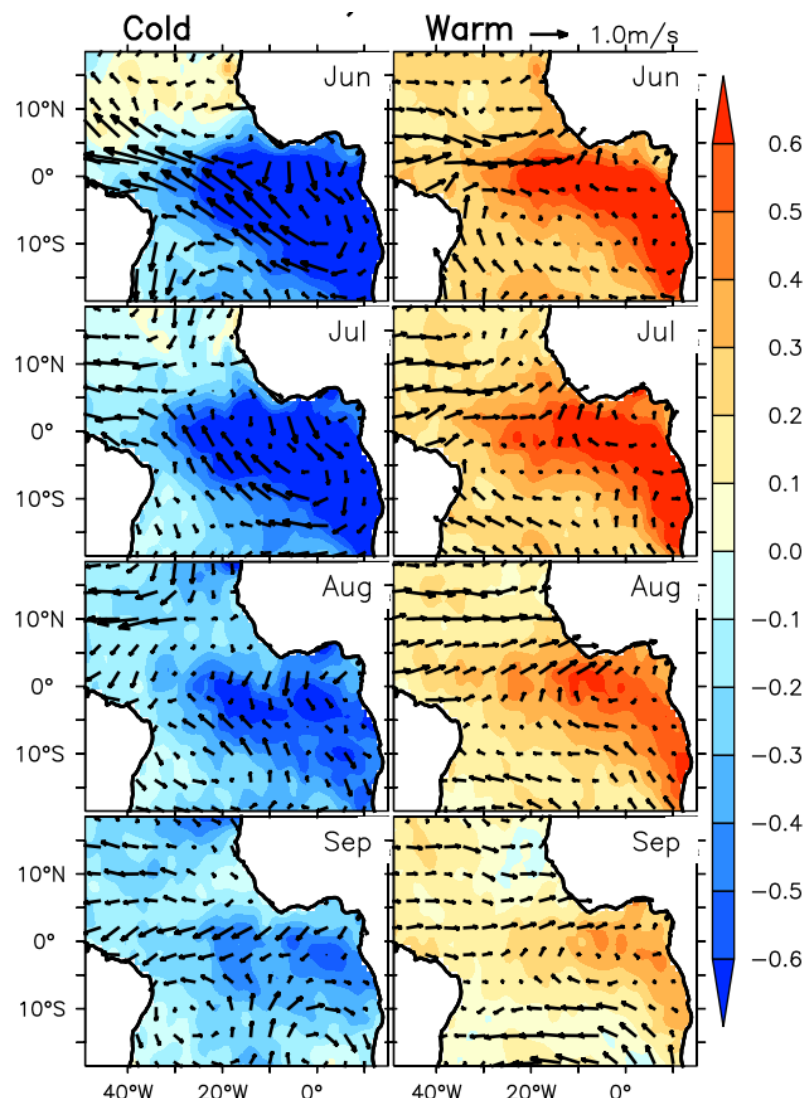


Figure 1.10: Monthly evolution of anomalies of SST and low level winds at 850 hPa associated with the cold (left) and warm (right) phases of AZM. The SST and winds are taken from HadISST (Rayner et al., 2003) and ERA-Interim Reanalysis (Dee et al., 2011), respectively. The period of analysis is 1979–2013.

Significant departures from the seasonal cycle of tropical Atlantic described above can

be found in a given year and the interannual variability of SST in the equatorial Atlantic is dominated by the AZM (e.g., Zebiak, 1993; Servain et al., 2000). The AZM, variously called as Atlantic Niño (e.g., Ruiz-Barradas et al., 2000; Polo et al., 2015a), Atlantic Equatorial Mode (e.g., Servain et al., 2000; Mohino and Losada, 2015) and Atlantic Equatorial Cold Tongue Mode (e.g., Haarsma and Hazeleger, 2007; De Almeida and Nobre, 2012), is a coupled ocean-atmosphere phenomenon housed in the tropical Atlantic (e.g., Zebiak, 1993; Lübbecke et al., 2018). As mentioned already, it is similar to ENSO but weaker and more heavily damped (Philander, 1986; Zebiak, 1993; Xie and Carton, 2004; Lübbecke et al., 2010; Burls et al., 2012; Lübbecke and McPhaden, 2013; Lübbecke et al., 2018). The relative heavy damping of the AZM compared to ENSO is attributed to the weaker thermocline feedback in the tropical Atlantic (Lübbecke and McPhaden, 2013). The AZM can be most readily identified by its signatures in the SST. It is associated with an anomalous cooling (warming) in the southeastern tropical Atlantic and is called a cold (warm) AZM event (Fig. 1.10). Earlier studies defined different indices to identify AZM events based on various analyses of Empirical Orthogonal Function (e.g., Servain et al., 2000; Ruiz-Barradas et al., 2000; Murtugudde et al., 2001; Huang et al., 2004; Haarsma and Hazeleger, 2007) and averages of SST anomalies over different regions (Zebiak, 1993; Kucharski et al., 2007; Ding et al., 2010; Barimalala et al., 2012; Caniaux et al., 2011; Lutz et al., 2013). However, in this thesis, we will use the Atlantic 3 index (average of SST anomalies over 3°S-2°N and 20°W-0°E) first introduced by Zebiak (1993), as it is the most widely used (e.g., Latif and Grötzner, 2000; Illig et al., 2006; Keenlyside and Latif, 2007; Rodríguez-Fonseca et al., 2009; Foltz and McPhaden, 2010; Burls et al., 2012; Lübbecke and McPhaden, 2013; Pottapinjara et al., 2014; Martín-Rey et al., 2019). The AZM is strongly phase locked to the seasonal cycle (e.g., Keenlyside and Latif, 2007; Lübbecke et al., 2010; Richter et al., 2017). The AZM starts to develop in boreal spring, peaks in the late spring to early summer and decays thereafter (Fig. 1.10). Further, the interannual standard deviation of June–August Atlantic 3 index is 0.48°C. Apparently, the signals associated with the AZM are short lived, lasting only for 3–4 months and are weak compared to that of ENSO. However, analogous to ENSO, the Bjerknes feedback mechanism which involves a positive feedback between anomalies of SST, equatorial zonal winds and thermocline depth, explains a significant part of variability of the AZM (e.g., Zebiak, 1993; Carton and Huang, 1994; Keenlyside and Latif, 2007; Lübbecke et al., 2010; Lübbecke and McPhaden, 2013). Further, the equatorial wave dynamics play a critical role in the life cycle of the AZM (e.g., Illig et al., 2006; Ding

et al., 2010; Foltz and McPhaden, 2010). These earlier studies have shown that an anomalous weakening (strengthening) of equatorial easterly trade winds in the western equatorial Atlantic triggers an eastward moving downwelling (upwelling) Kelvin wave which deepens (shallows) the thermocline and ultimately results in a warm (cold) SST anomaly in the eastern equatorial Atlantic (Fig. 1.10). The SST anomalies of the AZM are confined mostly to the south of equator in a southeastward direction and extend up to the African coast. Note that these SST anomalies are collocated with the seasonal cold tongue in the tropical Atlantic (compare Fig. 1.9 and Fig. 1.10). The eastern equatorial Atlantic SST anomalies are often preceded by the SST anomalies off the coast of Angola (Florenchie et al., 2003, 2004). Previous studies treated these SST anomalies off Angola as a separate phenomenon called the Benguela Niño (e.g., Shannon et al., 1986; Gammelsrød et al., 1998; Rouault et al., 2003; Florenchie et al., 2003, 2004). Although some Benguela events can be generated by local processes, most of the Benguela Niño events coincide with the eastern equatorial Atlantic events and the two are shown to be related via different pathways such as the propagation of equatorial and coastal Kelvin waves, off equatorial Rossby waves, and meridional along shore winds off the coast of Africa (Florenchie et al., 2003; Huang et al., 2004; Reason et al., 2006; Rouault et al., 2007; Polo et al., 2008; Lübbecke et al., 2010; Richter et al., 2010; Lutz et al., 2013). Hence, the Benguela Niño is treated as part of the AZM in this thesis.

The AZM has been shown to be interacting with different modes of variability both local and remote to the Atlantic such as the Atlantic Meridional Mode, the atmospheric/oceanic conditions in the south Atlantic (South Atlantic Anticyclone/South Atlantic Subtropical Dipole/South Atlantic Ocean Dipole) and ENSO (Lübbecke et al., 2018, and references therein). The Atlantic Meridional Mode (AMM) or the Inter-hemispheric Mode is characterized by SST anomalies of opposite sign on either side of the equator and is the second dominant mode of interannual variability in the tropical Atlantic (e.g., Nobre and Shukla, 1996; Carton et al., 1996; Chang et al., 1997; Chiang and Vimont, 2004; Xie and Carton, 2004). It is active during boreal spring, and varies on interannual and decadal timescales. The AMM drives cross-equatorial low level wind anomalies flowing from the cooler hemisphere to the warmer hemisphere. The spring Atlantic ITCZ is sensitive to the SST gradient of the AMM and moves towards the warmer hemisphere. The AMM has been shown to be related to the AZM via the meridional displacement of the spring ITCZ (Servain et al., 1999; Murtugudde et al., 2001). Anomalous migrations of the spring Atlantic ITCZ influences the concurrent equatorial zonal winds and thereby induce

the development of the AZM in the following summer (see Chapter 4 for more details on this relationship).

The variations in the strength of the South Atlantic Anticyclone (comprising midlatitude westerlies, southeast trades and equatorward winds along the coast of Africa) during boreal spring can precondition the development of an AZM event via the anomalous weakening or strengthening of the southeast trade winds and the cold tongue (Lübbecke et al., 2010; Richter et al., 2010; Hu et al., 2013; Lübbecke et al., 2014). The AZM, which is predominantly a southeastern tropical Atlantic phenomenon, is shown to be oppositely related to the concurrent SST anomalies in the southwestern subtropical Atlantic (Nnamchi et al., 2011, 2016). Further, these studies propose that the AZM should be viewed as an equatorial arm of their unified South Atlantic Ocean Dipole but obviously more research is required before this view can be accepted. This dipole is closely related to the South Atlantic Subtropical Dipole (a similar SST structure modulated by the strength and position of south Atlantic subtropical High) which also is shown to be similarly related to the AZM (e.g., Venegas et al., 1996, 1997; Haarsma et al., 2005; Colberg and Reason, 2007; Trzaska et al., 2007; Morioka et al., 2011; Nnamchi et al., 2017)

Earlier studies reported an opposite relationship between ENSO and AZM: an El Niño (La Niña) peaking in boreal winter can lead to a cold (warm) AZM event in the following boreal summer (Latif and Barnett, 1995; Latif and Grötzner, 2000; Ruiz-Barradas et al., 2003; Münnich and Neelin, 2005; Handoh et al., 2006; Tokinaga et al., 2019). These studies proposed different pathways by which ENSO influences the AZM. The heating associated with an El Niño can induce changes in the Walker circulation and lead to low level easterlies in the western equatorial Atlantic during boreal spring which result in the cooler SST anomalies in the eastern equatorial Atlantic in the following boreal summer via the equatorial dynamics and the Bjerknes feedback mechanism (Latif and Barnett, 1995; Ruiz-Barradas et al., 2003; Münnich and Neelin, 2005). This delayed response in the tropical Atlantic can be explained by the dynamical adjustment of the equatorial Atlantic to the slowly varying wind anomalies and seasonally changing background state in the tropical Atlantic (Latif and Grötzner, 2000). In addition, an El Niño in the preceding winter can affect the AZM via the north tropical Atlantic pathway by inducing warming in the north tropical Atlantic in the following boreal spring (Enfield and Mayer, 1997; Huang et al., 2002) which sets up an inter-hemispheric SST gradient. This gradient in turn leads to concurrent cross-equatorial low level winds towards the north tropical Atlantic

which can cause a cold AZM event in the following summer through the Bjerknes feedback mechanism (Chang et al., 2006). Further, an El Niño can lead to a cold AZM via the south tropical Atlantic pathway by a wavetrain emanating from the central equatorial Pacific which travels via south America to reach the tropical South Atlantic after about a season to influence the low level winds there and consequently the SST anomalies (Handoh et al., 2006). All these studies showed the existence of a relationship between ENSO and AZM but this relationship is inconsistent. For instance, an El Niño is sometimes followed by a warm AZM event contrary to what the above studies showed. Several studies discuss the causes for this fragile relationship between ENSO and AZM (Chang et al., 2006; Lübbecke and McPhaden, 2012; Tokinaga et al., 2019). Based on the analyses of response in the tropical Atlantic to an El Niño in various model experiments and observational data sets, these studies attribute the fragility of the relationship to i) the competing effects of warming induced by the tropospheric temperature response in the Atlantic, and cooling produced by the surface easterlies and subsequent Bjerknes feedback (Chang et al., 2006) ii) generation of downwelling Rossby wave to the north of equator in the tropical Atlantic during boreal spring, which upon reflection at the western boundary, tends to kill the AZM cold event which resulted from the direct response in the surface easterlies (Lübbecke and McPhaden, 2012), and iii) differential impacts of El Niño events lasting over single versus multiple years (Tokinaga et al., 2019). Thus far, we have discussed the influence of ENSO on the AZM with a delay of about six months but even a developing ENSO event active in boreal summer has a similar opposite relationship with the contemporaneous AZM during the satellite period (e.g., Kucharski et al., 2009; Wang et al., 2009; Pottapinjara et al., 2014). Normally, the opposite phases of ENSO and AZM co-occur, i.e., an El Niño (La Niña) event accompanies a cold (warm) AZM event. However, the relationship between ENSO and AZM, either contemporaneous or with a delay, depends on the period of analysis and is not stationary (Chiang et al., 2000; Wang, 2006b; Kucharski et al., 2009; Martín-Rey et al., 2018). From the analysis of observational and reanalysis data sets, Chiang et al. (2000) argue that the relationship between ENSO and its induced surface winds in the western equatorial Atlantic in boreal spring has an interdecadal variability which is controlled by the spring maximum of the ENSO SST anomaly. Further, Martín-Rey et al. (2018) show that the relationship between ENSO and the tropical Atlantic can be modulated by the Atlantic Multidecadal Oscillation. From the above discussion, it is clear that different factors, both local and remote to the Atlantic, control the generation of AZM events. The causative mechanisms of the AZM will be discussed in detail in Chapter 4.

Earlier studies showed that the AZM can affect the weather patterns of the regions adjoining the tropical Atlantic such as South America (e.g., Nobre and Shukla, 1996; Lübbecke et al., 2018) and West Africa (e.g., Rodríguez-Fonseca et al., 2015), and the remotely located regions like Europe (e.g., García-Serrano et al., 2011), Mediterranean (e.g., Losada et al., 2012), equatorial Pacific (e.g., Keenlyside et al., 2013; Polo et al., 2015b) and Indian Ocean (e.g., Wang et al., 2009).

The effect of AZM on the ISM is of particular interest to us. This effect reported in various previous studies till date is summarized in the following. The warm (cold) SST anomalies associated with the AZM are shown to induce anomalous subsidence (rising motion) over India reducing (enhancing) the ISMR (Kucharski et al., 2007, 2008). Given that the SST anomalies associated with ENSO and AZM are anti-correlated, Kucharski et al. (2007) suggest that the weakening of the ENSO-ISM relation in the recent decades could be due to the strengthening of the AZM SSTs which tend to negate the effect of ENSO on ISM. Sabeerali et al. (2019a) also show that the inverse relation between the AZM and ISM is strengthening in the recent decades. Kucharski et al. (2008) and Wang et al. (2009) highlight the importance of the AZM in impacting the ISM by showing that when the effect of summer time ENSO SST anomalies on the ISMR is linearly regressed out, the resulting ISMR correlates the strongest with the SST anomalies associated with the AZM. On a similar note, from the analysis of an ensemble of Atmospheric General Circulation Model (AGCM) experiments and considering only the contribution of summer time SST anomalies in the tropical oceans, Cherchi et al. (2018) argue that the strongest factor next to ENSO in influencing the monsoon extremes is the AZM. Using an AGCM, Kucharski et al. (2009) propose a physical mechanism wherein the response to the heating associated with a warm AZM is a quadrupole in the upper level stream function. The northeastern arm of the quadrupole is situated over India with an upper level convergence and lower level divergence leading to a reduction in precipitation over India. The heating in the tropical Atlantic also weakens the low level monsoon flow in the Arabian Sea and causes an increase in the SST in the Arabian Sea due to reduced upwelling and evaporation (Wang et al., 2009). Further, using a regional ocean model coupled with an ecosystem model, Barimalala et al. (2013a) demonstrate that a cold (warm) AZM strengthens (weakens) the Somali Jet, favors more (less) upwelling and results in more (less) phytoplankton concentrations in the Arabian Sea. In addition, Barimalala et al. (2012) examine the simulation of relation between the AZM and ISM in some state-of-the-art Coupled Model Intercomparison (CMIP) 3 models,

with an emphasis on the physical mechanism proposed by Kucharski et al. (2009). They find that a majority of the coupled models examined, display the teleconnection but with a weaker intensity which they attribute to the warm SST bias in the tropical Atlantic. While the physical mechanism proposed by Kucharski et al. (2009) is constrained to the tropics, Yadav (2017) argues that the AZM can affect the ISM also via an extratropical pathway by inducing alternate highs and lows in the geopotential. In this mechanism, a warm (cold) AZM induces an upper level low (high) to the northwest of India which weakens (reinforces) the monsoon especially over the northwest India (Yadav, 2017; Yadav et al., 2018). Analyzing the hindcast simulations initialized in two different months in a coupled general circulation model, Sabeerali et al. (2019b) show that the hindcast which simulates the AZM and its teleconnection to the ISM has higher prediction skill for the ISMR.

1.4 Modulation of the frequency of monsoon depressions in the Bay of Bengal by the AZM

As can be seen from the above, while several studies focused on the impact of AZM on ISM on interannual timescales, none examined if the AZM can also affect the monsoon transients, for example, the monsoon depressions. As mentioned already in Section 1.1, the monsoon depressions forming during boreal summer in the Bay of Bengal (BoB) can account for about 50% of the monsoon rainfall over the core monsoon region and eventually contribute to seasonal total monsoon rainfall (e.g., Krishnamurti, 1979; Goswami et al., 2003; Yoon and Chen, 2005; Krishnamurthy and Ajayamohan, 2010; Krishnan et al., 2011; Praveen et al., 2015). Hence, any change in the frequency of monsoon depressions can be expected to cause a change in the total monsoon rainfall. In our recent related study Pottapinjara et al. (2014), we have investigated the influence of the AZM on the characteristics of monsoon depressions in the Bay of Bengal. Further, we have also suggested a plausible physical mechanism which links the tropical Atlantic and the ISM. This study, conducted before the formal beginning of the thesis, led to and forms the basis of body of work documented in this thesis. Therefore, the key results of our study Pottapinjara et al. (2014) are discussed in some detail in the below.

Segregating the monsoon (June-July-August) depressions into those that occurred dur-

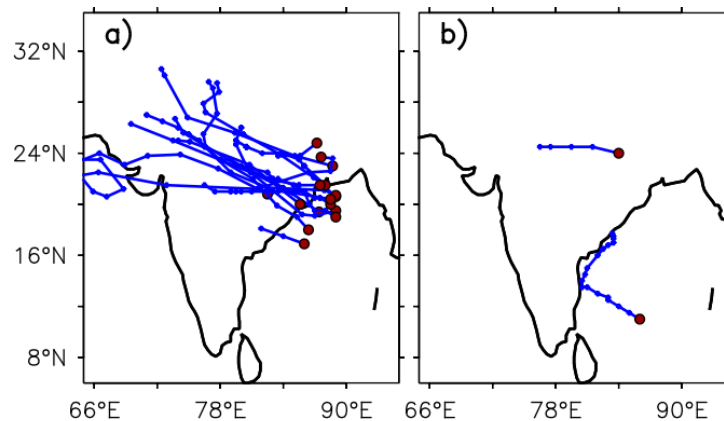


Figure 1.11: The locations of genesis (brown circles), and tracks (blue lines) of monsoon (June-July-August) depressions in the BoB that occurred during a) cold and b) warm phases of AZM. The AZM events that co-occur with ENSO events are omitted in the analysis to highlight the intrinsic influence of AZM on the depressions. The period of analysis is 1975–2012. The depressions data provided by the IMD is available at http://www.imdchennai.gov.in/cyclone_eatlas.htm. The AZM and ENSO events are identified using the June-July-August Atlantic 3 and ONI indices, respectively. The indices are prepared from the HadISST (Rayner et al., 2003). The identification of AZM and ENSO events, and their respective lists are the same as in Chapter 3.

ing cold, warm and neutral phases of AZM, we have found that the tendency of formation of monsoon depressions in the BoB is significantly more during the cold AZM compared to that of the warm AZM (Pottapinjara et al., 2014). Further, the difference between the average number of depressions in the season between the cold and warm AZM remains statistically significant even after accounting for the co-occurrence of AZM warm (cold) with the La Niña (El Niño) (see Chapter 3 for details of AZM and ENSO events; Pottapinjara et al., 2014). It indicates that this difference in the frequency of monsoon depressions in the BoB is an intrinsic response of the AZM. Further, a majority of depressions during cold AZM are found to form in the northeastern part of BoB, and their tracks are found to be long and clustered along the monsoon trough axis. However, during the warm AZM, the genesis of depressions occurs over a broader region in the BoB, and the tracks are short and more divergent. This observation also holds even when the AZM events co-occurring with ENSO events are omitted from the analysis (Fig. 1.11). Interestingly, we could not find any significant difference either in the frequency, or in the organization of tracks of monsoon depressions in the BoB between El Niño and La Niña.

In Pottapinjara et al. (2014), we have also suggested a plausible mechanism by which the AZM can influence the frequency of monsoon depressions in the BoB during June-July-August. The mechanism takes a tropical pathway to connect the AZM operating in the southeastern

equatorial Atlantic, and (rainfall over) India and (frequency of monsoon depressions in) the BoB located to the north of equator in the Indian Ocean. Previous studies showed that the formation of monsoon depressions in the BoB depends on large scale atmospheric conditions such as cyclonic vorticity at lower levels, vertical wind shear, and moisture transport into the BoB, among others (e.g., Goswami et al., 2003; Krishnan et al., 2011; Yanase et al., 2012). That is, the enhancement of low level cyclonic vorticity and moisture transport, and reduction of vertical wind shear in the BoB favor the formation of monsoon depressions in the BoB. During the cold (warm) AZM, the cross equatorial moisture transport into the BoB and cyclonic vorticity at lower levels (850 hPa) increase (decrease), and the vertical wind shear between lower (850 hPa) and upper (200 hPa) levels weakens (strengthens), creating more (less) favorable conditions for the formation of monsoon depressions in the BoB (Fig. 1.12). A teleconnection between the tropical Atlantic and the Indian Ocean is shown in Fig. 1.13. The diabatic heating associated with the convection anomalies of AZM can trigger a response in the tropospheric temperature (TT). The response has a Rossby wave-like structure in the tropical Atlantic with its two lobes on either side of the equator, and has a Kelvin wave-like structure which extends eastward and reaches the Indian Ocean. The positive correlations shown in Fig. 1.13 indicate that a warm (cold) AZM can increase (decrease) the mid-tropospheric temperature over the Indian Ocean in the equatorial belt. As discussed earlier in Section 1.1, the TT gradient between over the Indian subcontinent and the Indian Ocean (TT over land – TT over ocean) during summer drives the mean monsoon circulation (Webster et al., 1998; Wang, 2006a). The enhancement (reduction) of TT over the Indian Ocean induced by the warm (cold) AZM can weaken (enhance) the strength of TT gradient between the land and ocean, and lead to an anomalously weaker (stronger) than normal monsoon circulation which in turn decreases (increases) rainfall over India. It also decreases (increases) moisture transport into the BoB. As shown in Fig. 1.12, the warm (cold) AZM also induces a weakening (an enhancement) of low level cyclonic vorticity, and an increase (a decrease) in vertical wind shear in the BoB. In effect, the warm (cold) AZM creates less (more) favorable conditions for the formation of monsoon depressions in the BoB which in turn contribute to decreasing (increasing) rainfall over India. This teleconnection mechanism entails the thermodynamic manifestation of the influence of the AZM on ISM, and is consistent with the mechanism proposed by Kucharski et al. (2009).

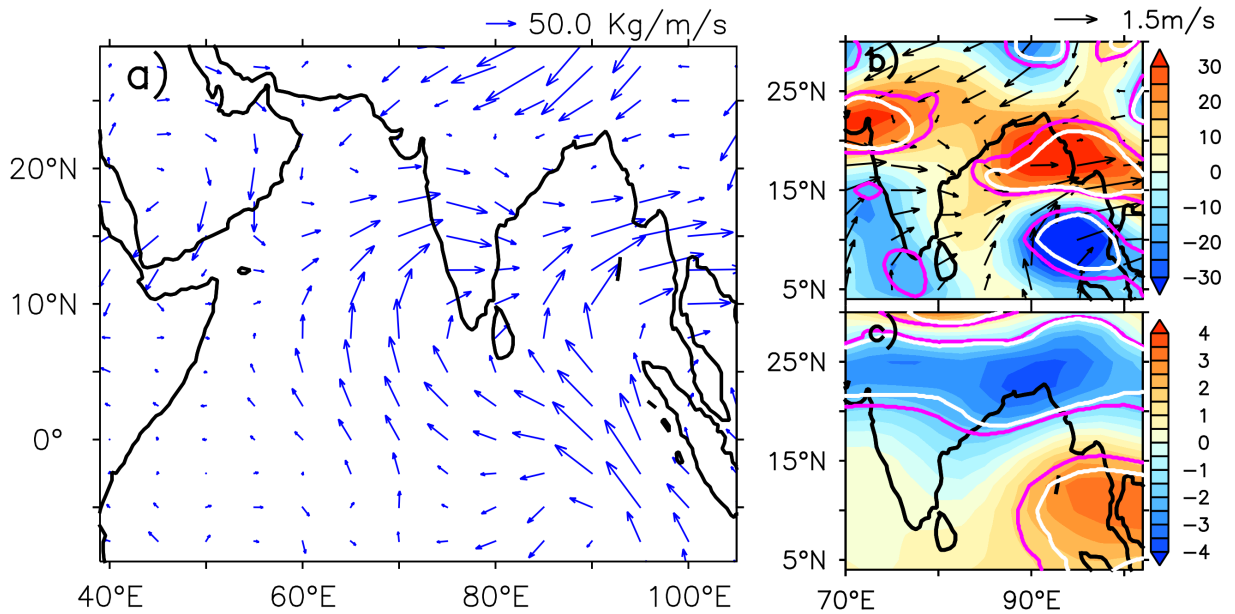


Figure 1.12: The differences of seasonal (June-July-August) composites of anomalies of a) vertically integrated moisture transport b) vorticity (10^{-7} s^{-1}) overlaid by winds at 850 hPa, and c) vertical wind shear (m s^{-1}) between levels 850 and 200 hPa. The composites of anomalies of each variable are first computed during the cold and warm phases of AZM separately, and the difference of cold and warm (cold–warm) composites, is presented here. The contours in pink and white (in b and c) indicate the significance levels of 20% and 10%, respectively as per Student's t -test. The variables are taken from NCEP's Reanalysis-2 (Kanamitsu et al., 2002). The period of analysis is 1979–2012. The list of AZM events used in this analysis is a subset of that in Chapter 3. See Chapter 2 for details on how to compute the composites and determine the level of statistical significance.

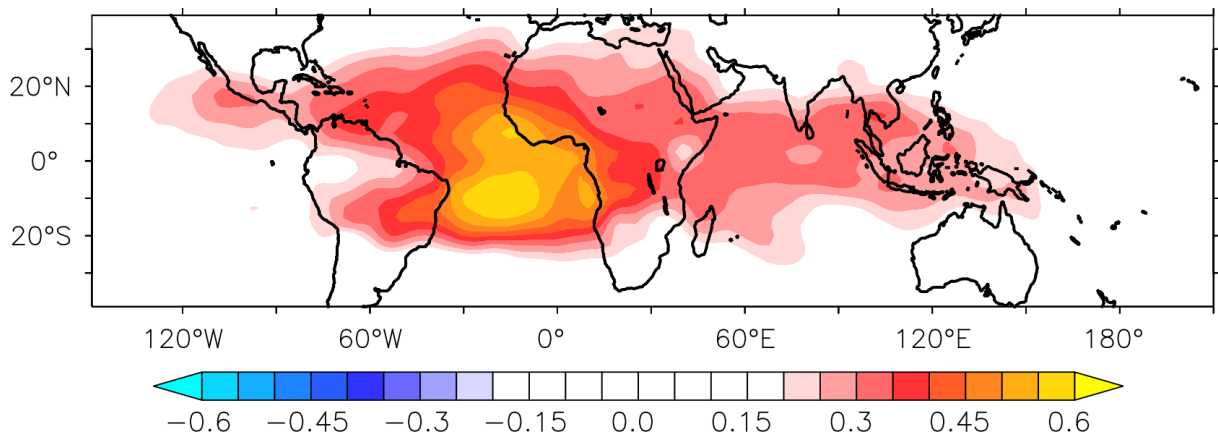


Figure 1.13: The simultaneous correlation between monthly time series of tropospheric temperature (TT) anomalies averaged over 1000 through 200 hPa, and the Atlantic 3 index. The influence of ENSO is regressed out from these variables before computing the correlation to highlight the impact of AZM on the TT anomalies. All the shaded values are statistically significant at the 10% level as per Student's t -test. The tropospheric temperature is taken from NCEP's Reanalysis-2 (Kanamitsu et al., 2002). The period of analysis is 1979–2012. See Chapter 3 for details on why and how to regress out the influence of ENSO on the target variable. See Pottapinjara et al. (2014) for further details such as development and decay of this response with time.

1.5 Scope of the work

While considerable research has been carried out on understanding the relation between the AZM and ISM, and possible physical mechanisms at work, a lot of gaps still remain. Importantly, studies by Keenlyside and Latif (2007) and Ding et al. (2010) show that winds, heat content, and SST in the equatorial Atlantic during boreal spring are significantly related to the AZM during boreal summer. Further, Servain et al. (1999) and Murtugudde et al. (2001) demonstrated that the meridional migration of the ITCZ during spring also is closely related to the AZM. That is, precursors to the summer AZM are available during boreal spring. However, it is not yet known if the evolution of cold and warm AZM events is symmetric as in the case of ENSO. Also, the relation between the AZM and ISM as such does not provide any lead relationship of the AZM to the ISM as both of them are active during almost the same time in boreal summer, and none of the above studies addressed it. Addressing these issues is of course important and eventually would lead to a better understanding, and therefore a better handle on the prediction, of the impacts of cold and warm AZMs on global climate, including the ISM. In this background, the objectives of the thesis are set as follows, and will be addressed in the subsequent chapters.

- (i) To explore the lead association of the known precursors of the AZM in boreal spring to the following ISM
- (ii) To investigate if the evolution of warm and cold AZM in the boreal spring is symmetric which would enhance our understanding of the AZM
- (iii) To explore the capability of a current day seasonal forecast model in simulating the relationship between the AZM and ISM

1.6 Summary

In this chapter, an up-to-date status of the prior research on the AZM-Indian summer monsoon rainfall is presented, along with some other useful background information. The important gaps are identified, based on which, a list of objectives to be achieved in the thesis are set. Chapter 2 provides a description of different datasets and analysis techniques used in the

thesis. Chapter 3, Chapter 4 and Chapter 5 address the Objectives i, ii and iii, respectively. Chapter 6, the last chapter, presents a summary and elucidates the results in light of the objectives.

Chapter 2

Description of Datasets and Statistical Methods

In this chapter, the datasets and statistical techniques that are common to several subsequent chapters are described. Any specific datasets and analysis techniques used in a certain chapter will be discussed in the respective chapter.

2.1 Datasets used

The results presented in this thesis are, in general, based on the analysis of different datasets during the period of 1979–2012. However, several other results are presented for a broader period of 1975–2013. The 1979–2012 period was chosen because of the availability of good quality datasets which was made possible by the advent of satellites and other improved observation platforms. Further, notwithstanding that the research presented in this thesis was carried out over a period of time, efforts have been made to keep the datasets used uniform throughout the study. Having said this, a few variables have been taken from different datasets depending on the problem at hand and these choices have been justified below. In addition, for the variables of winds and ocean temperature, we chose to work with the data sets of improved quality and higher resolution as they became available. Given the qualitative nature of the results, even though the choice of datasets should not have any bearing on the results, we have made efforts to ensure that there is always a qualitative agreement across the data sets. Since

this is mainly concerned with the results of Chapter 3, we demonstrate the robustness of the results across the data sets by reproducing some important analyses of Chapter 3 using the newer datasets and presented them in Appendix A.

2.1.1 Sea Surface Temperature

We have used the Hadley Centre Sea Ice and Sea Surface Temperature (HadISST; Rayner et al., 2003) developed by the Hadley Centre for Climate Prediction and Research of UK Met Office. It is a globally complete gridded dataset with a spatial resolution of $1^\circ \times 1^\circ$ and temporal resolution of a month, available from 1871 to date. The input data used to prepare HadISST are taken from various observational platforms. They are quality controlled for biases, errors, inhomogeneities, etc. and interpolated to reconstruct the data in the data-sparse regions. Further details are available from Rayner et al. (2003). This dataset is mainly used to identify the AZM and ENSO events throughout the study to maintain the list of events uniform.

2.1.2 Rainfall

For the study of rainfall variations over India, a high resolution rainfall dataset prepared by the India Meteorological Department (IMD) has been used (Pai et al., 2014). The IMD is the official agency that collects meteorological data, through its numerous stations spread all over India. The IMD converts the data thus collected into various useful products. This dataset is a daily gridded product prepared after quality controlling for errors and interpolation. It can be obtained from the website of IMD, Pune (<http://dsp.imdpune.gov.in/>). It has a spatial resolution of $0.25^\circ \times 0.25^\circ$ and is available for the period 1901–2013 (Pai et al., 2014). This dataset is mainly used in Chapter 3.

In Chapter 5, to compare the simulation of the relationship between the AZM and rainfall associated with ISM in the model against the observations, we have used the precipitation from the Global Precipitation Climatology Project (GPCP; Adler et al., 2003). It is a monthly dataset with a spatial resolution of $2.5^\circ \times 2.5^\circ$. This dataset provides global coverage of precipitation on both land and oceans. Given that models often misrepresent the rainfall distribution, it is reasonable to compare the simulation of the relationship in the both over land and ocean (north

Indian Ocean). Hence, a dataset with contiguous coverage such as GPCP is more relevant from this context than the IMD's rainfall dataset discussed above which is available only on land (India).

2.1.3 Winds

The wind data used are from two well documented reanalysis products. In Chapter 3, the National Centres for Environmental Prediction (NCEP)'s Reanalysis 2 (Kanamitsu et al., 2002) winds were used. The NCEP Reanalysis 2 is a daily/monthly gridded atmospheric reanalysis product that provides various atmospheric parameters at a spatial resolution of $2.5^\circ \times 2.5^\circ$ and is available for the period 1979 to date. It can be downloaded from the website of NOAA/OAR/ESRL PSD, Boulder, Colorado, USA, i.e., <https://www.esrl.noaa.gov/psd/>.

Tracking the position of Inter-tropical Convergence Zone (ITCZ) is crucial to Chapter 4 but to trace its position, wind data of a high spatial resolution is necessary, as the criterion for tracking the ITCZ is based on winds (see Chapter 4 for details). Therefore, in Chapter 4, we chose to use the wind data from the European Centre for Medium Range Weather Forecast (ECMWF)'s Re-analysis (ERA) Interim (Dee et al., 2011). This is a daily/monthly atmospheric reanalysis dataset with varying spatial resolutions but the resolution of data we used is $0.7^\circ \times 0.7^\circ$ which is higher compared to NCEP's Reanalysis 2 used in Chapter 3. This dataset is available for the period 1979–2019. It can be downloaded from the ECMWF's website at <https://apps.ecmwf.int/datasets/data/interim-full-daily/>. This dataset has also been used in Chapter 5.

2.1.4 Ocean Temperature

The oceanic subsurface temperature data is mainly used to compute the upper ocean heat content. The ocean temperature data used in Chapter 3, is obtained from Simple Ocean Data Analysis (SODA; Carton and Giese, 2008) version 2.2.4, jointly developed by the University of Maryland and Texas A&M University. The dataset is a monthly gridded product of spatial resolution $0.25^\circ \times 0.25^\circ$ with 40 vertical levels for the period 1871–2010. It is available for

download from multiple data providers including the Asia Pacific Data Research Center from their website at http://apdrc.soest.hawaii.edu/datadoc/soda_2.2.4.php.

In Chapter 4, we have used EN4 subsurface analysis version 4.2.0 of the UK Met Office (Good et al., 2013). It provides monthly global objective analyses of subsurface temperature and salinity with a spatial resolution of $1^\circ \times 1^\circ$ with 40 vertical levels for the period 1900 to the present. The temperature and salinity vertical profiles from various collections of *in situ* data were quality controlled for errors before preparing the objective analyses. This product does not involve any ocean model, and thus avoids errors introduced by the ocean model. It can be obtained from their website at <https://www.metoffice.gov.uk/hadobs/en4/download.html>. As stated already, some important analyses of Chapter 3 are reproduced using this data set and presented in Appendix A.

2.2 Statistical Methods

In this study, the most common statistical techniques used to analyze the datasets mentioned above are, the composite analysis, the linear correlation, and the linear regression. Although most of these methods are routinely used (Von Storch and Zwiers, 1999; Wilks, 2011), we discuss them here briefly for the sake of completeness. The statistical tests to determine the significance of the statistics calculated using these methods, will be explained immediately after. Note that there are many details to these methods but we describe only those aspects which are relevant to this thesis. As our study is concerned with inter-annual timescales, the monthly or seasonal mean anomalies are computed by removing the monthly or seasonal climatology, respectively. These anomalies are de-trended before any further analysis, as will be explained later in the chapter.

2.2.1 Composite Analysis

As the name itself suggests, the composite analysis involves compositing or segregating events of interest from a collection of data and analyzing the data employing statistical measures, most often the mean. The composite analysis provides insights into patterns or structures associated with phenomena such as ENSO, which are otherwise masked in the totality of the

data (e.g., Guan et al., 2003; Saji and Yamagata, 2003; Ashok et al., 2004a; Ashok and Saji, 2007; Kao and Yu, 2009; Welhouse et al., 2016). The segregation of events usually requires a certain criterion. The sequence of steps involved in the composite analysis is as follows. Suppose that we want to study the relation between two variables, x (or $x_i, i = 1, ..n$) and y (or $y_i, i = 1, ..n$), with i denoting the index of x . The events of x are defined depending on the value of i : whenever i assumes a certain value or a range of values, the corresponding values of y are segregated and their average is computed. The analysis does not make any assumptions as to the relation between the two variables, whether linear or non-linear (Von Storch and Zwiers, 1999; Xie et al., 2017).

The difference of composite means has also been used to highlight the contrast between two sets of events (e.g., Lau and Nath, 2003; Ashok et al., 2004b; Tejavath et al., 2019). For instance, the difference between the averages of wind anomalies during AZM cold events and AZM warm events contrasts the effect of a cold AZM event on winds against that of a warm AZM event (Fig. 4.7). This difference of composite means is also useful to determine whether the aspects of x captured by their respective segregating criterion are also expressed in y (Von Storch and Zwiers, 1999). For example, the events of El Niño and La Niña are defined depending on the value of ONI index, and by using the difference of composite means, it can be checked whether or not the rainfall over India is also different during El Niño and La Niña. Given that the climate is variable, care must be taken while compositing the data and interpreting the results.

2.2.2 Linear Correlation

The linear correlation is a measure of association between two variables, say x and y (Wilks, 2011). The most common correlation is the Pearson correlation, which is what we use in this thesis. The correlation coefficient r_{xy} is given by,

$$r_{xy} = \frac{1}{n-1} \frac{\sum_{i=1}^n [(x_i - \bar{x})][(y_i - \bar{y})]}{\sqrt{\frac{1}{n-1} \sum_{i=1}^n (x_i - \bar{x})^2} \sqrt{\frac{1}{n-1} \sum_{i=1}^n (y_i - \bar{y})^2}} \quad (2.1)$$

where (x_i, y_i) forms a data pair, \bar{x} and \bar{y} are the averages of all corresponding data points x_i and y_i each totaling to n , respectively. The correlation coefficient is a scalar and its value ranges

between -1 and 1. The higher the magnitude of correlation coefficient (excluding the sign), the stronger is the association between the variables. However, a low or zero correlation does not necessarily mean that the variables are not related, as the correlation we discussed tells us only the linear relation between the variables and does not give us any idea of non-linear association between them. Therefore, they can be still be related non-linearly and yet have a correlation of zero (Von Storch and Zwiers, 1999).

In addition to the simple linear correlation discussed above, a lead and lagged correlation analysis has also been used. The lead or lagged correlation between time series of two variables is useful to find if a change in one variable is associated with that in the other with a time delay (e.g., McPhaden, 2003; Ashok and Saji, 2007; Ren and Jin, 2011). A lead (lagged) correlation coefficient is obtained essentially in the same manner as above except that x_i s are shifted below (above) and data pairs are formed with the undisturbed y_i s, i.e., x_{i+l}, y_i (x_{i-l}, y_i), where l is the number of steps by which x_i are shifted and called the lead (lag). In a lead or lagged correlation, the total number of data pairs decrease by the same number as lead or lag, respectively.

2.2.3 Linear Regression

The simple linear regression is a linear approach which seeks to summarize the relationship between two variables using a straight line (Wilks, 2011). One of the two variables is an independent variable and the other is a dependent variable, often denoted by x and y , respectively. The value of y as predicted by the regression given the observations of x , i.e., \hat{y} , is given by,

$$\hat{y} = a + bx \quad (2.2)$$

where a and b are the y intercept and slope of the line, respectively. The parameters a and b can be obtained as follows.

$$b = \frac{\sum_{i=1}^n (x_i - \bar{x})(y_i - \bar{y})}{\sum_{i=1}^n (x_i - \bar{x})^2} \quad (2.3)$$

$$a = \bar{y} - b\bar{x} \quad (2.4)$$

The linear regression line has the least error for the predictions of y . The most common criterion used for error minimization is the least of the sum of the squared differences between y and \hat{y} .

As can be seen, the correlation coefficient r_{xy} (Eq. (2.1)) described earlier and linear regression slope b (Eq. (2.3)) are related. Note that neither regression nor correlation imply causality, hence these statistics must be interpreted with caution.

The geophysical time series often exhibit a trend which originates from various sources including the low frequency internal variability, and systematic changes in the forcing of climate system (Von Storch and Zwiers, 1999; Kumar et al., 1999). In this thesis, the focus is neither on the low frequency variability nor on the climate change but the interannual variations of AZM and its impact on the ISMR. Therefore, the trend in various parameters has been removed. The de-trended time series of $x(t)$, i.e., $x_{det}(t)$ can be obtained by,

$$x_{det}(t) = x(t) - b \times t \quad (2.5)$$

where b is the slope of the linear regression between the time series $x(t)$ and time t .

As discussed in Chapter 1, ENSO is a major driver of climate variability around the globe. Further, the SST anomalies associated with AZM are weak compared to ENSO, and ENSO and AZM often co-occur. Hence, to delineate the effect of AZM on a certain target field, as is our interest, removing the effect of ENSO on that field is necessary. It can be partially achieved by regressing out the impact of ENSO linearly on the target field (e.g., Kucharski et al., 2008; Joseph et al., 2011) as described in the following. Assuming that the target field time series $T(t)$ is significantly related to ENSO that is characterized by the *ONI* index (or the Niño 3.4 index), residual of $T(t)$, i.e., $T_{res}(t)$, which is free from the linear effect of ENSO is given by,

$$T_{res}(t) = T - b \times ONI(t) \quad (2.6)$$

where b is the slope of the linear regression between $T(t)$ and $ONI(t)$. This is a linear method based on linear regression and does not guarantee to remove the influence of ENSO on the target field completely. It is used in Chapter 5 and its extended variant is used in Chapter 3.

2.2.4 Determination of statistical significance

Thus far, we have discussed various statistical techniques that will be employed in this thesis. However, a statistic not accompanied by a measure of its significance is not helpful,

and can often lead to incorrect interpretations. The significance of a statistic is determined by a procedure called hypothesis testing. The elements of hypothesis testing are: 1) identification of an appropriate test statistic that is computed from the sample data, 2) defining a null hypothesis, which usually is that the sample data are a result of chance but not of a systematic process, 3) defining an alternative hypothesis, which often is that the null hypothesis is not true, 4) obtaining a sampling distribution that the test statistic follows, assuming that the null hypothesis is true, and 5) the comparison of the observed test statistic to the sampling distribution. If the test statistic falls in the improbable region, then the null hypothesis is rejected. Otherwise, the alternative hypothesis is accepted (Wilks, 2011). These steps will become clear when we apply the procedure to determine the significance of statistics discussed in the following.

To gauge the significance of composite mean of members (monthly mean SST anomalies associated with cold AZM events, for example) from a small sample size ($n < 30$; n is the sample size or the number of observations), the test statistic t is given by,

$$t = \frac{\bar{x} - \mu_0}{SE(\bar{x})} \quad (2.7)$$

$$SE(\bar{x}) = \frac{s}{\sqrt{n}} \quad (2.8)$$

where SE is the standard error, \bar{x} is the sample mean, μ_0 is the population mean and s is the sample standard deviation. The population refers to the collection of all possible values of the members. The statistic t follows the Student's t distribution with $n - 1$ degrees of freedom (the number of independent values of the sample that enter the final calculation of test statistic). The computation of t as defined in Eq. (2.7), requires the sample standard deviation s which in turn needs the sample mean \bar{x} to be calculated. It implies that the number of independent sample data points entering the computation of t goes down by 1 from n , and hence the value of degrees of freedom is $n - 1$. The null hypothesis is that the population mean μ_0 is zero, and the alternative hypothesis is that $\mu_0 \neq 0$ because the mean of the anomalies can take either a positive or a negative value. To account for the possibility of mean going in either direction, the two-tailed Student's t -test is used. The null hypothesis is rejected if the test statistic is greater than or equal to the critical value of t , i.e., t_{crit} , which is associated with a given significance level. The critical value t_{crit} can be read from standard t -tables. The significance levels of 0.05 (or 5%) and 0.1 (or 10%) are often used. The rejection of null hypothesis here implies that it is

less probable that the composite mean is the result of chance and conversely, it is probable (at the specified level of significance) that the mean is a result of systematic process (Von Storch and Zwiers, 1999; Wilks, 2011; Gonick and Smith, 1993). The level of significance has been indicated wherever it is used in the thesis.

The test statistic to estimate the significance of difference of means of two composites for small samples is the same as in Eq. (2.7) except that the standard error in the equation is given by,

$$SE(\bar{x}_1 - \bar{x}_2) = S_{pool} \sqrt{\frac{1}{n_1} + \frac{1}{n_2}}, \quad (2.9)$$

where,

$$S_{pool} = \sqrt{\frac{(n_1 - 1)s_1^2 + (n_2 - 1)s_2^2}{n_1 + n_2 - 2}} \quad (2.10)$$

In Eq. (2.9) and Eq. (2.10), \bar{x}_1 and \bar{x}_2 are means of samples of sizes n_1 and n_2 , respectively. Further, s_1 and s_2 are standard deviations of the samples in the same order. The test statistic thus constructed follows a t distribution, assuming that the population standard deviations are equal. The degrees of freedom of this t distribution is $n_1 + n_2 - 2$ (Wilks, 2011).

In the case of linear correlation, the test statistic is similar to Eq. (2.7), and is given by,

$$t = \frac{r}{SE(r)}, \quad (2.11)$$

where,

$$SE(r) = \sqrt{\frac{1 - r^2}{n - 2}}, \quad (2.12)$$

and r is the sample correlation coefficient given by Eq. (2.1). The null hypothesis is that the correlation coefficient is zero, implying that there is no association between the two variables, whereas the alternative hypothesis is that the correlation coefficient is non-zero. The test statistic in Eq. (2.11) follows the t distribution and the significance of correlation coefficient can be determined in the same manner as discussed above (Von Storch and Zwiers, 1999). The two-tailed Student's t -test has been used to determine the significance of the correlation coefficients throughout this thesis, unless mentioned otherwise.

Chapter 3

Exploring clues of predictability of the Indian Summer Monsoon Rainfall in the tropical Atlantic¹

In Chapter 1, we have discussed the relationship between the Atlantic Zonal Mode and Indian Summer Monsoon Rainfall as reported by earlier studies including our recent study Pottapinjara et al. (2014). However, since both AZM and ISM are contemporaneous, the relationship between the two does not provide us any predictive value for the ISMR. Therefore, in this chapter, we seek a predictive relationship between the tropical Atlantic and the ISMR based on the known teleconnections, by exploiting the fact that a great part of the variability of AZM is explained by ENSO-like dynamics. Our attempt is based on the expectation that any prior clues of an oncoming AZM event eventually lead to a better forecasting of the monsoon in advance via the physical pathways discussed in Chapter 1.

¹An edited version of this chapter appeared in *International Journal of Climatology* as Pottapinjara et al. (2016): 'Relation between the upper ocean heat content in the equatorial Atlantic during boreal spring and the Indian monsoon rainfall during June–September' ©Royal Meteorological Society
Further, *Nature India*, a publication of Nature Publishing Group, highlighted this work in their article entitled 'Indian monsoon prediction clues in equatorial Atlantic' (available at <https://www.natureasia.com/en/nindia/article/10.1038/nindia.2015.140>).

3.1 Introduction

India's food security and 60% of the employment base depend on rain fed agriculture, which in turn depends on 80% of the seasonal rainfall received during June–September, i.e., Indian Summer Monsoon Rainfall (ISMR). It is well known that the ISMR exhibits significant interannual variability in both intensity and spatial distribution leading to extreme events like floods and droughts (e.g., Parthasarathy et al., 1994; Gadgil, 2003). Hence, it is of immense socioeconomic importance to forecast these variations in advance to devise better policies to mitigate possible disasters and plan for suitable crops. Even though significant improvements have been made in the simulation and prediction of ISMR, the skill of statistical, atmospheric, and coupled models in predicting the ISMR leaves a lot to be desired (Rajeevan and Nanjundiah, 2009; Gadgil and Srinivasan, 2011; Kim et al., 2012). For example, the monsoon predictions using atmosphere or coupled ocean-atmosphere models by most of the leading centers in the world could not predict the large deficit in rainfall during the summer monsoon of 2009 (Nanjundiah, 2009). Fortunately, steady progress in dynamical seasonal prediction of the ISMR is being made (Rao et al., 2019; Pattanaik et al., 2019). Nonetheless, in addition to the necessary improvements in the modeling and data assimilation, a critical need is to understand the system better, particularly on interannual time scales, and identify hitherto undiscovered drivers of the Indian monsoon variability. As discussed in Chapter 1, earlier studies have examined the influence of different climate modes on the interannual variability of ISMR (e.g., Webster and Yang, 1992; Webster et al., 1998). Among them, El Niño-Southern Oscillation (ENSO) and the Indian Ocean Dipole (IOD) are the dominant interannual modes in the tropics. In general, a La Niña (an El Niño) or a positive (negative) IOD event leads to an enhancement (a reduction) of the ISMR. A strong relationship exists between ENSO (Philander et al., 1989) and the ISMR (Webster et al., 1998), even though the relationship is not stationary and depends on the type of ENSO (Kumar et al., 1999, 2006; Ashok and Saji, 2007). The recent failures of monsoon predictions in 2012 and 2014 were also accompanied by the unexpected demise of ENSO highlighting the tenuousness of relying on ENSO for monsoon predictions. Further, ENSO explains only 30% of the interannual variability of ISMR (Rajeevan and McPhaden, 2004; Gadgil, 2014). It indicates that the development of an ENSO event may not always have its impact on the ISMR. For example, in the year 1997, a strong El Niño occurred but the ISMR was normal. This is demonstrated to be associated with an opposing impact from the co-occurring strong IOD event

(e.g., Webster et al., 1999; Murtugudde et al., 2000; Ashok et al., 2001, 2004b). Moreover, there are a few dry and wet years, which cannot be explained by either ENSO or IOD events (Varikoden and Preethi, 2013). For instance, the ISMR was above normal in 2013, even though there was no ENSO or IOD event. Hence, it is imperative to find out the influence of other tropical teleconnections to the Indian monsoon, especially during non-ENSO years. This motivates us to explore any likely skill from another tropical ocean, viz., the tropical Atlantic.

As described in Chapter 1, the Atlantic Zonal Mode (AZM; also called as Atlantic Niño), a coupled ocean-atmosphere phenomenon from the tropical Atlantic, is similar to ENSO in terms of coupled dynamics but weaker (Zebiak, 1993; Xie and Carton, 2004; Burls et al., 2012). The AZM is phase locked to seasonal cycle and usually peaks during the boreal summer (June–August; Lübbecke et al., 2010) coinciding with the Indian summer monsoon period (June–September), although some AZM events can occur later in the fall (Monger et al., 1997; Okumura and Xie, 2006). A series of studies have shown that a warm (cold) AZM event can decrease (increase) the ISMR (Kucharski et al., 2007, 2008; Wang et al., 2009; Barimalala et al., 2013b). In Pottapinjara et al. (2014), we have extended these earlier studies by investigating how the AZM can influence the ISMR by altering the number of monsoon depressions in the Bay of Bengal which contribute significantly to the ISMR.

Although the existence of a relation between the AZM and ISMR is shown by the earlier studies as well as in our recent study Pottapinjara et al. (2014), there is no predictive value in the SST associated with AZM to ISMR since both of them are active almost at the same time during boreal summer. Understanding the dynamics of AZM may help us in eventually deriving a predictive relation for the ISMR. Keenlyside and Latif (2007) showed the existence of Bjerknes feedback (Bjerknes, 1969) involving a positive feedback between the zonal winds, thermocline, heat content, and SST in the equatorial Atlantic in the evolution of AZM, similar to the case of ENSO. Further, Ding et al. (2010) showed that variations in upper ocean heat content (or heat content; see Section 3.3 for details) averaged in the equatorial Atlantic belt precede SST anomalies in the cold tongue region (6°S – 2°N and 20°W – 0°W) by 4–5 months. That indicates a potentially predictive value from heat content to the SST anomalies during the AZM. Hence, it is worthwhile to examine the changes in heat content in the equatorial Atlantic which precede the AZM to determine if those changes can foretell the ensuing summer monsoon anomaly sufficiently in advance. Our interest in the heat content variability in the equatorial Atlantic and

ISMR is motivated by a study by Rajeevan and McPhaden (2004). They have shown that heat content or, its equivalent - the volume of warm water in the tropical Pacific, can act as a better predictor for ISMR with a lead time of at least one season, compared to ENSO SST indices which do not have any predictive value for the ensuing monsoon rainfall. Moreover, McPhaden and Nagura (2014) have shown that the heat content in the Indian Ocean equatorial belt can be a predictor of the IOD development through a mechanism similar to that of ENSO in the Pacific. They explained these results in the framework of the recharge oscillator theory (Jin, 1997b). However, the relationship between heat content variability in the equatorial Atlantic and ISMR is not investigated thus far, to the best of our knowledge. The primary objective of this chapter is to describe and explain the existence and the mechanistic connection between the heat content and other Bjerknes feedback components in the equatorial Atlantic, and ISMR. This might shed some light on the ensuing monsoon, especially during non-ENSO years.

3.2 Relationship between the AZM and ISMR

In Chapter 1, we have discussed the relation between the AZM and ISMR as reported by earlier studies and our recent study (Pottapinjara et al., 2014). However, as will be noted in the following, the effect of AZM on rainfall over India is not uniform. In this chapter, we pay attention to the spatial variability of the relationship, and to examine its details, the daily high resolution ($0.25^\circ \times 0.25^\circ$) gridded rainfall data provided by the India Meteorological Department (Pai et al., 2014) is used. The method of selection of AZM and ENSO events for the analysis presented in this chapter is discussed here. The same method is followed in the subsequent chapters as well. The Atlantic 3 (Atl3; average of SST anomalies over 3°S – 2°N and 20°W – 0°E) index that is characteristic of the AZM, is used to identify the AZM events. Whenever the Atl3 index crosses one standard deviation (0.48°C) during June–August (JJA) season, it is called a warm (cold) event, if the sign of the anomalies is positive (negative) (Burls et al., 2012). The Atl3 index is based on the detrended Hadley Centre Sea Ice and Sea Surface Temperature (HadISST) product (Rayner et al., 2003). Due to the constraints posed by the availability of different data sets, we will restrict ourselves only to the period 1975–2010. During this period, AZM cold events are found to occur in years 1976, 1978, 1982, 1983, 1992, 1994, 1997, and 2005 (a total of 8), and warm events during 1984, 1987, 1988, 1995, 1996, 1998, 1999, 2008, and 2010 (a

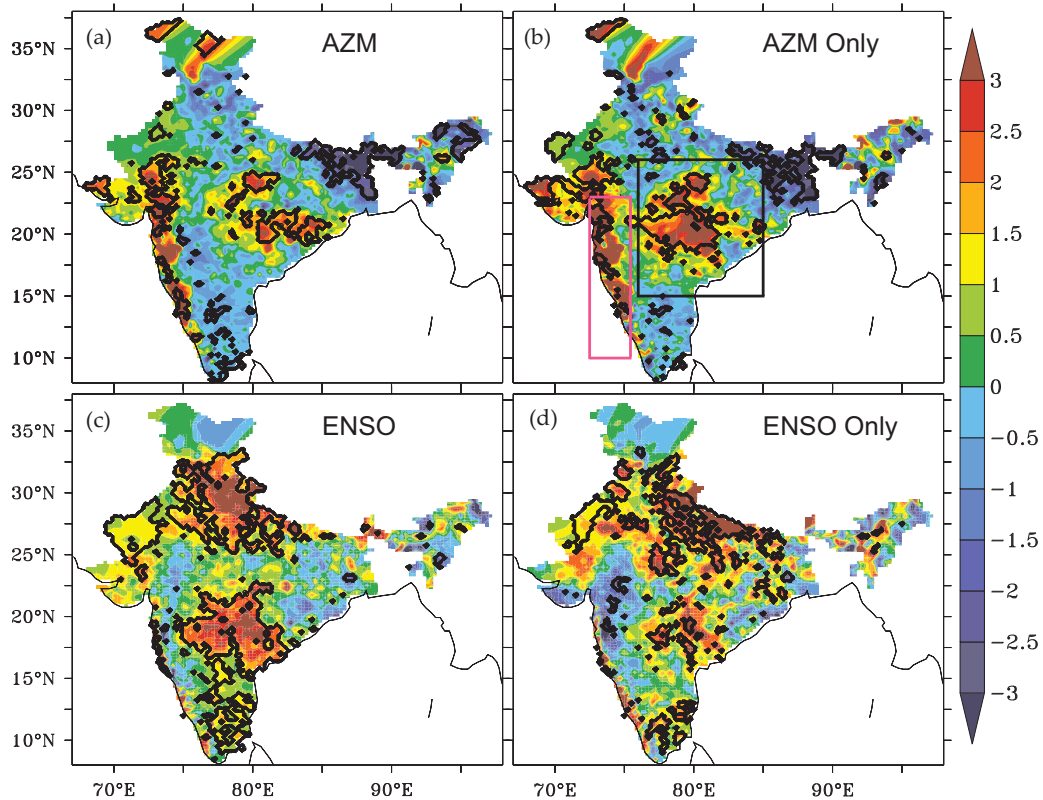


Figure 3.1: Differences of composites of rainfall (mm) between the cold and warm events of (a) AZM, (b) AZM only (excluding those co-occurring with ENSO), (c) ENSO and (d) ENSO only (excluding ENSO events co-occurring with AZM). The two regions selected for the analysis, i.e., Central India (15°N–26°N and 76°E–85°E; black box) and the Western Ghats (10°N–23°N and 72.5°E–75.5°E; pink box) are shown in (b). The contours in black color indicate 10% significance level.

total of 9). Following the same criterion for selecting ENSO years as for AZM, but using ONI index (SST anomalies averaged over 5°S–5°N and 170°W–120°W; standard deviation 0.5°C), years of La Niña events are identified to be 1975, 1985, 1988, 1998, 1999, 2000, and 2010 (a total of 7); and, El Niño events to be 1982, 1987, 1991, 1997, 2002, 2004, and 2009 (a total of 7) (consistent with the list of ENSO events given at http://www.cpc.ncep.noaa.gov/products/analysis_monitoring/ensostuff/ensoyears.shtml). It can be noted that there are some years in which both the AZM and ENSO occurred. The cold AZM events which did not occur along with ENSO are 1976, 1978, 1983, 1992, 1994, and 2005 (a total of 6), and the warm events independent of ENSO are 1984, 1995, 1996, and 2008 (a total of 4). The differences (cold–warm) between seasonal (June–September) composites of rainfall over India during the cold and warm AZM years, including and excluding the co-occurring ENSO events are shown in Fig. 3.1a and Fig. 3.1b, respectively.

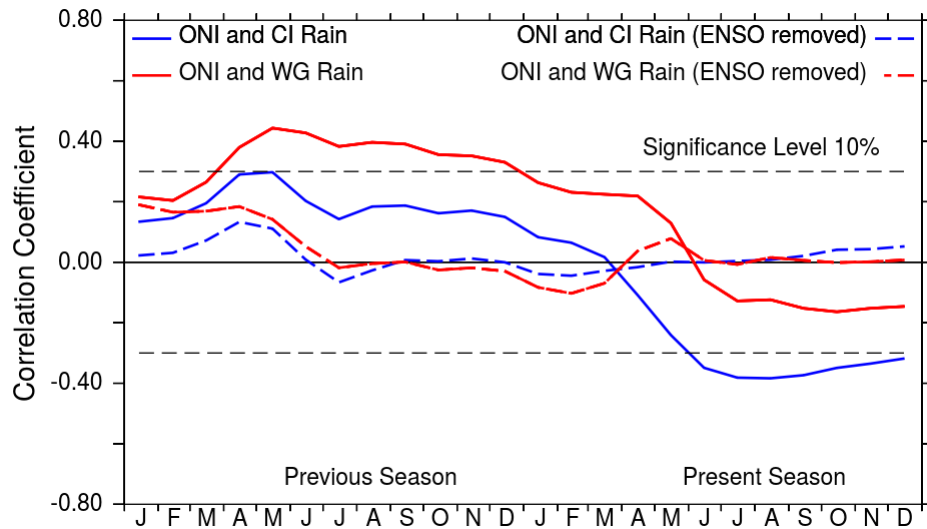


Figure 3.2: The lead-lag correlations between ONI index, and rainfall over Central India (blue) and the Western Ghats (red) before (thick line) and after (dashed) removing the effect of ENSO over the respective regional rainfall. The dashed straight lines indicate the 10% significance level for the correlations using the two-tailed Student's t-test.

Consistent with the earlier studies (Kucharski et al., 2007, 2008, 2009; Pottapinjara et al., 2014), Fig. 3.1a and Fig. 3.1b clearly depict the relationship between the AZM and ISMR with enhanced (reduced) rainfall in the lower parts of the Western Ghats and over Central India but with decreased (increased) rainfall over northeastern India and southeastern India during a cold (warm) AZM event. Similar maps of difference (La Niña–El Niño) of seasonal composites of rainfall over India during La Niña and El Niño phases of ENSO including and excluding the co-occurring AZM events are shown in Fig. 3.1c and Fig. 3.1d, respectively. From the figure, it can be seen that the spatial patterns of rainfall composites for the AZM (Fig. 3.1a and Fig. 3.1b) and ENSO (Fig. 3.1c and Fig. 3.1d) are different. It is also clear from the figure that the spatial pattern of rainfall for the AZM where ENSO years are excluded (i.e., for only non-ENSO AZM events; Fig. 3.1b) becomes more prominent. From this, we can discern that the AZM does affect the rainfall over India independently of ENSO, and its effects are not homogeneous over India. To capture the variation of the influence of AZM over rainfall, two dominantly affected regions, i.e., Central India (15°N – 26°N and 76°E – 85°E ; shown as a black box in Fig. 3.1b) and the Western Ghats (10°N – 23°N and 72.5°E – 75.5°E ; shown as a pink box in Fig. 3.1b), that show significant difference in rainfall between the cold and warm phases of AZM, are selected to analyze the problem further.

It is well known that ENSO is a dominant phenomenon remotely affecting the Indian

monsoon. The lead-lag correlation analysis between the rainfall over Central India and the Western Ghats (regions shown in Fig. 3.1b), and the ONI index yields (Fig. 3.2) significant correlations both in the present and previous year's monsoon seasons. The previous year's monsoon correlations represent the cyclic nature of the correlation pattern between the rainfall and ENSO (Rajeevan and McPhaden, 2004). In order to highlight the relation between the AZM and monsoon rainfall, the effect of ENSO on rainfall needs to be removed first. The details of a statistical method that can remove the effect of ENSO on the rainfall in both seasons are given here. The method to remove simultaneous effect of ENSO on a given target field as described in Section 2.2.3, is extended here to serve our purpose. The effect of ENSO on June–September (JJAS) rainfall time series is removed by taking JJAS ONI index (or Niño 3.4 index) both during the previous, and present monsoon seasons as shown in Eq. (3.1). In the equation, the SST leads are with respect to the JJAS rainfall during the present monsoon season. The residual time series of rainfall which is free from the linear effect of ONI index is given by,

$$Rainfall_{res} = Rainfall - Slope_1 \times ONI(present) - Slope_2 \times ONI_{res}(previous), \quad (3.1)$$

where,

$$ONI_{res}(previous) = ONI(previous) - Slope_3 \times ONI(present)$$

In Eq. (3.1), $Slope_1$ and $Slope_2$ are the least square regression fit slopes between the rainfall, and ONI index during the present monsoon season and $ONI_{res}(previous)$ (residual of ONI index in the previous monsoon season that is uncorrelated with ONI index in the present monsoon season), respectively. And, $Slope_3$ is the slope of the least square regression fit between ONI index in the present and previous monsoon seasons. The second term in the equation (involving $Slope_2$) accounts for the effect of ONI index of the previous season on rainfall that is not related to ONI index of the present season. Correlating the residual of JJAS rainfall anomaly time series with the ONI index confirms that the correlations after removing the effect of ENSO are well below the significance levels (Fig. 3.2). These residual rainfall time series of the two regions are used in the analysis. If we wish to keep it simple by removing the influence of ENSO on ISMR only during the present season, the results presented in this chapter still hold although the strength of correlation might drop. As mentioned already, in this chapter, we have used the method described above (Eq. (3.1)), to account for the biennial relation between ENSO and ISMR involving cyclic correlations (Webster et al., 1998).

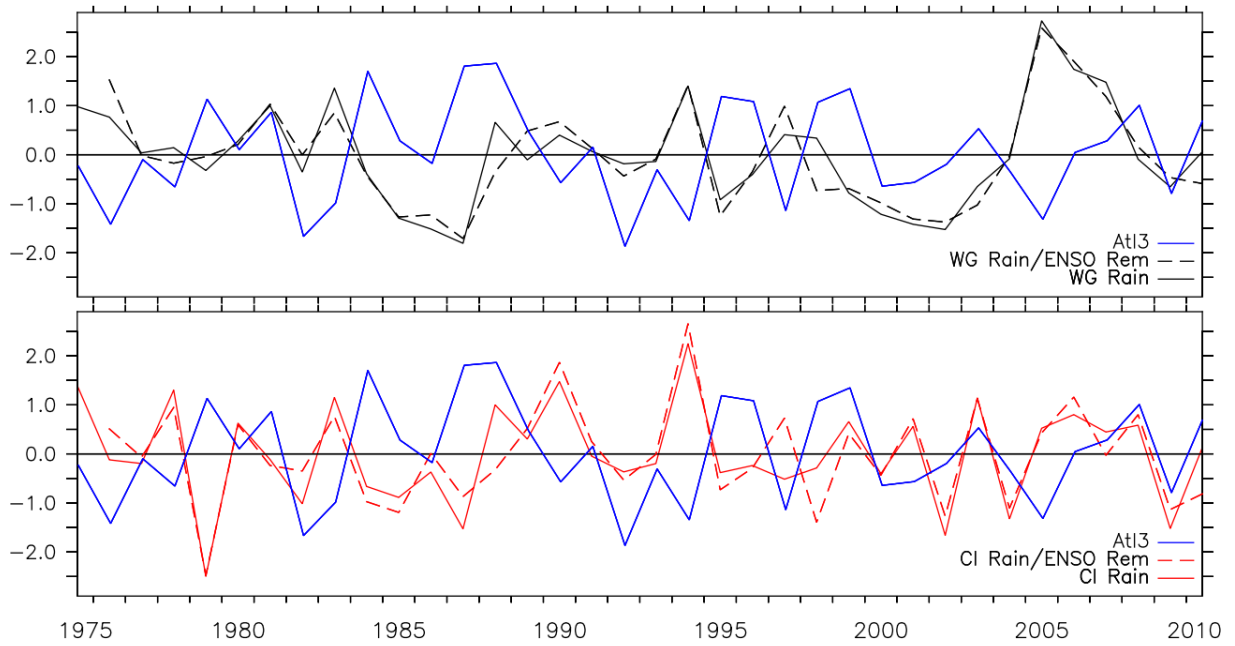


Figure 3.3: a) The time series of JJA AtI3 (blue line) and JJAS rainfall over the Western Ghats and Central India before (line) and after (dashed line) removing the influence of ENSO on the rainfall. While the rainfall over the Western Ghats is marked in black, that over Central India is marked in red. All time series are normalized by their respective standard deviation.

Central India rainfall versus JJA AtI3	Western Ghats rainfall versus JJA AtI3
-0.15	-0.29
After removing the ENSO effect over the respective rainfall	
-0.34	-0.35

Table 3.1: Correlation coefficients between JJA AtI3 index and JJAS rainfall anomalies over Central India (15°–26°N and 76°–85°E) and Western Ghats (10°–23°N and 72.5°–75.5°E) before and after removing the effect of ENSO on the respective rainfall series. The coefficients marked in bold are significant at the 10% level.

Resuming our discussion on the relation between the AZM and ISMR, Fig. 3.3 shows the JJA AtI3 index, and JJAS rainfall anomalies averaged over the Western Ghats and Central India (as shown in Fig. 3.1), before and after removing the effect of ENSO over the respective regional rainfall time series following the method described above. Further, simultaneous correlations among the time series are presented in Table 3.1. From the table, it may be noted that the correlations (–0.15 over Central India; –0.29 over the Western Ghats) improve and become statistically more significant after removing the effect of ENSO (–0.34 over Central India; –0.35 over the Western Ghats) over the respective rainfalls. It may also be noted that the sign of correlations agrees with the difference of seasonal composites of rainfall maps presented in

Fig. 3.1a and Fig. 3.1b and also is consistent with our result from (Pottapinjara et al., 2014). In addition, it implies that the AZM can explain about 12% (square of the correlation coefficient) of variability of the rainfall over the Western Ghats or Central India after removing the effect of ENSO on rainfall. Given the shortage of reliable predictors of ISMR when there is no ENSO event, it is worthwhile to pursue the study of the linkages between AZM and ISMR, and any potential lead relationship for the AZM may eventually translate into a predictive signal of the ISMR.

3.3 Evolution of the zonal wind, heat content and SST in the equatorial Atlantic associated with AZM

Having shown the existence of a relation between the AZM and ISMR and its spatial variability, we seek indicators portending the SST anomalies associated with AZM which might serve as predictors for ISMR anomalies. To see if any lead-time indicators exist for an impending AZM event, dynamics associated with the AZM are examined in the below.

A dynamical positive feedback between the winds, SST and thermocline depth was proposed by Bjerknes to explain the growing phase of ENSO (Bjerknes, 1969) as discussed in Chapter 1. In an equatorial ocean basin where the normal conditions are characterized by a warm pool in the west and a cold tongue in the east, the feedback can be explained as follows. A warm SST anomaly in the east (produced by local reduction in upwelling or a remotely driven deepening of the thermocline, typically by a Kelvin wave from the west), weakens the temperature gradient between the western warm pool and the eastern cold tongue, which further weakens the easterly trade winds. Weakened trades will further weaken the upwelling and surface cooling, and allow the warming to persist or grow in the east driving a positive coupled ocean-atmosphere feedback that needs to be terminated by other processes (Wang and Picaut, 2004). The relations between these three components of the Bjerknes feedback are examined below in the context of AZM.

To show the changes in wind field associated with the Bjerknes feedback in the equatorial Atlantic, the National Centers for Environmental Prediction's (NCEP) Reanalysis-2 product for wind (1979–2010; Kanamitsu et al., 2002) is used. The upper ocean heat content per unit area

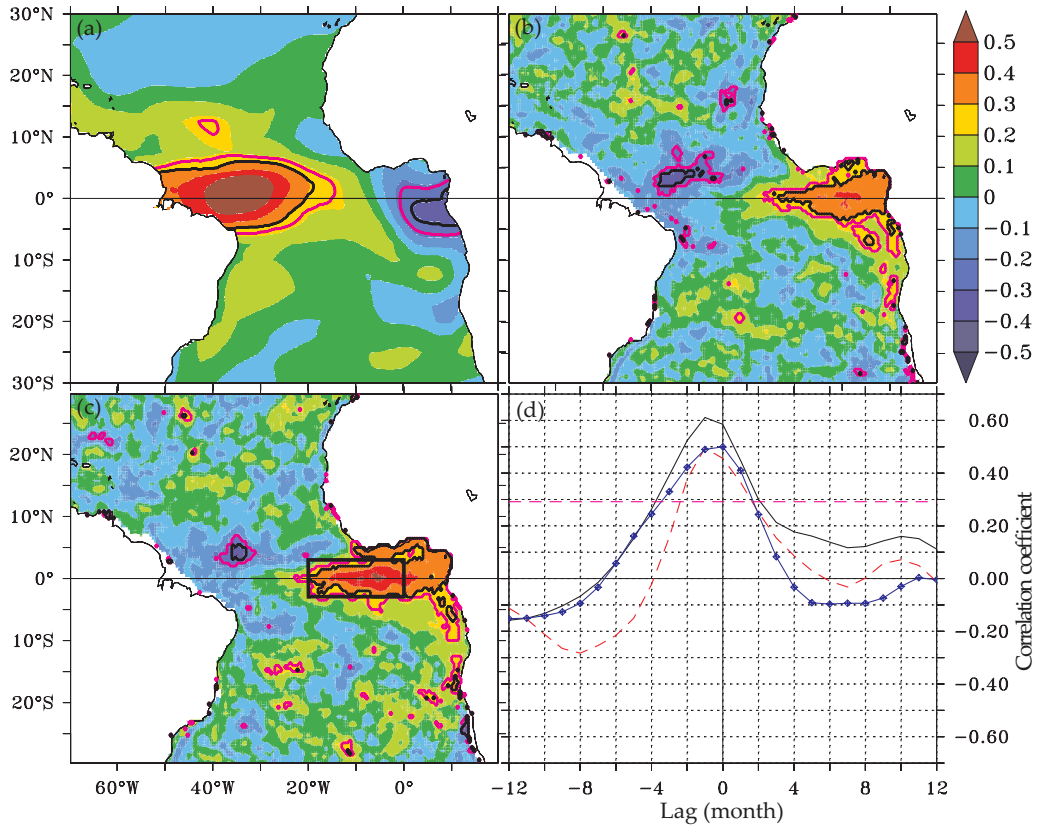


Figure 3.4: Spatial correlations between the anomalies of (a) SST in the Atl3 region and zonal winds, (b) western equatorial Atlantic (3°S – 3°N and 40°W – 20°W ; WEA) zonal winds and heat content, (c) eastern equatorial Atlantic (3°S – 3°N and 5°W – 10°E ; EEA) heat content and SST, and (d) monthly lead-lag correlations between anomalies of SST in the Atl3 region and WEA zonal wind (black), WEA zonal wind and EEA heat content (red) and EEA heat content and Atl3 (blue). The zonal winds are taken at 850 hPa level. In spatial correlation plots (a, b and c), contours of 20% and 10% significance are indicated in pink and black colors respectively and in (d), the level of 10% significance is indicated by a pink dashed line. The correlations over land are masked in (a) to highlight the same over the ocean. The black box in (c) indicates the Atl3 region.

above 20°C isotherm (‘heat content’ hereafter) is synonymous with the thermocline depth and is given by Eq. (3.2). The heat content is calculated using ocean temperature data obtained from the Simple Ocean Data Assimilation (SODA) v2.2.4 (Carton and Giese, 2008).

$$\frac{1}{A}Q_{tot} = \rho C_p \int_{z=0m}^{z(T=20^{\circ}\text{C})} T(z)dz \quad (3.2)$$

In Eq. (3.2), Q_{tot} is the total heat content; A is the surface area; ρ is the density of water; C_p is the specific heat of water; T is the temperature of water; and, z is the depth of the ocean. Spatial correlations between the anomalies of low level zonal wind (850hPa), heat content and SST are shown in Fig. 3.4. The correlations between the Atl3 index and low level zonal wind anomaly

presented in Fig. 3.4a tell us that warm SST anomalies in the Atl3 region are associated with positive wind anomalies in the western equatorial Atlantic (WEA; 3°S – 3°N and 40°W – 20°W). The zonal wind anomalies averaged over the WEA are positively correlated with heat content anomalies in the eastern equatorial Atlantic (EEA; 3°S – 3°N and 5°W – 10°E ; Fig. 3.4b), which indicates that westerly (easterly) zonal wind anomaly in the WEA drives an enhancement (a reduction) of heat content in the EEA. The heat content anomalies averaged in the EEA are positively correlated with SST anomaly in the Atl3 region (Fig. 3.4c) indicating that anomalous increase in heat content in the EEA is tied to an increase in SST in the east, likely through thermocline-mixed layer interactions. From Fig. 3.4a, Fig. 3.4b, and Fig. 3.4c, note that the three components (the wind anomalies in the WEA, heat content anomalies in the EEA, and SST anomalies in the Atl3 region) can potentially work together to form a positive feedback. Also, note that these are all simultaneous correlations and do not give us any clue on the possible leads or lags. Monthly lead-lag correlations between the three components shown in Fig. 3.4d indicate a lag of one month in peak correlations both between SST in the Atl3 region and winds in the WEA, and between winds in the WEA and heat content in the EEA. It also shows a lag of about one month in the peak correlation between heat content in the EEA and SST in the Atl3. These different correlations are significant with at least two months lead. These results are consistent with Keenlyside and Latif (2007) where the Bjerkenes feedback is shown to be at work in the tropical Atlantic as in the case of ENSO but with a weaker intensity. All these are monthly correlation analyses from which we can say with confidence that the development of an AZM event involves coupled ocean-atmosphere feedbacks.

To gain more confidence in the causal links, monthly composite analyses of the three components mentioned above are presented in Fig. 3.5 for both the cold and warm AZM events. In the figure, during a cold (warm) AZM event, the low level zonal winds in the WEA reaches its farthest in April (May) followed by the heat content in the EEA in May (June) and SST in the Atl3 region in June (June). From the above and Fig. 3.4, it may be argued that during a warm (cold) AZM event, anomalous westerlies (easterlies) in the western equatorial Atlantic lead to an anomalous increase (decrease) in heat content in the EEA with a lag of one month. It can be further argued that the anomalies in the heat content are reflected in SST in the Atl3 region within one month's time which in turn feeds back to winds in the WEA, thus completing a positive feedback loop. It can be noticed that zonal surface winds in the EEA become the strongest (weakest) in June (June) during the cold (warm) events of AZM acting as a dampening

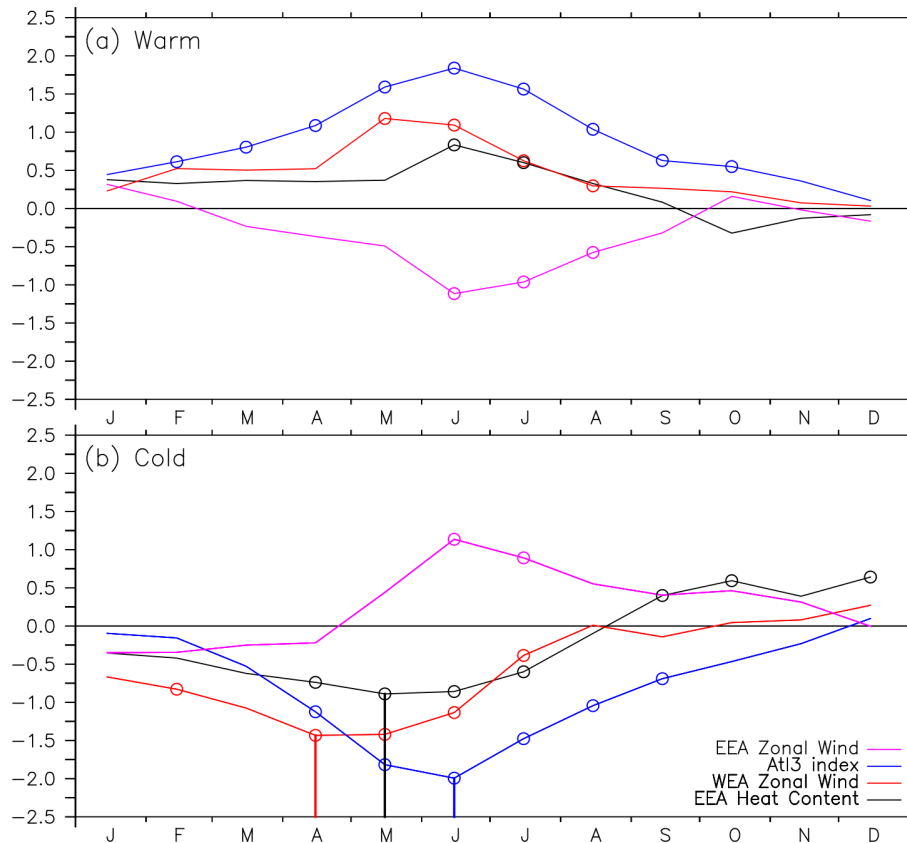


Figure 3.5: Evolution of composites of anomalies of western equatorial zonal wind (red), eastern equatorial zonal wind (pink), eastern equatorial heat content (black) and SST in the Atl3 region (blue) during the warm (a) and cold (b) events of AZM. All the fields are normalized before compositing. The zonal winds are taken at 850 hPa level. The peaks of different fields plotted are marked as vertical lines in their respective colors. The statistical significance of the composites at the 10% is indicated by circles in their respective colors.

factor in the feedback loop. Once again, the chain of events in the feedback loop agrees well with Keenlyside and Latif (2007).

The most important observation from Fig. 3.5 is that the development of different signals during the cold and warm AZM events is clearly distinct, and it is indicative of the impending AZM event as early as early spring itself. This suggests that wind anomalies in the WEA and heat content anomalies in the EEA during boreal spring might offer potential predictability of the development of an AZM event in the ensuing summer. Hence, the key question is whether this information can provide some clue on the ISMR anomalies associated with AZM. The relationship between equatorial Atlantic winds and heat content, and the ISMR is examined below.

3.4 Relationship between the ISMR, and the variability of heat content and winds in the equatorial Atlantic in boreal spring

The spatio-temporal evolution of correlations between the heat content in the Atlantic, and JJAS rainfall anomalies over Central India and the Western Ghats, before and after removing the effect of ENSO over the respective rainfall time series are shown in Fig. 3.6 (Fig. 3.6a and Fig. 3.6b: Central India; Fig. 3.6c and Fig. 3.6d: the Western Ghats; see Section 3.2 for the details of method to remove the effect of ENSO over rainfall). It is evident from the figure that consistent signals are present in the eastern equatorial Atlantic Ocean in nearly the same regions as in Fig. 3.4b. The correlations of the equatorial Atlantic heat content with ISMR over both the regions start to build up from January and become strongest in February and March and weaken later. It can also be seen that the correlations further improve after removing the effect of ENSO on rainfall (Fig. 3.6b and Fig. 3.6d). It is worth re-emphasizing that the correlations between the rainfall and Atl3 SST also improve similarly as shown in Table 3.1. After removing the effect of ENSO over respective rainfall time series, the correlations between the heat content and rainfall over the Western Ghats persist from January to May, whereas the correlations between rainfall over Central India and heat content, get weaker in April and May. However, this figure clearly indicates that the heat content in the EEA in January–May may hold some clues for the summer rainfall anomalies over these Indian land regions. The Bjerknes feedback component that precedes the heat content in the Atlantic as shown in Fig. 3.5 is the anomalous westerly surface winds in the WEA. Similar to Fig. 3.6, the correlations between the low level (850hPa) zonal winds and rainfall are shown in Fig. 3.7. For rainfall over the Western Ghats, there are clear signals in low level zonal winds in the WEA, both before and after removing the effect of ENSO. However, for Central India rainfall, after removing the effect of ENSO, there seems to be some association with the low level wind in the WEA in April and May, but it is comparatively weaker than that for the Western Ghats. From the above analysis, it may be concluded that low level winds in the WEA may be a potential predictor for rainfall anomalies over Western Ghats and Central India one season in advance.

Synthesizing the different arguments made above, we can state that the coherent changes in low level zonal winds, heat content, and SST (Bjerknes feedback) precede an AZM event

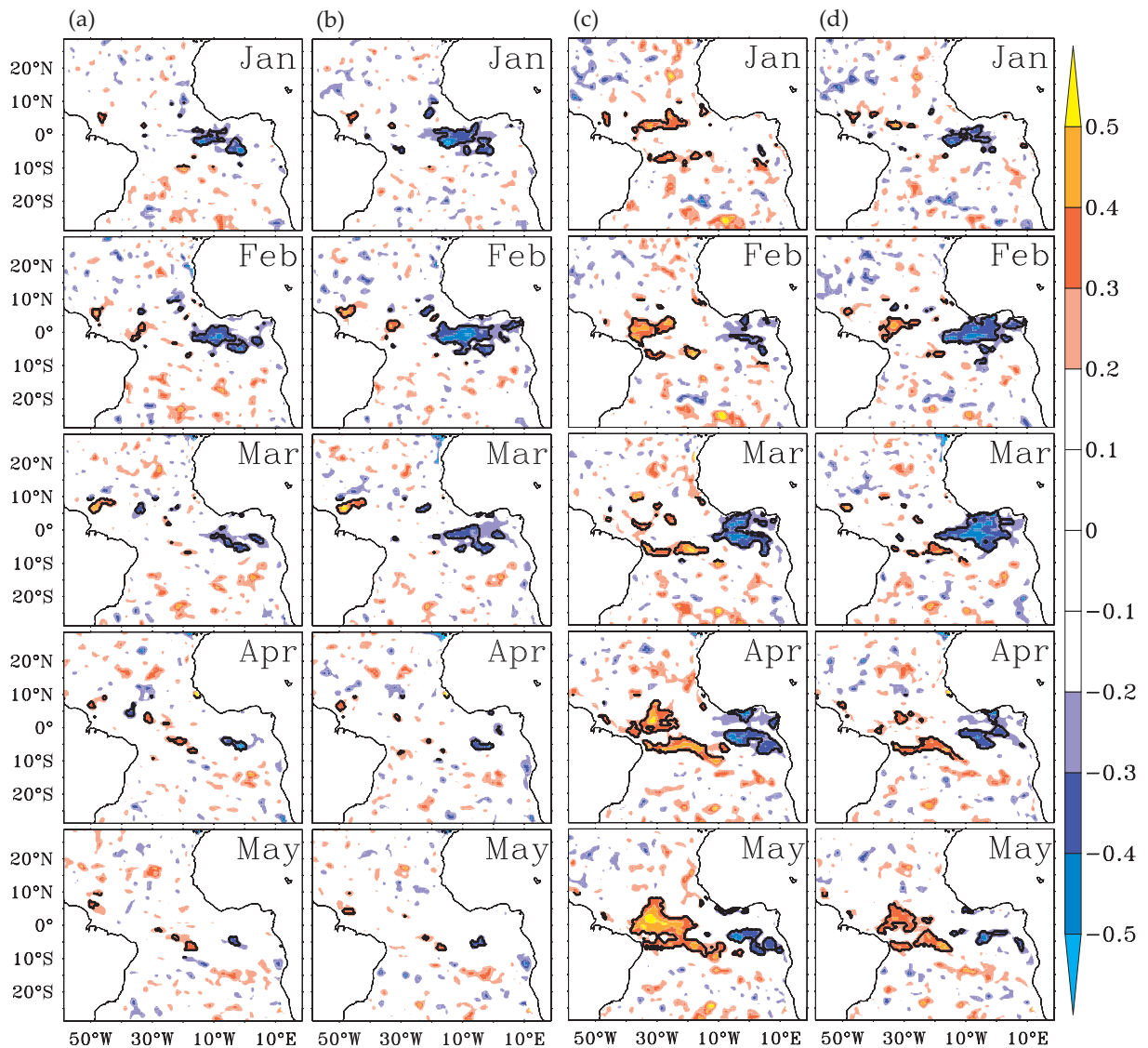


Figure 3.6: Monthly correlations, during January–May, between anomalies of heat content and JJAS rainfall anomalies over Central India (a and b), and the Western Ghats (c and d), before (a and c) and after (b and d) removing the effect of ENSO on the respective regional rainfall during the monsoon season. Correlations above 10% significance level around the equator are shown in black contours. This figure is consistent with Fig. A.1 which is repeated using a different dataset to demonstrate the robustness of the results across datasets.

as shown in Fig. 3.4 and Fig. 3.5. The extant relation between the AZM and ISMR is shown in Table 3.1 and is consistent with the earlier studies discussed in Chapter 1. The Bjerknes feedback components of heat content in the EEA and surface zonal winds in the WEA during January–May are shown to be related to the rainfall over India in June–September in Fig. 3.6 and Fig. 3.7. In addition, it is also shown that the relationship improves after removing the effect of ENSO over the rainfall. In summary, we can conclude that by tracking the zonal surface winds in the WEA and heat content and SST in the EEA, we may gain some short lead-time potential

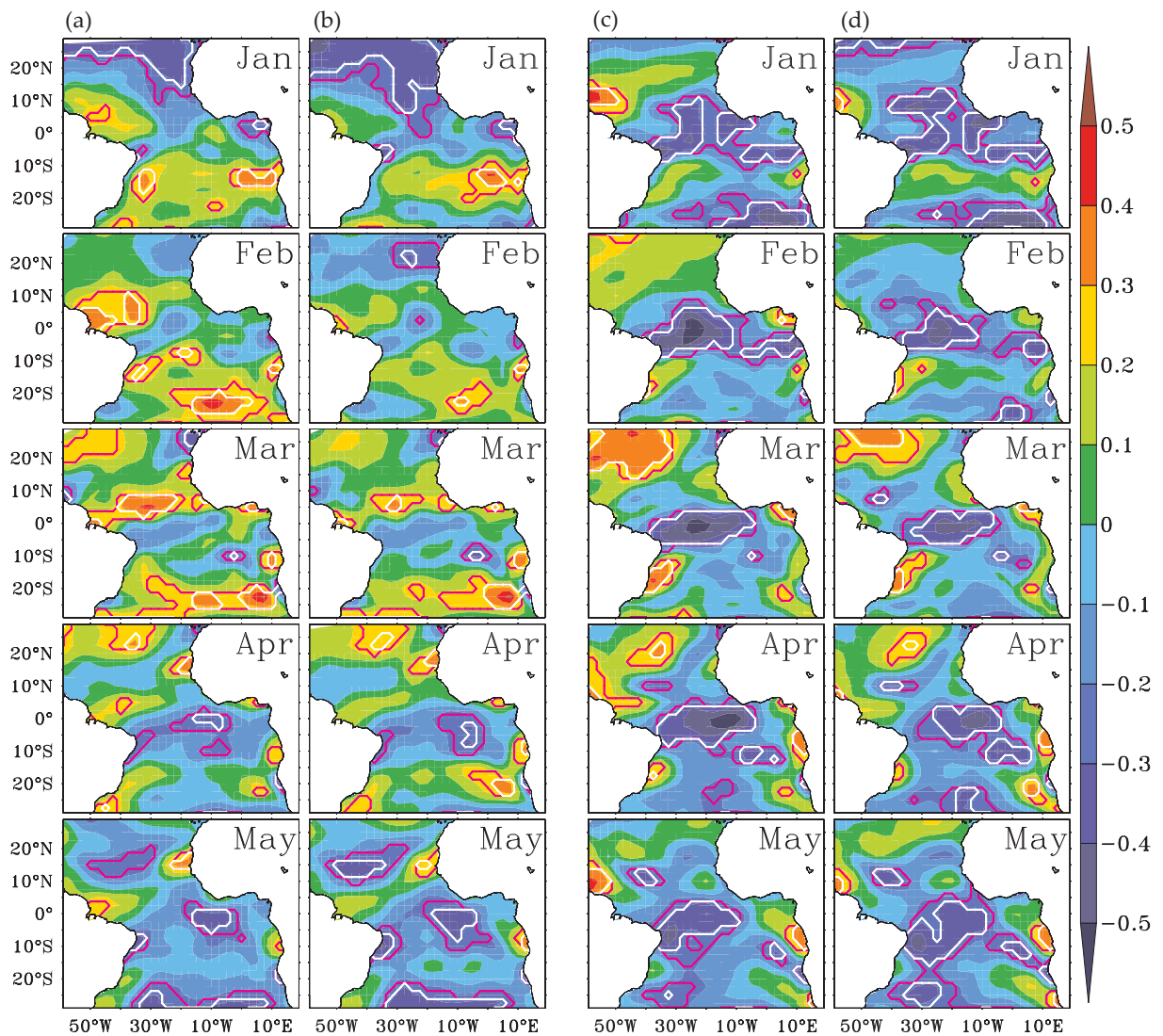


Figure 3.7: Monthly correlations, during January–May, between anomalies of low level winds, and JJAS rainfall anomalies over Central India (a and b), and the Western Ghats (c and d), before (a and b) and after (b and d) removing the effect of the ENSO on the respective regional rainfall during the monsoon season. The contours of 20% and 10% significance levels are indicated in pink and white colors, respectively. Correlations over land are masked to highlight the same over the ocean. This figure is consistent with Fig. A.2 which is repeated using a different dataset to demonstrate the robustness of the results across datasets.

predictability in monsoon anomalies, especially during non-ENSO years.

It may be worthwhile to sum up different analysis methods used in this chapter to alleviate any confusion. The major analysis techniques used are the linear correlation and composite analysis which have been discussed already in Chapter 2. Fig. 3.1 and Fig. 3.5 are the result of composite analysis whereas Fig. 3.2, Fig. 3.4, Fig. 3.6, and Fig. 3.7 are obtained using linear correlation analysis. In the composite analysis, the AZM (or ENSO) years are used including or excluding the other to elucidate the distinct patterns in different fields associated with

the AZM (or ENSO). The linear correlation analyses (Fig. 3.4, Fig. 3.6, and Fig. 3.7) are performed with the total time series. To clearly depict the impact of AZM that is otherwise masked by ENSO, Eq. (3.1) is used to remove the effect of ENSO from the rainfall, as ENSO confounds the analysis in the full time series. The residual rainfall time series is used for further correlation analysis.

3.5 Summary and Discussion

Several recent studies have highlighted the relationship between the AZM and ISMR (e.g., Wang et al., 2009). The SST anomaly associated with the AZM in the eastern equatorial Atlantic affects the ISMR via both dynamical and thermodynamical pathways as reported in earlier studies (Kucharski et al., 2009; Pottapinjara et al., 2014). Extending these earlier studies, in Pottapinjara et al. (2014), we have examined how the AZM influences the ISMR by modulating the frequency of monsoon depressions in the Bay of Bengal. In this chapter, we have attempted to find a potential predictor that may give some indication of the ensuing AZM event in the Atlantic which might in turn offer predictive value for the ISMR. As shown by (Keenlyside and Latif, 2007), Bjerknes feedback is the dominant causative mechanism for the evolution of AZM events. Consistent with earlier studies, we find that the evolution of low level zonal winds, heat content, and SST are different for warm or cold AZM events starting as early as boreal spring of the same year. Importantly, our analysis shows that the upper ocean heat content in the eastern equatorial Atlantic and zonal surface winds in the western equatorial Atlantic during boreal spring season are indicators of an impending AZM event. This in turn should provide us with valuable early clues to an imminent ISMR anomaly through the AZM's impact on monsoon depressions and via its teleconnection to the monsoon with a reasonable lead-time. We believe that these novel causal linkages offer a testable hypothesis for the state-of-the-art coupled climate models used to forecast the Indian summer monsoon, especially during non-ENSO years.

Our analysis shows that there is a clear and consistent correlation between the rainfall over the Western Ghats, and heat content and low level zonal winds in the equatorial Atlantic (Fig. 3.6d and Fig. 3.7d). However, the same cannot be observed in the case of correlation between rainfall over Central India and equatorial Atlantic zonal winds (Fig. 3.7b) although the

correlation is a bit more convincing between the heat content and the rainfall (Fig. 3.6b). This may be because the rainfall over Central India has several contributing factors like the monsoon depressions in the Bay of Bengal and the direct moisture transport by the southwest monsoon winds (see Chapter 3 of Pant and Kumar, 1997). The rainfall distribution over India is not uniform and different mechanisms may be operating in determining the rainfall over different parts of India (e.g., Rao, 1976; Krishnamurthy and Shukla, 2000; Vecchi and Harrison, 2004). As depicted in Fig. 3.1, the influence of AZM too is not uniform over India and that might explain why there is a difference in correlations with rainfall over Central India and the Western Ghats (Fig. 3.6 and Fig. 3.7). For example, a relation between the heat content of the eastern Indian Ocean and monsoon droughts was reported by (Krishnan et al., 2006). It is possible that the impact of AZM on ISMR is not only confounded by ENSO but also by the IOD.

Although different generation mechanisms of AZM have been proposed (Enfield and Mayer, 1997; Latif and Grötzner, 2000; Huang et al., 2002; Foltz and McPhaden, 2010; Lübbecke et al., 2010; Lübbecke, 2013; Lübbecke et al., 2014), none of them can explain the occurrence of all AZM events. Hence, in a sense, the total interannual variability of the equatorial Atlantic can be said to be achieved only through the synthesis of different mechanisms. However, at the heart of almost all of these mechanisms lies the Bjerknes feedback, which is often initiated by a wind anomaly in the western equatorial Atlantic, and is found to explain most of the variability associated with AZM. In this chapter, we are primarily interested in the coherent changes in different components of the Bjerknes feedback that may foretell the occurrence of AZM events and thereby the ISMR, specifically during non-ENSO years.

Our findings are essentially consistent with Ding et al. (2010) in that the heat content anomalies in the equatorial Atlantic precede the changes in Atl3 SST associated with the AZM. In addition, the existence of a relationship between the AZM and rainfall over India is reported by some earlier studies (e.g., Kucharski et al., 2008) as well as in our recent study Pottapinjara et al. (2014). Naturally, as one would expect, a predictive value for the Indian monsoon in the heat content in the equatorial Atlantic is of utmost importance, especially during non-ENSO years, and is indeed shown to exist by our analysis. Unfortunately, with our current analysis, why the correlations between the seasonal (JJAS) mean rainfall and the heat content in the EEA drop in May (Fig. 3.4) cannot be explained. These require some sensitivity experiments with models and this analysis can be performed with forced ocean and coupled climate models

separately but we will not pursue this problem in this thesis.

Unlike Ding et al. (2010), the local relation we seek between the EEA heat content and SST is driven by maximum correlation specifically for predictive value to ISMR. It should be noted that the local and remote forcing of the thermocline variability in the EEA and the east-west contrast (Busalacchi and Picaut, 1983) is lost in the analysis of (Ding et al., 2010) due to their averaging of the heat content over the tropical Atlantic and thus the lead time of their heat content with the AZM is about a season in contrast to the one-month lead we find here between the EEA heat content and the AZM. The role of the Bjerknes feedback and the east-west contrast we report must play a role in determining the anomalous ITCZ position and the strength of the correlation between the meridional and zonal modes and thereby the link between the ITCZ and Indian monsoon. This aspect partly motivates our effort presented in Chapter 4.

In our analysis, the composite evolution of different components of the Bjerknes feedback of the warm AZM events does not appear to be a mirror image of that of cold events (Fig. 3.3). It may be due to differences in the timing and strength of the associated cold tongue. The possibility of other processes playing a role in generating AZM warm events and the likely absence of Bjerknes feedback in some events might be a reason why composites of winds and heat content for the warm AZM events do not appear so smooth (Fig. 3.3). This possibility is addressed in part in Chapter 4.

Chapter 4

Asymmetric relation between boreal spring position of Atlantic Inter-tropical Convergence Zone and Atlantic Zonal Mode¹

In Chapter 3, by taking the advantage of the inherent Bjerknes feedback mechanism of the Atlantic Zonal Mode (AZM), we have shown that the early signs of an AZM event in surface zonal winds and heat content in the equatorial Atlantic during boreal spring can give us valuable clues to the ensuing Indian Summer Monsoon (ISM) through the teleconnections discussed in Chapter 1. Extending that effort in this chapter, we examine the relationship between the AZM and the meridional movement of the spring Atlantic Intertropical Convergence Zone (ITCZ), another precursor to the AZM. Additionally, we gain some important insights into different causative mechanisms of AZM including that in which spring ITCZ movement plays a crucial role. These results can be expected to enhance our understanding of the AZM as well as that of chronic model biases and contribute ultimately to the predictability of the ISM, among other things.

¹An edited version of this chapter appeared in *Journal of Climate* as Pottapinjara et al. (2019): ‘On the Relation between the Boreal Spring Position of the Atlantic Intertropical Convergence Zone and Atlantic Zonal Mode’ ©American Meteorological Society

4.1 Introduction

It is well known that the interannual variability of the Indian Summer Monsoon Rainfall (ISMR) is governed by both internal dynamics and external factors such as El Niño-Southern Oscillation (ENSO; Sikka, 1980; Keshavamurty, 1982; Mooley and Parthasarathy, 1984; Philander et al., 1989; Webster et al., 1998), Indian Ocean Dipole (IOD; Saji et al., 1999; Behera et al., 1999; Ashok et al., 2001; Slingo and Annamalai, 2000), the dominant interannual modes in the tropical climate. As discussed in Chapter 1, the Atlantic Zonal Mode (AZM), akin to but weaker than ENSO (Zebiak, 1993), is active during boreal summer (June–August) contemporaneous with the Indian Summer Monsoon (ISM). It has been shown to influence the ISMR by recent studies (Kucharski et al., 2008, 2009; Wang et al., 2009; Pottapinjara et al., 2014; Richter et al., 2014; Kucharski et al., 2016; Yadav, 2017) as well as in Chapter 3. The warm (cold) phase of AZM tends to reduce (enhance) rainfall over India with its effect being especially significant when there is no co-occurring ENSO event (Chapter 3; Wang et al., 2009). On the other hand, the AZM can sow the seeds for the development of an ENSO event (Rodríguez-Fonseca et al., 2009; Ham et al., 2013; Martín-Rey et al., 2015; Kucharski et al., 2016). Therefore, an enhanced understanding of different causative mechanisms of AZM will aid in better prediction of the ISM as well as a better understanding of ENSO dynamics, among other things.

In addition to the AZM, the interannual variability in the tropical Atlantic is dominated by the Atlantic Meridional Mode (AMM; Nobre and Shukla, 1996; Chiang and Vimont, 2004; Xie and Carton, 2004), which is active during boreal spring. It is characterized by SST anomalies of opposite sign on either side of the equator (Fig. 4.1; see Section 4.2 for the definition). The two modes, AMM (active in boreal spring) and AZM (active in boreal summer), are related via the meridional displacement of the Inter-tropical Convergence Zone (ITCZ) in boreal spring (Servain et al., 1999; Murtugudde et al., 2001). These early studies indicate that the anomalous meridional movement of ITCZ during spring is an important precursor to the AZM. The factors that influence the variability of the boreal spring ITCZ are discussed in the following. Chiang et al. (2002) attribute the variability of the ITCZ position in the Atlantic to two factors, namely, the cross-equatorial SST gradient (or AMM) and the remote forcing from the equatorial Pacific through ENSO. The SSTs in the tropical North Atlantic (TNA), the northern lobe of AMM, can be influenced by ENSO (e.g., Huang, 2004; Amaya and Foltz, 2014), among other things. The TNA SST warming occurs a season after the mature phase of ENSO warm

event (Enfield and Mayer, 1997; Giannini et al., 2000; Yang et al., 2018). The role of AMM in the meridional movement of the ITCZ during spring has already been discussed in previous studies (Servain et al., 1999; Murtugudde et al., 2001). Apart from reiterating the importance of AMM, Chiang et al. (2002) suggest that ENSO can also modulate the meridional position of the ITCZ during spring in the Atlantic through Walker circulation. An El Niño peaking in boreal winter suppresses convection over equatorial Atlantic in the following spring via the descending branch of anomalous Walker circulation. Without presenting the details, they note that as a secondary effect of the suppression of rainfall over the equatorial Atlantic, the ITCZ moves north. Lee et al. (2008) stress the importance of persistence of the tropical Pacific forcing into boreal spring in determining the tropical north Atlantic (TNA) SST and thus the ITCZ movement. García-Serrano et al. (2017) suggest that ENSO influences TNA SST through a remote secondary Gill-type mechanism. In this mechanism, for example, a decaying El Niño that persists into boreal spring can suppress the convection over the deep tropical Atlantic and generate two upper-level cyclonic circulations as though a heat sink is located over the same region. From the above we conclude that the Atlantic ITCZ during spring can be affected directly (without much time lag) by AMM and also via convective processes by a decaying ENSO (Neelin and Su, 2005), or indirectly (with a time lag of few months) via TNA variability (Czaja et al., 2002; Czaja and Frankignoul, 2002; Wu and Liu, 2002; Yang et al., 2018). Putting it in the context of the relationship between the AMM, ITCZ and AZM we mentioned earlier, the ITCZ captures different remote influences apart from the influence of AMM and preconditions the development of the AZM. Hence, in this chapter, we focus on the spring ITCZ movement rather than on AMM.

As mentioned earlier, the meridional movement of the Atlantic ITCZ during spring is an important precursor to the AZM. The relation between the two concisely is that the spring ITCZ migration, through the resulting spring zonal wind anomalies over the equator, triggers the Bjerknes feedback and leads to an AZM event in the following summer. The Bjerknes feedback involves western equatorial Atlantic zonal wind anomalies forcing thermocline depth variations in the eastern equatorial Atlantic which then influence the SST anomalies in the east which in turn positively feedback to the wind anomalies (Keenlyside and Latif, 2007). The correlation between the ITCZ position during spring and concurrent western equatorial Atlantic zonal winds is -0.82 , significant at 5% level (see Table 4.1 and Section 4.2 for details). Given the apparent criticality of the spring western equatorial Atlantic zonal winds in the formation of

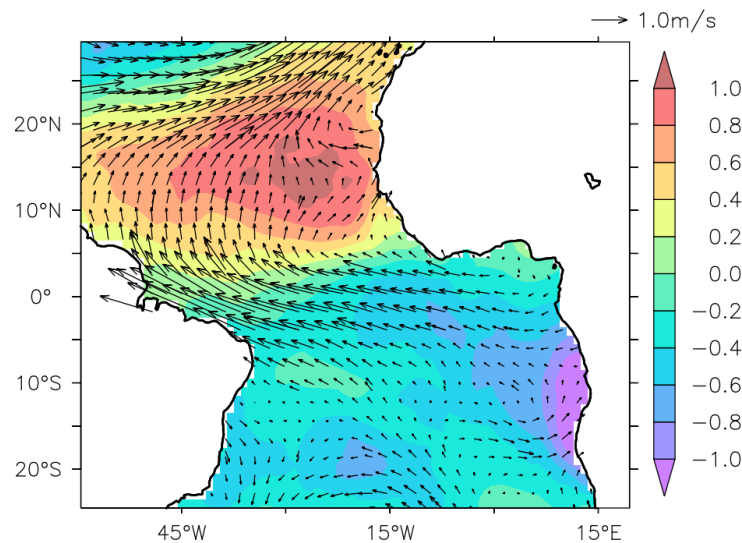


Figure 4.1: Regressions of the Atlantic Meridional Mode (AMM) index onto March–May anomalies of SST ($^{\circ}\text{C}$) and winds (m s^{-1}). See Section 4.2 for the definition of AMM index.

an AZM event, it may appear that the relation between the spring ITCZ and AZM is quite robust. However, the correlation between spring ITCZ and Atlantic 3 SST index (Atl3; see Section 4.2 for definition) that characterizes the AZM reduces to a moderate -0.34 , still significant at 5% level but just above the threshold of significance (Table 4.1). This raises an interesting set of questions: what causes the drop in correlations? Is there a limiting factor in the Bjerknes feedback chain that may explain the drop? Does the relation hold equally well for both cold and warm AZM events? In other words, is the ITCZ–AZM relation symmetric? More broadly, are the generation mechanisms of warm AZM events the same as that of cold events? This question is motivated by a result from ENSO diversity studies which highlight that there is more diversity in the warm events in the tropical Pacific (El Niño) and that differences between the cold events (La Niña) are subtle (Kug and Ham, 2011; Ren and Jin, 2011; Capotondi et al., 2015; Chen et al., 2015; Ashok et al., 2017; Timmermann et al., 2018). With regard to the questions we have raised, a few recent reports make a passing mention of this knowledge gap as discussed below.

Notably, extending the earlier studies (Servain et al., 1999; Murtugudde et al., 2001), a recent study by Foltz and McPhaden (2010) shows that the equatorial zonal winds caused by positive AMM (anomalously warm north and/or cold south; Fig. 4.1), force off-equatorial oceanic Rossby waves which are reflected as downwelling Kelvin waves from the western equatorial Atlantic opposite in sign to the directly forced Kelvin waves. The reflected downwelling Kelvin waves in turn terminate the AZM warm event towards the end of summer. The conclu-

	CC		CC
MAM AMM <i>vs</i> MAM ITCZ	0.81	MAM AMM <i>vs</i> JJA Atl3	-0.31
MAM ITCZ <i>vs</i> MAM zonal wind	-0.82	MAM ITCZ <i>vs</i> JJA Atl3	-0.34
MAM zonal zind <i>vs</i> AMJ EEA HC	0.65	MAM zonal wind <i>vs</i> JJA Atl3	0.54
AMJ EEA HC <i>vs</i> MJJ WEA HC	-0.69	AMJ EEAHC <i>vs</i> JJA Atl3	0.50
		MJJ WEAHC <i>vs</i> JJA Atl3	-0.43

Table 4.1: Correlation Coefficients (CC) between different parameters averaged over different months (MAM: March–May; AMJ: April–June; MJJ: May–July; JJA: June–August). AMM: Atlantic Meridional Mode; AZM: Atlantic Zonal Mode; zonal wind: central to western equatorial Atlantic zonal winds; EEA HC: Eastern Equatorial Atlantic Heat Content; WEA HC: Western Equatorial Atlantic Heat Content; ITCZ: Inter-tropical Convergence Zone. See Section 4.3 and Fig. 4.3 for the regions over which different parameters are averaged.

sion of Foltz and McPhaden (2010) that AMM and AZM are related, is from a correlation analysis which is insensitive to the asymmetry, if any, in the relation. With regards to differences between cold and warm AZM events during their lifetime, Lübbecke and McPhaden (2017) show, based on a composite analysis, that the Bjerknes feedback components of cold events are mirror images of those of warm events, i.e., AZM is essentially symmetric. However, Lübbecke and McPhaden (2017) do not rule out the possibility of existence of an asymmetry in forcing of cold and warm events. While the former study did not raise the question of existence of any asymmetry between the ITCZ (or AMM) and AZM, the latter did not rule out such a possibility. Putting these in context, almost all of these previous studies imply that the anomalous northward (southward) shift of the ITCZ in spring can lead to a cold (warm) AZM event, which implicitly implies a symmetric relation between the ITCZ in spring and AZM. Further, the studies on the diversity of generation mechanisms of AZM are absent, to the best of our knowledge. Hence, despite the above mentioned studies, the questions we raised remain unanswered and we attempt to address them in this study. These answers should contribute to the predictability of the monsoon (ISM), especially during non-ENSO AZM years by improving our understanding of the AZM which is shown to influence the ISM in Chapter 3.

It may be recollected that in Chapter 3, we have shown that from the early signs in the zonal wind and heat content in the equatorial Atlantic in boreal spring, an oncoming AZM event may be foretold which might in turn give us clues about the ISMR one season in advance. However, the causative mechanisms that trigger wind anomaly in the equatorial Atlantic which is a necessary factor for the development of AZM are not yet fully understood. Understanding

different causative mechanisms of AZM events may contribute to the predictability of the ISMR by providing any signals that stretch further back in time giving an advanced warning of a forthcoming AZM event and thus of the impact on ISMR. It may also contribute to the knowledge of different biases that can arise in the coupled models especially those that are used to forecast the monsoon and thereby provide process understanding for the improvement of such models.

4.2 The relevance of AMM and spring ITCZ to the AZM

As already discussed above, studies such as Servain et al. (1999), Murtugudde et al. (2001), and Foltz and McPhaden (2010) demonstrate the existence of a relationship between the AMM, ITCZ, and AZM. This relation is shown in Table 4.1 as well but before going into details, we briefly discuss here the indices of AZM, AMM, and ITCZ, and the datasets used to obtain those indices. In this chapter, we have used the same method of identifying the AZM events and the SST data product (HadISST; Rayner et al., 2003) as in Chapter 3 (see Section 3.2). As discussed in Chapter 3, a warm (cold) AZM is considered to occur in any year when the June–August average of Atl3 index exceeds (falls below) $+1$ (-1) standard deviation (Zebiak, 1993; Burls et al., 2012). Following this definition, during the study period (1979–2013), we identify nine warm AZM events which occurred in 1984, 1987, 1988, 1995, 1996, 1998, 1999, 2008, and 2010 and six cold AZM events in years 1982, 1983, 1992, 1994, 1997, and 2005. This list is consistent with that in Chapter 3. Further, following Foltz and McPhaden (2010), AMM index is defined as the difference between SST anomalies averaged over northern (5°N – 28°N and 60°W – 20°W) and southern (20°S – 5°N and 30°W – 10°E) tropical Atlantic. The meridional movement of ITCZ is tracked using the latitude of the zero meridional surface wind speed along the longitude of 28°W in the latitudinal range of 5°S – 20°N (Servain et al., 1999). And the wind data used is taken from the European Centre for Medium Range Weather Forecasting (ECMWF)'s Reanalysis (ERA-Interim; Dee et al., 2011). In the remainder of this study, all seasons used are from the perspective of the northern hemisphere, unless mentioned otherwise.

As evident from Table 4.1, the AMM which is active during boreal spring is significantly correlated with the concurrent Atlantic ITCZ position (correlation coefficient of 0.81 significant at 5% level), and both AMM and spring Atlantic ITCZ are also related to the AZM in the following summer. Note that the correlation between Atl3 index and MAM ITCZ (-0.34)

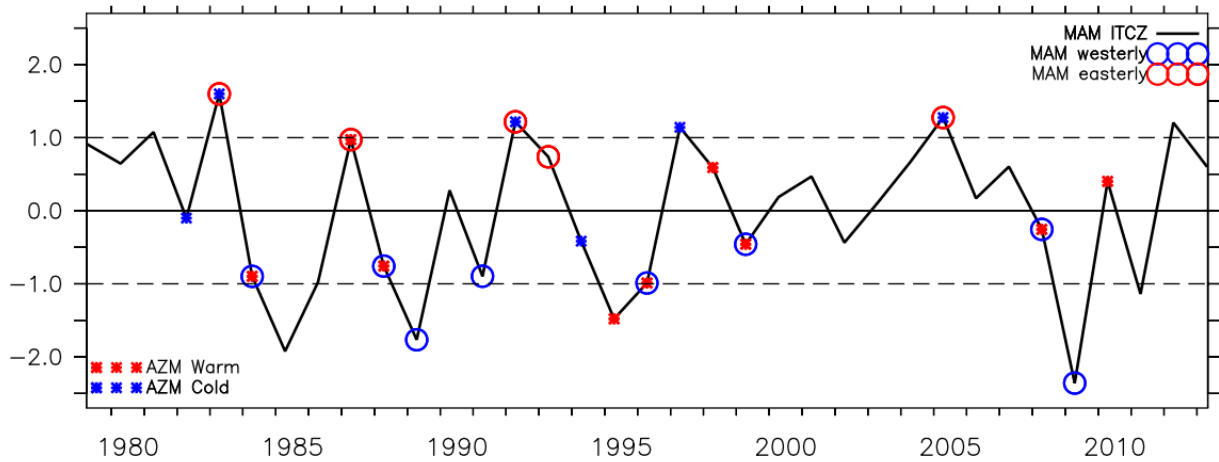


Figure 4.2: Interannual variations of anomalous meridional position of ITCZ in March–May (black). The time series is normalized by its standard deviation and standard deviation is indicated by a black dashed line. Whenever the central to western equatorial zonal wind in March–May is sufficiently strong crossing $+0.9$ (-0.9) of its respective standard deviation, i.e., westerly (easterly), it is indicated by blue (red) circles. Whenever the Atl3 SST in June–August crosses $+1$ (-1) of its respective standard deviation, i.e., when there is a warm (cold) AZM event, it is indicated by red (blue) stars.

is marginally higher than that with AMM (-0.31). Further, the correlation between MAM zonal winds (crucial for the development of AZM) and MAM ITCZ (-0.82) is also larger than that with zonal wind and AMM (-0.73). As discussed in Section 4.1, we focus on the ITCZ movement rather than on AMM in this study, and the above comparison of correlations supports our choice. In addition, these significant correlations suggest that understanding the ITCZ movement will give a fresher and potentially a different perspective on the asymmetry in its relation with AZM.

Concentrating on the spring ITCZ movement, Table 4.1 also shows that during the study period, the correlation between the spring ITCZ position and spring zonal winds is -0.82 but the correlation between ITCZ and JJA Atl3 index is -0.34 (0.33 is the threshold correlation at 5% significance level for a sample size of 35). The reduction in correlation implies that not all the meridional excursions of the spring ITCZ lead to AZM events in the following summer despite the variations in the position of ITCZ strongly affecting the spring equatorial zonal winds, a prerequisite for an AZM event.

4.3 Asymmetry in the relationship between the Atlantic spring ITCZ position and AZM

To see how many meridional excursions of ITCZ ultimately lead to the AZM events, the interannual variations of spring ITCZ position along with the indicator of the AZM occurrence (listed in Section 4.2) are plotted in Fig. 4.2. Whenever the spring ITCZ position exceeds its $+1$ (-1) standard deviation, the ITCZ is considered to be located anomalously north (south) from its mean position. From the figure, it can be seen that the ITCZ in spring is anomalously north in six years (1981, 1983, 1992, 1997, 2005 and 2012) and in four of these years (1983, 1992, 1997 and 2005), the AZM cold events occurred in the following summer. On the other hand, while the ITCZ is anomalously south in six years (1985, 1986, 1989, 1995, 2009 and 2011), an AZM warm event occurred in the subsequent summer in only one of these years (1995). It is worth mentioning that two AZM warm events that occurred in 1984 and 1996 have spring ITCZ position just short of the threshold of anomalous southward position, i.e., -1 standard deviation. The ratio of AZM cold (warm) events that are preceded by anomalous northward (southward) ITCZ in spring is 4:6 (1:9), i.e., 66% (11%). Even if we include the two ‘just-below-the-threshold’ warm events of 1984 and 1996, the ratio of warm AZM events preceded by southward migration of ITCZ in spring is 3:9 (33%), which is still significantly less than its counterpart for the cold AZM. Therefore, while an anomalous northward ITCZ in spring tends to give rise to an AZM cold event in the following summer, an anomalous southward position of the same is less likely to lead to an AZM warm event. Clearly, there is an asymmetry in the relation between the position of ITCZ in spring and AZM in the ensuing summer, an important result which has not been reported thus far.

Since the relation between ITCZ and AZM is skewed towards the cold events, to understand different processes involved when the northward displacement of ITCZ in spring leads to an AZM cold event in the following summer, we show the monthly evolution of composite anomalies of different fields including heat content in Fig. 4.3. The upper ocean heat content (per unit area) above 20°C isotherm as given by Eq. (3.2) is calculated using ocean temperature data from EN4 analysis of UK Met Office Hadley Centre (Good et al., 2013). A positive AMM type of SST configuration (relatively warm in the north and/or cold in the south; similar to Fig. 4.1) during February–May moves the ITCZ anomalously north in spring (MAM).

The resultant cross-equatorial winds strengthen the concurrent southeast trades and weaken the northeast trades around the equator in spring. The net result is an enhancement in the strength of easterlies over the equatorial band, a prerequisite for the development of a cold AZM event. The strengthened equatorial easterlies, in turn, result in the increased heat content in the western equatorial Atlantic by deepening the thermocline. An upwelling Kelvin wave propagates to the east to shoal the thermocline and leads to cooler SSTs in the following summer, thus leading to a cold AZM event. As already mentioned in Section 4.1, the AMM is not the only factor influencing the spring Atlantic ITCZ position but the other factors are not discussed here in Fig. 4.3 for the sake of simplicity.

It is interesting to inquire what gives rise to the asymmetry in the relation between the position of the ITCZ in spring and AZM. We pose a question as to whether the asymmetry can be explained by the findings of (Richter et al., 2014). Taking monthly means of ITCZ position and equatorial zonal winds, and compositing the winds over each unique ITCZ position during the entire study period, Richter et al. (2014) show that as the ITCZ moves from its southern most to its northern most position, equatorial zonal winds remain easterly and grow stronger almost linearly. Given that anomalous equatorial easterlies in spring are a precondition to a cold AZM, if a relation between anomalous spring ITCZ and contemporaneous anomalous equatorial zonal winds holds as presented in Richter et al. (2014), i.e., if any anomalous meridional movement of spring ITCZ produces concurrent anomalous equatorial easterlies, it would explain the skewness between spring ITCZ and AZM. But does such a relation exist in reality? The high negative and significant correlation in spring between the ITCZ and central to western equatorial Atlantic zonal winds of -0.82 (Table 4.1) tells us that the anomalous northward migration of ITCZ in spring is indeed associated with anomalous easterly winds over the central to western equatorial Atlantic. However, a southward migration of the ITCZ in spring is associated with westerly anomalies. A scatter plot between these two quantities (Fig. 4.4), underscores the same implying that the finding of Richter et al. (2014) cannot serve us to explain the asymmetry. Therefore, considering the importance of spring wind anomalies for AZMs, the reason for the asymmetry must lie elsewhere and the interaction of the seasonal cycle and the interannual anomalies may be crucial. The supposed contradiction between the result of Richter et al. (2014) and ours is discussed later in Section 4.7. The seemingly counterintuitive westerlies in the equatorial band associated with the anomalous southward movement of ITCZ in spring (analyzed in Table 4.1 and Fig. 4.4) can be explained by a careful observation of evolution of composites of wind

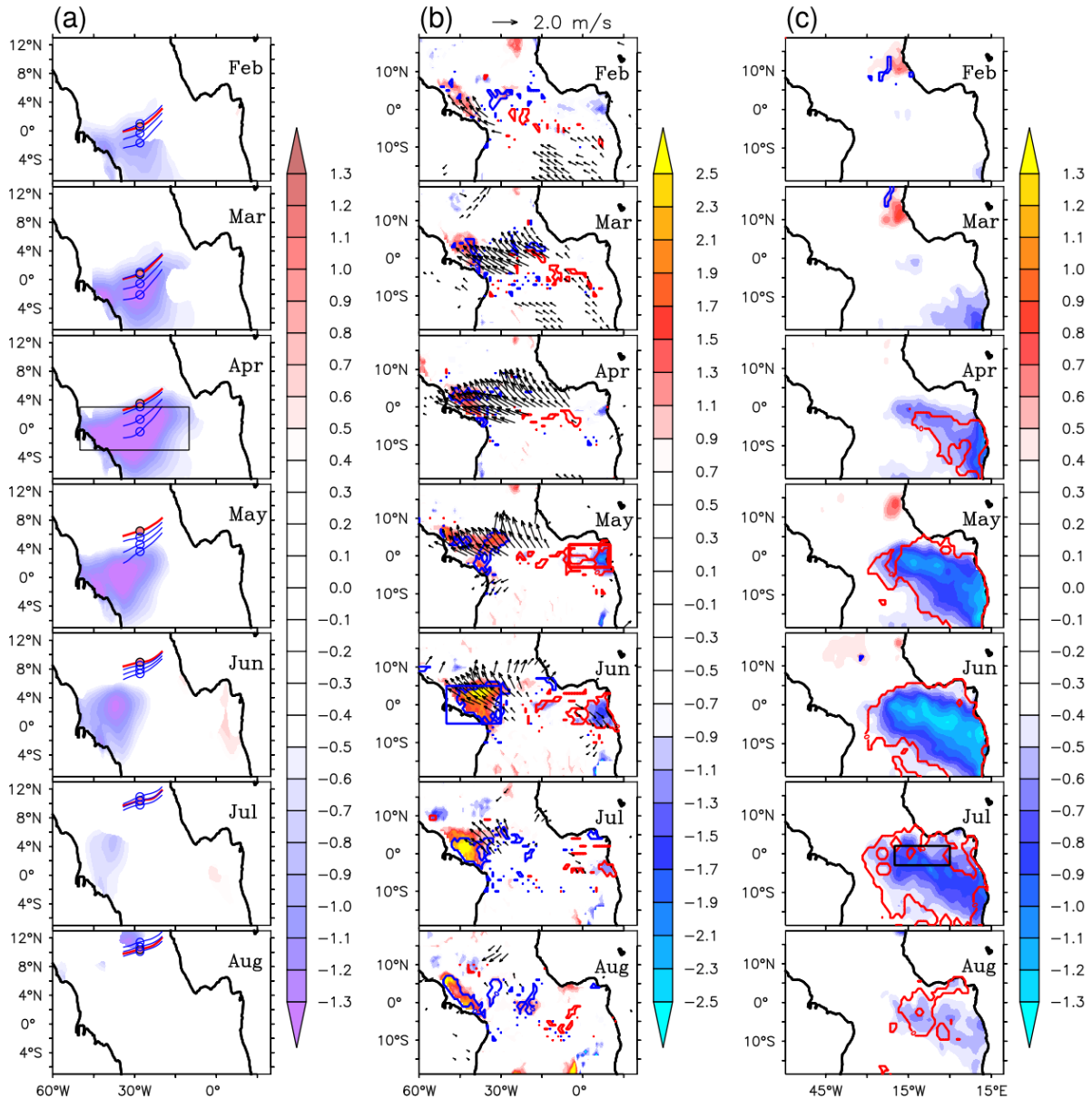


Figure 4.3: Monthly (February–August) evolution of composites of (a) ITCZ position (lines) and zonal wind anomalies (shading; ms^{-1}); (b) anomalies of winds (vector) and heat content (shading; 10^{10}Jm^{-2}) and (c) SST (shading; $^{\circ}\text{C}$) when the spring Atlantic ITCZ is anomalously northwards and gave rise to a cold AZM event. In (a), red line (dot inside a black circle) indicates the ITCZ position at respective longitudes (along 28°W) whereas the blue lines (circle) indicate the envelope of ITCZ variability, i.e., middle blue line (circle) indicates the climatological ITCZ position in that month, and the top and bottom blue lines (circles) indicate ± 1 standard deviation of the position from the mean in the same month. The calendar month is indicated on each subpanel. Only those zonal winds in (a) and vectors in (b) that are significant at the 5% level are shown. The significance of heat content anomalies in (b) and SST anomalies in (c) are indicated by line contours. The rectangular boxes in black [in (a); April], red [in (b); May], and blue [in (b); June] and thick black [in (c); July] indicate the regions over which anomalies of winds, eastern equatorial Atlantic heat content, western equatorial Atlantic heat content and SST are averaged respectively, for use in other analyses.

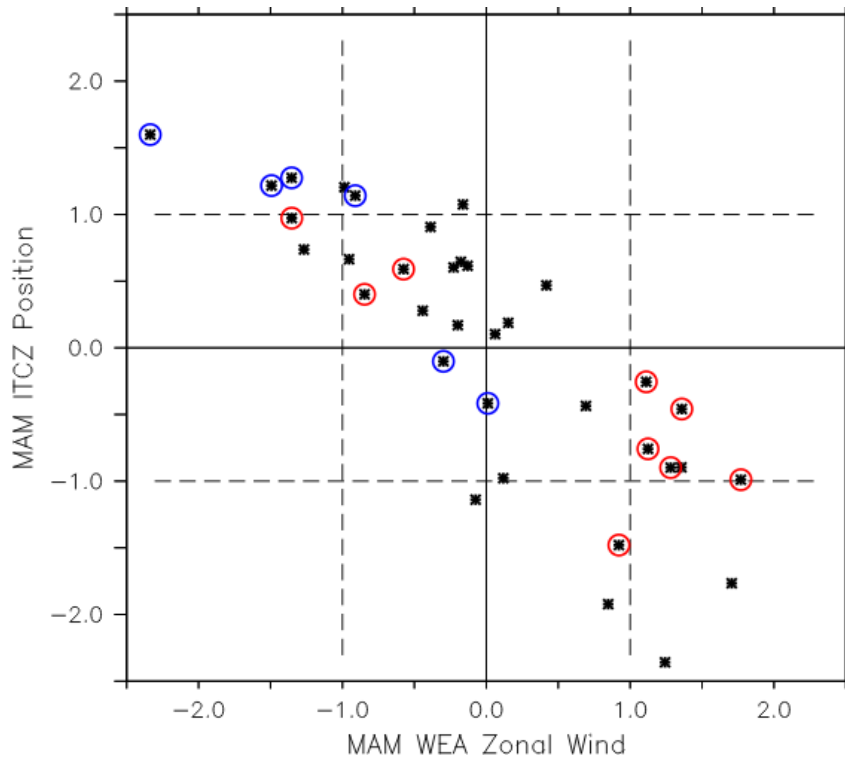


Figure 4.4: Scatter plot between the normalized indices of MAM western equatorial Atlantic (WEA) zonal winds (averaged over 3°S–3°N and 40°W–10°W) and MAM ITCZ position. The black dashed horizontal (vertical) lines indicate the ± 1 standard deviation of ordinate (abscissa). The points surrounded by blue (red) circles indicate the years in which cold (warm) AZM events occurred in the following summer.

anomalies of individual events when the ITCZ is anomalously south in spring (Fig. 4.5). The wind anomalies in spring that are northerly or northeasterly just north of the equator turn and develop a westerly component as they cross the equator (Fig. 4.5b). The westerly component just south of the equator is stronger than the easterly component just north of the equator, giving rise to net westerly winds when averaged in the equatorial band for the analysis in Table 4.1 and Fig. 4.4. The mechanisms for these westerly anomalies need further investigation but we will not discuss it in this study.

The reason for the asymmetry in fact lies in the peculiar features of climatological movement of the ITCZ in the Atlantic (Fig. 4.6). From the figure, it may be noted that during January–April the mean position of the ITCZ is relatively close to the equator and the variability of the position of ITCZ is at its highest. The drastic change both in the mean position and the variability occurs during May–June, with the position of the mean ITCZ moving north by about 6 degrees and the standard deviation falling to about $\frac{1}{3}$ of that in April (standard deviation is 1.743 and 0.576 degrees latitude in April and June, respectively). During the study period, i.e.,

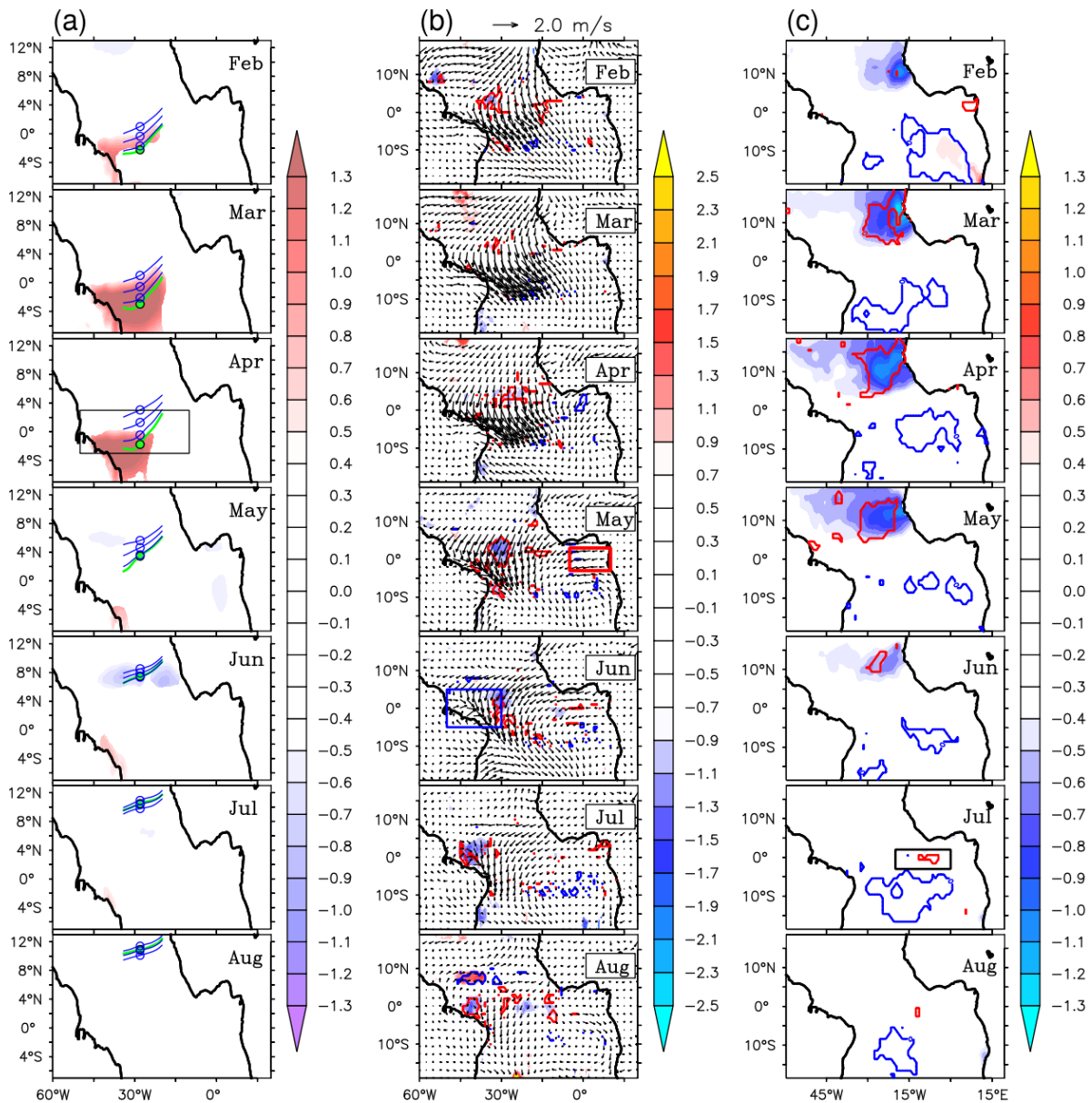


Figure 4.5: Same as Fig. 4.3 but the composites of different fields presented here are of events when the spring ITCZ is anomalously in the south. As discussed in Section 4.3, except in the year 1995, no southward movement of spring ITCZ led to a warm AZM event in the ensuing summer. This singular event is excluded while computing the composite to ensure its homogeneity as well as to highlight the predominantly westerly nature of winds in the western equatorial Atlantic in all events included. The composite of ITCZ position in (a) is shown in green for better visibility. In (b), even the non-significant wind anomalies are also shown to highlight the variation of their strength across the equator.

1979–2013, the position of ITCZ in spring is anomalously southward in six years and in four of those years, winds that are northerly or northeasterly just north of equator develop a strong westerly component upon crossing the equator in spring, as noted above (winds during individual events are not shown but it can be observed from their composite in Fig. 4.5b as well). The

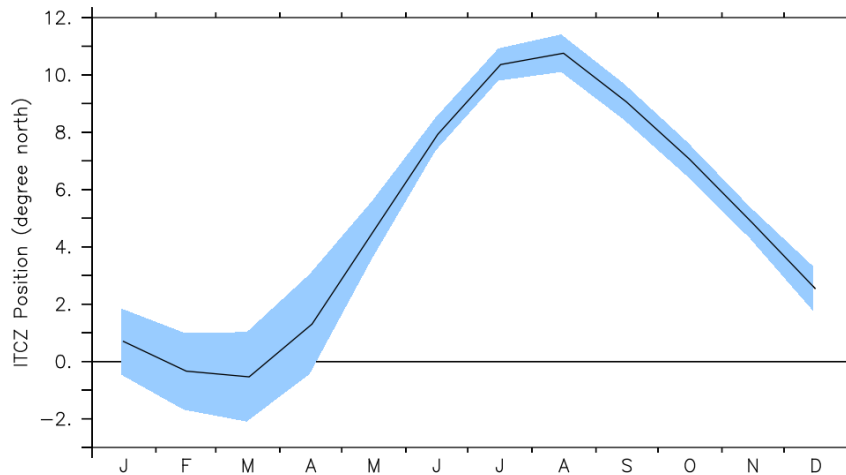


Figure 4.6: Monthly evolution of the mean position of the ITCZ in the Atlantic (black line; along 28°W; °N) with the shading indicating the ± 1 standard deviation about the mean in the respective months.

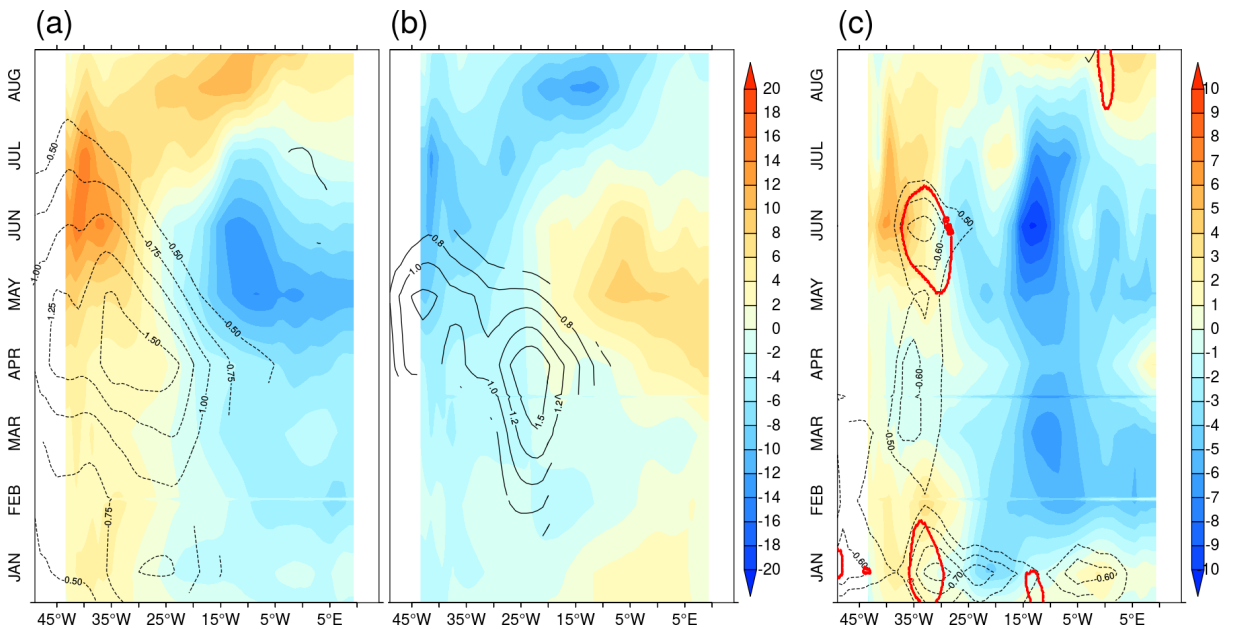


Figure 4.7: (a),(b): Hovmöller diagram of the composite of anomalies of thermocline depth (shading) overlaid by zonal winds (contours) over the equator in the Atlantic when the MAM ITCZ is anomalously north (south) and zonal wind anomalies over WEA are easterly (westerly). (c) Hovmöller diagram obtained by adding the anomalies shown in (a) and (b) [= anomalies in (a) – negative of anomalies in (b)], intended to show the dominance of anomalies in (a) over that in (b). In (a) and (b), only the wind anomalies that are significant at the 5% level are shown. In (c), the significant wind anomalies are indicated by the contour lines in red. Significance contour lines become discontinuous if the zonal winds between the two ends of a contour are not significant.

maximum of this wind anomaly is centered around 7°S with weaker westerlies over the western equatorial Atlantic (WEA) compared to easterlies in spring in the same region when the ITCZ is anomalously north shown in Fig. 4.3b. The westerlies can drive an equatorial downwelling

Kelvin wave and remotely deepen the thermocline in the east, if they are sufficiently strong. Nonetheless, the westerlies weaken further in May–June as the climatological ITCZ moves into the northern hemisphere and the inherent variability of the ITCZ itself reduces as shown in Fig. 4.6. This leads to a premature death of a weak incipient warm event resulting ultimately in a very low proportion of AZM warm events surviving into the summer. Fig. 4.7 shows that in the years when spring ITCZ position is anomalously south and winds are westerly over the WEA, the westerlies are not as strong and are less persistent in contrast to those years when the position of ITCZ in spring is anomalously north and winds over WEA are easterly.

In light of the above explanation, a reconsideration of why an anomalous northward movement of ITCZ in spring is highly likely to lead to a cold AZM event, is necessary. The fact that the mean position of the ITCZ in February–March is south of the equator, implies that even when the ITCZ is anomalously north, the center of maximum easterly wind anomalies is closer to the equator and thus the magnitude of the easterlies over the WEA is stronger than that of the westerly wind anomalies associated with anomalous southward position of the ITCZ (Fig. 4.7). The strong spring easterlies shoal the thermocline in the east preparing the ground for an oncoming AZM cold event but weaken in early summer as the mean ITCZ itself moves further north. Nevertheless, the easterlies persist albeit restricted to an area to the west of 30°W. In a nutshell, the asymmetry in the relation between the position of Atlantic ITCZ in spring and AZM is inherent in the seasonal cycle itself.

From earlier studies (Murtugudde et al., 2001; Lübbecke and McPhaden, 2017), and our analysis presented in Fig. 4.3 and Table 4.2, we identify the different factors involved in the mechanism where the anomalous spring migration of ITCZ leads to an AZM in the following summer to be: (i) position of ITCZ in spring (MAM ITCZ), (ii) the concurrent zonal winds averaged over the central to western equatorial Atlantic (3°S–3°N and 50°W–10°W), (iii) heat content averaged over the eastern equatorial Atlantic in mid-spring to early summer (AMJ EEA HC; 3°S–3°N and 5°W–15°E), (iv) heat content averaged over the western equatorial Atlantic in late spring to mid summer (MJJ WEA HC; 5°S–5°N and 50°W–30°W) and (v) SST averaged over the Atl3 region in summer (JJA Atl3; 3°S–2°N and 20°W–0°W). Note that these are closely related to the Bjerknes feedback components discussed in Chapter 3. Monthly evolution of composites of these different factors averaged in their respective regions are presented in Fig. 4.8 to identify any distinct signatures associated with the cold AZM events that are pre-

	MAM ITCZ	MAM Zonal Wind	AMJ Zonal Wind	MJJ Zonal Wind	MAM WEA HC	AMJ WEA HC	MJJ WEA HC	MAM EEA HC	AMJ EEA HC	MJJ EEA HC	JJA Atl3
MAM AMM	0.81	-0.73	-0.62	-0.47	0.78	0.82	0.82	-0.47	-0.60	-0.53	-0.31
MAM ITCZ		-0.82	-0.70	-0.47	0.63	0.70	0.79	-0.35	-0.47	-0.41	-0.34
MAM Zonal Wind			0.96	0.82	-0.71	-0.82	-0.89	0.51	0.65	0.54	0.54
AMJ Zonal Wind				0.93		-0.76	-0.83		0.65	0.56	0.66
MJJ Zonal Wind							-0.67			0.53	0.76
MAM WEA HC								-0.45	-0.47	-0.34	-0.29
AMJ WEA HC								-0.56	-0.65	-0.52	-0.39
MJJ WEA HC								-0.53	-0.69	-0.60	-0.43
MAM EEA HC											0.52
AMJ EEA HC											0.50
MJJ EEA HC											0.44

Table 4.2: Correlations between different factors representing a chain of processes with respect to relation between AMM, ITCZ and AZM. The abbreviations are the same as in Table 4.1. Additionally, the first three lettered string of each factor represents the season in which the factor is averaged (e.g., MAM: March-April-May; AMJ: April-May-June). The cross-correlations among the factors MAM ITCZ, MAM zonal wind, AMJ EEA HC, MJJ EEA HC, JJA Atl3 are the highest and are shown in blue color. These factors are used in further analysis in 4.9.

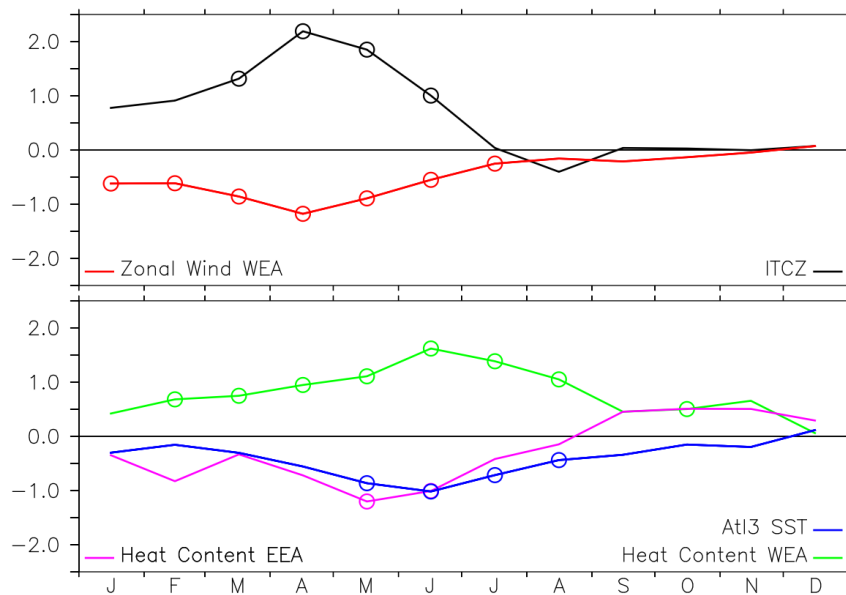


Figure 4.8: Monthly evolution of composites of anomalies of (top) zonal winds (ms^{-1}) in the western equatorial Atlantic and position of ITCZ ($^{\circ}$ latitude) and (bottom) SST averaged over Atl3 region ($^{\circ}\text{C}$), heat content (10^{10} Jm^{-2}) averaged in the western/eastern equatorial Atlantic, composited in the years when MAM ITCZ is north and leads to the development of a cold AZM event in the subsequent summer. The circles on each line indicate when the respective composite means become significant at the 5% level.

ceded by northward spring ITCZ. From the figure, it can be seen that the maximum northward displacement of the ITCZ occurs during March-April-May (MAM) with the central to western equatorial easterlies peaking simultaneously. The heat content in the eastern equatorial Atlantic reaches its minimum during April-May-June (AMJ) while the heat content in the western equatorial Atlantic attains its maximum during May-June-July (MJJ). The SST anomalies in the Atl3 region are at their coldest during June-July-August (JJA). The timings of these factors agree with the previous studies (Keenlyside and Latif, 2007) and with Fig. 3.5, and also yield the highest correlations with the links above and below in the chain of processes (Table 4.2). These seasonal timings of when different factors become important will be used later to show the distinction of the cold AZM events preceded by northward ITCZ in spring.

4.4 Relationship between the meridional migration of spring ITCZ and strong canonical AZM events

In the above, we have shown the existence and cause of asymmetry in the relation between the spring Atlantic ITCZ and AZM. We will now explore if the cold AZM events preceded by anomalous northward spring ITCZ, have any distinct features. However, before doing that, a useful background information is provided first. As mentioned earlier, the Bjerknes feedback is a dominant mechanism that explains AZM (Keenlyside and Latif, 2007) although there are several other mechanisms contributing (Foltz and McPhaden, 2010; Zhu et al., 2012; Lübbecke, 2013; Richter et al., 2013; Lübbecke et al., 2018). Richter et al. (2013) classify AZM events into those that can and cannot be explained by ENSO-like dynamics. The distinctive criterion that Richter et al. (2013) adopt for the classification is that if a warm (cold) AZM event in summer is preceded by westerly (easterly) winds in the central to western equatorial Atlantic in spring, then it is referred to as a canonical warm (cold) event. On the other hand, if it is preceded by winds of opposite sign, it is called a non-canonical event. It is worth noting that oceanic subsurface changes, which are an important part of the Bjerknes feedback, are not taken into account in this classification. Also, those events which have near neutral winds cannot be covered by their classification. Modifying their definition to account for the above events as well, we classify a ‘strong canonical’ warm (cold) event to be one that is preceded by westerly winds in March–May, positive (negative) heat content in the eastern equatorial Atlantic in April–June and negative (positive) heat content in the western equatorial Atlantic in May–July. All those events that do not meet this criterion are classified as ‘non-strong-canonical’ warm (cold) events. Note that the respective timings when different Bjerknes components become important are only for a typical AZM event (Keenlyside and Latif, 2007). Interannual variations of these different factors are normalized by their respective standard deviations and plotted in Fig. 4.9. To categorize an AZM event as ‘strong canonical’, the amplitude of these factors (with the exception of winds) are required to exceed one respective standard deviation. This condition is relaxed in the case of winds as they tend to be noisy. The threshold of amplitude is lowered to 0.9 times their standard deviation. In addition, the relaxation accommodates several events for which the amplitude of winds falls short of the threshold imposed on all other factors, i.e., one standard deviation.

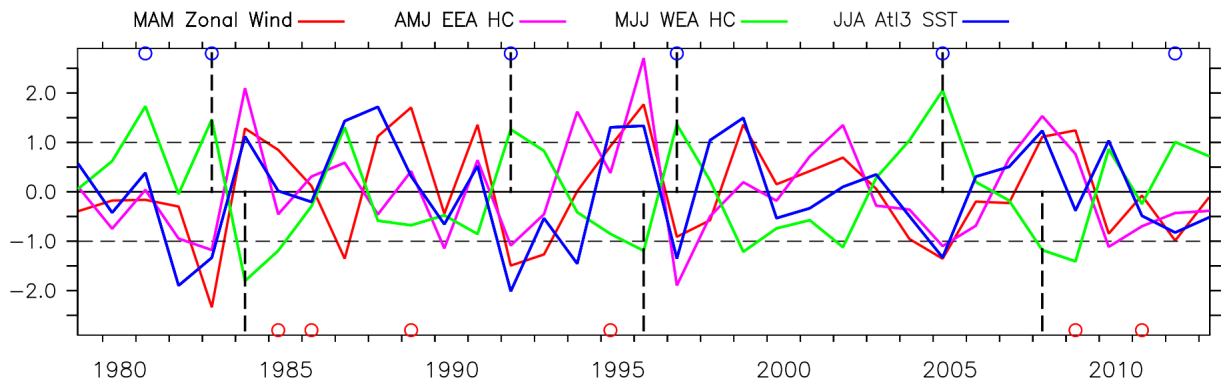


Figure 4.9: Interannual variations of anomalies of western equatorial Atlantic zonal winds in March–May (red; ms^{-1}), eastern equatorial Atlantic heat content in April–June (purple; 10^{10} J m^{-2}), western equatorial Atlantic heat content in May–July (green; 10^{10} J m^{-2}) and SST in the characteristic Atl3 region in June–August (blue; $^{\circ}\text{C}$). Strong canonical cold (warm) events are indicated with black dashed line in upper (lower) portion. All the time series are normalized by their respective standard deviation. Whenever the spring ITCZ crosses +1 (–1) standard deviation, i.e., north (south), it is indicated with blue (red) thick circles.

Going by this definition, it can be seen from Fig. 4.9 that the strong canonical (non-strong-canonical) cold AZM events are 1983, 1992, 1997 and 2005 (1981 and 1994). For every strong canonical cold event, normalized factors clearly exceed one respective standard deviation along with the spring ITCZ position in Fig. 4.2. The strong canonical (non-strong-canonical) warm events are 1984, 1996 and 2008 (1987, 1988, 1995, 1998, 1999 and 2010). None of the strong canonical warm events have the spring ITCZ located further southwards than the threshold position, although the ITCZ was appreciably southwards in 1984 and 2008. The proportion of strong canonical cold (warm) AZM events is 4:6 (3:9), i.e., 66% (33%). In other words, the proportion of strong canonical events is larger in case of cold events than that of warm events. It is interesting to note that all strong canonical cold AZM events are preceded by northward movement of ITCZ in spring whereas only two out of three strong canonical warm events are preceded by southward movement of ITCZ in spring. The proportion of strong canonical events, either warm or cold, that can be explained by the spring movement of ITCZ is 86%. From this, we may conclude that most of the strong canonical AZM events can be explained by anomalous spring position of ITCZ and this relation is stronger in the case of cold events compared to that of the warm events. This point is also demonstrated by the drop in correlation between anomalous ITCZ position in MAM and JJA Atl3 index. The correlation when the cold events preceded by ITCZ northward movement in spring are included is -0.34 and is significant at 5% level (Table 4.1). The correlation drops to a statistically insignificant -0.13 , when those events are removed. A major reason for the reduction in the correlation

may be attributed to changes in the heat content in the western equatorial Atlantic (MJJ WEA HC) as it is the only factor whose correlation falls below significance after removing the strong canonical cold AZM events. The correlations between JJA Atl3, and MAM zonal wind, AMJ EEA HC and MJJ WEA HC, the factors plotted in Fig. 4.9, dip from 0.54, 0.50, -0.43 as shown in Table 4.1 to 0.36, 0.34 and -0.20 , respectively, when the events are excluded. It must be clarified that we separate AZM events into ‘strong canonical’ and ‘non-strong-canonical’ as opposed to the separation of ‘canonical’ and ‘non canonical’ of Richter et al. (2013) that is based on Bjerknes feedback mechanism and our classification of ‘non-strong-canonical’ does not imply that those events cannot be explained by the said mechanism. On a related note, it should also be mentioned that our classification of AZM events into ‘strong canonical’ and ‘non-strong-canonical’ events is sensitive to the data product used and the classification of a few events may change. However, it does not alter our result that almost all the ‘strong canonical’ AZM events can be explained by the spring Atlantic ITCZ movement and that the relation is stronger for the cold AZM events.

It may be noted that not all anomalous northward excursions of ITCZ in spring lead to AZM cold events in summer. There are two years (1981 and 2012) in which despite the ITCZ being anomalously north in spring, a cold AZM event did not follow (details are discussed separately in Section 4.6 for the sake of lucidity). Although the northward excursion of ITCZ in spring is a necessary condition for the development of a cold event, it is not sufficient unless its position and resulting easterlies over the equatorial Atlantic are sustained throughout spring.

4.5 Diversity of causative mechanisms of cold and warm AZM events

In the above, we have shown that most of the strong canonical AZM events are explained by the ITCZ movement in spring and subsequent Bjerknes feedback. It is interesting to explore what other mechanisms may explain the AZM events apart from the ITCZ movement and/or the dominant Bjerknes feedback. As it is difficult to show spatial evolution of each and every event, we present a novel pictorial representation of the evolution of the Bjerknes components of all the AZM events during the study period in Fig. 4.10. This representation serves multiple

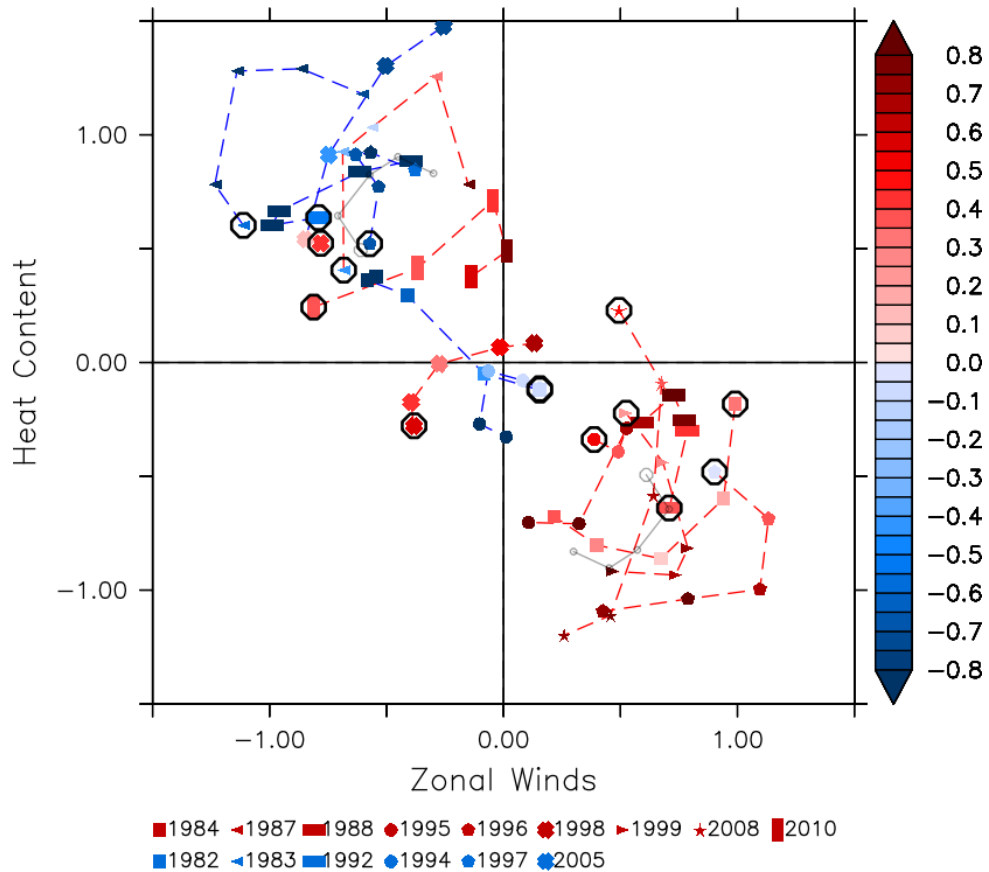


Figure 4.10: Evolution of different Bjerknes components during March–July of each AZM event in the phase space of zonal winds averaged over central to western equatorial Atlantic (abscissa; m s^{-1}) and heat content in the western equatorial Atlantic (ordinate; 10^{10} J m^{-2}) with the color of each point/symbol representing the SST in the Atl3 region ($^{\circ}\text{C}$). Different symbols are used to mark different AZM events and the red (blue) dashed lines connecting them indicate a warm (cold) AZM event. The starting point of each year, i.e., March, is indicated by a black circle. The gray line connects the one standard deviation points in the phase space during March–July and the March point is indicated with a bigger gray circle. This line serves as a reference against which the strength of a particular event can be compared. All the Bjerknes components plotted are smoothed by a 3-month running mean for better appearance. For the Bjerknes feedback to be considered active all three elements of (Keenlyside and Latif, 2007) have to be present. While the heat content and zonal wind anomalies are used as the axes, SST in the Atl3 region is shown filling different symbols used to differentiate between the events and is easy to miss. Since only the AZM events which we already know have an SST response (AZM definition is based on Atl3 SST index) are plotted, this representation is adequate to tell us whether or not an AZM event can be explained by the Bjerknes feedback.

purposes: (i) whether or not a particular event can be explained by the Bjerknes feedback can be conveniently determined (ii) evolution of multiple events can be summarized in one frame. For an easy interpretation of the figure, tracking of the cold event in 1983 is explained. While the equatorial zonal winds remain almost steady during March–May, the heat content in the

western equatorial Atlantic increases. Both the winds and heat content decrease in strength after May. The SST in the Atl3 region reaches its peak in May–June. The movement along the trajectory in a clockwise direction indicates that the changes in the zonal winds precede those in the heat content. From the figure, it can be noted that normally the trajectories of cold (warm) events are in the top left (bottom right) quadrant. All such events can be explained by Bjerknes mechanism to one degree or another whether preceded by an appropriate ITCZ movement in spring or not. However, there are exceptions: cold event of 1994 and warm events of 1987, 1998 and 2010. The cold event of 1982 is a slight exception in that its track is close to the origin due to weak Bjerknes components but ultimately moves to the top left quadrant when the components become strong enough. Apparently, the two exceptions among cold events (1982 and 1994) are also the events that are not preceded by a spring northward movement of ITCZ. This figure is clearly reminiscent of Kessler (2002) and captures similar aspects of the recharge-discharge processes involved in AZM, although the focus there was on whether ENSO is an oscillation or a series of events. A similar question is relevant for AZM as well but we will not discuss it in this study.

What are the mechanisms by which cold AZM events form without a northward movement of ITCZ and/or the Bjerknes feedback? As mentioned earlier, the AZM cold events that are not preceded by northward ITCZ in spring occurred in 1982 and 1994. In both of these events, a negative SST anomaly forms due to winds off the equator (either southerly alongshore or easterlies parallel to the equator) and spreads over to the equator to eventually become a cold event (see Section 4.6 for detailed discussion of the events). Thus, during the study period, most of the cold AZM events are explained by Bjerknes feedback associated with the spring movement of ITCZ and the rest by the wave activity induced by alongshore winds off Angola and/or off-equatorial winds.

The causative mechanisms and timing of the triggers of a warm event appear to be more diverse than that of a cold event. As mentioned earlier, only two out of nine warm events are explained by ITCZ movement in spring and subsequent Bjerknes feedback. The remaining warm events are: 1987, 1988, 1995, 1999, 2008 and 2010. Most of them can be broadly explained by the Bjerknes feedback mechanism if we do not adhere strictly to the requirement of a strong subsurface response (1988, 1995, 1999 and 2008; Fig. 4.2 and Fig. 4.9). The exceptions are the warm events of 1998, 1987 and 2010 (see Section 4.6 for details). Although, the Bjerknes

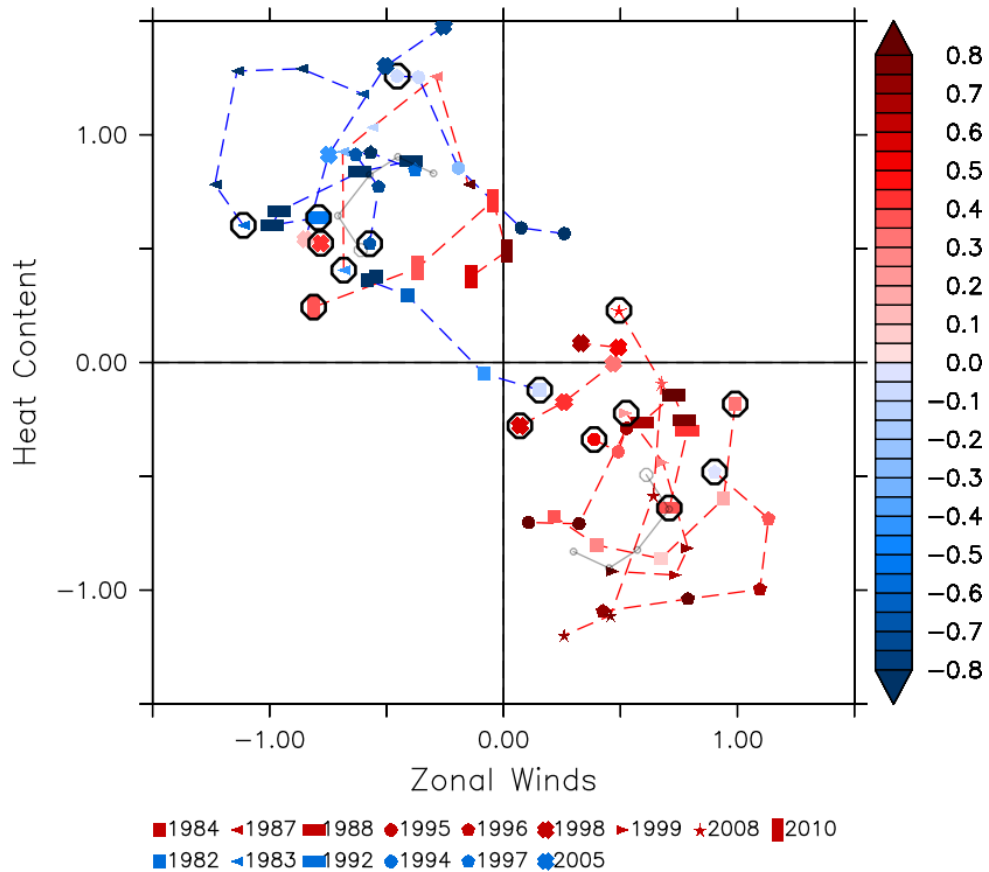


Figure 4.11: Same as Fig. 4.10 except that in case of the cold event in 1994, the zonal winds are averaged in the region centered around 5°S (7°S–3°S and 20°W–10°E) and the heat content is negative of that averaged in the eastern Atlantic centered around 5°S (7°S–3°S and 0°E–15°E). In the case of warm event in 1998, the zonal winds are averaged over 3°S–3°N and 5°W–15°E.

feedback mechanism seems to be at the centre of most of the warm events, only a few events are triggered by a southward spring transition of ITCZ. On a side note, it is interesting to see that after accounting for the change of centre of action as in the case of the cold event of 1994 and the warm event of 1998, trajectories of all the cold events move in a clockwise direction which means that the changes in the zonal winds precede the changes in heat content (Fig. 4.11). However, the trajectories of warm events of 1988 and 1998 move in an anticlockwise direction.

Several previous studies have discussed different mechanisms by which a warm AZM event can occur. Richter et al. (2013) show that AZM warm events that cannot be explained by ENSO-like dynamics are driven by a mechanism in which surface wind anomalies just north of the equator induce warm heat content anomalies which are advected towards the equator and propagate to the east. They argue that such warm events are caused by AMM with warm SST anomalies in the TNA. This is different in details compared to the mechanism suggested by

Foltz and McPhaden (2010) which involves waves described earlier in Section 4.1. Zhu et al. (2012) show an interesting relation between the AMM and AZM on a 3–4 year time scale. The positive heat content anomalies in northern tropical Atlantic resulting from positive AMM, can discharge into the equatorial waveguide when the AMM weakens, and stimulate a warm AZM event about 12–15 months later (the warm event of 1987 is an example of this mechanism but on shorter timescales). Lübbecke (2013) summarizes different mechanisms causing a warm event. Our findings here add a finer point via the asymmetry in the ITCZ-AZM interactions. In this study, we are more specifically focused on the asymmetry of cold and warm events related to ITCZ variability and not on proposing any new mechanism for the AZM itself.

4.6 The peculiar AZM events

We discuss the events which do not fit the general patterns described above and examine the possible reasons for their departure in the following. These events are mentioned earlier but their details are presented here separately for the sake of lucidity of main results.

As mentioned before in Section 4.4, in the years of 1981 and 2012, despite the ITCZ in spring being in the north, a cold AZM event did not follow. In the year 1981, although the ITCZ was north in March–April, it did not stay north in May (Fig. 4.12). More importantly, the northward ITCZ did not result in southeasterlies over the equator due to the presence of an SST anomaly in the southern tropical Atlantic west of 5°W , which caused the cross-equatorial winds to be mostly southerly, i.e., lacking the easterly component. If it were not for this SST anomaly, there could have been a cold AZM event as all other signs were favorable. In the year 2012, the ITCZ position did not fall as drastically as in the year 1981 and as a result, the required sustained easterly winds were present (Fig. 4.13; compare it with Fig. 4.12). However, requisite changes in heat content (enhanced in the west and reduced in the east) did not occur (Fig. 4.13). Therefore, although the northward excursion of ITCZ in spring is a necessary condition to the development of a cold event, it is not sufficient unless its position and resulting easterlies over the equatorial Atlantic are sustained throughout spring.

The mechanisms by which cold AZM events form without a northward movement of ITCZ in spring and/or the Bjerknes feedback are discussed here. As noted previously in Section 4.5, the AZM cold events that are not preceded by northward ITCZ in spring occurred in

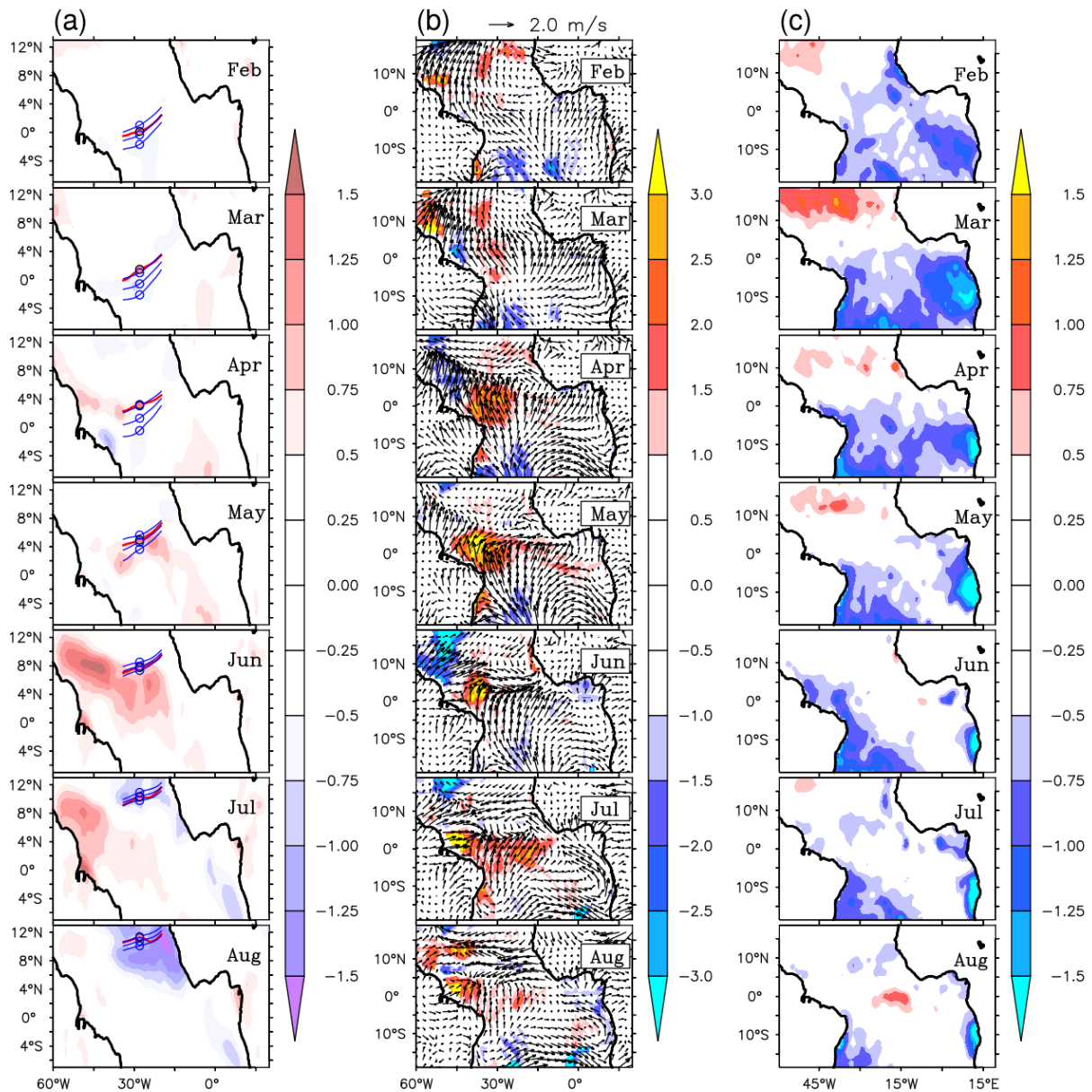


Figure 4.12: Same as Fig. 4.3 but the anomalies of corresponding variables in the year 1981 are presented instead of the composites.

1982 and 1994. In the year 1982, upwelling favorable northward alongshore winds near the coast of Angola from January-onwards helped develop an initial negative SST anomaly which spread and evolved into an AZM cold event that lasted into the following winter (Fig. 4.14). The equatorial easterly wind anomalies did not precede the event: rather they occurred as a result of the already developed SST anomaly. It is also reflected in its trajectory which is close to the origin on the vertical initially (Fig. 4.10). However, once all the feedback components kick in, the event evolves like any other cold event. The persistence of negative heat content anomalies in the eastern equatorial Atlantic helped maintain the cold SST even after the summer. This

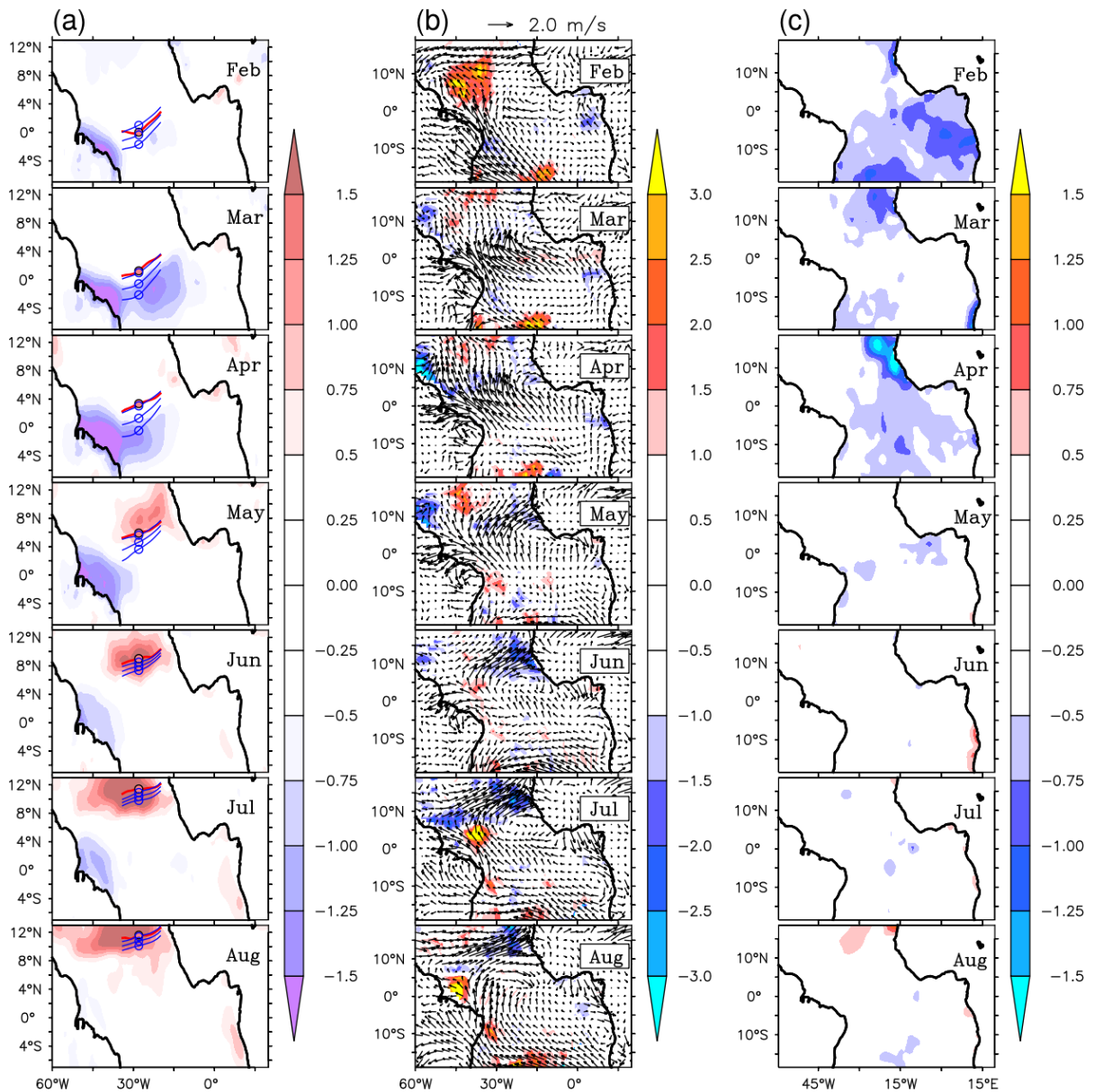


Figure 4.13: Same as Fig. 4.12 but for the year 2012.

event can be deemed special owing to the dominance of SST over other Bjerknes feedback components and due to the persistence of the SST anomalies into winter by which time a typical AZM event ends. The other event in 1994 also seems to be special for several reasons. The Bjerknes feedback components such as equatorial easterly winds, negative (positive) heat content in the east (west) either do not favor or instead disfavor the formation of a cold AZM event, explaining why its track is close to the origin and passes into the bottom right corner where usually the warm events are found (Fig. 4.10). However, it is the off-equatorial easterly winds centered around 5°S in March–May that shoal the thermocline in the east along African coast centered around 5°S and form an initial SST anomaly which subsequently spreads to lower lat-

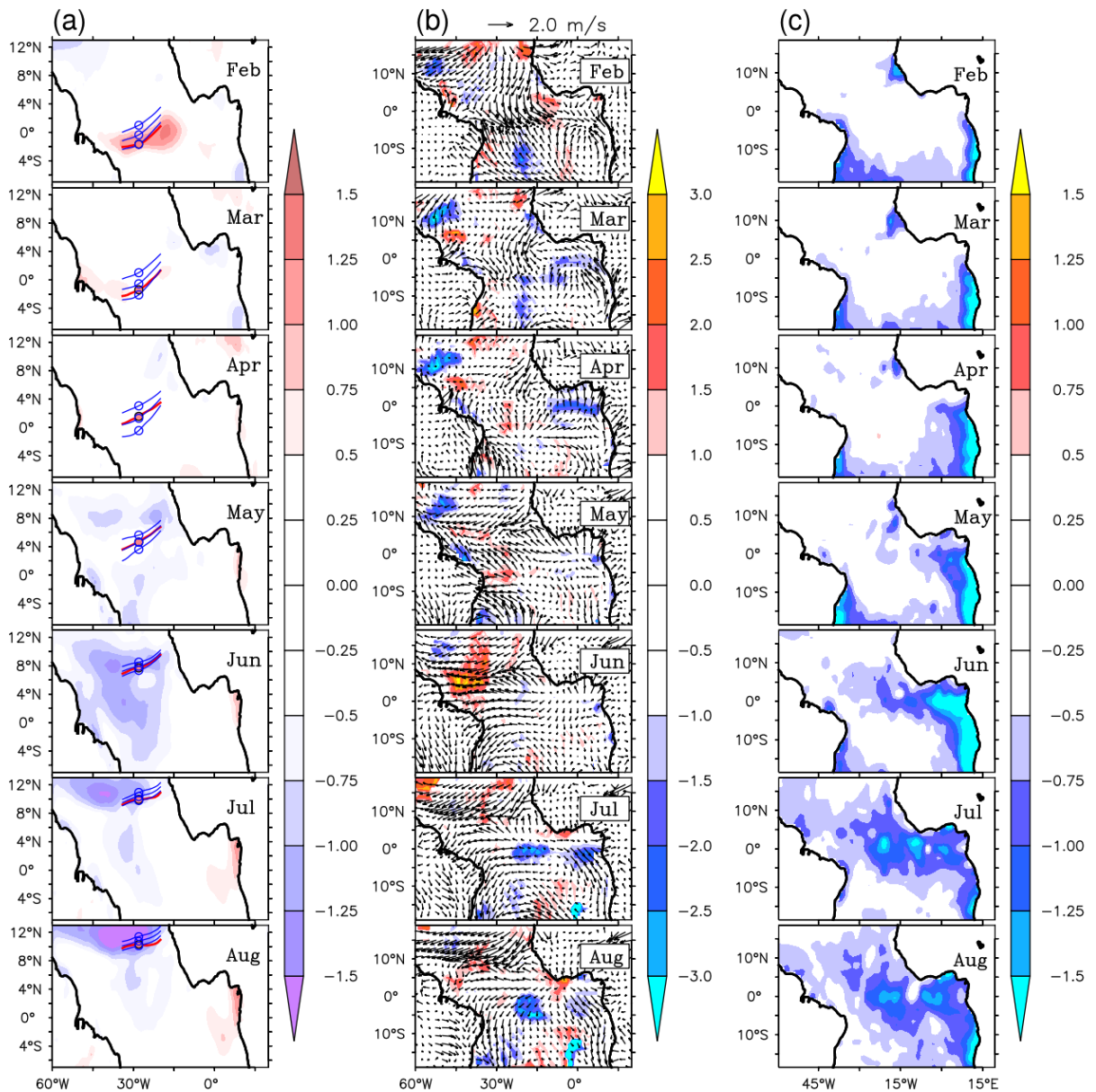


Figure 4.14: Same as Fig. 4.12 but for the year 1982

itudes developing into a cold AZM event (Fig. 4.15). So, this event has the essential Bjerknes components at play but the centre of action is shifted to 5°S. Accounting for such a change of centre of action, moves its trajectory to the usual top left quadrant (compare Fig. 4.10 and Fig. 4.11). However, we must say our current understanding of the mechanism of such events is incomplete and further investigations are required. Nonetheless, in both of these events, a negative SST anomaly forms due to winds off the equator (either southerly alongshore or easterlies parallel to the equator) and spreads over to the equator to eventually become a cold event.

The causative mechanisms of a warm event other than the Bjerknes feedback mechanism are discussed here. As noted already in Section 4.5, the warm events that cannot be

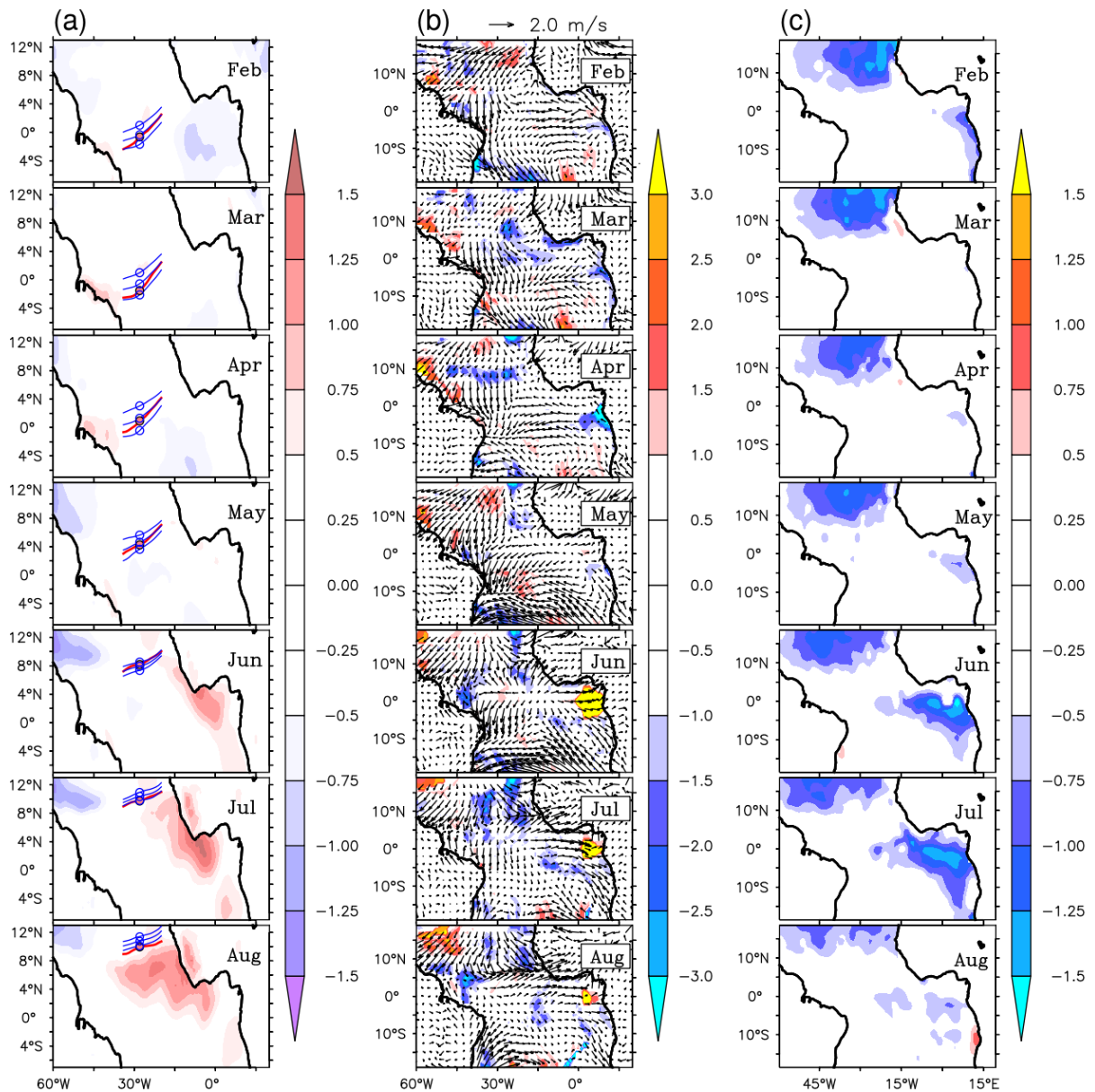


Figure 4.15: Same as Fig. 4.12 but for the year 1994.

explained by the Bjerknes feedback mechanism are 1998, 1987 and 2010. The warm event of 1998 has the spring westerly winds in the eastern part of the equatorial Atlantic (3°S–3°N and 5°W–15°E) but easterlies in the western equatorial Atlantic. The opposing zonal winds are manifest in its weak subsurface response or heat content (Fig. 4.16). Upon accommodating the change of location of the favorable zonal winds, its trajectory moved to bottom right corner (compare Fig. 4.10 and Fig. 4.11). However, the Bjerknes components of westerly winds and heat content are the weakest compared to any other warm event which explains why its trajectory is the closest to the origin. The warm event of 1987 is associated with northward migration of ITCZ in spring which usually causes a cold event so its track evolves the same as a cold

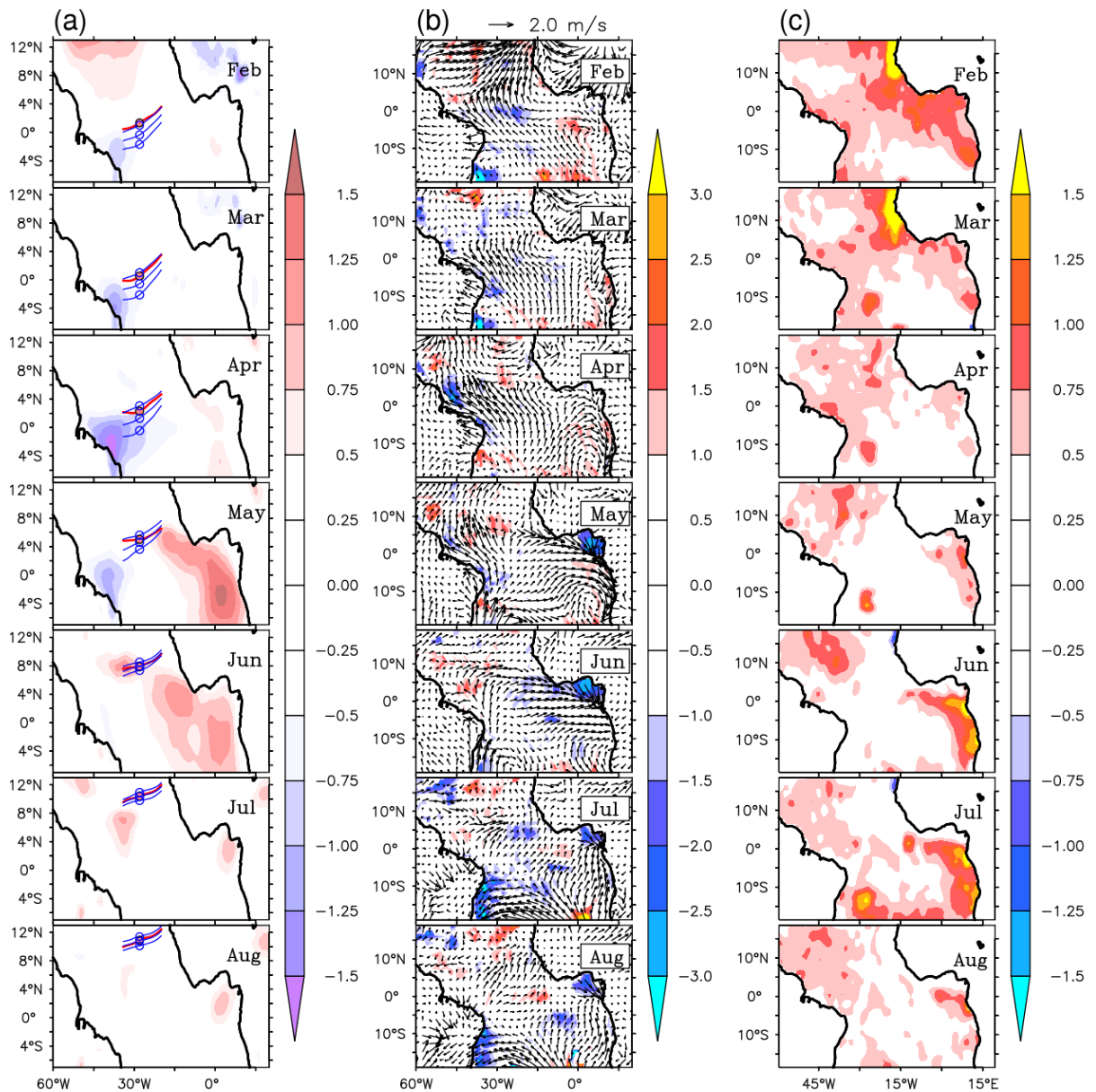


Figure 4.16: Same as Fig. 4.12 but for the year 1998.

event but with a warm SST (Fig. 4.2, Fig. 4.9 and Fig. 4.10). This special event is explained by a mechanism proposed by Zhu et al. (2012), whose key points are already discussed earlier in Section 4.5. This event was discussed by Richter et al. (2013) as well. In 2010, all the Bjerknes components indicated the development of a cold AZM but a warm AZM event occurred instead (Fig. 4.2, Fig. 4.9 and Fig. 4.10) which cannot easily be explained in the absence of sufficient data.

4.7 Summary and Discussion

Earlier studies have discussed the existence of a relationship between the ITCZ position in spring in the tropical Atlantic and the AZM in summer, using correlation analyses (Servain et al., 1999; Murtugudde et al., 2001). In this chapter, we go into the details of this relationship and begin our investigation with a question why the high correlation between the anomalous position of ITCZ and equatorial zonal winds in spring, a prerequisite for the development of an AZM event, does not translate into strong association between the ITCZ position in spring and AZM in summer. To the best of our knowledge, none of the previous studies addressed this question. By starting from an initial hypothesis that the ITCZ-AZM relation may have an asymmetry with regards to cold and warm AZM events, we show that the relation between the ITCZ in spring and AZM is stronger for cold AZMs than warm AZMs with a skew towards cold events (Fig. 4.17). It implies that the evolution of cold and warm AZM events with respect to the meridional position of Atlantic ITCZ during boreal spring is asymmetric. We further show that the asymmetry is inherent in the seasonal cycle itself. The weakened and less persistent westerly winds in the western equatorial Atlantic during warm events preceded by southward spring ITCZ and the resultant lack of support from the subsurface ocean response, an important factor in Bjerknes feedback, is argued to result in a weak association between the ITCZ and warm AZM. We also show that the AZM events caused by ITCZ movement are ‘strongly canonical’, i.e., associated not only with zonal surface winds in spring but also an oceanic subsurface response in late spring to mid-summer.

Further, we observe that the timing and causative mechanisms of a cold AZM event are less diverse than that of a warm event. We infer that the asymmetry in the diversity may be explained by the fact the AZM is phase locked to the seasonal cycle (Keenlyside and Latif, 2007), which is due to the seasonal ITCZ movement (Richter et al., 2014, 2017). Further, the cold AZM being simply an enhancement of the climatological condition and the warm AZM being an anomaly in its true sense, may also be important to consider. It should be noted that there are more warm events in the study period than cold events and thus inadequate sampling may be an issue. However, it must be observed that almost all the studies that propose a different mechanism other than the straight forward Bjerknes feedback do it only for a warm AZM case. We opine that the asymmetry is inherent in the strong association of the AZM with the seasonal cycle.

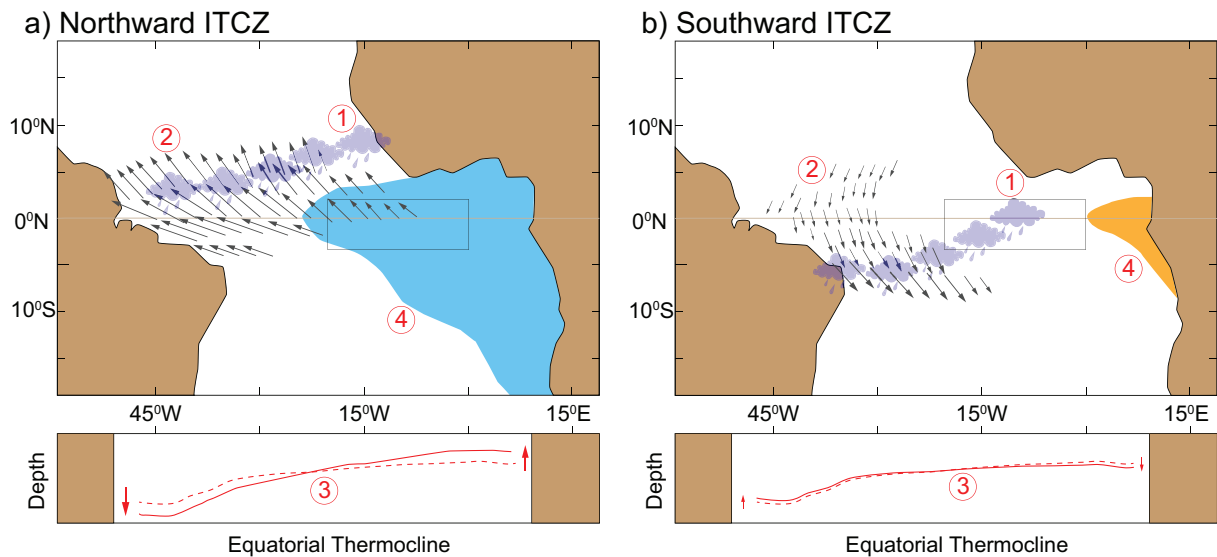


Figure 4.17: A schematic diagram summarizing the most likely scenario when the Atlantic ITCZ in spring is anomalously (a) north and (b) south. When the Atlantic ITCZ in spring is anomalously north as shown in (a) at point 1, it leads to concurrent anomalous winds that have strong easterly component over the WEA (point 2), which in turn shoals the equatorial thermocline in the east and deepens the same in the west with a delay of 1 or 2 months (point 3; dashed line: mean thermocline; thick line: shifted thermocline), finally resulting in a cold AZM event in the following summer (point 4). On the contrary, when the ITCZ in spring is anomalously south as shown in (b) at point 1, it leads to concurrent anomalous winds that are predominantly northerly in the vicinity of the equator but develop a strong westerly component upon crossing into the south but away from the equator (point 2). The westerly component of the winds in the WEA is so weak that they cause insufficient deepening of equatorial thermocline in the east (point 3) inducing weak warm SST anomalies and thus no warm AZM event (point 4). In summary, while the anomalous northward spring ITCZ leads to a cold AZM event in the following summer most of the times, the converse is less likely and hence the skewness in the relation between spring ITCZ position and AZM. Atl3 region is marked with a rectangular box. The above is only for representative purposes and not to scale.

We started our investigation of the relation between the spring Atlantic ITCZ and AZM with a question of what causes the drop in correlation between the ITCZ in spring and AZM despite a high correlation between ITCZ and equatorial zonal winds in spring, and apparent criticality of these winds for the development of an AZM. However, a related question of why the relation between wind anomalies in spring and SST anomalies in summer is weaker than the correlation between equatorial trades and ITCZ latitude (Table 4.1), can be also posed. This has been addressed by several studies either overtly or implicitly. Foltz and McPhaden (2010), Lübbecke and McPhaden (2012) and Richter et al. (2013) talk about how spring warm SST anomalies in the TNA can sometimes cause a warm AZM event in the following summer instead of the usual cold AZM event. The positive meridional mode is associated with equatorial

easterly winds in boreal spring which normally is a precondition for a cold AZM. However, in some special cases, via the mechanisms discussed in earlier studies (Foltz and McPhaden, 2010; Lübbecke and McPhaden, 2012; Richter et al., 2013), warm AZM events can occur which weakens the relation between the spring equatorial winds and the summer SSTs. On a related note, Chang et al. (2006) talk about how the tropospheric warming over the tropical Atlantic induced by an El Niño destructively interferes with the spring equatorial easterly winds which leads to a summer SST cooling in the STA. This can contribute to reducing the association between the spring winds and summer SST anomalies. Nonetheless, as shown in Table 4.1, the correlation between the spring ITCZ position and summer Atl3 index is lower than that between spring WEA zonal winds and summer Atl3 index making our set goal worthwhile.

A close relation between equatorial zonal winds and position of the ITCZ has been noted in an earlier study by Richter et al. (2014) who show that the equatorial easterlies grow strong almost linearly when the ITCZ is to the north of equator but they are uniformly weak when the ITCZ is in the south, nevertheless the winds remain easterly throughout. Although their result appears to be at odds with our observation that anomalous northward (southward) movement of ITCZ during spring is associated with concurrent anomalous easterlies (westerlies), it is not in reality, owing to differences in methodology and time period of the two studies. While Richter et al. (2014) average the monthly mean absolute equatorial zonal wind stress over each unique absolute ITCZ position during their entire study period which represents the mean picture and removes some of the seasonal preferences, we focused on the relation between anomalies of ITCZ and equatorial zonal winds only during spring. Therefore, we posit that our findings are novel in eliciting the asymmetric relation between the spring position of the ITCZ and AZM and its explanation through interaction between the seasonal cycle and interannual anomalies.

We have described different processes involved when an anomalous northward spring ITCZ, which can be influenced by AMM among other things, leads to a cold AZM in the following summer in Fig. 4.3. Contrary to our intention, the figure might give an impression that a northward ITCZ shift and easterly wind anomalies occur before the development of significant cool SST anomalies in the southeast Atlantic in the late spring to summer, leading to the question of causality: is the AMM a result of anomalous spring ITCZ position rather than a cause? We clarify this apparent contradiction here. Note that Fig. 4.3 shows the composite of anomalies of different fields including SST and winds for all those cold AZM events preceded by the

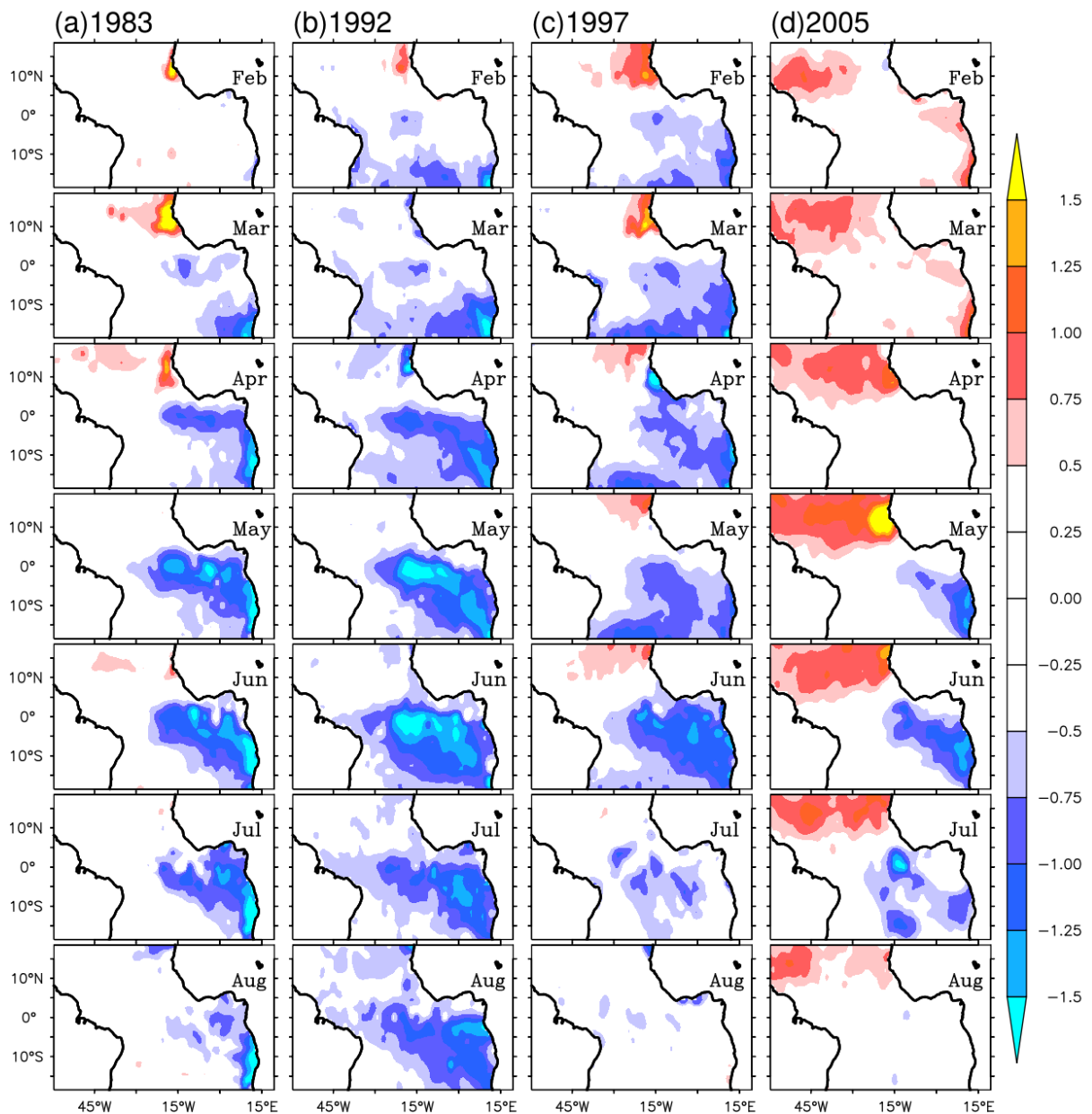


Figure 4.18: Monthly (February–August) evolution of SST anomalies in the years a) 1983, b) 1992, c) 1997 and d) 2005 when the anomalous spring ITCZ in the north leads to a cold AZM event in the following summer. These are the SST anomalies used to compute the respective monthly composite shown in Fig. 4.3c

ITCZ displaced anomalously north in spring. A positive AMM type of SST structure (warm north and/or cool south) during spring is not present in all the composite years but whenever it is present (in 1997 and 2005) it persists from February itself followed by a northward displacement of ITCZ in spring and the associated equatorial easterlies (Fig. 4.18). In the composite picture (Fig. 4.3), the AMM pattern appears weak in the north but strong in the south because AZM has early SST anomalies of the same sign in the south overlapping with that of AMM

there but no signal in the north which adds to the fact that AMM SST pattern is not present in all the constituent years. The question of causality is also not supported by earlier studies (e.g., Hu and Huang, 2006) which show that the development of an AMM event can span from boreal fall to boreal spring preceding the anomalous meridional displacement of ITCZ in spring with the associated equatorial easterlies.

Our observation that causative mechanisms of the cold AZM (counterpart of La Niña in the tropical Atlantic) are less diverse than that of warm AZM (counterpart of El Niño) is supported by studies about ENSO diversity reporting similar results (Kug and Ham, 2011; Ren and Jin, 2011; Chen et al., 2015; Ashok et al., 2017). Chen et al. (2015) attribute the cause of asymmetry, irregularity and extremes of El Niño to westerly wind bursts and also point out that the wind bursts strongly affect El Niño but not La Niña. Capotondi et al. (2015) and Ashok et al. (2017) suggest that while different types of El Niño are distinguishable, the La Niña events are not. Timmermann et al. (2018) also note that La Niña events exhibit less diversity in their spatial patterns compared to El Niño events pointing to an asymmetry in the dynamical processes involved. These results lend a hand to our speculation that cold AZMs have less diversity compared to warm AZMs. The verification of the validity of this hypothesis can form the subject of a separate study but we will not undertake it in this thesis.

Chapter 5

Simulation of interannual relationship between the Atlantic Zonal Mode and the Indian Summer Monsoon in CFSv2

As discussed in Chapter 1, previous studies have shown that the Atlantic Zonal Mode (AZM) can influence the Indian Summer Monsoon (ISM) on interannual timescales. Expanding on these studies, in our recent study Pottapinjara et al. (2014), we have proposed a plausible thermodynamics-baesd mechanism by which the AZM can influence the ISM. In this chapter, we report from various sensitivity experiments we carry out using the CFS version 2, a state-of-the-art coupled dynamical model, whose high resolution variant is utilized for monsoon forecasts in India on operational basis. We examine whether the model simulates the observed relationships between the AZM and ISM, and the physical mechanisms proposed in earlier studies.

5.1 Introduction

The importance of understanding the relation between the Indian summer monsoon (ISM) and its external drivers is discussed elaborately in Chapter 1 and the focus in this thesis is on the relation between the ISM and climate mode of interannual variability housed in the tropical Atlantic, i.e., the Atlantic Zonal Mode (AZM). Earlier studies have shown that the AZM

influences the ISM on interannual timescales (Kucharski et al., 2008, 2009; Wang et al., 2009; Barimalala et al., 2013b; Pottapinjala et al., 2014; Kucharski et al., 2016; Yadav et al., 2018; Sabeerali et al., 2019a,b). A series of studies conducted by Kucharski et al. (2007, 2008, 2009) show the existence of a relation between AZM and Indian Summer Monsoon Rainfall (ISMR) in which a warm (cold) AZM event leads to a low-level divergence (convergence) over India and thereby reduced (increased) ISMR. Further, in Pottapinjala et al. (2014), we have shown that the AZM can affect the monsoon transients: in response to a warm (cold) AZM event, the number of monsoon depressions forming in the Bay of Bengal decreases (increases) and thereby contributes to a reduction (an enhancement) of rainfall over India. We have also suggested a physical mechanism in which the AZM influence propagates in tropospheric temperature via Kelvin-like waves to the east to reach the Indian Ocean and influences the monsoon by modulating the mid-tropospheric land-sea thermal gradient and thereby the seasonal mean flow. This mechanism entails a thermodynamic manifestation of the response of ISM to the AZM. The changes thus induced in the mean flow were shown to affect the monsoon depressions in the Bay of Bengal and rainfall over India (see Section 1.4 for an outline of these results).

For optimum societal benefit, understanding the variability of the monsoon and efforts to forecast it must go hand in hand. In this context, the operational/semi-operational efforts of forecasting the ISM are discussed here briefly. The India Meteorological Department (IMD) is the agency tasked with the responsibility of providing the meteorological services in India including the monsoon forecasts. Currently, the IMD uses a suite of statistical and dynamical models to forecast the monsoon (Pai et al., 2011; Kumar et al., 2012; Pai et al., 2017, 2019). In addition to the existing models, the IMD has recently adopted a variant of the Coupled Forecasting System version 2 (CFSv2; Saha et al., 2014a) for the operational monsoon forecasts (Ramu et al., 2016; Pokhrel et al., 2016; Saha et al., 2017, 2019; Krishna et al., 2019; Pattanaik et al., 2019; Pai et al., 2019). The CFSv2 is a state-of-the-art coupled ocean-atmosphere general circulation model, originally developed by the National Centers for Environmental Prediction (NCEP).

The CFSv2 simulates the general features of the monsoon and its variability reasonably well (e.g., Jiang et al., 2013; Saha et al., 2014a). However, it has some serious biases, importantly, a dry bias over land (Saha et al., 2014b; Narapusetty et al., 2016, 2018). The success of monsoon forecasts using the CFSv2 depends on, among other things, how well the model

simulates the links of the monsoon with external factors. Previous studies have investigated the simulation of ENSO and IOD, and their relation to the ISMR in the model (e.g., George et al., 2016; Saha et al., 2016) and report that while the ENSO-monsoon relation is too strong compared to observations, the IOD-monsoon relation is completely out of phase due to inadequate representation of coupled dynamics in the Indian Ocean. However, the simulation of AZM and its relation to the ISMR in the model is yet to receive its due attention. In a recent study, Sabeerali et al. (2019b) analyze the hindcasts of CFSv2 initialized in different months and show that a simulation that erroneously forecasts the AZM loses predictive skill for the monsoon. While their interest was on assessing the predictive skill of the AZM in the model, in this study, we will focus more on the simulation of observed AZM-ISM relation and teleconnections in the model, particularly as proposed in our recent study Pottapinjara et al. (2014) and outlined in Section 1.4. This helps in identifying the shortcomings, if any, in the model with respect to AZM-ISM relation and would potentially contribute to improving the forecasts of ISM issued using this model. We will at first examine the representation of the mean state in the tropical Atlantic in Section 5.3 and the simulation of the AZM and its relation to the ISMR in a free-run we carried out with the model in Section 5.4. Further, in Section 5.5, we will present the details of a complementary sensitivity experiment in which the SST anomalies associated with the AZM in the tropical Atlantic are imposed and the response of ISM to those anomalies is examined.

5.2 The model, observed data and design of the sensitivity experiment

As mentioned earlier, in this chapter, we use the standard configuration of the CFSv2 model developed by the NCEP (Saha et al., 2014a,b). The atmospheric component of the model has a resolution of T126 (0.9°) in the horizontal and has 64 sigma-pressure hybrid levels. The oceanic component has a horizontal resolution of $0.25\text{-}0.5^\circ$ and 40 vertical levels. This model is used in understanding of the monsoon processes (e.g., Roxy et al., 2015). The performance of the model free-run in simulating the climatology in the tropical Atlantic, the AZM and its relation with the ISM is validated against various observational and reanalysis data products. The Hadley Centre Sea Ice and Sea Surface Temperature (HadISST; Rayner et al., 2003) is

used for model forcing. The Atlantic 3 index (Atl3) and Oceanic Nino Index (ONI) are used to identify the AZM and ENSO events, respectively the same way as described in Chapter 3 and Chapter 4. The monthly precipitation data from the Global Precipitation Climatology Project (GPCP; Adler et al., 2003) is also used. The position of the Atlantic ITCZ is identified as the latitude at which the meridional component of the surface winds vanishes along 28°W between the latitudes of 5°S and 20°N (Servain et al., 1999), again the same way as in Chapter 4. The wind data from the European Centre for Medium Range Weather Forecasting (ECMWF)'s Reanalysis, known as the ERA-Interim (Dee et al., 2011), for the period 1979–2012 is used to validate the model performance. The Tropospheric Temperature (TT) data is also taken from ERA-Interim reanalysis.

As will be shown later from the model free-run analysis, the model simulates climatology of the tropical Atlantic, and the AZM and its relation with the ISM reasonably well, despite some biases. Therefore, the model is used to conduct the sensitivity experiment to see how the ISM responds to imposed SST anomalies associated with AZM.

In our simulations, we use a 100-year free-run with the CFSv2 coupled model (henceforth referred to as the CFSv2_{REF}), starting with well-balanced ocean and atmospheric initial conditions. As mentioned earlier, before conducting the sensitivity experiments, the performance of the model in simulating different systems involved such as AZM and ISMR is evaluated using 20 years of the model free-run, leaving the first 50 years of the free-run for allowing the model to reach dynamical stability. The results of this analysis are presented in Section 5.3. In addition to this reference run, we carry out a sensitivity experiment (referred to as the CFSv2_{SST} run) designed as follows. We start from the model state in the month of May of every year of the 20-year free-run and impose the SST anomalies associated with an observed warm AZM event in the tropical Atlantic (Fig. 5.7) from June through September (when both the AZM and ISM are active) of each year. This ensemble of runs with different initial conditions but with the same imposed SST anomalies in the Atlantic constitutes the sensitivity experiment (CFSv2_{SST} run). The details of how the imposed SST anomalies are constructed is discussed later. The average of the differences between the sensitivity run (CFSv2_{SST}) and the reference run (CFSv2_{REF}), i.e., the average of (CFSv2_{SST} – CFSv2_{REF}), over the period of experiment is considered as the response of the model to the imposed SST anomalies and this response is analyzed to examine the if the model simulates the mechanisms proposed.

The SST anomalies imposed (Fig. 5.7) are prepared from the observed SST data as follows: 1) monthly SST anomalies (SSTA) are averaged over the period of June–August (JJA) of each year 2) JJA SSTA are de-trended and 3) the detrended anomalies are composited in all those years when there is a warm AZM event during the period 1950–2012. It may be noted that although in reality the AZM SST anomalies vary both in spatial extent and magnitude during its life cycle, i.e., June–August, the SST anomaly pattern imposed in the experiment is not changed during the experiment to keep it simple.

5.3 The mean state of the tropical Atlantic in CFSv2

Before examining how the ISM in the model responds to the imposed AZM SST anomalies, it is imperative to see if the model simulates the climatological features in the two ocean basins. As mentioned earlier, the model simulates the climatological features of summer monsoon including the tropospheric temperature over the land and ocean reasonably well (Jiang et al., 2013; Saha et al., 2014a,b). Hence we will not present the simulation of the mean monsoon or its variability but will focus on the simulation of the seasonal cycle in the tropical Atlantic here. Fig. 5.1 shows the observed monthly climatological evolution of SST and surface winds in the tropical Atlantic. The high SST band with temperatures above 25°C transits in the north-south direction with the season. Notably, it is followed by a zone of convergence of the trade winds (or the Inter-tropical Convergence Zone; ITCZ) from either hemisphere with a delay of about one month. With the progress of the season, and as a result of intensified winds and northward excursion of the ITCZ during late boreal spring–early boreal summer, the thermocline in the southeastern Atlantic is lifted up. The associated upwelling leads to a drop of about 5°C in SST and thereby to the development of a distinctive seasonal cold SST tongue with temperatures below 25°C in the eastern equatorial Atlantic during boreal summer (Fig. 5.1; Dippe et al., 2018). The cold tongue region has the highest SST variability and its interannual modulation in the timing and/or strength leads to an AZM event (e.g., Burls et al., 2012; Lübbecke et al., 2018). This observed seasonal cycle of the tropical Atlantic has already been discussed in Chapter 1. Fig. 5.2 shows the bias of the model in simulating the seasonal cycle in SST and surface winds in the Atlantic. It can be seen from the figure that there is a warm SST bias of about 3°C in the tropical South Atlantic during May–September and the bias

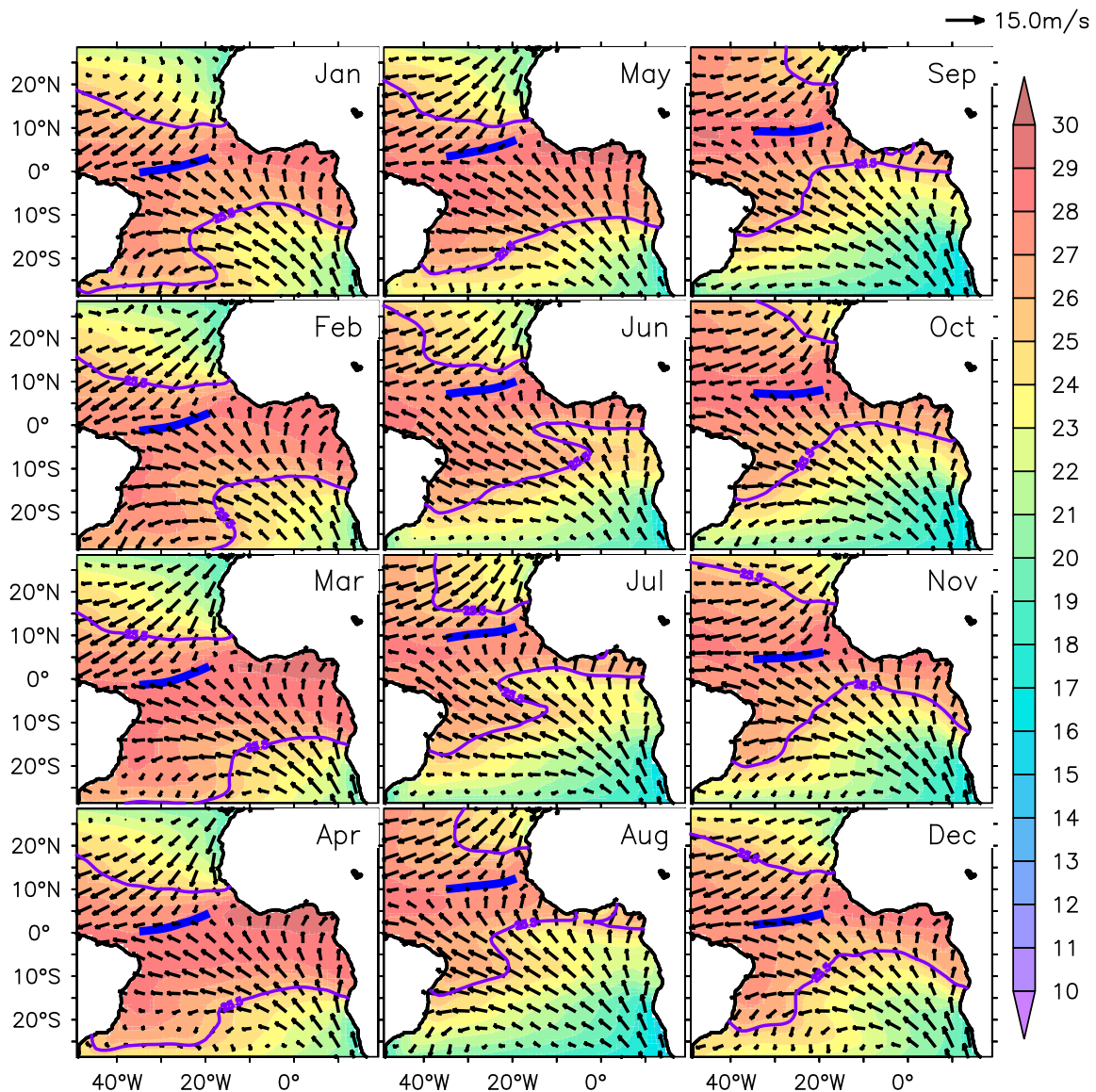


Figure 5.1: The observed monthly climatology of SST ($^{\circ}\text{C}$; shaded) overlaid by surface winds (vectors), and position of the oceanic ITCZ (thick blue line) in the tropical Atlantic. The SST contour of 25.5°C is overlaid (blue) to show the development of the seasonal cold tongue in the southern tropical Atlantic during boreal spring–summer. The corresponding month is indicated on each subpanel. This figure is the same as Fig. 1.9.

has the highest spatial extent in June–July. The winds over the equator have a northerly bias and the highest bias is in April–May with a reduction in the later months. The SST bias follows that of equatorial winds. Note that the model bias in SST in summer has a structure similar to that of seasonal cold tongue shown in Fig. 5.1. Simulation of the development of seasonal cold tongue in the tropical Atlantic is important for the model to capture the AZM properly. The movement of ITCZ is strongly tied to the seasonal cycle and it may reveal more about the SST

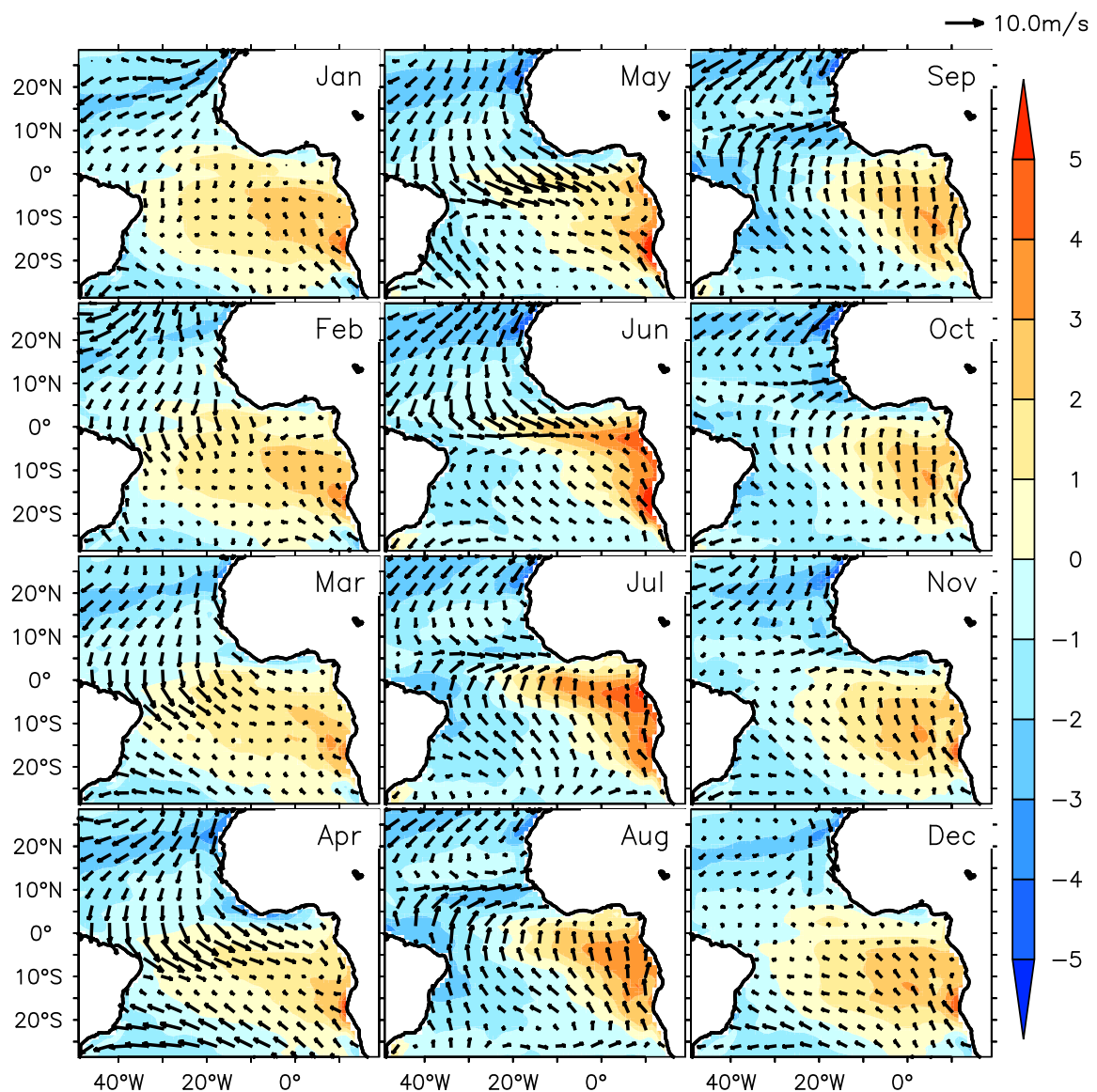


Figure 5.2: Monthly evolution of the bias ($\text{CFSv2}_{\text{REF}} - \text{Observations}$) in the annual cycle of SST (shaded; $^{\circ}\text{C}$) and surface winds (vectors; ms^{-1}) when the reference run is compared against the observations.

bias. A comparison of the monthly climatological position of the ITCZ in the model with that of the observations is shown in Fig. 5.3. General features of the Atlantic ITCZ spending most of its time in the northern hemisphere and occupying the southernmost position in or around spring and northernmost position in or around summer are captured accurately by the model (as discussed in Chapter 4). However, the model ITCZ lags behind the observed ITCZ reflecting the delayed seasonal cycle in the model which leads to a late development of cold tongue and causes the warm SST bias (Fig. 5.2). The model ITCZ is the farthest from the observed ITCZ in boreal spring but the difference between their positions reduces in the later months. It should

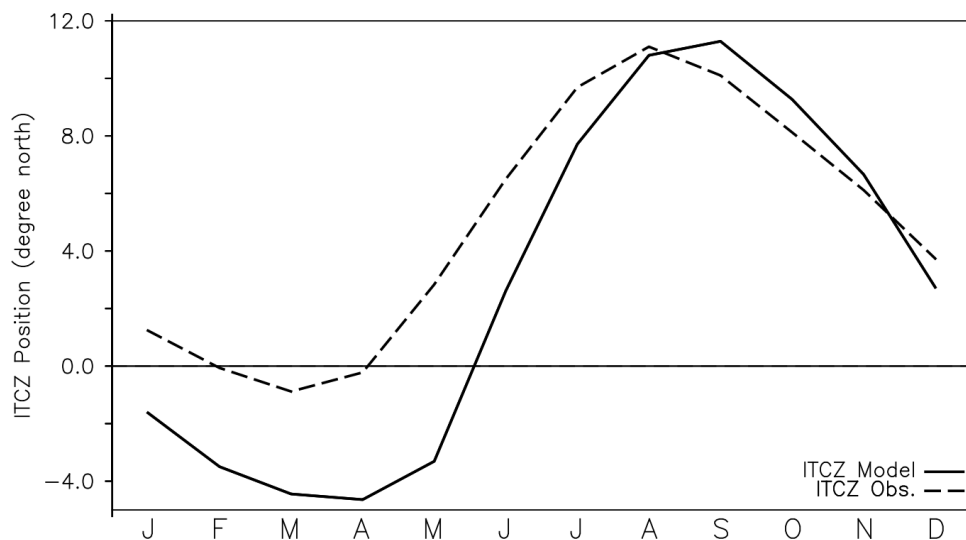


Figure 5.3: The monthly climatological position of the ITCZ (degree north) in the Atlantic in the model reference run (CFSv2_{REF}; solid line) and in the observations (dashed line).

be noted that the position of the ITCZ in the model almost coincides with that of observations in August. As we will see later, this point becomes important when interpreting the results of the sensitivity experiment. From the above, we can conclude that the model simulates the development of seasonal cold tongue that is characteristic of the tropical Atlantic but with a delay of about two months, giving rise to the warm SST bias. The biases in SST in the cold tongue region, surface winds over the equator and the position of ITCZ are intimately connected with each other and they decrease after July. As may be noted, the interannual SST anomaly of this cold tongue, its accompanying anomalous winds, and the thermocline depth, among other things, manifest as an AZM event. Hence, we may expect that the occurrence of the AZM in the model may be late compared to that in the observations. We examine in the below how well the model simulates the AZM using the free-run (CFSv2_{REF}) of the model.

5.4 Simulation of the AZM and its links with the Indian summer monsoon in CFSv2 free-run

The composites of anomalies of SST and wind of cold and warm AZM events (see Section 5.2 for the identification of events) in CFSv2 free-run (or CFSv2_{REF}) are compared with that of the observations in Fig. 5.4. In the observations, the SST anomalies associated with an AZM event peak in June or July and decay thereafter. These SST anomalies extend from the coast

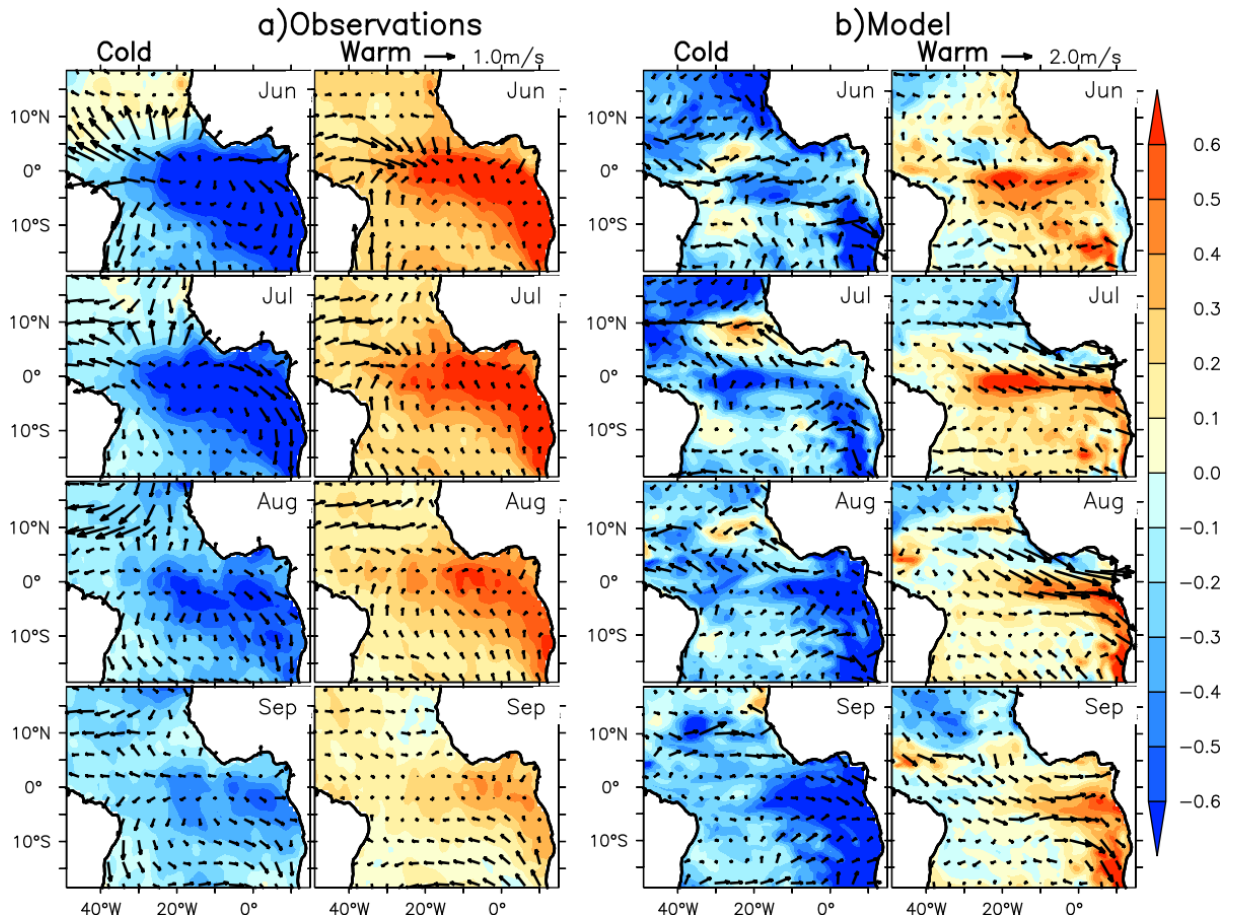


Figure 5.4: Monthly composites of anomalies of SST (shaded; °C) and low level winds at 850 hPa (vectors; ms^{-1}) of cold and warm AZM events in a) observations and b) in the reference run during June–September. a) is the same as Fig. 1.10

of Angola to the Atl3 region (3°S – 2°N and 20°W – 0°E) over the equator (Fig. 5.4a) and are accompanied by divergent (convergent) surface winds during a cold (warm) event. The northerly (southerly) wind anomalies along the Angolan coast in the latter months of July and August contribute to the decay of a cold (warm) event. However, in the model, although the SST anomalies in the proximity of equator are present from June onward, a clear sign of an AZM event in SST, i.e., the SST anomalies extending from coast of Angola to the Atl3 region, emerges only in July and peaks in August or September (Fig. 5.4b) which is late compared to the observations (Fig. 5.4a). Further, the magnitude and spatial extent of SST anomalies in the model are smaller compared to that in the observations. Interestingly, the least bias in the climatological position of the ITCZ during the season (June–September) occurs in August/September. Furthermore, the reduction of bias in ITCZ position is intimately connected to the delayed development of cold tongue as discussed above (Fig. 5.2 and Fig. 5.3). Given that the modulation of the seasonal cold tongue manifests as an AZM event, the delayed development of cold tongue leads to a

delayed AZM event compared to the observations. Nonetheless, the important feature of phase locking of AZM to the seasonal cycle is captured by the model. Hence, although delayed and weak compared to the observations, the model simulates the AZM.

As mentioned earlier in Chapter 2 and Chapter 3, ENSO influences the global climate. The relation between the AZM and ENSO in the model is discussed here. The standard deviation of the JJA Atl3 index in the observations is 0.48 but it is 0.23 in the model implying that the AZM is less variable in the model compared to the observations. The correlation between JJA Atl3 and JJA ONI in the model is 0.5 against -0.41 in the observations. While the AZM and ENSO have an opposite phase relation in the observations (also see Section 3.2), they are cooperative in the model. We have tried to take care of this issue by removing the effect of ENSO on a target field as described in Chapter 2, whenever necessary. However, it must be noted that this approach cannot remove the effect of ENSO completely.

As mentioned earlier in Section 5.1 and outlined in Chapter 1, Pottapinjara et al. (2014) proposed a physical mechanism by which the AZM in the tropical Atlantic can affect the ISM: an AZM excites a response in the mid-tropospheric temperature (TT) field which propagates to the east and disturbs the thermal gradient between over the Indian subcontinent and over the Indian ocean (Webster et al., 1998; Goswami and Xavier, 2005) and thereby affects the mean circulation and rainfall over India (Fig. 5.5a). In Fig. 5.5, the key element of eastward propagation of TT response is shown both for the model and observations. The positive correlation between the Atl3 index and the TT shown in the figure indicates that as a response to SST and convection anomalies associated with a warm (cold) AZM event, the tropospheric temperature over the Atlantic and Indian oceans rises (falls). In the observations (Fig. 5.5a; similar to Fig. 10 of Pottapinjara et al. (2014)), the TT response in the Atlantic grows (before -1 month TT lead), peaks (between -1 and 1 months lead) and decays (after 1 month lead) with time. This Matsuno-Gill-type response (Matsuno, 1966; Gill, 1980) has a Rossby wave-like structure with two lobes of high positive correlation on either side of the equator in the Atlantic and has an eastward propagating Kelvin wave like-structure in the equatorial band. The response propagates to the east through the Indian Ocean and reaches as far as 140°E in the Pacific at its peak. The warming of the troposphere in the equatorial belt (confined to 10°S and 10°N) in the Indian Ocean can weaken the positive TT gradient between the land (Indian subcontinent) and ocean (Indian Ocean) that is shown to be critical for the circulation of ISM (e.g., Webster et al., 1998;

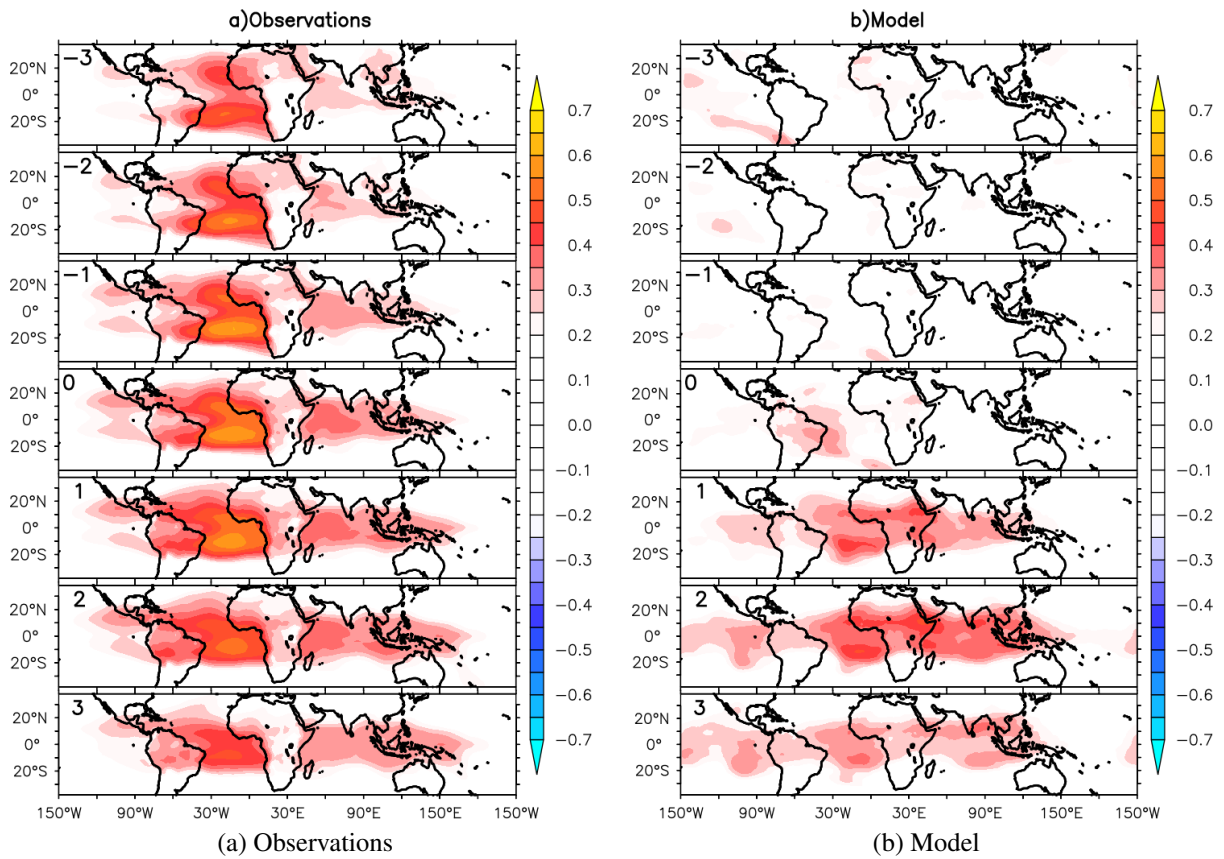


Figure 5.5: The monthly lead-lag correlations between the Atl3 index and Tropospheric Temperature (TT) integrated over 600 hPa to 200 hPa after removing the effect of ENSO on both TT and Atl3 index in a) Observations and b) Model. The lead of TT in months is indicated on each subpanel. The effect of ENSO is removed to elicit the signal clearly (as discussed in Section 3.2). The removal also takes care of the wrong AZM-ENSO relation in the model, albeit partially. The correlations are statistically significant at the 10% level.

Goswami and Xavier, 2005). In Pottapinjara et al. (2014), the modulation of TT gradient by the AZM is argued to be intimately connected to the lower level moisture transport to the Indian subcontinent, low level cyclonic vorticity in the Bay of Bengal (BoB), number of depressions in the BoB and finally the rainfall over India (see Section 1.4 for an outline). A similar figure (Fig. 5.5b) for the model tells us that an AZM indeed excites a response in TT. Although it is weaker and decays faster compared to observations, the key features of the response in terms of structural similarity, propagation to the east into the IO, and growth and decay are all captured by the model.

It is interesting to see if the simulation of the relation between the AZM SST and TT in the model is reflected in AZM-ISMR relation as well. Fig. 5.6 shows the correlation between the Atl3 index and precipitation over India both in the observations and in the model. As reported

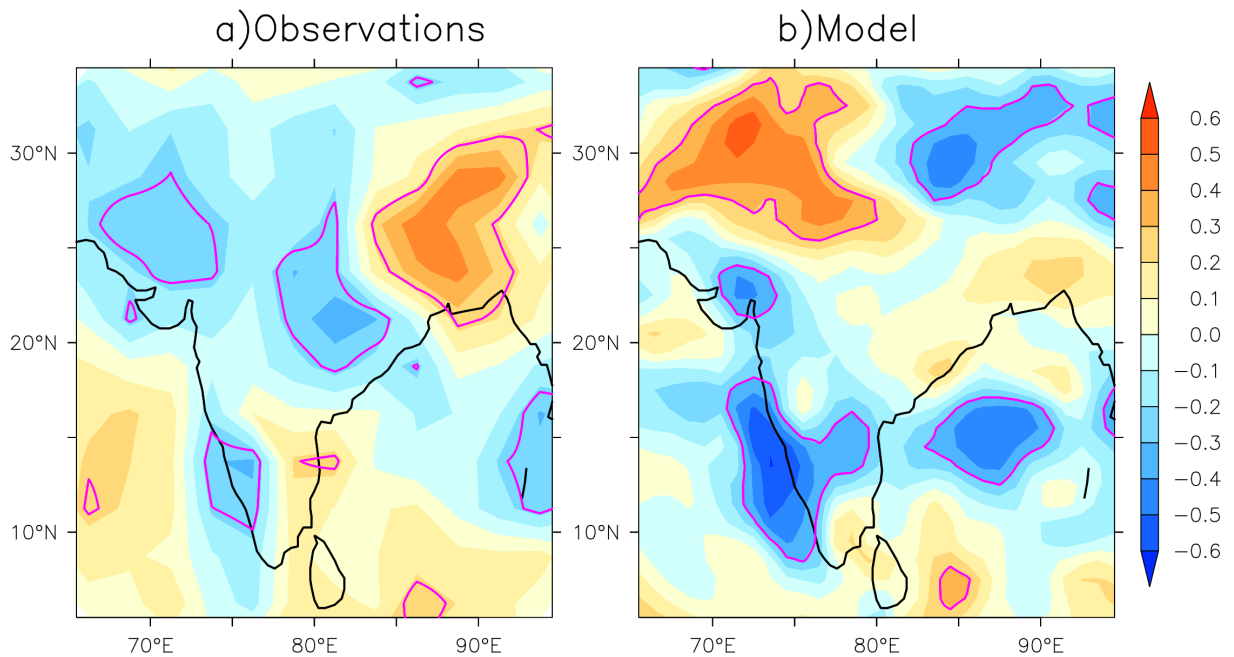


Figure 5.6: The correlation between the JJA AtI3 index and the JJAS precipitation over India in the a) observations and b) model reference run (CFSv2_{REF}), after removing the effect of ENSO over precipitation. The correlations are significant at the 20% level.

in previous studies (e.g., Kucharski et al., 2008; Wang et al., 2009; Pottapinjara et al., 2014), the observed relationship between the AZM and ISMR is that a warm (cold) AZM decreases (increases) rainfall over the Western Ghats and central India and enhances (reduces) rainfall over northeastern India (Fig. 5.6a). An opposite relation between the AZM and rainfall over a band extending from the Bay of Bengal to the northwest India can be seen as well. However, in the model, only the relationship between the AZM and rainfall along the Western Ghats is captured correctly (Fig. 5.6b). Note that the rainfall along the Western Ghats is directly influenced by changes in the mean flow. Further, the rainfall over central India has several contributors apart from variations in the mean flow (e.g., Pant and Kumar, 1997) and for the model to capture its relation with the AZM, all such factors need to be simulated properly.

5.5 Response of the ISM to the imposed warm AZM SST anomalies

In the above, examining the model free-run (CFSv2_{REF}), we have shown that the model simulates the relation between the AZM and ISMR through Kelvin wave-like in the TT field

reasonably well despite some shortcomings. To gain insights and more confidence about the influence of AZM on the ISM in the model, a sensitivity experiment is conducted as described in Section 5.2.

The response of the ISM to the imposed warm AZM SST anomalies shown in Fig. 5.7, i.e., the CFSv2_{SST} is analyzed here. The observed relation between the AZM and the rainfall and low level winds is shown in Fig. 5.8a. A warm AZM causes easterly wind anomalies in the eastern tropical Indian Ocean and north-easterly wind anomalies in the Arabian Sea; the net effect being the weakening the boreal summer seasonal mean flow. As a result, a warm AZM suppresses rainfall over the Western Ghats and over a band extending from the Bay of Bengal to the Northwest India but enhances the rainfall over the eastern equatorial Indian Ocean. The seasonal (June–September) average of the response in precipitation and low level winds is shown in Fig. 5.8b. It appears that the imposition of warm SST anomalies in the tropical Atlantic weakens the low level mean flow in the Arabian Sea (in agreement with the observations; compare with Fig. 5.8a) but enhances precipitation along and to the west of Western Ghats (contrary to the observations; compare with Fig. 5.8a). It also seems to cause an anticyclonic low level flow over central India and an increase in rainfall over the same region. The response in the low level winds in the eastern equatorial Indian Ocean is easterly, in agreement with the observations (compare with Fig. 5.8a). While the response in the low level winds is roughly as we would expect based on our earlier results in Pottapinjara et al. (2014) and the analysis shown in Fig. 5.8a, the response in the precipitation is not. Further, note that the responses in the low level winds and precipitation are not consistent with each other. This apparent inconsistency

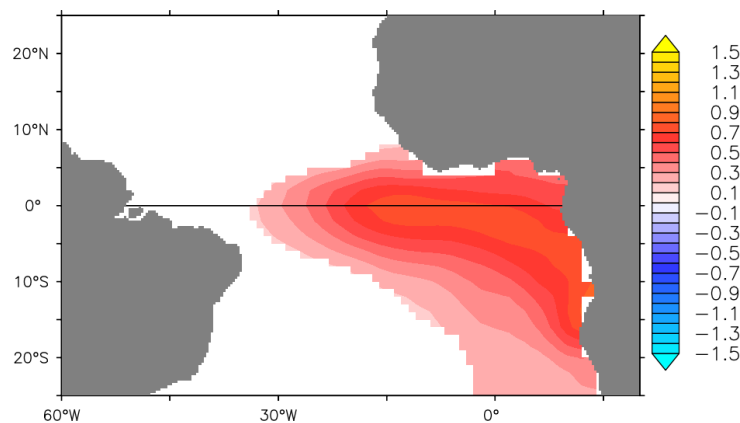


Figure 5.7: Composite of observed JJA SST anomalies (shaded; °C) of warm AZM events that is imposed in the sensitivity experiment. The composite is statistically significant at 10% level. The construction of the composite is described in Section 5.2.

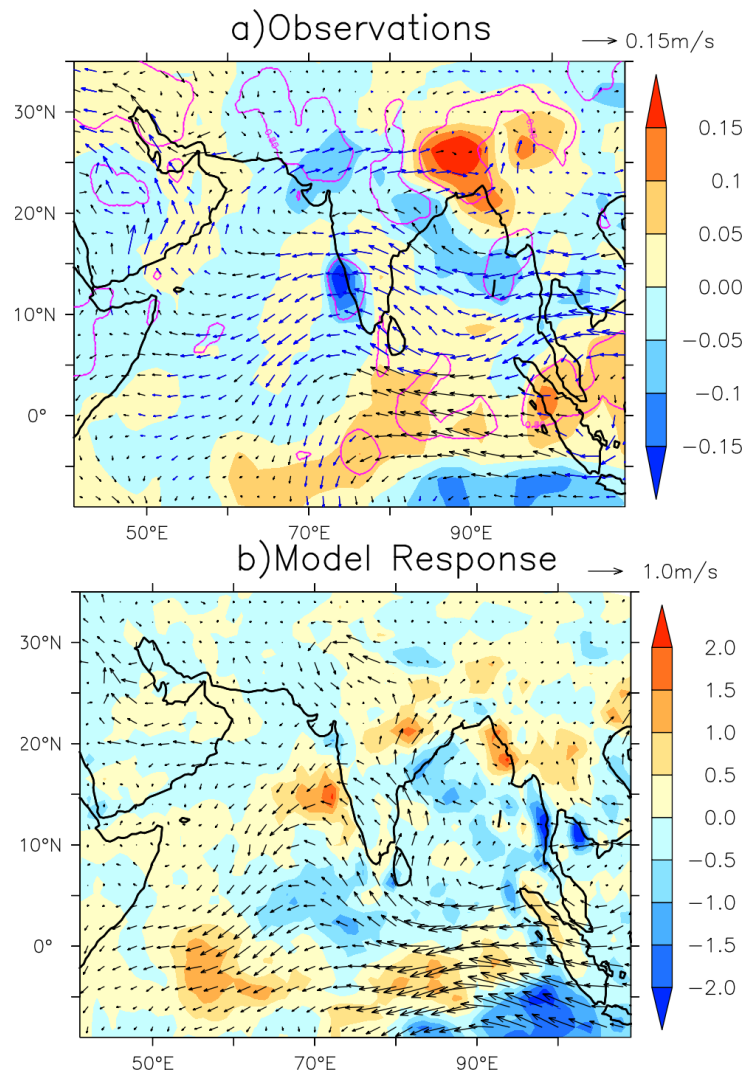


Figure 5.8: Influence of the AZM on the seasonal mean precipitation and low level circulation in the Indian Ocean in the a) observations and b) model sensitivity experiment (CFSv2_{SST}). a) Regression of JJA At13 index onto anomalies of JJAS precipitation (shading; mm day^{-1}) and low level winds (850 hPa; vectors; m s^{-1}) after removing the influence of ENSO b) JJAS mean response in precipitation (shading; mm day^{-1}) overlaid by winds (vectors; m s^{-1}). In (a), the statistically significant regressions at 20% in precipitation (winds) are shown in red contours (blue vectors).

must be investigated first before delving into further details. A similar plot of monthly mean responses in precipitation and winds during June–September shown in Fig. 5.9 tells us that the two fields are consistent with each other in all individual months of the season. Whenever the response in winds opposes (strengthens) the seasonal mean flow, the precipitation is less (more) than the corresponding climatological mean. However, note that the response in neither the precipitation nor winds is uniform in sign in the season and the precipitation response is disproportionate to that of winds. For instance, the wind response of about 2 ms^{-1} along the west coast of India in September (5.9d) generates disproportionately widespread and stronger

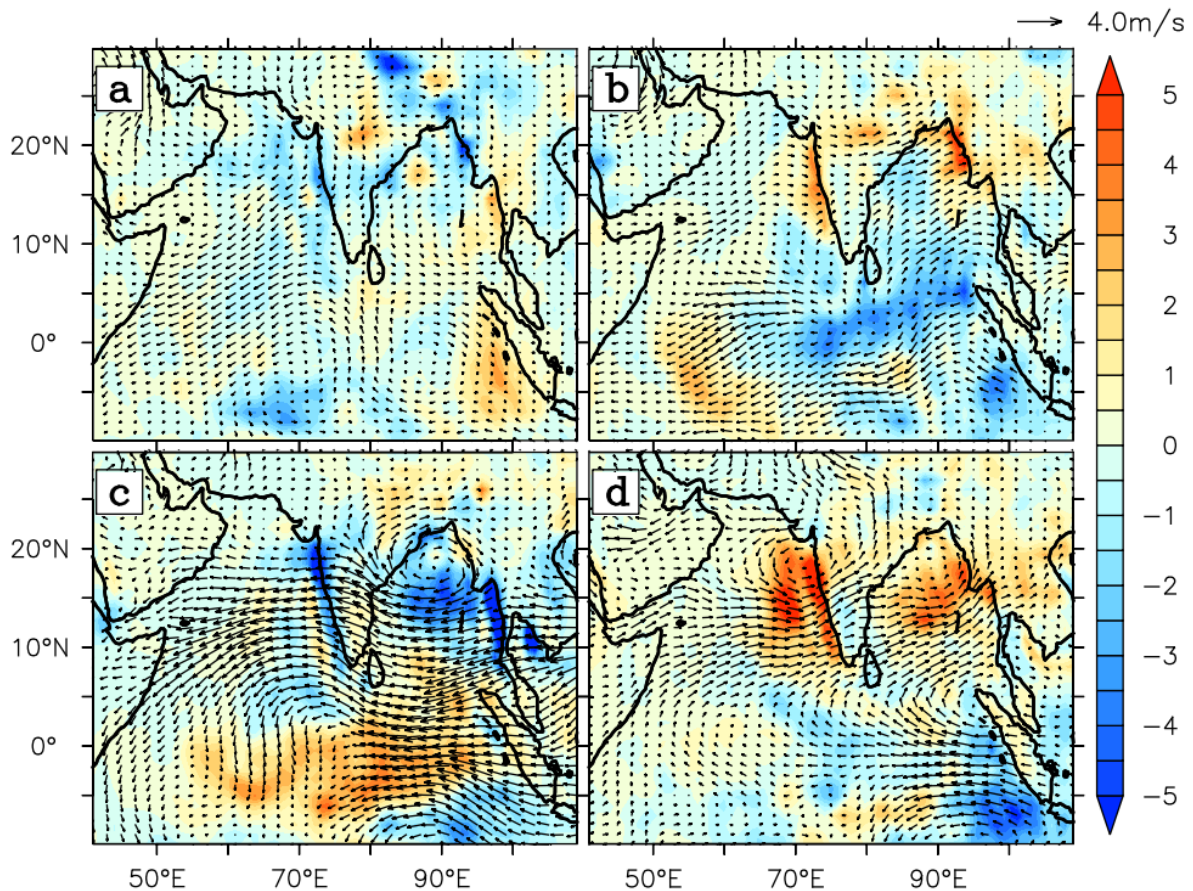


Figure 5.9: Monthly mean response of precipitation (shading; mm day⁻¹) overlaid by low level winds (vectors) in each month during June–September (a: June; b: July; c: August; d: September).

precipitation response compared to the wind response of about 4 ms⁻¹ in the same region in August (5.9c). Hence, the inconsistency between the wind and precipitation in the seasonal mean response shown in Fig. 5.8 arises from averaging their respective responses which are non-linearly related in individual months.

From the earlier analysis (Fig. 5.8a) and Chapter 3, the warm SST anomaly in the tropical Atlantic leads to a reduction in precipitation along the Western Ghats and over central India as well as non-conducive conditions for the formation of monsoon depressions in the Bay of Bengal (Pottapinjara et al., 2014). However, this relation in the sensitivity experiment can be seen only in the month of August and the response in other months is either weak, or the opposite (Fig. 5.9). In the month of August, a strong easterly flow extending from the west Pacific to the Somali coast that opposes the seasonal mean can be observed (Fig. 5.9 and Fig. 5.11a).

A strong anti-cyclonic circulation in the Bay of Bengal which tends to oppose the formation of monsoon depressions can also be noticed (compare Fig. 5.9c and Fig. 5.11a with Fig. 5.8 and Fig. 1.12b). This response in winds is accompanied by a reduction in precipitation along the Western Ghats and over the Bay of Bengal, and an enhancement in precipitation over the central to eastern Indian Ocean between 10°S and the equator. All this response is consistent with the observations (Fig. 5.8a). However, the precipitation response over central India is mixed with reduction over some place and the enhancement over the other. It must be borne in mind that rainfall over central India has several contributing factors and obtaining the right response over there needs proper simulation of all those contributing factors in the model (Pant and Kumar, 1997). As may be noted, this relation between AZM and precipitation over central India could not be simulated in the model reference run (CFSv2_{REF}) as well (Fig. 5.6). Nonetheless, on the whole, the response in the month of August (5.9c) is very close to the observations. Before addressing the question of whether or not the response in August is consistent across different fields, we must examine why the experiment yields observed response only in August and not in other months.

A relevant study by Richter et al. (2014) provides us a clue. Analyzing the Coupled Model Intercomparison Project 5 (CMIP5) models, Richter et al. (2014) note that the development of the cold tongue in the eastern equatorial Atlantic is not adequately captured by most of the models and that it may be partly due to westerly wind stress biases in boreal spring. Using the pre-industrial runs of the CMIP5 models, the study shows that there is a high correspondence between the latitudinal position of Atlantic ITCZ and the strength of the equatorial easterlies over the cold tongue region. Further, many models place the Atlantic ITCZ southward than is observed during boreal spring which weakens the equatorial easterlies causing a warm bias over the cold tongue region in the boreal summer and reversing the observed zonal SST gradient. The position of the ITCZ during boreal spring is very sensitive to the SST gradient between the north and south tropical Atlantic, and thus links the meridional and zonal modes in the tropical Atlantic (Servain et al., 1999; Murtugudde et al., 2001). Following (Richter et al., 2014), to find out why the model response is as observed only in August, the simulation of the Atlantic seasonal cycle in the model is examined here. The proper simulation of the Atlantic seasonal cycle in the model is essential because the AZM is tightly phase locked to the seasonal cycle. The movement of the Atlantic ITCZ is an important aspect of the seasonal cycle and the comparison of movement of Atlantic ITCZ both in the model and observation shows that the

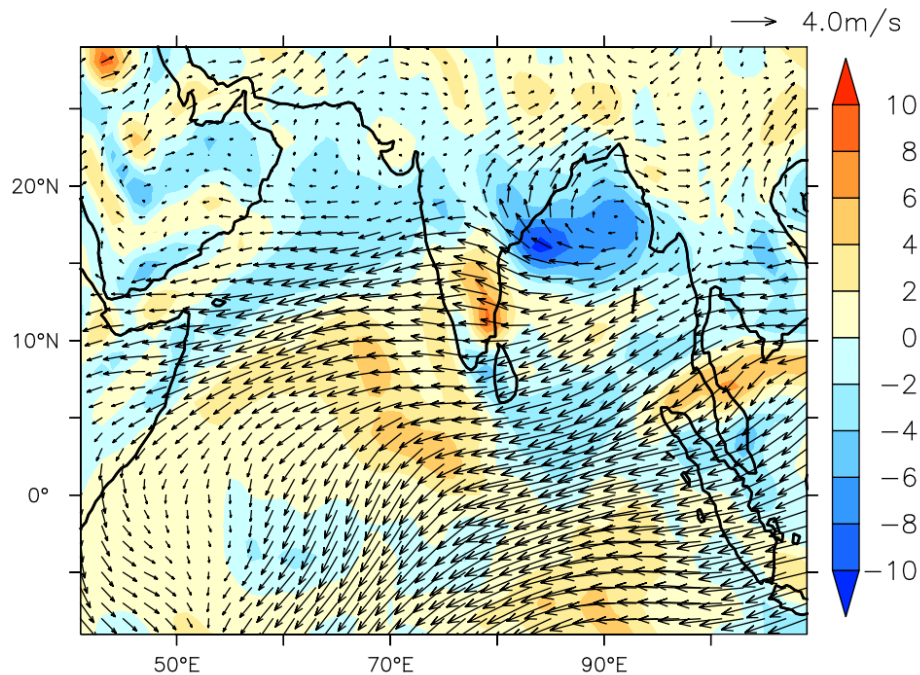


Figure 5.10: The response in vorticity at 850 hPa (shading; 10^{-6} s^{-1}) overlaid by vectors of shear between at 850 hPa and 200 hPa (winds at 850 hPa – winds at 200 hPa; ms^{-1}) in August.

seasonal cycle in the model is delayed compared to the observation (Fig. 5.3). However, the ITCZ in the model is located where it should be as per the observation only in the month of August and it is off by at least 3 degree latitude in other months during boreal spring–summer. The timing of the least bias in the position of the ITCZ coincides with that of the western equatorial Atlantic zonal winds (Fig. 5.2). As may be noted from Fig. 5.2, the SST bias also starts to decrease in August. Given that the SST anomalies imposed in the tropical Atlantic in the experiment ride on the climatology, it may be concluded that the close-to-right background conditions in the model in August gives us the desired response in the Indian ocean. Therefore, we will concentrate on the response in different fields only in August. Henceforth, the model response in the following would mean the response in August unless mentioned otherwise.

As discussed in Section 1.4, the AZM can influence the rainfall over central India by modulating the frequency of monsoon depressions forming in the Bay of Bengal (Pottapinjara et al., 2014). As shown in Fig. 5.10, as a response to the imposed warm SST anomalies in the tropical Atlantic, there is a negative vorticity and high wind shear between upper and lower levels, which together oppose the formation of depressions there. The reduced number of mon-

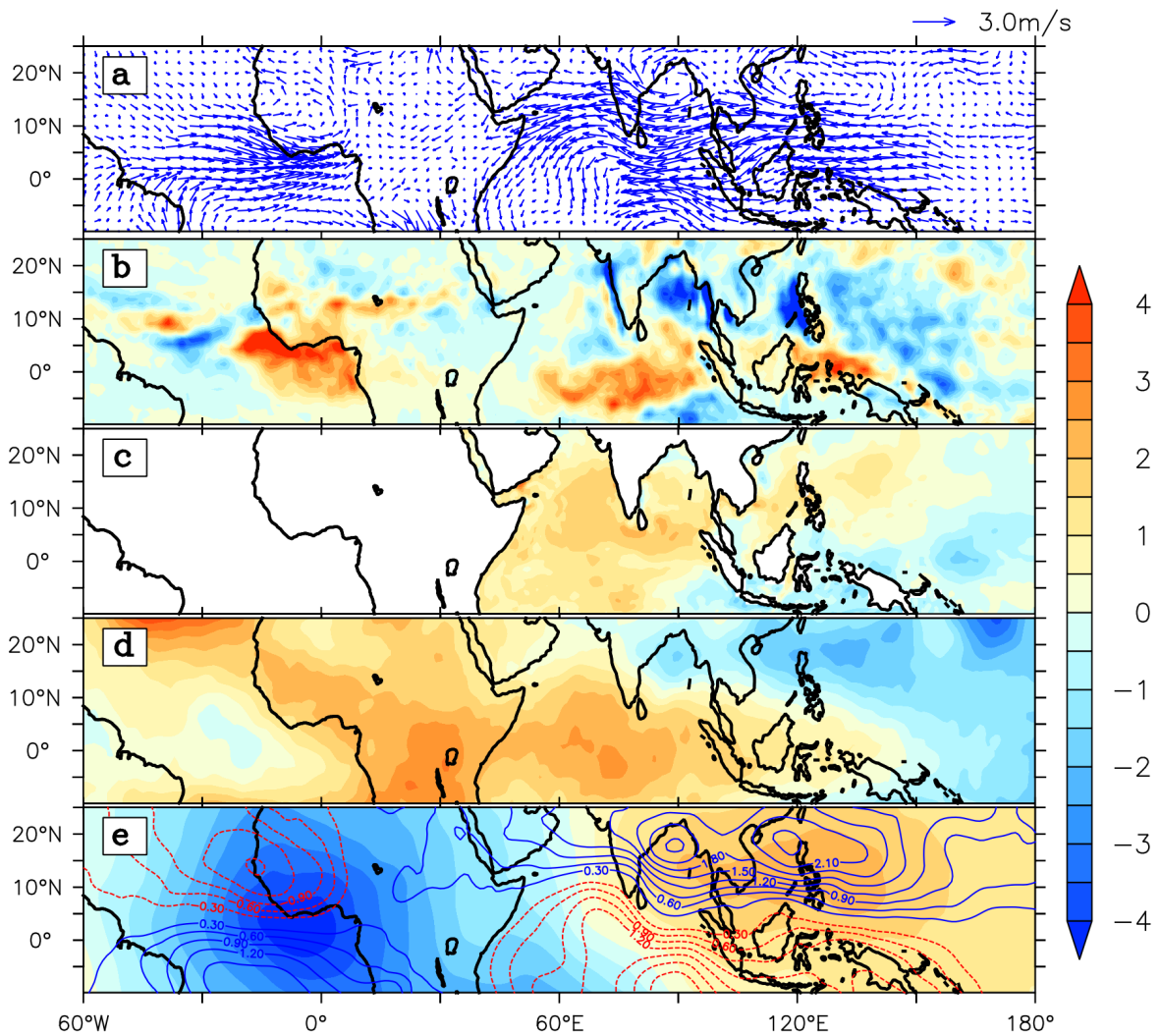


Figure 5.11: The response and analyses of different fields covering the tropical Atlantic and Indian oceans: a) low level wind vectors at 850 hPa (m s^{-1}); b) precipitation (mm day^{-1}); c) SST ($^{\circ}\text{C}$; multiplied by 0.25); d) mid-tropospheric temperature averaged between 600 and 200 hPa (0.1 K) e) upper level velocity potential at 200 hPa (shading; $10^6 \text{ m}^2\text{s}^{-1}$) and low level stream function at 850 hPa (contours; $10^6 \text{ m}^2\text{s}^{-1}$). The specified fields are scaled to have a common color scale. In c), the SST response in the tropical Atlantic is masked because that is where we impose the warm AZM SST anomalies. In (d), the positive (negative) contours of stream function are shown in blue (red) colors to highlight the quadrupole structure of Kucharski et al. (2009).

soon depressions tend to cause less rainfall over central India region that is normally frequented by the monsoon depressions. So, the model simulates an important result of Pottapinjara et al. (2014).

A major aspect of the teleconnection mechanism, between the Atlantic and Indian oceans is through Kelvin wave-like propagating in the tropospheric temperature field as discussed earlier (see Section 1.4 and Pottapinjara et al., 2014). To demonstrate this, the response in different

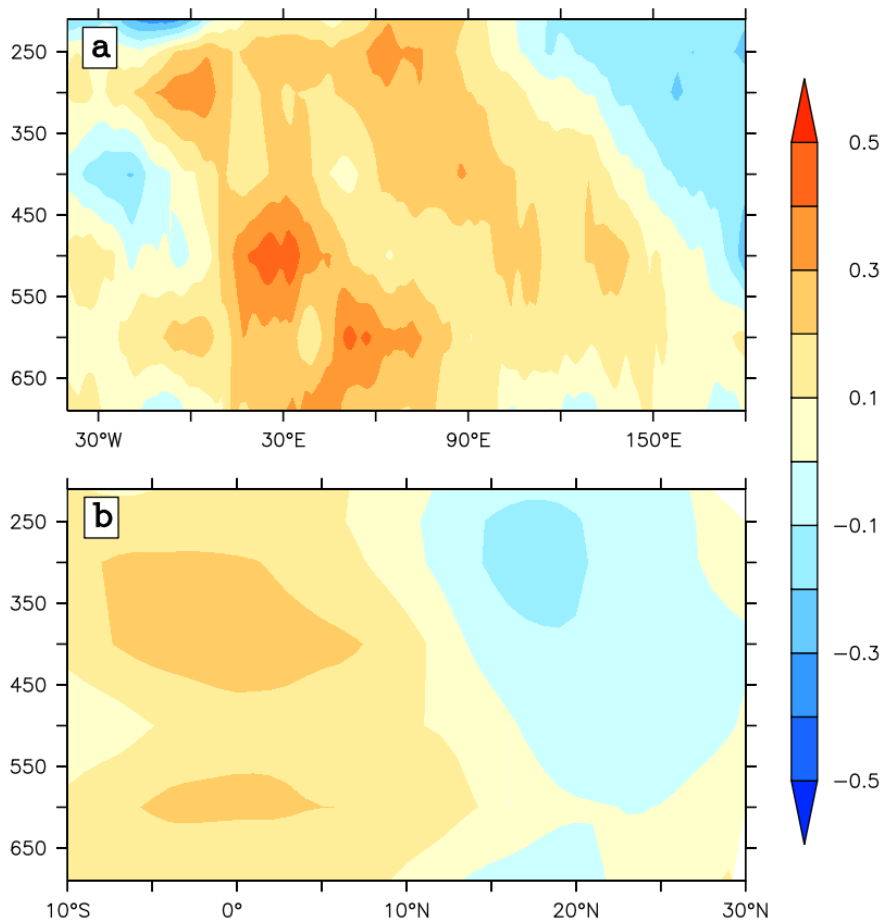


Figure 5.12: Vertical cross sections of the response in mid-tropospheric temperature (TT; K) in August, a) after averaging over the latitudinal band of 5°S – 5°N to show the TT teleconnection between the Atlantic and Indian oceans and b) after averaging over the longitudinal band of 60°E – 120°E to show the gradient in TT between over the Indian subcontinent and Indian Ocean.

fields covering the tropical Atlantic and Indian oceans is shown in Fig. 5.11. In response to the imposed warm SST anomalies in the tropical Atlantic, the convection over the eastern equatorial Atlantic results in precipitation over the same region (Fig. 5.11b). A consistent low level westerly wind response in the central to western equatorial Atlantic can be also noticed (Fig. 5.11a). Further, a weak warm response in SST in the Arabian Sea due to the weakened monsoonal flow can also be seen (Fig. 5.11c). Excited by the warm AZM anomalies and its resultant convection anomalies, a warm response in the mid-tropospheric temperature can be seen extending into the Indian Ocean and reach up to 150°E in the western Pacific (Fig. 5.11d). The vertical section of TT averaged over the equatorial belt covering the Atlantic and Indian oceans shows us that the TT in the mid-tropospheric column over the longitudes of Atlantic indeed warms up and extends into the Indian Ocean (Fig. 5.12a). Further, the vertical section of the TT re-

sponse in the longitudinal band of 60°E–120°E covering both Indian subcontinent and Indian Ocean reveals that the TT response over the Indian Ocean is warm, consistent with the warm TT response originating from the Atlantic and is cold over the subcontinent (Fig. 5.12b). This warm TT response over the ocean and cold TT response over land weakens the mean land-sea mid-tropospheric thermal gradient and consequently reduces the strength of mean monsoonal flow as shown in Fig. 5.10 and Fig. 5.11a. Note that this TT response is consistent with the response in precipitation and winds shown in Fig. 5.9.

As mentioned earlier in Section 5.1, a dynamical manifestation of the response of ISM to the AZM is reported by Kucharski et al. (2009). From a sensitivity experiment conducted using an Atmospheric General Circulation Model (AGCM), they find that a positive (negative) AZM SST anomaly in the tropical Atlantic causes a Gill-Matsuno type baroclinic quadrupole response in the stream function. Further, from the the upper level velocity potential, they showed that the heating associated with the warm AZM event induces an upper level divergence over the Atlantic and Africa region, and an upper level convergence over India and the western Pacific which is attributed to the reduction of rainfall over India. Interestingly, the upper level velocity potential in the model response presented in 5.11 shows a similar structure with upper level divergence over Atlantic and convergence over India. In addition, the quadrupole response in lower level stream function can also be seen (Fig. 5.11e). Consistent with this, a reduced precipitation over India and the Bay of Bengal can be also noticed (Fig. 5.11b).

From the above discussion of the sensitivity experiment, we may conclude with more confidence that the observed teleconnection between the AZM and ISM is simulated by the model reasonably well although it misses some finer details due to biases in the model.

5.6 Summary and Discussion

Earlier studies have shown the existence of a relation between the AZM and ISM (e.g., Kucharski et al., 2008; Wang et al., 2009; Pottapinjara et al., 2014). (Kucharski et al., 2009) showed that the warm (cold) AZM SST anomaly induces a Matsuno-Gill type quadrupole structure causing a sinking (rising) motion over India which in turn reduces (enhances) rainfall over India. In our recent study Pottapinjara et al. (2014), we proposed a thermodynamic aspect of the teleconnection by which the AZM affects the ISM. As per our hypothesis, the signal of the

AZM propagates eastwards and reaches the Indian Ocean as Kelvin-like wave in tropospheric temperature. Further, by modulating the mid-tropospheric temperature gradient between over the Indian subcontinent and the Indian Ocean, it affects the seasonal mean flow and thereby the rainfall over India (e.g., Goswami and Xavier, 2005).

The IMD, the agency responsible for the monsoon prediction in India, employs the NCEP CFSv2 coupled model as one of its dynamical models for the seasonal prediction of monsoon. In the present study, we examine the fidelity of the simulation of the AZM-ISM relation in the low resolution variant of the same model (CFS version 2). Further, we conduct a complementary sensitivity experiment to examine if the physical mechanism proposed in Pottapinjara et al. (2014) is simulated by the model. An analysis of the 20 years of the free-run (or CFSv2_{REF}) by the model suggests that variability of the AZM and its relation to the monsoon, i.e., a warm (cold) AZM suppressing (enhancing) the rainfall over India, are captured reasonably well in the model but are subject to the biases linked to the mean state. Further analyses of the sensitivity experiment are analyzed in the context of these biases to advance the process understanding of the AZM-monsoon interactions. Because of the delayed seasonal cycle in the tropical Atlantic in the model, the response to the imposed warm AZM SSTA in the precipitation and low level winds are not consistent throughout the summer, as reflected in their seasonal mean response. However, in the month of August, when the Atlantic ITCZ in the model is in its correct position, the response of the ISM to imposed warm AZM SST anomalies is consistent across precipitation, low level winds, mid-tropospheric temperature, vorticity and shear; all simulating the physical mechanism suggested in Pottapinjara et al. (2014) as mentioned earlier. The reduction in rainfall along the Western Ghats as a response to warm AZM SSTA is prominently seen as it is directly affected by the changes in the mean flow. However, the precipitation response over central India is not clearly seen owing to limitations of the model. Further, the experiment also shows that the model simulates the dynamics-based physical mechanism proposed by Kucharski et al. (2009) wherein a warm AZM SST anomaly has a Gill-Matsuno type quadrupole response and induces an upper level convergence over India leading to reduced rainfall. The two mechanisms may not be totally independent of each other but are different manifestations of the total coupled nonlinear system. As shown in this study, the CFSv2 model has some serious biases in simulating the seasonal cycle in the tropical Atlantic. This problem is also seen in many coupled models participating in the CMIP5 as well (Richter et al., 2014). This study highlights the need for improving the mean state of tropical Atlantic in CFSv2 in

order to account for a realistic AZM-ISM connections, which will lead to better forecasts of the ISM.

Although we have shown that the CFSv2 simulates the different manifestations of response of ISM to AZM (of Kucharski et al., 2009; Pottapinjara et al., 2014), we have not investigated the relative importance of these mechanisms. The response of winds and precipitation in the Indian Ocean (Fig. 5.11a and Fig. 5.11b) seem a bit stronger for the imposed SST anomalies. The strong response could be due to local positive feedbacks in the Indian Ocean or a stronger dynamic response in addition to the thermodynamic response. The cooling of TT in the Bay of Bengal and western Pacific (Fig. 5.11d) could not be seen in the observations or in the reference run of model (Fig. 5.5). It is likely that this cooling is induced by the sinking motion as a secondary response. The enhancement of precipitation in the southeastern Indian Ocean, and reduction of precipitation over the Bay of Bengal (Fig. 5.11b) are likely linked by the local Hadley cell in the Indian Ocean. A slight cooling of TT in the central equatorial Atlantic in Fig. 5.11d is due to the cooling between the levels of 400 and 350 hPa (Fig. 5.12a) but we do not understand why this occurs. In this study, while examining the simulation of the results reported in Pottapinjara et al. (2014), we did not actually track the monsoon depressions in the model as the coarse resolution of the model does not support it. Rather, we have only shown the response in the vorticity and wind shear that are crucial for the formation of monsoon depressions in the Bay of Bengal. Further, in the experiment we have conducted only the response to warm SST anomalies in the tropical Atlantic is studied. A subsequent experiment imposing the cold SST anomalies can offer us more insights into possible non-linearity in the teleconnection between the AZM and ISM with respect to the phase of AZM but we will not pursue it here in this thesis.

Chapter 6

Conclusion and scope for future work

The Indian summer monsoon (ISM) is the lifeline of the south Asian region, a heavily populated region in the world. The ISM contributes to about 80 % of the annual total rainfall of India. The ISM varies on a spectrum of timescales but we focus on its inter-annual variability given the implications of these year-to-year variations of ISM for the economy and food production of India. Understanding the variability of the monsoon and predicting the same has an immense value. Motivated by this great societal need, in this thesis, we have attempted to understand the interannual variability of the monsoon induced by the AZM, an aspect that has not been explored in detail. The detailed summary of results and their limitations, if any, are already discussed at the end of each of Chapter 3, Chapter 4 and Chapter 5. This chapter casts the key findings of the thesis in the context of the set objectives and throws some ideas that can be taken up for further study.

As the interannual variability of the ISM is a result of both internal dynamics and external factors, and the influence of the external factors form the basis of prediction of the ISM, we have surveyed the literature in Chapter 1 to understand the external drivers of the ISM, especially those operating in the tropics. Our literature survey informs us that the El Niño-Southern Oscillation (ENSO) and Indian Ocean Dipole (IOD), the coupled ocean-atmosphere modes of variability operating in the tropical Pacific and Indian oceans respectively, are two major drivers of the ISM. The survey also informs us that there is a similar mode of variability housed in the tropical Atlantic called the Atlantic Zonal Mode (AZM) whose influence on the ISM is relatively less studied compared to that of ENSO and IOD. We chose to focus on this relationship

between the AZM and ISM, and conducted a thorough review of the prior research on the relationship in Chapter 1. The prior research includes a recent relevant study of ours Pottapinjara et al. (2014) which is the basis for the body of work presented in the thesis. From the review of the earlier research on AZM-ISM relationship, we identify important gaps based on which we set the following objectives.

- (i) To explore the lead association of the known precursors of the AZM in boreal spring to the following ISM
- (ii) To investigate if the evolution of warm and cold AZM in the boreal spring is symmetric, which would enhance our understanding of the AZM
- (iii) To explore the capability of a current day seasonal forecast model in simulating the relationship between the AZM and ISM

We have used a variety of well documented observational and reanalysis datasets in our analysis and described them in Chapter 2. We have tried to use the same set of datasets throughout the thesis to maintain the uniformity, and discussed any exceptions and reasons thereof. Nevertheless, we have demonstrated that the choice of datasets does not alter our results. In addition, we have used CFSv2 model for the analysis discussed in Chapter 5 and the model is described in the same chapter for the ease of readability. Further, different statistical techniques employed to analyze these datasets have also been discussed in Chapter 2.

One of our goals is to investigate the lead associations of the ISM and our focus here is on the relationship between the AZM and ISM. However, both the AZM and ISM are active during boreal summer and hence the relation between the two does not provide any predictive value for the ISM. Earlier studies showed that the Bjerknes feedback mechanism, which involves the SST, surface winds and heat content in the equatorial region, explains a great part of variability of the AZM. The previous studies also showed that these Bjerknes feedback components in the tropical Atlantic during boreal spring indicate the development of an oncoming AZM event in the following summer. Based on this prior research, in Chapter 3, we explore the lead association of the Bjerknes components during boreal spring to the ISM (Objective i). We find that the coherent evolution of the surface zonal winds and heat content in the equatorial Atlantic during boreal spring is significantly related to the summer monsoon rainfall over two important regions in India. It gives us a clue of the ISMR one season in advance through the teleconnections reported in the previous studies discussed in Chapter 1. This result is especially important and

can offer us hope when ENSO, a major driver of the inter-annual variability around the globe including the ISM, is not active.

Having shown the lead association for the ISM in the spring precursors of the AZM in Chapter 3, we delve deep into the details of the evolution of AZM events in Chapter 4 (Objective ii). As discussed in Section 3.5, some analyses of Chapter 3 also provide a good background for our efforts presented in Chapter 4. Earlier studies showed that meridional migrations of the Atlantic Inter-tropical Convergence Zone (ITCZ) during boreal spring affects the concurrent surface zonal winds in the equatorial Atlantic which is a precursor of the AZM. We observe that the relationship between the meridional position of spring Atlantic ITCZ and AZM is not as strong as that between the location of spring Atlantic ITCZ and concurrent surface zonal winds in the equatorial Atlantic. We find that it is due to an asymmetry in the relationship between the spring Atlantic ITCZ position and AZM: while an anomalously northward spring ITCZ is highly likely to lead to a cold AZM event in the following summer, an anomalously southward spring ITCZ is less likely to cause a warm event. We also find that the asymmetry is inherent to the Atlantic seasonal cycle. Putting it in the context of Objective ii, the evolution of cold and warm AZM events with respect to the meridional position of Atlantic ITCZ during boreal spring is asymmetric. In addition, we observe that the causative mechanisms of warm AZM events are more diverse than that of cold events. This could imply that the AZM cold events are inherently more predictable compared to the warm events. This important result paves the way for further AZM diversity studies. The results presented in this chapter enhance our understanding of the AZM and contribute to the predictability of different phenomena including the ISM via the teleconnections discussed in Chapter 1 and Chapter 3.

In Chapter 3 and Chapter 4, we have investigated the relationship of the AZM with its precursors, and the lead association of these precursors for the ISM through its teleconnections with the AZM. However, these results based on the analysis of observational and reanalysis datasets find their practical application when they are simulated by the numerical models used for prediction of the ISM. In Chapter 5, we examine whether the relationship between the AZM and ISM reported in earlier studies is simulated in the Coupled Forecast System version 2 (CFSv2), a state-of-the-art dynamical model used for the seasonal prediction of monsoon in India (Objective iii). Our emphasis is on the simulation of results reported in our earlier study Pottapinjara et al. (2014), importantly, the influence of the AZM on the ISM rainfall and the

thermodynamics-based teleconnection between the AZM and ISM via the Kelvin-like waves in the tropospheric temperature field. From the analysis of the model free-run and the complementary sensitivity experiment we conducted, we find that the model simulates the AZM and its relationship with the ISM as reported in our earlier study and other important studies reasonably well despite some mean state biases. However, these biases, manifest in the delayed development of the seasonal cycle in the Atlantic, determine the simulation of timing and strength of the AZM-ISM relationship in the model. Our results strongly advocate that the simulation of the annual cycle of the Atlantic ITCZ, and the AZM are critically important to capture the teleconnections between the AZM and ISMR. It is relevant to note that many of the CMIP5 models also fail to simulate the interannual ENSO-Monsoon relationship owing to a poor capability in accurate simulation of the seasonal cycle of ENSO (e.g., Jourdain et al., 2013). Such improvement will, in turn, potentially contribute to improving the forecasts of the monsoon issued using the model (CFSv2).

A brief summary of the key results is provided here.

1. The boreal spring zonal surface winds and heat content in the equatorial Atlantic, which are precursors of AZM, are significantly related to the ISMR and can give us a clue of the ensuing ISM one season in advance
2. The evolution of cold and warm AZM events with respect to the meridional position of the spring Atlantic ITCZ, a precursor of the AZM, is asymmetric. In addition, the causative mechanisms of warm AZM events seem to be more diverse than that of cold AZM events
3. The CFSv2, a state-of-the-art dynamical model used for the seasonal prediction of the ISM in India, simulates the observed relationship between the AZM and ISM reasonably well, despite mean state biases in the tropical Atlantic. However, the timing and strength of the AZM-ISM relationship in the model are affected by the biases.

Having elucidated the key results of the thesis in the context of the set objectives, we discuss some ideas which are offshoots of these results in the following. These research problems can be taken up in a future study.

In Chapter 3, we have shown that the spring precursors of AZM have a lead association with the ISM. As discussed in Chapter 1, the climate modes of variability such as the the

Atlantic Meridional Mode (AMM), the South Atlantic Anticyclone (SAA) and ENSO can trigger the AZM events. In addition to the different causative mechanisms of the AZM discussed in Chapter 5, there may be further unknown processes leading to AZM events. Hence, it is likely that the different phenomena affecting the development of AZM (e.g., AMM, SAA and ENSO) may influence the ISM via the AZM. The connections between such phenomena and the monsoon either directly or via the AZM can be the subject of further studies.

As mentioned in Section 4.1, one of the factors affecting the spring Atlantic ITCZ movement is, a decaying ENSO. This result from previous studies, together with our results discussed in Chapter 4, hint at an interesting linkage between the tropical Pacific and the ISM in a novel way. Previous studies show that a persistent (into spring) yet decaying El Niño can suppress the rainfall over the deep tropical Atlantic and move the ITCZ north in spring. The northward spring ITCZ can cause a cold AZM event in the following summer which in turn can enhance the rainfall over India. Normally, an El Niño that is active in summer tends to reduce the ISMR. However, an El Niño peaking in preceding winter and decaying thereafter can enhance the ISMR through the cold AZM, El Niño's reincarnation. This should at least motivate focused model sensitivity studies to better understand the ITCZ-AZM-ISM interactions and its asymmetries. In addition, a potential question to address is, can the AZM influence the following Indian winter monsoon through its 'capacitor effect' in the equatorial Indian ocean?

In Chapter 5, we have shown that the CFSv2 has biases in the simulation of the mean state in the tropical Atlantic. Such biases may initiate false AZM events which in turn may affect monsoon predictions via the teleconnection mechanisms discussed in Chapter 1 and Chapter 5. The impact of these biases on the ISM in the models used for monsoon forecasts (CFSv2) needs to be studied. Further, efforts must be made to reduce these biases to improve the simulation of AZM variability and thus the monsoon forecasts issued using the CFSv2.

Appendix A

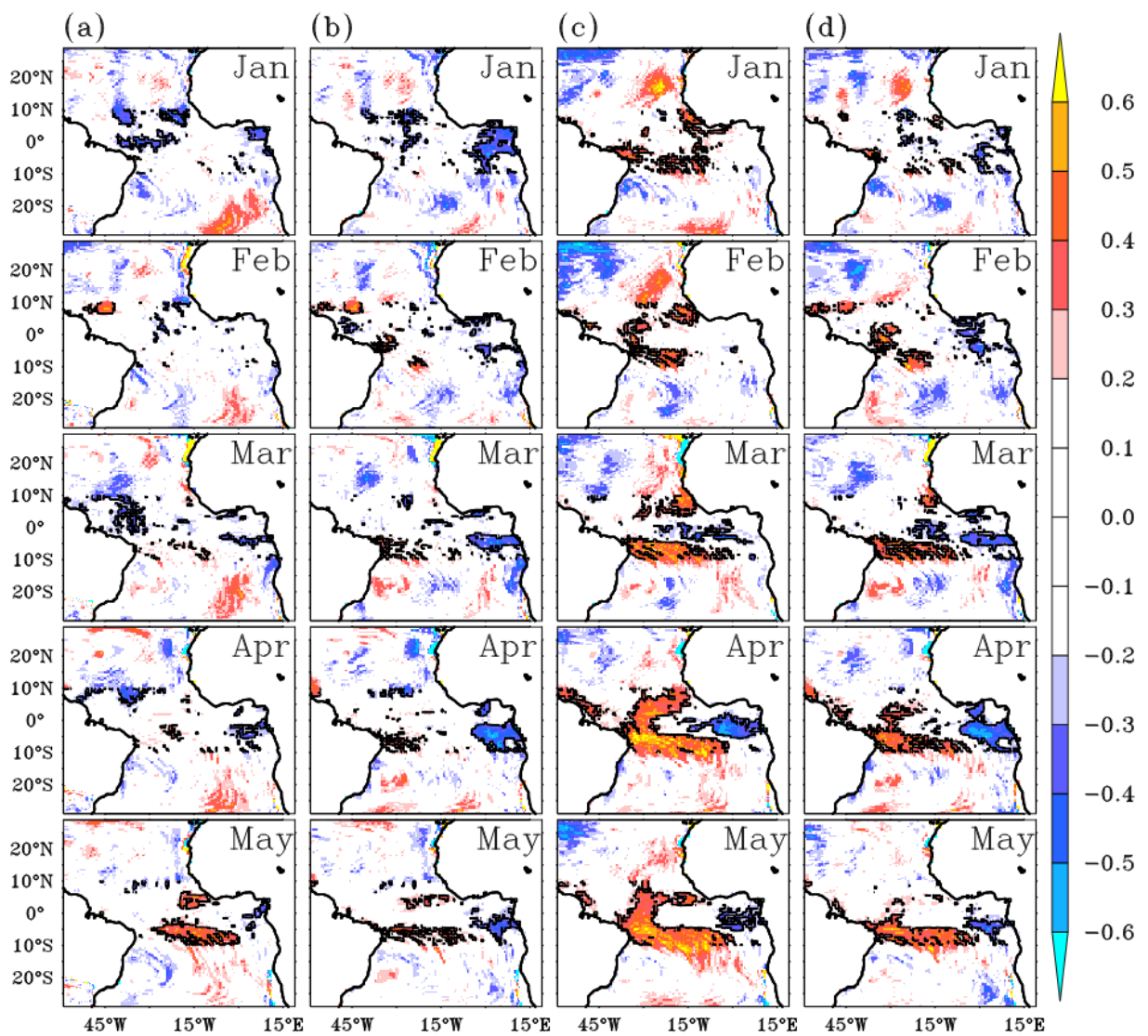


Figure A.1: Same as Fig. 3.6 but using EN4 subsurface analysis version 4.2.0 of the UK Met Office (Good et al., 2013) for the computation of heatcontent.

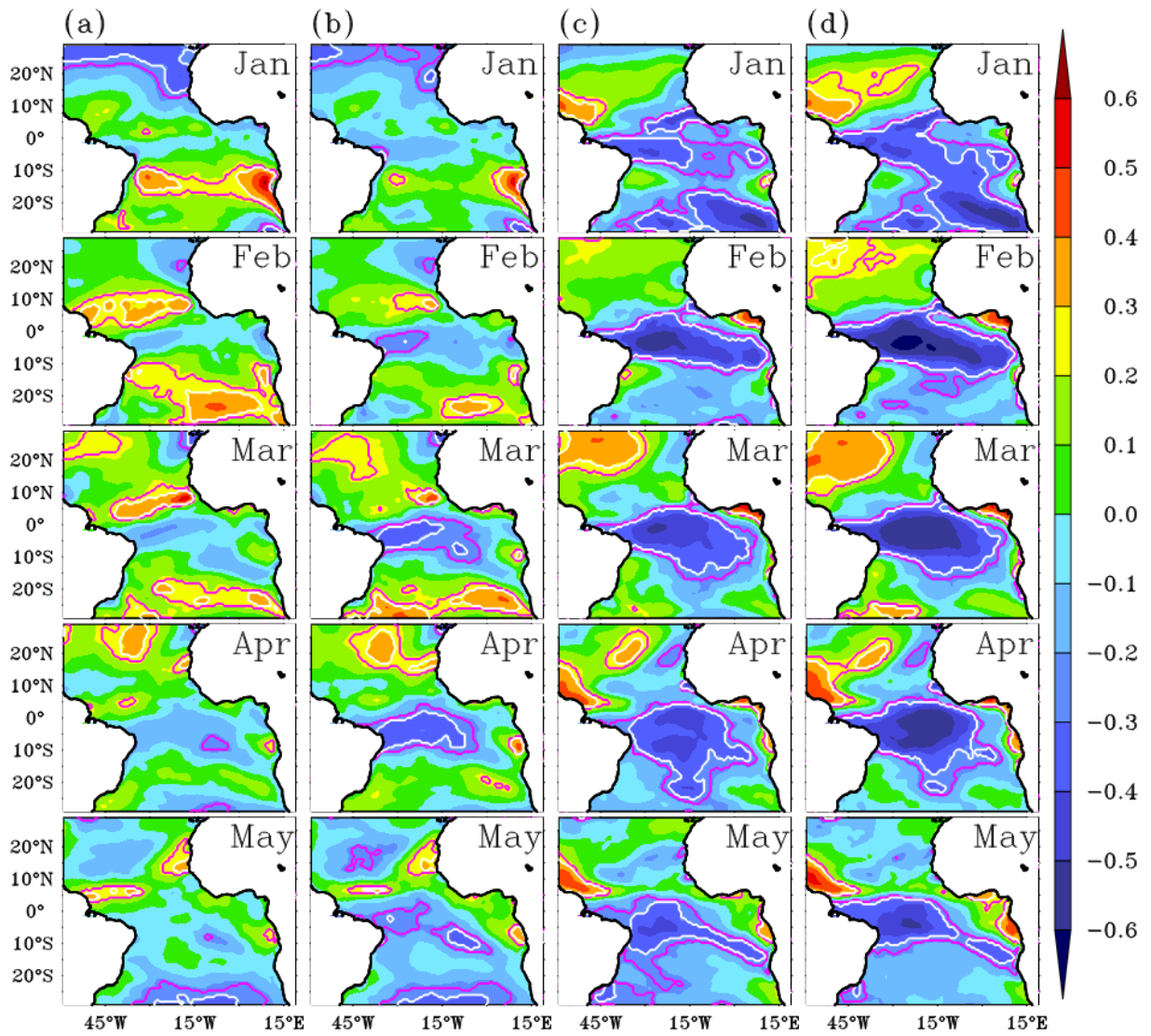


Figure A.2: Same as Fig. 3.7 but using the wind data from the ERA-Interim (Dee et al., 2011).

References

- Adler, R. F., and Coauthors, 2003: The Version-2 Global Precipitation Climatology Project (GPCP) Monthly Precipitation Analysis (1979–Present). *Journal of Hydrometeorology*, **4** (6), 1147–1167, doi:10.1175/1525-7541(2003)004<1147:TVGPCP>2.0.CO;2.
- Alexander, M. A., I. Bladé, M. Newman, J. R. Lanzante, N.-C. Lau, and J. D. Scott, 2002: The atmospheric bridge: The influence of ENSO teleconnections on air–sea interaction over the global oceans. *Journal of climate*, **15** (16), 2205–2231.
- Amat, H. B., and K. Ashok, 2018: Relevance of Indian summer monsoon and its tropical indo-Pacific climate drivers for the Kharif crop production. *Pure and Applied Geophysics*, **175** (6), 2307–2322.
- Amaya, D. J., and G. R. Foltz, 2014: Impacts of canonical and Modoki El Niño on tropical Atlantic SST. *Journal of Geophysical Research: Oceans*, **119** (2), 777–789.
- Annamalai, H., R. Murtugudde, J. Potemra, S. Xie, and B. Wang, 2002: Coupled dynamics in the Indian Ocean: Externally or internally forced? *EGS General Assembly Conference Abstracts*, Vol. 27.
- Annamalai, H., R. Murtugudde, J. Potemra, S.-P. Xie, P. Liu, and B. Wang, 2003: Coupled dynamics over the Indian Ocean: Spring initiation of the zonal mode. *Deep Sea Research Part II: Topical Studies in Oceanography*, **50** (12-13), 2305–2330.
- Ashok, K., S. K. Behera, S. A. Rao, H. Weng, and T. Yamagata, 2007: El Niño Modoki and its possible teleconnection. *Journal of Geophysical Research: Oceans*, **112** (C11).
- Ashok, K., F. Feba, and C. T. Tejavath, 2019: The Indian summer monsoon rainfall and ENSO. *Mausam*, **70** (3), 443–452.

-
- Ashok, K., Z. Guan, N. Saji, and T. Yamagata, 2004a: Individual and combined influences of ENSO and the Indian Ocean dipole on the Indian summer monsoon. *Journal of Climate*, **17** (16), 3141–3155.
- Ashok, K., Z. Guan, N. H. Saji, and T. Yamagata, 2004b: Individual and Combined Influences of ENSO and the Indian Ocean Dipole on the Indian Summer Monsoon. *Journal of Climate*, **17** (16), 3141–3155, doi:10.1175/1520-0442(2004)017<3141:IACIOE>2.0.CO;2.
- Ashok, K., Z. Guan, and T. Yamagata, 2001: Impact of the Indian Ocean dipole on the relationship between the Indian monsoon rainfall and ENSO. *Geophysical Research Letters*, **28** (23), 4499–4502.
- Ashok, K., Z. Guan, and T. Yamagata, 2003: A look at the relationship between the ENSO and the Indian Ocean dipole. *Journal of the Meteorological Society of Japan. Ser. II*, **81** (1), 41–56.
- Ashok, K., and N. Saji, 2007: On the impacts of ENSO and Indian Ocean dipole events on sub-regional Indian summer monsoon rainfall. *Natural Hazards*, **42** (2), 273–285.
- Ashok, K., M. Shamal, A. Sahai, and P. Swapna, 2017: Nonlinearities in the evolutionary distinctions between El Nino and La Nina types. *Journal of Geophysical Research: Oceans*, **122** (12), 9649–9662.
- Ashok, K., C.-Y. Tam, and W.-J. Lee, 2009: ENSO Modoki impact on the Southern Hemisphere storm track activity during extended austral winter. *Geophysical Research Letters*, **36** (12).
- Ashok, K., and T. Yamagata, 2009: The El Niño with a difference. *Nature*, **461** (7263), 481–484.
- Barimalala, R., A. Bracco, and F. Kucharski, 2012: The representation of the South Tropical Atlantic teleconnection to the Indian Ocean in the AR4 coupled models. *Climate dynamics*, **38** (5-6), 1147–1166.
- Barimalala, R., A. Bracco, F. Kucharski, J. P. McCreary, and A. Crise, 2013a: Arabian Sea ecosystem responses to the South Tropical Atlantic teleconnection. *Journal of Marine Systems*, **117-118**, 14 – 30.

-
- Barimalala, R., A. Bracco, F. Kucharski, J. P. McCreary, and A. Crise, 2013b: Arabian Sea ecosystem responses to the South Tropical Atlantic teleconnection. *Journal of Marine Systems*, **117**, 14–30.
- Behera, S., R. Krishnan, and T. Yamagata, 1999: Unusual ocean-atmosphere conditions in the tropical Indian Ocean during 1994. *Geophysical Research Letters*, **26 (19)**, 3001–3004.
- Bjerknes, J., 1969: Atmospheric teleconnections from the equatorial Pacific. *Monthly weather review*, **97 (3)**, 163–172.
- Burls, N., C. C. Reason, P. Penven, and S. Philander, 2012: Energetics of the tropical Atlantic zonal mode. *Journal of Climate*, **25 (21)**, 7442–7466.
- Busalacchi, A. J., and J. Picaut, 1983: Seasonal variability from a model of the tropical Atlantic Ocean. *Journal of Physical Oceanography*, **13 (9)**, 1564–1588.
- Cadet, D. L., 1985: The southern oscillation over the Indian Ocean. *Journal of climatology*, **5 (2)**, 189–212.
- Caniaux, G., H. Giordani, J.-L. Redelsperger, F. Guichard, E. Key, and M. Wade, 2011: Coupling between the Atlantic cold tongue and the West African monsoon in boreal spring and summer. *Journal of Geophysical Research: Oceans*, **116 (C4)**.
- Capotondi, A., and Coauthors, 2015: Understanding ENSO diversity. *Bulletin of the American Meteorological Society*, **96 (6)**, 921–938.
- Carton, J. A., X. Cao, B. S. Giese, and A. M. Da Silva, 1996: Decadal and interannual SST variability in the tropical Atlantic Ocean. *Journal of Physical Oceanography*, **26 (7)**, 1165–1175.
- Carton, J. A., and B. S. Giese, 2008: A Reanalysis of Ocean Climate Using Simple Ocean Data Assimilation (SODA). *Monthly Weather Review*, **136 (8)**, 2999–3017, doi:10.1175/2007MWR1978.1.
- Carton, J. A., and B. Huang, 1994: Warm events in the tropical Atlantic. *Journal of Physical Oceanography*, **24 (5)**, 888–903.
- Chang, P., Y. Fang, R. Saravanan, L. Ji, and H. Seidel, 2006: The cause of the fragile relationship between the Pacific El Niño and the Atlantic Niño. *Nature*, **443 (7109)**, 324.

-
- Chang, P., L. Ji, and H. Li, 1997: A decadal climate variation in the tropical Atlantic Ocean from thermodynamic air-sea interactions. *Nature*, **385 (6616)**, 516–518.
- Chen, D., and Coauthors, 2015: Strong influence of westerly wind bursts on El Niño diversity. *Nature Geoscience*, **8 (5)**, 339–345.
- Cherchi, A., F. Kucharski, and F. Colleoni, 2018: Remote SST forcing on Indian summer monsoon extreme years in AGCM experiments. *International Journal of Climatology*, **38**, e160–e177.
- Chiang, J. C., Y. Kushnir, and A. Giannini, 2002: Deconstructing Atlantic Intertropical Convergence Zone variability: Influence of the local cross-equatorial sea surface temperature gradient and remote forcing from the eastern equatorial Pacific. *Journal of Geophysical Research: Atmospheres*, **107 (D1)**, ACL–3.
- Chiang, J. C., Y. Kushnir, and S. E. Zebiak, 2000: Interdecadal changes in eastern Pacific ITCZ variability and its influence on the Atlantic ITCZ. *Geophysical Research Letters*, **27 (22)**, 3687–3690.
- Chiang, J. C., and D. J. Vimont, 2004: Analogous Pacific and Atlantic meridional modes of tropical atmosphere–ocean variability. *Journal of Climate*, **17 (21)**, 4143–4158.
- Chiodi, A. M., and D. Harrison, 2015: Global seasonal precipitation anomalies robustly associated with El Niño and La Niña events: An OLR perspective. *Journal of Climate*, **28 (15)**, 6133–6159.
- Colberg, F., and C. Reason, 2007: Ocean model diagnosis of low-frequency climate variability in the South Atlantic region. *Journal of climate*, **20 (6)**, 1016–1034.
- Czaja, A., and C. Frankignoul, 2002: Observed impact of Atlantic SST anomalies on the North Atlantic Oscillation. *Journal of Climate*, **15 (6)**, 606–623.
- Czaja, A., P. Van der Vaart, and J. Marshall, 2002: A diagnostic study of the role of remote forcing in tropical Atlantic variability. *Journal of Climate*, **15 (22)**, 3280–3290.
- Dai, A., and T. Wigley, 2000: Global patterns of ENSO-induced precipitation. *Geophysical Research Letters*, **27 (9)**, 1283–1286.

-
- De Almeida, R., and P. Nobre, 2012: On the Atlantic cold tongue mode and the role of the Pacific ENSO. *Ocean Science Discussions*, **9** (1), 163–185.
- Dee, D. P., and Coauthors, 2011: The ERA-Interim reanalysis: configuration and performance of the data assimilation system. *Quarterly Journal of the Royal Meteorological Society*, **137** (656), 553–597, doi:10.1002/qj.828.
- Ding, H., N. S. Keenlyside, and M. Latif, 2010: Equatorial Atlantic interannual variability: Role of heat content. *Journal of Geophysical Research: Oceans*, **115** (C9).
- Dippe, T., M. Krebs, J. Harlaß, and J. F. Lübbecke, 2018: Can climate models simulate the observed strong summer surface cooling in the equatorial Atlantic? *YOUMARES 8–Oceans Across Boundaries: Learning from each other*, Springer, 7–23.
- Enfield, D. B., and D. A. Mayer, 1997: Tropical Atlantic sea surface temperature variability and its relation to El Niño-Southern Oscillation. *Journal of Geophysical Research: Oceans*, **102** (C1), 929–945.
- Findlater, J., 1969: A major low-level air current near the Indian Ocean during the northern summer. *Quarterly Journal of the Royal Meteorological Society*, **95** (404), 362–380.
- Florenchie, P., J. R. Lutjeharms, C. Reason, S. Masson, and M. Rouault, 2003: The source of Benguela Niños in the south Atlantic Ocean. *Geophysical Research Letters*, **30** (10).
- Florenchie, P., C. Reason, J. Lutjeharms, M. Rouault, C. Roy, and S. Masson, 2004: Evolution of interannual warm and cold events in the southeast Atlantic Ocean. *Journal of Climate*, **17** (12), 2318–2334.
- Foltz, G. R., and M. J. McPhaden, 2010: Interaction between the Atlantic meridional and Niño modes. *Geophysical Research Letters*, **37** (18).
- Gadgil, S., 2003: The Indian monsoon and its variability. *Annual Review of Earth and Planetary Sciences*, **31** (1), 429–467.
- Gadgil, S., 2014: El Niño and the summer monsoon of 2014. *Current Science*, **106** (10), 1335–1336.
- Gadgil, S., 2018: The monsoon system: Land–sea breeze or the ITCZ? *Journal of Earth System Science*, **127** (1), 1.

-
- Gadgil, S., Y. Abrol, and S. P. Rao, 1999: On growth and fluctuation of Indian foodgrain production. *Current Science*, **76** (4), 548–556.
- Gadgil, S., and S. Gadgil, 2006: The Indian monsoon, GDP and agriculture. *Economic and Political Weekly*, 4887–4895.
- Gadgil, S., M. Rajeevan, and P. Francis, 2007: Monsoon variability: Links to major oscillations over the equatorial Pacific and Indian oceans. *Current Science*, **93** (2), 182–194.
- Gadgil, S., and J. Srinivasan, 2011: Seasonal prediction of the Indian monsoon. *Current Science (Bangalore)*, **100** (3), 343–353.
- Gadgil, S., P. Vinayachandran, and P. Francis, 2003: Droughts of the Indian summer monsoon: Role of clouds over the Indian Ocean. *Current Science*, 1713–1719.
- Gammelsrød, T., C. Bartholomae, D. Boyer, V. Filipe, and M. Otoole, 1998: Intrusion of warm surface water along the Angolan Namibian Coast in February–March 1995: the 1995 Benguela niño. *African Journal of Marine Science*, **19**.
- García-Serrano, J., C. Cassou, H. Douville, A. Giannini, and F. J. Doblas-Reyes, 2017: Revisiting the ENSO teleconnection to the tropical North Atlantic. *Journal of Climate*, **30** (17), 6945–6957.
- García-Serrano, J., T. Losada, and B. Rodríguez-Fonseca, 2011: Extratropical atmospheric response to the Atlantic Niño decaying phase. *Journal of climate*, **24** (6), 1613–1625.
- George, G., D. N. Rao, C. Sabeerali, A. Srivastava, and S. A. Rao, 2016: Indian summer monsoon prediction and simulation in CFSv2 coupled model. *Atmospheric Science Letters*, **17** (1), 57–64.
- Giannini, A., Y. Kushnir, and M. A. Cane, 2000: Interannual variability of Caribbean rainfall, ENSO, and the Atlantic Ocean. *Journal of Climate*, **13** (2), 297–311.
- Gill, A. E., 1980: Some simple solutions for heat-induced tropical circulation. *Quarterly Journal of the Royal Meteorological Society*, **106** (449), 447–462.
- Gonick, L., and W. Smith, 1993: *The cartoon guide to statistics*. Collins.

-
- Good, S. A., M. J. Martin, and N. A. Rayner, 2013: EN4: Quality controlled ocean temperature and salinity profiles and monthly objective analyses with uncertainty estimates. *Journal of Geophysical Research: Oceans*, **118** (12), 6704–6716.
- Goswami, B., R. Ajayamohan, P. K. Xavier, and D. Sengupta, 2003: Clustering of synoptic activity by Indian summer monsoon intraseasonal oscillations. *Geophysical Research Letters*, **30** (8).
- Goswami, B., and S. Chakravorty, 2017: Dynamics of the Indian summer monsoon climate. *Oxford Research Encyclopedia of Climate Science*.
- Goswami, B., and P. K. Xavier, 2005: ENSO control on the south Asian monsoon through the length of the rainy season. *Geophysical Research Letters*, **32** (18).
- Gualdi, S., E. Guilyardi, A. Navarra, S. Masina, and P. Delecluse, 2003: The interannual variability in the tropical Indian Ocean as simulated by a CGCM. *Climate dynamics*, **20** (6), 567–582.
- Guan, Z., K. Ashok, and T. Yamagata, 2003: Summertime Response of the Tropical Atmosphere to the Indian Ocean Dipole Sea Surface Temperature Anomalies. *Journal of the Meteorological Society of Japan. Ser. II*, **81** (3), 533–561, doi:10.2151/jmsj.81.533.
- Haarsma, R. J., E. J. Campos, W. Hazeleger, C. Severijns, A. R. Piola, and F. Molteni, 2005: Dominant modes of variability in the South Atlantic: A study with a hierarchy of ocean–atmosphere models. *Journal of climate*, **18** (11), 1719–1735.
- Haarsma, R. J., and W. Hazeleger, 2007: Extratropical atmospheric response to equatorial Atlantic cold tongue anomalies. *Journal of climate*, **20** (10), 2076–2091.
- Halley, E., 1753: An historical account of the trade winds, and monsoons, observable in the seas between and near the Tropicks, with an attempt to assign the physical cause of the said winds. *Philosophical Transactions of the Royal Society of London*, **16** (183), 153–168.
- Ham, Y.-G., J.-S. Kug, and J.-Y. Park, 2013: Two distinct roles of Atlantic SSTs in ENSO variability: North tropical Atlantic SST and Atlantic Niño. *Geophysical Research Letters*, **40** (15), 4012–4017.

-
- Handoh, I. C., G. R. Bigg, A. J. Matthews, and D. P. Stevens, 2006: Interannual variability of the Tropical Atlantic independent of and associated with ENSO: Part II. The South Tropical Atlantic. *International Journal of Climatology: A Journal of the Royal Meteorological Society*, **26** (14), 1957–1976.
- Hu, Z.-Z., and B. Huang, 2006: Physical processes associated with the tropical Atlantic SST meridional gradient. *Journal of climate*, **19** (21), 5500–5518.
- Hu, Z.-Z., A. Kumar, B. Huang, and J. Zhu, 2013: Leading modes of the upper-ocean temperature interannual variability along the equatorial Atlantic Ocean in NCEP GODAS. *Journal of climate*, **26** (13), 4649–4663.
- Huang, B., 2004: Remotely forced variability in the tropical Atlantic Ocean. *Climate Dynamics*, **23** (2), 133–152.
- Huang, B., P. S. Schopf, and Z. Pan, 2002: The ENSO effect on the tropical Atlantic variability: A regionally coupled model study. *Geophysical Research Letters*, **29** (21), 35–1.
- Huang, B., P. S. Schopf, and J. Shukla, 2004: Intrinsic ocean–atmosphere variability of the tropical Atlantic Ocean. *Journal of Climate*, **17** (11), 2058–2077.
- Hunt, K. M., A. G. Turner, P. M. Inness, D. E. Parker, and R. C. Levine, 2016: On the structure and dynamics of Indian monsoon depressions. *Monthly Weather Review*, **144** (9), 3391–3416.
- Iizuka, S., T. Matsuura, and T. Yamagata, 2000: The Indian Ocean SST dipole simulated in a coupled general circulation model. *Geophysical Research Letters*, **27** (20), 3369–3372.
- Illig, S., D. Gushchina, B. Dewitte, N. Ayoub, and Y. Du Penhoat, 2006: The 1996 equatorial Atlantic warm event: Origin and mechanisms. *Geophysical research letters*, **33** (9).
- Jeong, H.-I., and Coauthors, 2012: Assessment of the APCC coupled MME suite in predicting the distinctive climate impacts of two flavors of ENSO during boreal winter. *Climate dynamics*, **39** (1-2), 475–493.
- Jiang, X., S. Yang, Y. Li, A. Kumar, X. Liu, Z. Zuo, and B. Jha, 2013: Seasonal-to-interannual prediction of the Asian summer monsoon in the NCEP Climate Forecast System version 2. *Journal of Climate*, **26** (11), 3708–3727.

-
- Jin, F.-F., 1997a: An equatorial ocean recharge paradigm for ENSO. Part I: Conceptual model. *Journal of the atmospheric sciences*, **54** (7), 811–829.
- Jin, F.-F., 1997b: An equatorial ocean recharge paradigm for ENSO. Part I: Conceptual model. *Journal of the atmospheric sciences*, **54** (7), 811–829.
- Jin, F.-F., 1997c: An equatorial ocean recharge paradigm for ENSO. Part II: A stripped-down coupled model. *Journal of the Atmospheric Sciences*, **54** (7), 830–847.
- Joseph, P., and P. Raman, 1966: Existence of low level westerly jet stream over peninsular India during July. *Indian J Meteorol Geophys*, **17** (1), 407–410.
- Joseph, S., A. Sahai, R. Chattopadhyay, and B. Goswami, 2011: Can El Niño–Southern Oscillation (ENSO) events modulate intraseasonal oscillations of Indian summer monsoon? *Journal of Geophysical Research: Atmospheres*, **116** (D20).
- Jourdain, N. C., A. S. Gupta, A. S. Taschetto, C. C. Ummenhofer, A. F. Moise, and K. Ashok, 2013: The Indo-Australian monsoon and its relationship to ENSO and IOD in reanalysis data and the CMIP3/CMIP5 simulations. *Climate dynamics*, **41** (11-12), 3073–3102.
- Kanamitsu, M., W. Ebisuzaki, J. Woollen, S.-K. Yang, J. J. Hnilo, M. Fiorino, and G. L. Potter, 2002: NCEP/DOE AMIP-II Reanalysis (R-2). *Bulletin of the American Meteorological Society*, **83** (11), 1631–1644, doi:10.1175/BAMS-83-11-1631.
- Kao, H.-Y., and J.-Y. Yu, 2009: Contrasting eastern-Pacific and central-Pacific types of ENSO. *Journal of Climate*, **22** (3), 615–632.
- Keenlyside, N. S., H. Ding, and M. Latif, 2013: Potential of equatorial Atlantic variability to enhance El Niño prediction. *Geophysical Research Letters*, **40** (10), 2278–2283.
- Keenlyside, N. S., and M. Latif, 2007: Understanding equatorial Atlantic interannual variability. *Journal of climate*, **20** (1), 131–142.
- Keshavamurty, R., 1982: Response of the atmosphere to sea surface temperature anomalies over the equatorial Pacific and the teleconnections of the Southern Oscillation. *Journal of the Atmospheric Sciences*, **39** (6), 1241–1259.
- Kessler, W. S., 2002: Is ENSO a cycle or a series of events? *Geophysical Research Letters*, **29** (23), 40–1.

-
- Kim, H.-M., P. J. Webster, J. A. Curry, and V. E. Toma, 2012: Asian summer monsoon prediction in ECMWF System 4 and NCEP CFSv2 retrospective seasonal forecasts. *Climate dynamics*, **39** (12), 2975–2991.
- Klein, S. A., B. J. Soden, and N.-C. Lau, 1999: Remote sea surface temperature variations during ENSO: Evidence for a tropical atmospheric bridge. *Journal of climate*, **12** (4), 917–932.
- Koteswaram, P., 1958: The easterly jet stream in the tropics. *Tellus*, **10** (1), 43–57.
- Kothawale, D., and M. Rajeevan, 2017: Monthly, seasonal and annual rainfall time series for all-India, homogeneous regions and meteorological subdivisions: 1871–2016. *IITM Research Report No. RR-138*.
- Krishna, R. P. M., S. A. Rao, A. Srivastava, H. P. Kottu, M. Pradhan, P. Pillai, R. A. Dandi, and C. Sabeerali, 2019: Impact of convective parameterization on the seasonal prediction skill of Indian summer monsoon. *Climate Dynamics*, **53** (9-10), 6227–6243.
- Krishnamurthy, V., and R. Ajayamohan, 2010: Composite structure of monsoon low pressure systems and its relation to Indian rainfall. *Journal of Climate*, **23** (16), 4285–4305.
- Krishnamurthy, V., and J. Shukla, 2000: Intraseasonal and interannual variability of rainfall over India. *Journal of Climate*, **13** (24), 4366–4377.
- Krishnamurti, T., 1979: Tropical Meteorology. *Compendium of Meteorology II*, A. Wiin-Nielsen, Ed., World Meteorological Organization.
- Krishnamurti, T. N., and H. Bhalme, 1976: Oscillations of a monsoon system. Part I. Observational aspects. *Journal of the Atmospheric Sciences*, **33** (10), 1937–1954.
- Krishnan, R., D. Ayantika, V. Kumar, and S. Pokhrel, 2011: The long-lived monsoon depressions of 2006 and their linkage with the Indian Ocean Dipole. *International Journal of Climatology*, **31** (9), 1334–1352.
- Krishnan, R., K. Ramesh, B. Samala, G. Meyers, J. Slingo, and M. Fennessy, 2006: Indian Ocean-monsoon coupled interactions and impending monsoon droughts. *Geophysical Research Letters*, **33** (8).

-
- Kucharski, F., A. Bracco, J. Yoo, and F. Molteni, 2007: Low-frequency variability of the Indian monsoon–ENSO relationship and the tropical Atlantic: The weakening of the 1980s and 1990s. *Journal of Climate*, **20** (16), 4255–4266.
- Kucharski, F., A. Bracco, J. Yoo, and F. Molteni, 2008: Atlantic forced component of the Indian monsoon interannual variability. *Geophysical Research Letters*, **35** (4).
- Kucharski, F., A. Bracco, J. Yoo, A. Tompkins, L. Feudale, P. Ruti, and A. Dell’Aquila, 2009: A Gill–Matsuno-type mechanism explains the tropical Atlantic influence on African and Indian monsoon rainfall. *Quarterly Journal of the Royal Meteorological Society: A journal of the atmospheric sciences, applied meteorology and physical oceanography*, **135** (640), 569–579.
- Kucharski, F., and Coauthors, 2016: The teleconnection of the tropical Atlantic to Indo-Pacific sea surface temperatures on inter-annual to centennial time scales: a review of recent findings. *Atmosphere*, **7** (2), 29.
- Kug, J.-S., and Y.-G. Ham, 2011: Are there two types of La Nina? *Geophysical Research Letters*, **38** (16).
- Kumar, A., D. Pai, J. Singh, R. Singh, and D. Sikka, 2012: Statistical models for long-range forecasting of southwest monsoon rainfall over India using step wise regression and neural network. *Atmospheric and Climate Sciences*, **2** (03), 322.
- Kumar, K. K., B. Rajagopalan, and M. A. Cane, 1999: On the weakening relationship between the Indian monsoon and ENSO. *Science*, **284** (5423), 2156–2159.
- Kumar, K. K., B. Rajagopalan, M. Hoerling, G. Bates, and M. Cane, 2006: Unraveling the mystery of Indian monsoon failure during El Niño. *Science*, **314** (5796), 115–119.
- Kump, L. R., J. F. Kasting, R. G. Crane, and Coauthors, 2004: *The earth system*, Vol. 432. Pearson Prentice Hall Upper Saddle River, NJ.
- Latif, M., and T. P. Barnett, 1995: Interactions of the tropical oceans. *Journal of Climate*, **8** (4), 952–964.
- Latif, M., and A. Grötzner, 2000: The equatorial Atlantic oscillation and its response to ENSO. *Climate Dynamics*, **16** (2-3), 213–218.

-
- Lau, N.-C., and M. J. Nath, 2003: Atmosphere-Ocean Variations in the Indo-Pacific Sector during ENSO Episodes. *Journal of Climate*, **16** (1), 3–20, doi:10.1175/1520-0442(2003)016<0003:AOVITI>2.0.CO;2.
- Lee, S.-K., D. B. Enfield, and C. Wang, 2008: Why do some El Niños have no impact on tropical North Atlantic SST? *Geophysical Research Letters*, **35** (16).
- Losada, T., B. Rodríguez-Fonseca, and F. Kucharski, 2012: Tropical influence on the summer Mediterranean climate. *Atmospheric Science Letters*, **13** (1), 36–42.
- Lübbecke, J. F., 2013: Climate science: Tropical Atlantic warm events. *Nature Geoscience*, **6** (1), 22.
- Lübbecke, J. F., C. W. Böning, N. S. Keenlyside, and S.-P. Xie, 2010: On the connection between Benguela and equatorial Atlantic Niños and the role of the South Atlantic Anticyclone. *Journal of Geophysical Research: Oceans*, **115** (C9).
- Lübbecke, J. F., N. J. Burls, C. J. Reason, and M. J. McPhaden, 2014: Variability in the South Atlantic anticyclone and the Atlantic Niño mode. *Journal of Climate*, **27** (21), 8135–8150.
- Lübbecke, J. F., and M. J. McPhaden, 2012: On the inconsistent relationship between Pacific and Atlantic Niños. *Journal of Climate*, **25** (12), 4294–4303.
- Lübbecke, J. F., and M. J. McPhaden, 2013: A comparative stability analysis of Atlantic and Pacific Niño modes. *Journal of Climate*, **26** (16), 5965–5980.
- Lübbecke, J. F., and M. J. McPhaden, 2017: Symmetry of the Atlantic Niño mode. *Geophysical Research Letters*, **44** (2), 965–973.
- Lübbecke, J. F., B. Rodríguez-Fonseca, I. Richter, M. Martín-Rey, T. Losada, I. Polo, and N. S. Keenlyside, 2018: Equatorial Atlantic variability Modes, mechanisms, and global teleconnections. *Wiley Interdisciplinary Reviews: Climate Change*, **9** (4), e527.
- Lutz, K., J. Rathmann, and J. Jacobeit, 2013: Classification of warm and cold water events in the eastern tropical Atlantic Ocean. *Atmospheric Science Letters*, **14** (2), 102–106.
- Marathe, S., K. Ashok, P. Swapna, and T. Sabin, 2015: Revisiting El Niño Modoki. *Climate dynamics*, **45** (11-12), 3527–3545.

-
- Martín-Rey, M., I. Polo, B. Rodríguez-Fonseca, A. Lazar, and T. Losada, 2019: Ocean dynamics shapes the structure and timing of Atlantic Equatorial Modes. *Journal of Geophysical Research: Oceans*, **124** (11), 7529–7544.
- Martín-Rey, M., I. Polo, B. Rodríguez-Fonseca, T. Losada, and A. Lazar, 2018: Is there evidence of changes in tropical Atlantic variability modes under AMO phases in the observational record? *Journal of Climate*, **31** (2), 515–536.
- Martín-Rey, M., B. Rodríguez-Fonseca, and I. Polo, 2015: Atlantic opportunities for ENSO prediction. *Geophysical Research Letters*, **42** (16), 6802–6810.
- Matsuno, T., 1966: Quasi-geostrophic motions in the equatorial area. *Journal of the Meteorological Society of Japan. Ser. II*, **44** (1), 25–43.
- McPhaden, M. J., 2003: Tropical Pacific Ocean heat content variations and ENSO persistence barriers. *Geophysical research letters*, **30** (9).
- McPhaden, M. J., and M. Nagura, 2014: Indian Ocean dipole interpreted in terms of recharge oscillator theory. *Climate dynamics*, **42** (5-6), 1569–1586.
- Mohino, E., and T. Losada, 2015: Impacts of the Atlantic Equatorial Mode in a warmer climate. *Climate dynamics*, **45** (7-8), 2255–2271.
- Monger, B., C. McClain, and R. Murtugudde, 1997: Seasonal phytoplankton dynamics in the eastern tropical Atlantic. *Journal of Geophysical Research: Oceans*, **102** (C6), 12 389–12 411.
- Mooley, D., and B. Parthasarathy, 1984: Indian summer monsoon and the east equatorial Pacific sea surface temperature. *Atmosphere-Ocean*, **22** (1), 23–35.
- Morioka, Y., T. Tozuka, and T. Yamagata, 2011: On the growth and decay of the subtropical dipole mode in the South Atlantic. *Journal of climate*, **24** (21), 5538–5554.
- Münnich, M., and J. D. Neelin, 2005: Seasonal influence of ENSO on the Atlantic ITCZ and equatorial South America. *Geophysical research letters*, **32** (21).
- Murtugudde, R., J. P. McCreary Jr, and A. J. Busalacchi, 2000: Oceanic processes associated with anomalous events in the Indian Ocean with relevance to 1997–1998. *Journal of Geophysical Research: Oceans*, **105** (C2), 3295–3306.

-
- Murtugudde, R. G., J. Ballabrera-Poy, J. Beauchamp, and A. J. Busalacchi, 2001: Relationship between zonal and meridional modes in the tropical Atlantic. *Geophysical research letters*, **28 (23)**, 4463–4466.
- Nanjundiah, R., 2009: A quick look into assessment of forecasts for the Indian summer monsoon rainfall in 2009. *CAOS Report*, CAOS, IISc, Bangalore.
- Narapusetty, B., R. Murtugudde, H. Wang, and A. Kumar, 2016: Ocean–atmosphere processes driving Indian summer monsoon biases in CFSv2 hindcasts. *Climate Dynamics*, **47 (5-6)**, 1417–1433.
- Narapusetty, B., R. Murtugudde, H. Wang, and A. Kumar, 2018: Ocean–atmosphere processes associated with enhanced Indian monsoon break spells in CFSv2 forecasts. *Climate dynamics*, **51 (7-8)**, 2623–2636.
- Neelin, J. D., D. S. Battisti, A. C. Hirst, F.-F. Jin, Y. Wakata, T. Yamagata, and S. E. Zebiak, 1998: ENSO theory. *Journal of Geophysical Research: Oceans*, **103 (C7)**, 14 261–14 290.
- Neelin, J. D., and H. Su, 2005: Moist teleconnection mechanisms for the tropical South American and Atlantic sector. *Journal of Climate*, **18 (18)**, 3928–3950.
- Nnamchi, H. C., F. Kucharski, N. S. Keenlyside, and R. Farneti, 2017: Analogous seasonal evolution of the South Atlantic SST dipole indices. *Atmospheric Science Letters*, **18 (10)**, 396–402.
- Nnamchi, H. C., J. Li, and R. N. Anyadike, 2011: Does a dipole mode really exist in the South Atlantic Ocean? *Journal of Geophysical Research: Atmospheres*, **116 (D15)**.
- Nnamchi, H. C., J. Li, F. Kucharski, I.-S. Kang, N. S. Keenlyside, P. Chang, and R. Farneti, 2016: An equatorial–extratropical dipole structure of the Atlantic Niño. *Journal of Climate*, **29 (20)**, 7295–7311.
- Nobre, P., and J. Shukla, 1996: Variations of sea surface temperature, wind stress, and rainfall over the tropical Atlantic and South America. *Journal of climate*, **9 (10)**, 2464–2479.
- Okumura, Y., and S.-P. Xie, 2006: Some overlooked features of tropical Atlantic climate leading to a new Niño-like phenomenon. *Journal of climate*, **19 (22)**, 5859–5874.

-
- Pai, D., A. S. Rao, S. Senroy, M. Pradhan, P. A. Pillai, and M. Rajeevan, 2017: Performance of the operational and experimental long-range forecasts for the 2015 southwest monsoon rainfall. *Current Science*, **112**, 68–75.
- Pai, D., A. S. Rao, O. Sreejith, A. Bandgar, and D. Surendran, 2019: Forecasting the Monsoon. *Geography and You*, **19 (8)**, 10–15.
- Pai, D., O. Sreejith, S. Nargund, M. Musale, and A. Tyagi, 2011: Present operational long range forecasting system for southwest monsoon rainfall over India and its performance during 2010. *Mausam*, **62 (2)**, 179–196.
- Pai, D., L. Sridhar, M. Rajeevan, O. Sreejith, N. Satbhai, and B. Mukhopadhyay, 2014: Development of a new high spatial resolution (0.25×0.25) long period (1901–2010) daily gridded rainfall data set over India and its comparison with existing data sets over the region. *Mausam*, **65 (1)**, 1–18.
- Pant, G. B., and K. R. Kumar, 1997: *Climates of south Asia*. Wiley-Blackwell.
- Parthasarathy, B., and D. Mooley, 1978: Some features of a long homogeneous series of Indian summer monsoon rainfall. *Monthly weather review*, **106 (6)**, 771–781.
- Parthasarathy, B., A. Munot, and D. Kothawale, 1994: All-India monthly and seasonal rainfall series: 1871–1993. *Theoretical and Applied Climatology*, **49 (4)**, 217–224.
- Pattanaik, D., and Coauthors, 2019: Evolution of operational extended range forecast system of IMD: Prospects of its applications in different sectors. *MAUSAM*, **70 (2)**, 233–264.
- Philander, S., 1986: Unusual conditions in the tropical Atlantic Ocean in 1984. *Nature*, **322 (6076)**, 236–238.
- Philander, S., J. R. Holton, and R. Dmowska, 1989: *El Niño, La Niña, and the southern oscillation*, Vol. 46. Academic press.
- Philander, S. G., 1989: El Niño, La Niña, and the southern oscillation. *International geophysics series*, **46**, X–289.
- Picaut, J., F. Masia, and Y. Du Penhoat, 1997: An advective-reflective conceptual model for the oscillatory nature of the ENSO. *Science*, **277 (5326)**, 663–666.

-
- Pokhrel, S., and Coauthors, 2016: Seasonal prediction of Indian summer monsoon rainfall in NCEP CFSv2: forecast and predictability error. *Climate dynamics*, **46** (7-8), 2305–2326.
- Polo, I., A. Lazar, B. Rodriguez-Fonseca, and J. Mignot, 2015a: Growth and decay of the equatorial Atlantic SST mode by means of closed heat budget in a coupled general circulation model. *Frontiers in Earth Science*, **3**, 37.
- Polo, I., M. Martin-Rey, B. Rodriguez-Fonseca, F. Kucharski, and C. R. Mechoso, 2015b: Processes in the Pacific La Niña onset triggered by the Atlantic Niño. *Climate dynamics*, **44** (1-2), 115–131.
- Polo, I., B. Rodríguez-Fonseca, T. Losada, and J. García-Serrano, 2008: Tropical Atlantic variability modes (1979–2002). Part I: Time-evolving SST modes related to West African rainfall. *Journal of Climate*, **21** (24), 6457–6475.
- Pottapinjara, V., M. Girishkumar, M. Ravichandran, and R. Murtugudde, 2014: Influence of the Atlantic zonal mode on monsoon depressions in the Bay of Bengal during boreal summer. *Journal of Geophysical Research: Atmospheres*, **119** (11), 6456–6469.
- Praveen, V., S. Sandeep, and R. Ajayamohan, 2015: On the relationship between mean monsoon precipitation and low pressure systems in climate model simulations. *Journal of Climate*, **28** (13), 5305–5324.
- Preethi, B., T. Sabin, J. Adedoyin, and K. Ashok, 2015: Impacts of the ENSO Modoki and other tropical Indo-Pacific climate-drivers on African rainfall. *Scientific reports*, **5**, 16 653.
- Rajeevan, M., S. Gadgil, and J. Bhate, 2010: Active and break spells of the Indian summer monsoon. *Journal of earth system science*, **119** (3), 229–247.
- Rajeevan, M., and M. J. McPhaden, 2004: Tropical Pacific upper ocean heat content variations and Indian summer monsoon rainfall. *Geophysical Research Letters*, **31** (18).
- Rajeevan, M., and R. S. Nanjundiah, 2009: Coupled model simulations of twentieth century climate of the Indian summer monsoon. *Platinum jubilee special volume of the Indian Academy of Sciences*, 537–568.
- Ramage, C., 1971: [*Monsoon Meteorology*]. Academic Press.

-
- Ramu, D. A., and Coauthors, 2016: Indian summer monsoon rainfall simulation and prediction skill in the CFSv2 coupled model: Impact of atmospheric horizontal resolution. *Journal of Geophysical Research: Atmospheres*, **121** (5), 2205–2221.
- RAO, D. V. B., K. Ashok, and T. Yamagata, 2004: A numerical simulation study of the Indian summer monsoon of 1994 using NCAR MM5. *Journal of the Meteorological Society of Japan. Ser. II*, **82** (6), 1755–1775.
- Rao, S. A., and Coauthors, 2019: Monsoon Mission: A targeted activity to improve monsoon prediction across scales. *Bulletin of the American Meteorological Society*.
- Rao, Y., 1976: Southwest Monsoon (Meteorological Monograph, Synoptic Meteorology No. 1). *Indian Meteorological Department, New Delhi, 367pp*.
- Rasmusson, E. M., and T. H. Carpenter, 1982: Variations in tropical sea surface temperature and surface wind fields associated with the Southern Oscillation/El Niño. *Monthly Weather Review*, **110** (5), 354–384.
- Rayner, N., D. E. Parker, E. Horton, C. K. Folland, L. V. Alexander, D. Rowell, E. Kent, and A. Kaplan, 2003: Global analyses of sea surface temperature, sea ice, and night marine air temperature since the late nineteenth century. *Journal of Geophysical Research: Atmospheres*, **108** (D14).
- Reason, C., P. Florenchie, M. Rouault, and J. Veitch, 2006: Influences of large scale climate modes and agulhas system variability on the BCLME region. *Large marine ecosystems*, Vol. 14, Elsevier, 223–238.
- Ren, H.-L., and F.-F. Jin, 2011: Niño indices for two types of ENSO. *Geophysical Research Letters*, **38** (4).
- Richter, I., S. K. Behera, Y. Masumoto, B. Taguchi, N. Komori, and T. Yamagata, 2010: On the triggering of Benguela Niños: Remote equatorial versus local influences. *Geophysical Research Letters*, **37** (20).
- Richter, I., S. K. Behera, Y. Masumoto, B. Taguchi, H. Sasaki, and T. Yamagata, 2013: Multiple causes of interannual sea surface temperature variability in the equatorial Atlantic Ocean. *Nature Geoscience*, **6** (1), 43.

-
- Richter, I., S.-P. Xie, S. K. Behera, T. Doi, and Y. Masumoto, 2014: Equatorial Atlantic variability and its relation to mean state biases in CMIP5. *Climate dynamics*, **42** (1-2), 171–188.
- Richter, I., S.-P. Xie, Y. Morioka, T. Doi, B. Taguchi, and S. Behera, 2017: Phase locking of equatorial Atlantic variability through the seasonal migration of the ITCZ. *Climate Dynamics*, **48** (11-12), 3615–3629.
- Rodríguez-Fonseca, B., I. Polo, J. García-Serrano, T. Losada, E. Mohino, C. R. Mechoso, and F. Kucharski, 2009: Are Atlantic Niños enhancing Pacific ENSO events in recent decades? *Geophysical Research Letters*, **36** (20).
- Rodríguez-Fonseca, B., and Coauthors, 2015: Variability and predictability of West African droughts: a review on the role of sea surface temperature anomalies. *Journal of Climate*, **28** (10), 4034–4060.
- Rouault, M., P. Florenchie, N. Fauchereau, and C. J. Reason, 2003: South East tropical Atlantic warm events and southern African rainfall. *Geophysical Research Letters*, **30** (5).
- Rouault, M., S. Illig, C. Bartholomae, C. Reason, and A. Bentamy, 2007: Propagation and origin of warm anomalies in the Angola Benguela upwelling system in 2001. *Journal of Marine Systems*, **68** (3-4), 473–488.
- Roxy, M. K., K. Ritika, P. Terray, R. Murtugudde, K. Ashok, and B. Goswami, 2015: Drying of Indian subcontinent by rapid Indian Ocean warming and a weakening land-sea thermal gradient. *Nature communications*, **6**, 7423.
- Ruiz-Barradas, A., J. A. Carton, and S. Nigam, 2000: Structure of interannual-to-decadal climate variability in the tropical Atlantic sector. *Journal of Climate*, **13** (18), 3285–3297.
- Ruiz-Barradas, A., J. A. Carton, and S. Nigam, 2003: Role of the atmosphere in climate variability of the tropical Atlantic. *Journal of climate*, **16** (12), 2052–2065.
- Sabeerali, C., R. Ajayamohan, H. K. Bangalath, and N. Chen, 2019a: Atlantic Zonal Mode: An Emerging Source of Indian Summer Monsoon Variability in a Warming World. *Geophysical Research Letters*, **46** (8), 4460–4467.

-
- Sabeerali, C., R. Ajayamohan, and S. A. Rao, 2019b: Loss of predictive skill of Indian summer monsoon rainfall in NCEP CFSv2 due to misrepresentation of Atlantic zonal mode. *Climate Dynamics*, **52** (7-8), 4599–4619.
- Saha, S., and Coauthors, 2014a: The NCEP climate forecast system version 2. *Journal of Climate*, **27** (6), 2185–2208.
- Saha, S. K., and Coauthors, 2014b: Improved simulation of Indian summer monsoon in latest NCEP climate forecast system free run. *International Journal of Climatology*, **34** (5), 1628–1641.
- Saha, S. K., and Coauthors, 2016: Potential predictability of Indian summer monsoon rainfall in NCEP CFSv2. *Journal of Advances in Modeling Earth Systems*, **8** (1), 96–120.
- Sahai, A., R. Chattopadhyay, S. Joseph, P. M. Krishna, D. Pattanaik, and S. Abhilash, 2019: Seamless Prediction of Monsoon Onset and Active/Break Phases. *Sub-Seasonal to Seasonal Prediction*, Elsevier, 421–438.
- Sahai, A., and Coauthors, 2017: Potential predictability of wet/dry spells transitions during extreme monsoon years: optimism for dynamical extended range prediction. *Natural Hazards*, **88** (2), 853–865.
- Saji, N., B. Goswami, P. Vinayachandran, and T. Yamagata, 1999: A dipole mode in the tropical Indian Ocean. *Nature*, **401** (6751), 360.
- Saji, N., and T. Yamagata, 2003: Possible impacts of Indian Ocean Dipole mode events on global climate. *Climate Research*, **25**, 151–169, doi:10.3354/cr025151.
- Saji, N., and T. Yamagata, 2003: Structure of SST and surface wind variability during Indian Ocean dipole mode events: COADS observations. *Journal of Climate*, **16** (16), 2735–2751.
- Servain, J., I. Wainer, H. Ludos Ayina, and H. Roquet, 2000: The relationship between the simulated climatic variability modes of the tropical Atlantic. *International Journal of Climatology: A Journal of the Royal Meteorological Society*, **20** (9), 939–953.
- Servain, J., I. Wainer, J. P. McCreary Jr, and A. Dessier, 1999: Relationship between the equatorial and meridional modes of climatic variability in the tropical Atlantic. *Geophysical Research Letters*, **26** (4), 485–488.

-
- Shannon, L., A. Boyd, G. Brundrit, and J. Taunton-Clark, 1986: On the existence of an El Niño-type phenomenon in the Benguela system. *Journal of marine Research*, **44** (3), 495–520.
- Sikka, D., 1980: Some aspects of the large scale fluctuations of summer monsoon rainfall over India in relation to fluctuations in the planetary and regional scale circulation parameters. *Proceedings of the Indian Academy of Sciences-Earth and Planetary Sciences*, **89** (2), 179–195.
- Slingo, J., 2003: MONSOONS— Overview. *Encyclopedia of Atmospheric Sciences 2nd edition*.
- Slingo, J., and H. Annamalai, 2000: 1997: The El Niño of the century and the response of the Indian summer monsoon. *Monthly Weather Review*, **128** (6), 1778–1797.
- Soman, M., and J. Slingo, 1997: Sensitivity of the asian summer monsoon to aspects of sea-surface-temperature anomalies in the tropical pacific ocean. *Quarterly Journal of the Royal Meteorological Society*, **123** (538), 309–336.
- Suarez, M. J., and P. S. Schopf, 1988: A delayed action oscillator for ENSO. *Journal of the atmospheric Sciences*, **45** (21), 3283–3287.
- Tejavath, C. T., K. Ashok, S. Chakraborty, and R. Ramesh, 2019: A PMIP3 narrative of modulation of ENSO teleconnections to the Indian summer monsoon by background changes in the Last Millennium. *Climate Dynamics*, 1–17.
- Timmermann, A., and Coauthors, 2018: El Niño–southern oscillation complexity. *Nature*, **559** (7715), 535–545.
- Tokinaga, H., I. Richter, and Y. Kosaka, 2019: ENSO influence on the Atlantic Niño, revisited: Multi-year versus single-year ENSO events. *Journal of Climate*, **32** (14), 4585–4600.
- Trzaska, S., A. W. Robertson, J. D. Farrara, and C. R. Mechoso, 2007: South Atlantic variability arising from air–sea coupling: Local mechanisms and tropical–subtropical interactions. *Journal of climate*, **20** (14), 3345–3365.
- Varikoden, H., and B. Preethi, 2013: Wet and dry years of Indian summer monsoon and its relation with Indo-Pacific sea surface temperatures. *International Journal of Climatology*, **33** (7), 1761–1771.

-
- Vecchi, G. A., and D. Harrison, 2004: Interannual Indian rainfall variability and Indian Ocean sea surface temperature anomalies. *Earth Climate: The Ocean–Atmosphere Interaction, Geophys. Monogr*, **147**, 247–260.
- Venegas, S., L. Mysak, and D. Straub, 1997: Atmosphere–ocean coupled variability in the South Atlantic. *Journal of Climate*, **10** (11), 2904–2920.
- Venegas, S. A., L. A. Mysak, and D. N. Straub, 1996: Evidence for interannual and interdecadal climate variability in the South Atlantic. *Geophysical Research Letters*, **23** (19), 2673–2676.
- Vinayachandran, P., P. Francis, and S. Rao, 2009: Indian Ocean dipole: processes and impacts. *Current trends in science*, 569–589.
- Von Storch, H., and F. W. Zwiers, 1999: *Statistical analysis in climate research*. Cambridge university press.
- Walker, G., and E. Bliss, 1932: World weather. *Memoirs of the royal meteorological society*, **4**, 53–84.
- Wang, B., 2006a: *The asian monsoon*. Springer Science & Business Media.
- Wang, C., 2002: Atmospheric circulation cells associated with the El Niño–Southern Oscillation. *Journal of Climate*, **15** (4), 399–419.
- Wang, C., 2006b: An overlooked feature of tropical climate: Inter-Pacific-Atlantic variability. *Geophysical Research Letters*, **33** (12).
- Wang, C., F. Kucharski, R. Barimalala, and A. Bracco, 2009: Teleconnections of the tropical Atlantic to the tropical Indian and Pacific Oceans: A review of recent findings. *Meteorologische Zeitschrift*, **18** (4), 445–454.
- Wang, C., and J. Picaut, 2004: Understanding ENSO physics A review. *Earths Climate: The Ocean–Atmosphere Interaction, Geophys. Monogr*, **147**, 21–48.
- Wang, C., R. H. Weisberg, and J. I. Virmani, 1999: Western Pacific interannual variability associated with the El Niño–Southern Oscillation. *Journal of Geophysical Research: Oceans*, **104** (C3), 5131–5149.

-
- Webster, P., V. Magana, T. Palmer, and Coauthors, 2003: Dynamical theory. *Encyclopedia of Atmospheric Sciences*, 1370–1385.
- Webster, P. J., V. O. Magana, T. Palmer, J. Shukla, R. Tomas, M. Yanai, and T. Yasunari, 1998: Monsoons: Processes, predictability, and the prospects for prediction. *Journal of Geophysical Research: Oceans*, **103 (C7)**, 14 451–14 510.
- Webster, P. J., A. M. Moore, J. P. Loschnigg, and R. R. Leben, 1999: Coupled ocean–atmosphere dynamics in the Indian Ocean during 1997–98. *Nature*, **401 (6751)**, 356.
- Webster, P. J., and S. Yang, 1992: Monsoon and ENSO: Selectively interactive systems. *Quarterly Journal of the Royal Meteorological Society*, **118 (507)**, 877–926.
- Weisberg, R. H., and C. Wang, 1997: A western Pacific oscillator paradigm for the El Niño–Southern Oscillation. *Geophysical research letters*, **24 (7)**, 779–782.
- Welhouse, L. J., M. A. Lazzara, L. M. Keller, G. J. Tripoli, and M. H. Hitchman, 2016: Composite analysis of the effects of ENSO events on Antarctica. *Journal of Climate*, **29 (5)**, 1797–1808.
- Wilks, D. S., 2011: *Statistical methods in the atmospheric sciences*, Vol. 100. Academic press.
- Wu, L., and Z. Liu, 2002: Is tropical Atlantic variability driven by the North Atlantic Oscillation? *Geophysical Research Letters*, **29 (13)**, 31–1.
- Xie, S.-P., and J. A. Carton, 2004: Tropical Atlantic variability: Patterns, mechanisms, and impacts. *Earth Climate: The Ocean-Atmosphere Interaction, Geophys. Monogr.*, **147**, 121–142.
- Xie, Z., A. Duan, and Q. Tian, 2017: Weighted composite analysis and its application: an example using ENSO and geopotential height. *Atmospheric Science Letters*, **18 (11)**, 435–440, doi:10.1002/asl.786.
- Yadav, R. K., 2017: On the relationship between east equatorial Atlantic SST and ISM through Eurasian wave. *Climate Dynamics*, **48 (1-2)**, 281–295.
- Yadav, R. K., G. Srinivas, and J. S. Chowdary, 2018: Atlantic Niño modulation of the Indian summer monsoon through Asian jet. *Npj Climate and Atmospheric Science*, **1 (1)**, 23.

-
- Yamagata, T., S. K. Behera, S. A. Rao, Z. Guan, K. Ashok, and H. N. Saji, 2003: Comments on Dipoles, temperature gradients, and tropical climate anomalies. *Bulletin of the American Meteorological Society*, **84** (10), 1418–1422.
- Yanase, W., M. Satoh, H. Taniguchi, and H. Fujinami, 2012: Seasonal and intraseasonal modulation of tropical cyclogenesis environment over the Bay of Bengal during the extended summer monsoon. *Journal of Climate*, **25** (8), 2914–2930.
- Yang, Y., S.-P. Xie, L. Wu, Y. Kosaka, and J. Li, 2018: ENSO forced and local variability of North Tropical Atlantic SST: model simulations and biases. *Climate dynamics*, **51** (11-12), 4511–4524.
- Yeh, S.-W., and Coauthors, 2018: ENSO atmospheric teleconnections and their response to greenhouse gas forcing. *Reviews of Geophysics*, **56** (1), 185–206.
- Yoon, J.-H., and T.-C. Chen, 2005: Water vapor budget of the Indian monsoon depression. *Tellus A: Dynamic Meteorology and Oceanography*, **57** (5), 770–782.
- Zebiak, S. E., 1993: Air–sea interaction in the equatorial Atlantic region. *Journal of Climate*, **6** (8), 1567–1586.
- Zhu, J., B. Huang, and Z. Wu, 2012: The role of ocean dynamics in the interaction between the Atlantic meridional and equatorial modes. *Journal of Climate*, **25** (10), 3583–3598.

Publications reproduced verbatim

Relation between the upper ocean heat content in the equatorial Atlantic during boreal spring and the Indian monsoon rainfall during June–September

Vijay Pottapinjara,^a M. S. Girishkumar,^a S. Sivareddy,^a M. Ravichandran^{a*} and R. Murtugudde^b

^a Indian National Center for Ocean Information Services, Hyderabad, India

^b Earth System Science Interdisciplinary Center, University of Maryland, College Park, MD, USA

ABSTRACT: Earlier studies have identified a teleconnection between the Atlantic zonal mode (AZM) and Indian summer monsoon rainfall (ISMR), both of which are active during the boreal summer (AZM: June–August; ISMR: June–September). It is known that El Niño–Southern Oscillation (ENSO)-like coupled dynamics are operational in the tropical Atlantic during the AZM events. Our goal here is to extend this process understanding to seek a predictive relation between the tropical Atlantic and the ISMR based on these known teleconnections. Monthly composite analysis of the zonal surface winds, heat content, and sea surface temperature (SST) in the equatorial Atlantic tells us that signatures of a warm or cold AZM event begin to emerge as early as January of that year. We found significant correlations between the ISMR and the low level zonal winds in the western equatorial Atlantic and heat content in the eastern equatorial Atlantic in the boreal spring season. Tracking coherent changes in these winds and the evolution of the heat content in the deep tropical Atlantic in the boreal spring may offer the potential for skillful predictions of the ensuing summer monsoon anomalies, especially during non-ENSO years when the predictability of ISMR tends to be low.

KEY WORDS interannual variability; Atlantic zonal mode; Indian monsoon rainfall; heat content

Received 24 October 2014; Revised 25 July 2015; Accepted 18 August 2015

1. Introduction

India's food security and 60% of the employment base depend on rainfed agriculture, which in turn is dependent on 70% of the annual rainfall received during the months of June–September (JJAS) [Indian summer monsoon rainfall (ISMR)]. It is well known that the ISMR exhibits significant interannual variability in both intensity and spatial distribution leading to extreme events like floods and droughts (Parthasarathy *et al.*, 1994; Gadgil, 2003). So it is of immense socioeconomic importance to forecast these variations in advance to devise better policies to mitigate possible disasters and plan for suitable crops. Even though significant improvements have been made in the simulation and prediction of ISMR, the skill of statistical, atmospheric, and coupled models in predicting the ISMR leaves a lot to be desired (Rajeevan and Nanjundiah, 2009; Gadgil and Srinivasan, 2011; Kim *et al.*, 2012). For example, the monsoon predictions using atmosphere or coupled ocean–atmosphere models by most of the leading centres in the world could not predict the large deficit in rainfall during the summer monsoon of 2009 (Nanjundiah, 2009). It emphasizes the need to understand

the system better, particularly on interannual time scales. A strong relation exists between the El Niño–Southern Oscillation (ENSO; Philander *et al.*, 1989) and the ISMR (Webster *et al.*, 1998), even though the relation is not stationary and depends on the flavour of ENSO (Kumar *et al.*, 1999; Ashok *et al.*, 2007). The recent failures of monsoon predictions in 2012 and 2014 were also accompanied by the unexpected demise of ENSO (from what seemed like an evolving El Niño during the summer of 2014, the weak warm anomalies in the central-eastern equatorial Pacific have evolved to that of a weak El Niño by mid-March 2015 and persisted into September 2015; deficit in the ISMR is about 14%), highlighting the tenuousness of relying on ENSO for monsoon predictions. This motivates us to explore any likely skill from another tropical ocean, viz., the tropical Atlantic.

Earlier studies have examined the influence of different climate modes on the interannual variability of ISMR (Webster and Yang, 1992). Among them, ENSO and the Indian Ocean Dipole/Zonal Mode (IODZM) are the dominant interannual modes in the tropics. Their individual and combined effects on the ISMR have been investigated by a number of earlier studies using observational and modelling efforts (Neelin *et al.*, 1998; Webster *et al.*, 1998, 1999; Saji *et al.*, 1999; Clark *et al.*, 2000; Krishnamurthy and Shukla, 2000; Murtugudde *et al.*, 2000; Ashok *et al.*, 2001; Ashok and Saji, 2007; Cherchi *et al.*, 2007). In general, a La Niña (an El Niño) or a positive (negative)

* Correspondence to: Dr M. Ravichandran, Scientist-G & Head, Modelling and Observations Group, Indian National Center for Ocean Information Services, Ocean Valley, Pragathi Nagar, Hyderabad, Telangana, 500090, India. E-mail: ravi@incois.gov.in

IODZM event leads to an enhancement (a reduction) of the ISMR. The debate over whether an IODZM can occur independently of ENSO continues, including whether the IODZM is a real dipole at all (Annamalai *et al.*, 2003; Zhao and Nigam, 2015), but our goal is not to address this issue. Apart from influencing the ISMR, the IODZM can reduce the impact of ENSO on ISMR whenever modes of the same phase co-occur and the IODZM is even argued to impact an evolving ENSO (Ashok *et al.*, 2001; Annamalai *et al.*, 2005). It is worth mentioning here that ENSO explains only 30% of the interannual variability of ISMR (Rajeevan and McPhaden, 2004; Gadgil, 2014). It indicates that development of an ENSO event may not always have its impact on the ISMR. For example, despite the year 1997 being a strong El Niño, the ISMR was normal. Moreover, there are a few dry and wet years, which cannot be explained by either ENSO or IODZM events (Varikoden and Preethi, 2013). For instance, the ISMR was above normal in 2013, even though there was no ENSO or IODZM event. Hence, it is imperative to find out the influence of other tropical teleconnections to the Indian monsoon, especially during non-ENSO years.

A similar to, but weaker than ENSO, ocean–atmosphere interaction exists in the tropical Atlantic which is called the Atlantic zonal mode (AZM; also called as Atlantic Niño; Zebiak, 1993; Xie and Carton, 2004; Burls *et al.*, 2012). The study by Keenlyside and Latif (2007) showed the existence of Bjerknes feedback (Bjerknes, 1969) involving a positive feedback between the zonal winds, thermocline, heat content, and sea surface temperature (SST) in the equatorial Atlantic in the evolution of AZM, similar to the case of ENSO. The typical characteristics of a cold (warm) AZM event are manifested as an anomalous cooling (warming) and a reduction (an enhancement) of convection in the eastern equatorial Atlantic (EEA) (Xie and Carton, 2004; Burls *et al.*, 2012). However, these signals last only for a few months and the strength is also relatively low compared to ENSO. The AZM is phase locked to seasonal cycle and usually peaks during the boreal summer [June–August (JJA); Lübbecke *et al.*, 2010] coinciding with the Indian summer monsoon period (June–September), although some events can occur later in the fall (Monger *et al.*, 1997; Okumura and Xie, 2006). A series of studies has shown that a warm (cold) AZM event can decrease (increase) the ISMR (Kucharski *et al.*, 2007, 2008; Wang *et al.*, 2009; Barimalala *et al.*, 2011). A physical mechanism as to how the effect of AZM may reach the Indian subcontinent was demonstrated by Kucharski *et al.* (2009), where it is shown that the warm (cold) AZM SST in the tropical Atlantic drive a dynamic response producing a high (low) pressure over the Indian landmass, which leads to a decreased (increased) monsoonal flow. Consistent with this result, a recent study by Pottapinjara *et al.* (2014) showed that warm (cold) AZM SST can also convey its effect to the Indian Ocean through Kelvin-like waves in the tropospheric temperature field which tends to decrease (increase) the mid-tropospheric gradient between the Indian land mass

and tropical Indian Ocean leading to a weaker (stronger) monsoonal flow.

Although the existence of a relation between the AZM and ISMR is shown by these earlier studies, there is no predictive value in the SST associated with AZM to ISMR because both of them are active almost at the same time in the boreal summer. Ding *et al.* (2010) showed that variations in upper ocean heat content (or heat content; see Section 2) averaged in the equatorial Atlantic belt precede SST anomalies in the cold tongue region (6°S – 2°N and 20° – 0°W) by 4–5 months. That indicates a potentially predictive value from heat content to the SST anomalies during the AZM. Hence, it is worth examining the changes in heat content in the equatorial Atlantic which precede the AZM to determine if those changes can foretell the ensuing summer monsoon anomaly sufficiently in advance. Our interest in the heat content variability in the equatorial Atlantic and ISMR is motivated by a study by Rajeevan and McPhaden (2004). They have shown that heat content or its equivalent, volume of warm water in the tropical Pacific can act as a better predictor for ISMR with a lead time of 2 months, compared to ENSO SST indices which do not have any predictive value for the ensuing monsoon rainfall. Moreover, McPhaden and Nagura (2013) have shown that the heat content in the Indian Ocean equatorial belt can be a predictor of the IODZM development through a mechanism similar to that of ENSO in the Pacific. They explained these results in the framework of the recharge oscillator theory (Jin, 1997). However, the relationship between heat content variability in the equatorial Atlantic and ISMR is not investigated thus far, to the best of our knowledge. The primary objective of this study is to describe and explain the existence and the mechanistic connection between the heat content variability in the equatorial Atlantic and ISMR. This might shed some light on the ensuing monsoon, especially during non-ENSO years.

The remainder of this paper is organized as follows. Data sets used and methods employed are described in Section 2. Section 3 describes the analysis and results. Section 4 summarizes the results.

2. Data and methods

The AZM is characterized by the Atlantic 3 index (Atl3; analogous to the Niño 3 region for ENSO) which is the average of the SST anomalies over 3°S – 3°N and 20°W – 0°E . The AZM events are selected as follows. Whenever the Atl3 index crosses one standard deviation (0.48°C) during JJA season, it is called a warm (cold) event, if the sign of the anomalies is positive (negative) (Burls *et al.*, 2012). The Atl3 index is based on the detrended Hadley Centre Sea Ice and Sea Surface Temperature (HadISST) product (Rayner *et al.*, 2003). Because of the constraints posed by the availability of different data sets, we will restrict ourselves only to the period 1975–2010. During this period, AZM cold events are found to occur in years 1976, 1978, 1982, 1983, 1992,

1994, 1997, and 2005 (a total of eight), and warm events during 1984, 1987, 1988, 1995, 1996, 1998, 1999, 2008, and 2010 (a total of nine). Following the same criterion for selecting ENSO years as for AZM, but using Niño 3.4 (5°S–5°N and 170°–120°W) SST index (standard deviation 0.5 °C), years of La Niña events are identified to be 1975, 1985, 1988, 1998, 1999, 2000, and 2010 (a total of seven); and, El Niño events to be 1982, 1987, 1991, 1997, 2002, 2004, and 2009 (a total of seven) (consistent with the list of ENSO events given at http://www.cpc.ncep.noaa.gov/products/analysis_monitoring/ensostuff/ensoyears.shtml). It can be noted that there are some years in which both the AZM and ENSO occurred. The cold AZM events which did not occur along with ENSO are 1976, 1978, 1983, 1992, 1994, and 2005 (a total of six), and the warm events independent of ENSO are 1984, 1995, 1996, and 2008 (a total of four). These different sets of years are used to prepare different composite maps shown in the following section.

Ocean temperature data obtained from the Simple Ocean Data Assimilation (SODA) v2.2.4 (Carton and Giese, 2008) are used to calculate upper ocean heat content per unit area above 20 °C isotherm ('heat content' hereafter) as given by Equation (1).

$$\frac{1}{A} Q_{\text{tot}} = \rho C_p \int_{z=0\text{m}}^{z(t=20^\circ\text{C})} T(z) dz \quad (1)$$

In the equation, Q_{tot} is the total heat content; A is the surface area; ρ is the density of water; C_p is the specific heat of water; T is the temperature of water; and, z is the depth of the ocean. The daily high-resolution (0.25° × 0.25°) gridded rainfall data provided by the India Meteorological Department (Pai *et al.*, 2014) are used to show the relation between the AZM and ISMR. In addition, to show the changes in wind field associated with the Bjerknes feedback in the equatorial Atlantic, the National Centers for Environmental Prediction (NCEP) Reanalysis-2 product for wind (1979–2010; Kanamitsu *et al.*, 2002) is used. Seasonal composites and correlations are used in the analysis. The significance of correlations is determined using the two-tailed Student's t -test.

ENSO is the dominant phenomenon remotely affecting the Indian monsoon. The lead–lag correlation analysis between the rainfall over central India and the Western Ghats (see Section 3; regions shown in Figure 1(b)) and the Niño 3.4 index yields (figure not shown) significant correlations both in the present and previous year's monsoon seasons. The previous year's monsoon correlations represent the cyclic nature of the correlation pattern between the rainfall and ENSO (Rajeevan and McPhaden, 2004). In order to see which other phenomena affect the monsoon apart from ENSO, the effect of ENSO on rainfall needs to be removed. For this purpose, the method used in Kucharski *et al.* (2008) is extended to serve our analysis. The effect of ENSO on JJAS rainfall time series is removed by taking JJAS Niño 3.4 index both during the previous and present monsoons as shown in Equation (2). In the equation, the SST leads are with respect to the JJAS

rainfall during the present monsoon season. The residual time series of rainfall which is free from the linear effect of Niño 3.4 index is given by,

$$\begin{aligned} \text{Rainfall}_{\text{res}} = & \text{Rainfall} - \text{Slope}_1 \times \text{Niño 3.4 (pres)} \\ & - \text{Slope}_2 \times \text{Niño 3.4}_{\text{res}} (\text{prev}) \end{aligned} \quad (2)$$

where $\text{Niño 3.4}_{\text{res}}(\text{prev}) = \text{Niño 3.4}(\text{prev}) - \text{Slope}_3 \times \text{Niño 3.4}(\text{pres})$ and Slope_1 and Slope_2 are the least square regression fit slopes between the rainfall, and Niño 3.4 index during the present (pres) monsoon season and Niño 3.4_{res}(prev) (residual of Niño 3.4 index in the previous monsoon season that is uncorrelated with Niño 3.4 index in the present monsoon season), respectively. And, Slope_3 is the slope of the least square regression fit between Niño 3.4 index in the present and previous monsoon seasons. The second term in the equation (involving Slope_2) accounts for the effect of Niño 3.4 index of the previous season on rainfall that is not related to Niño 3.4 index of the present season. Correlating the residual of JJAS rainfall anomaly time series with the Niño 3.4 index confirms that the correlations after removing the effect of ENSO are well below the significance levels (figure not shown). These residual rainfall time series of the two regions (to be defined in the next section) are used in the analysis.

In this article, the major analysis techniques used are linear correlation and composite analysis. Figures 1 and 3 are the result of composite analysis whereas the rest (Figures 2, 4, and 5) are obtained using linear correlation analysis. In the composite analysis, the AZM (or ENSO) years are used including or excluding the other to elucidate the distinct patterns in different fields associated with the AZM (or ENSO). The linear correlation analyses (Figures 2, 4, and 5) are performed with the total time series. To clearly depict the impact of AZM that is otherwise masked by ENSO, Equation (2) is used to remove the effect of ENSO from the rainfall, as ENSO confounds the analysis in the full time series. The residual rainfall time series is used for further correlation analysis.

3. Results and discussion

3.1. Relationship between the AZM and ISMR

The differences (cold–warm) between seasonal (JJAS) composites of rainfall over India during the cold and warm AZM years, including and excluding the co-occurring ENSO years, are shown in Figure 1(a) and (b), respectively. Consistent with the earlier studies (Kucharski *et al.*, 2007, 2008, 2009; Pottapinjara *et al.*, 2014), Figure 1(a) and (b) clearly depicts the relationship between the AZM and ISMR with enhanced (reduced) rainfall in the lower parts of the Western Ghats and over central India but with decreased (increased) rainfall over northeastern India and southeastern India, during a cold (warm) AZM event. Similar maps of difference (La Niña–El Niño) of seasonal composites of rainfall over India during La Niña and El Niño phases of ENSO including and excluding the co-occurring AZM years are shown in Figure 1(c) and (d),

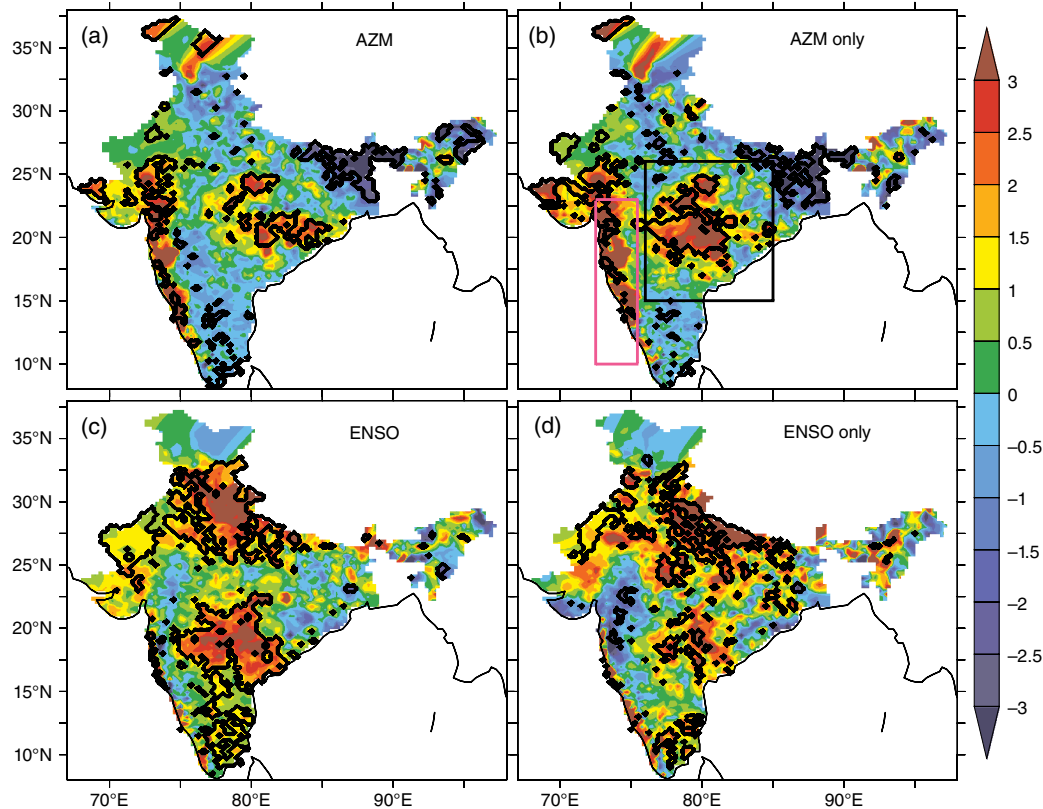


Figure 1. Differences of composites of rainfall between the cold and warm years of (a) AZM, (b) AZM only (excluding those co-occurring with ENSO), (c) ENSO, and (d) ENSO only (excluding ENSO co-occurring with AZM). The two regions selected for the analysis, i.e., central India (15° – 26° N and 76° – 85° E; big thick box (black in online)) and the Western Ghats (10° – 23° N and 72.5° – 75.5° E; small light box (pink in online)) are shown in (b). The contours in black colour indicate 90% significance level.

respectively. From the figure, it can be seen that the spatial patterns of rainfall composites for the AZM (Figure 1(a) and (b)) and ENSO (Figure 1(c) and (d)) are different. It is also clear from the figure that the spatial pattern of rainfall for the AZM where ENSO years are excluded (i.e., for only non-ENSO AZM events; Figure 1(b)) becomes more prominent. From this, we can discern that the AZM does seem to affect the rainfall over India independently of ENSO and its effects are not homogeneous over the sub-continent.

To capture the variation of the influence of AZM over rainfall, two dominant regions, i.e., central India (15° – 26° N and 76° – 85° E; shown as a black box in Figure 1(b)) and the Western Ghats (10° – 23° N and 72.5° – 75.5° E; shown as a pink box in the same), that show significant difference in rainfall between the cold and warm phases of AZM, are selected to analyse the problem further. The correlation coefficients between the JJA Atl3 index and JJAS rainfall anomalies averaged over the two regions as defined above, before and after removing the effect of ENSO over the respective regional rainfalls, are presented in Table 1 (see Section 2; correlations are simultaneous). It may be noted that the correlations (-0.15 over central India; -0.29 over the Western Ghats) improve and become statistically more significant after removing the effect of ENSO (-0.34 over central India; -0.35 over

Table 1. Correlation coefficients (CC) between JJA Atl3 index and JJAS rainfall anomalies over central India (15° – 26° N and 76° – 85° E) and Western Ghats (10° – 23° N and 72.5° – 75.5° E) before and after removing the effect of ENSO on the respective rainfall series.

Central India rainfall versus JJA Atl3	Western Ghats rainfall versus JJA Atl3
-0.15	-0.29
After removing the ENSO effect over the respective rainfall	
-0.34	-0.35

The CC marked in bold are above 90% significance level as per Student's *t*-test.

the Western Ghats) over the respective rainfalls. It may also be noted that the sign of correlations agrees with the difference of seasonal composites of rainfall maps presented in Figure 1(a) and (b) and is consistent with the result of Pottapinjara *et al.* (2014).

3.2. Evolution of the zonal wind, heat content, and SST in the equatorial Atlantic associated with AZM

Having shown the existence of a relation between the AZM and ISMR, we seek indicators portending the SST anomalies associated with AZM which might serve as predictors for ISMR anomalies. To see if any lead-time

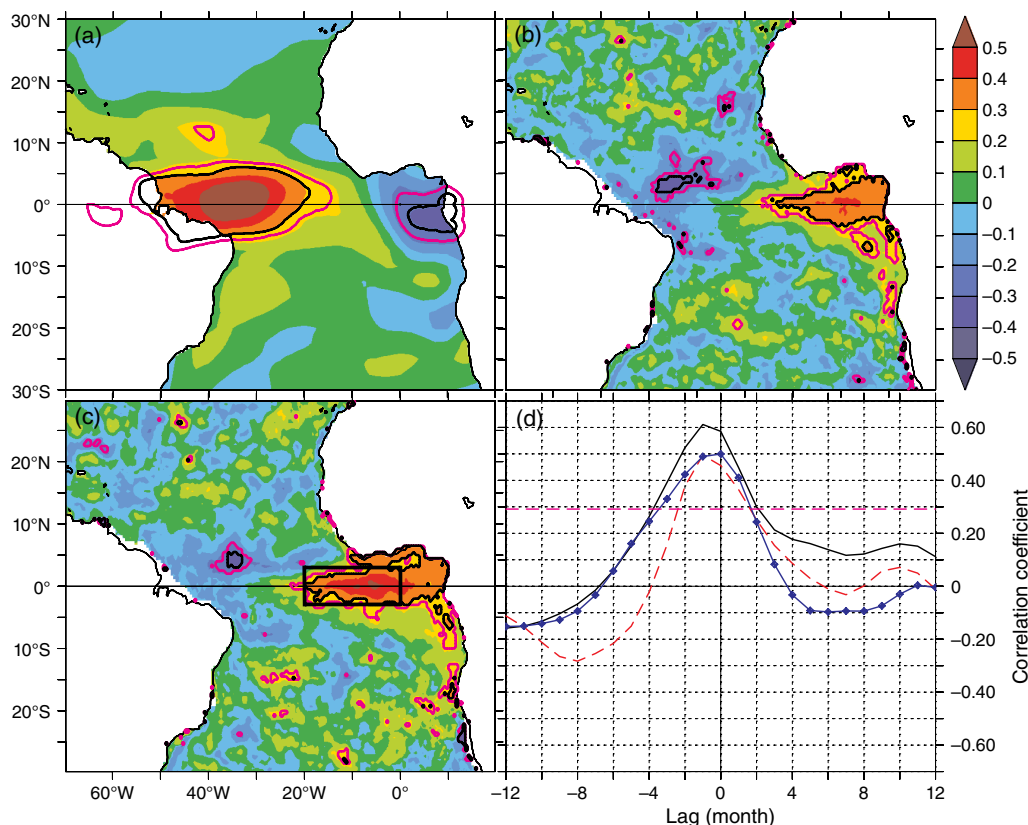


Figure 2. Spatial correlations between the anomalies of (a) SST in the AtI3 region and zonal winds, (b) western equatorial Atlantic (3°S–3°N and 40°–20°W; WEA) zonal winds and heat content, (c) east equatorial Atlantic (3°S–3°N and 5°W–10°E; EEA) heat content and SST, and (d) monthly lead–lag correlations between anomalies of SST in the AtI3 region and WEA zonal wind (black), WEA zonal wind and EEA heat content (dashes in red) and EEA heat content and AtI3 (diamonds in blue). The zonal winds are taken at 850 hPa level. In spatial correlation plots (a–c), contours of 80 and 90% significance are indicated in light and thick (pink and black colours) in online, respectively, and in (d), the level of 90% significance is indicated by a dashed horizontal (pink dashed in online) line. The correlations over land are masked in (a) to highlight the same over the ocean. The black box in (c) indicates the AtI3 region.

indicators exist for an impending AZM event, dynamics associated with the AZM are examined in below.

A dynamical positive feedback between the winds, SST, and thermocline depth was proposed by Bjerknes to explain the growing phase of ENSO (Bjerknes, 1969). In an equatorial ocean basin where the normal conditions are characterized by a warm pool in the west and a cold tongue in the east, the feedback can be explained as follows. A warm SST anomaly in the east (produced by local reduction in upwelling or a remotely driven deepening of the thermocline, typically by a Kelvin wave from the west) weakens the temperature gradient between the western warm pool and the eastern cold tongue which further weakens the easterly trade winds. Weakened trades will further weaken the upwelling and surface cooling and allow the warming to persist or grow in the east. Subsequently, equatorial upwelling in the east is weakened and also brings up water warmer than normal and hence further warms the SST in the east, driving a positive coupled ocean–atmosphere feedback that needs to be terminated by other processes (Wang and Picaut, 2004). The relations between these three components of the Bjerknes feedback are examined below in the context of AZM.

Spatial correlations between the anomalies of low level zonal wind (850 hPa), heat content (synonymous with the thermocline depth; see Section 2 for definition), and SST are shown in Figure 2(a)–(c). The correlation map between the AtI3 index and low level zonal wind anomaly presented in Figure 2(a) shows that warm SST anomalies in the AtI3 region are associated with positive wind anomalies in the western equatorial Atlantic (WEA; 3°S–3°N and 40°–20°W). The zonal wind anomalies averaged over the WEA are positively correlated with heat content anomalies in the EEA [3°S–3°N and 5°W–10°E; Figure 2(b)], which indicates that westerly (easterly) zonal wind anomaly in the WEA drives an enhancement (a reduction) of heat content in the EEA. The heat content anomalies averaged in the EEA are positively correlated with SST anomaly in the AtI3 region (Figure 2(c)) indicating that anomalous increase in heat content in the EEA is tied to an increase in SST in the east, likely through thermocline-mixed layer interactions. Note from Figure 2 (a)–(c) that the three fields (the wind anomalies in the WEA, heat content anomalies in the EEA, and SST anomalies in the AtI3) can potentially work together to form a positive feedback. Also, note that they are all simultaneous

correlations and do not give any clue on the possible leads or lags. Monthly lead–lag correlations between the three fields shown in Figure 2(d) indicate a lag of 1 month in peak correlations both between SST in the Atl3 region and winds in the WEA, and winds in the WEA and heat content in the EEA. It also shows a lag of about 1 month in the peak correlation between heat content in the EEA and SST in the Atl3. The different correlations are significant with at least 2 months lead. These results are consistent with Keenlyside and Latif (2007) where the Bjerknes feedback is shown to be at work in the tropical Atlantic as in the case of ENSO but with a weaker intensity. All these are monthly correlation analyses from which we can say with confidence that the development of an AZM event involves coupled ocean–atmosphere feedbacks.

To gain more confidence in the causal links, monthly composite analyses of these three fields mentioned above are presented in Figure 3 for both the cold and warm AZM years. In the figure, the zonal component of low level winds in the WEA reaches its farthest in April (May) followed by the heat content in the EEA in May (June) and SST in the Atl3 region in June (June) during a cold (warm) AZM event. From the above and Figure 2, it may be argued that during a warm (cold) AZM event, anomalous westerlies (easterlies) in the WEA lead to an anomalous increase (decrease) in heat content in the EEA with a lag of 1 month. It can be further argued that the anomalies in the heat content are reflected in SST in the Atl3 region within 1 month time which in turn feeds back to winds in the WEA, thus completing a positive feedback loop. It can be noticed that zonal surface winds in the EEA are strongest (weakest) in June (June) during the cold (warm) events of AZM acting as a dampening factor in the feedback loop. Once again, the chain of events in the feedback loop agrees well with Keenlyside and Latif (2007).

The most important observation from Figure 3 is that the development of different signals during the cold and warm AZM events is clearly distinct and that it is indicative of the impending AZM event as early as January itself. This suggests that wind anomalies in the WEA and heat content anomalies in the EEA during January–May might offer potential predictability of the development of an AZM event in the ensuing summer. Hence, the key question is whether this information can provide some clue on the ISMR anomalies associated with AZM. The relationship between equatorial Atlantic winds and heat content, and the ISMR is examined below.

3.3. Relationship between the ISMR and the heat content and wind variability in the equatorial Atlantic

The spatio-temporal evolution of correlations between the heat content in the Atlantic, and JJAS rainfall anomalies over central India and the Western Ghats, before and after removing the effect of ENSO over the respective rainfall time series are shown in Figure 4 [(a) and (b): central India; (c) and (d): the Western Ghats; see Section 2 for the method to remove the effect of ENSO over rainfall]. It is evident from the figure that consistent signals

are present in the eastern equatorial Atlantic Ocean in nearly the same regions as in Figure 2(b). The correlations of the equatorial Atlantic heat content with ISMR over both the regions start to build up from the month of January and become the strongest in the months of February and March and weaken later. It can also be seen that the correlations improve after removing the effect of ENSO on the rainfall (Figure 4(b) and (d)). It is worth reemphasizing that the correlations between the rainfall and Atl3 SST also improve similarly as shown in Table 1. After removing the effect of ENSO over respective rainfall time series, the correlations with the heat content persist from January to May for rainfall over the Western Ghats, whereas for the rainfall over central India, the signals get weaker in April and May. However, this figure clearly indicates that the heat content in the EEA in January–May may hold some clue for the summer rainfall anomalies over these Indian land regions. The Bjerknes feedback component that precedes the heat content in the Atlantic as shown in Figure 3 is the anomalous westerly surface winds in the WEA. Similar to Figure 4, the correlations between the low level (850 hPa) zonal winds and rainfall are shown in Figure 5. For rainfall over the Western Ghats, there are clear signals in low level zonal winds in the WEA, both before and after removing the effect of ENSO. However, for central India rainfall, after removing the effect of ENSO, there seems to be some signal in the wind during the months of April and May, but it is comparatively weaker than that for the Western Ghats. From the above analysis, it may be concluded that low level winds in the WEA may be a potential predictor for rainfall anomalies over Western Ghats and over central India one season in advance.

Synthesizing the different arguments made above, we can state that the coherent changes in low level zonal winds, heat content, and SST (Bjerknes feedback) precede an AZM event as shown in Figures 2 and 3. The extant relation between the AZM and ISMR is shown in Table 1 and is consistent with the earlier studies cited in Introduction. A physical mechanism conveying the influence of AZM to ISMR is discussed in Kucharski *et al.* (2009) and Pottapinjara *et al.* (2014). The Bjerknes feedback components of heat content in the EEA and surface zonal winds in the WEA during January–May are shown to be related to the rainfall over India in JJAS in Figures 4 and 5. In addition, it is also shown that the relation improves after removing the effect of ENSO over the rainfall. In summary, we can conclude that by tracking the zonal surface winds in the WEA and heat content and SST in the EEA, we may gain some short lead-time potential predictability in monsoon anomalies, especially during non-ENSO years.

4. Summary and conclusions

Several recent studies have highlighted the relationship between the AZM and ISMR (e.g., Wang *et al.*, 2009; Pottapinjara *et al.*, 2014). The SST anomaly associated with the AZM in the EEA affects the ISMR via both

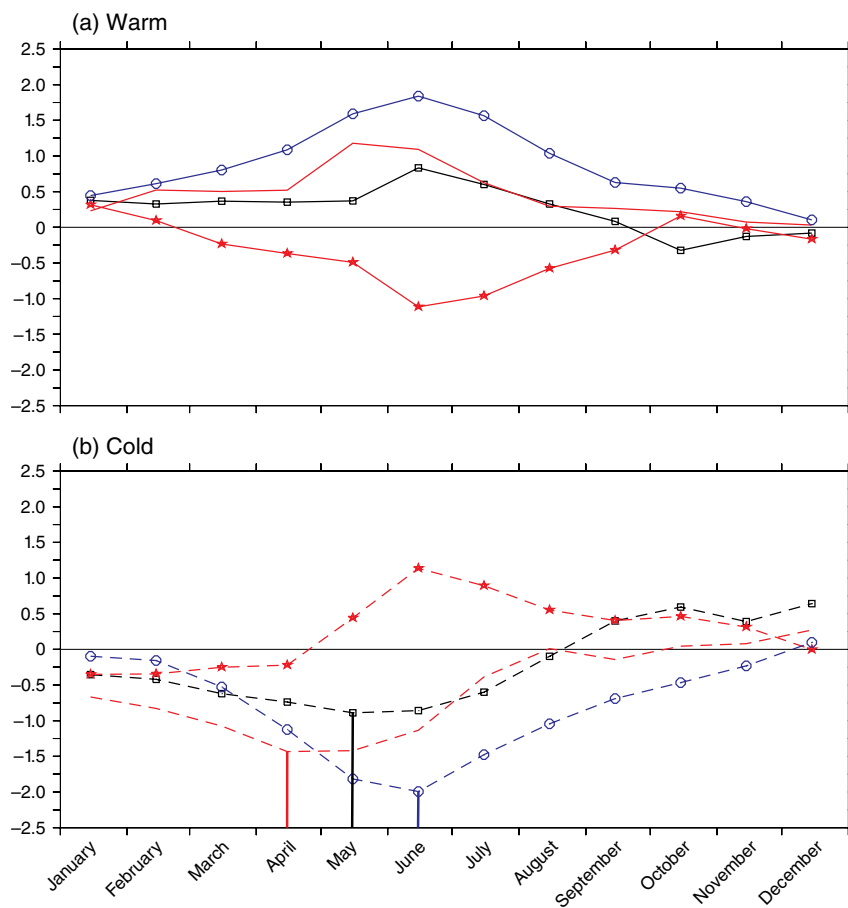


Figure 3. Evolution of composites of anomalies of western equatorial zonal wind (red; no symbol), eastern equatorial zonal wind (stars in red), eastern equatorial heat content (squares in black), and SST in the Atl3 region (circles in blue) during the warm (solid line) and cold (dashed line) years of AZM. All the fields are normalized before compositing. The zonal winds are taken at 850 hPa level. The peaks of different fields plotted are marked as vertical lines in their respective colours.

dynamical and thermodynamical pathways as reported in earlier studies (Kucharski *et al.*, 2009; Pottapinjara *et al.*, 2014). In this study, we attempted to find a predictor that may give some indication of the ensuing AZM event in the Atlantic which might in turn offer predictive value for the ISMR. As shown by Keenlyside and Latif (2007), Bjerknes feedback is the dominant causative mechanism for the evolution of warm or cold AZM events. Consistent with earlier studies, we find that the evolution of low level zonal winds, heat content, and SST is different for warm or cold AZM events starting as early as January of the same year. Our analysis shows that the upper ocean heat content in the EEA and zonal surface winds in the WEA during January–May season are indicators of an impending AZM event. This in turn should provide us with a valuable early clue to an imminent ISMR anomaly through the AZM's impact on monsoon depressions and via its teleconnection to the monsoon with a reasonable lead-time. We believe that these novel causal linkages offer a testable hypothesis for the state-of-the-art coupled climate models used to forecast the Indian summer monsoon, especially during non-ENSO years.

Our analysis shows that there is no clear and consistent correlation between the low level zonal winds in the equatorial Atlantic and rainfall over Central India (Figure 5), but the correlation is a bit more convincing between the heat content and the rainfall (Figure 4). This may be because the rainfall over central India has several contributing factors like the monsoon depressions in the Bay of Bengal and the direct moisture transport by the southwest monsoon winds (see chapter 3 of Pant and Rupakumar, 1997). The rainfall distribution over India is not uniform, and different mechanisms may be operating in determining the rainfall over different parts of India (Vecchi and Harrison, 2004). As depicted in Figure 1, the influence of AZM too is not uniform over India and that might explain why there is a difference in correlations with rainfall over central India and the Western Ghats (Figures 4 and 5). For example, a relationship between the heat content of the eastern Indian Ocean and monsoon droughts was reported by Krishnan *et al.* (2006). It is possible that the impact of AZM on ISMR is not only confounded by ENSO but also by the IODZM which needs further investigation.

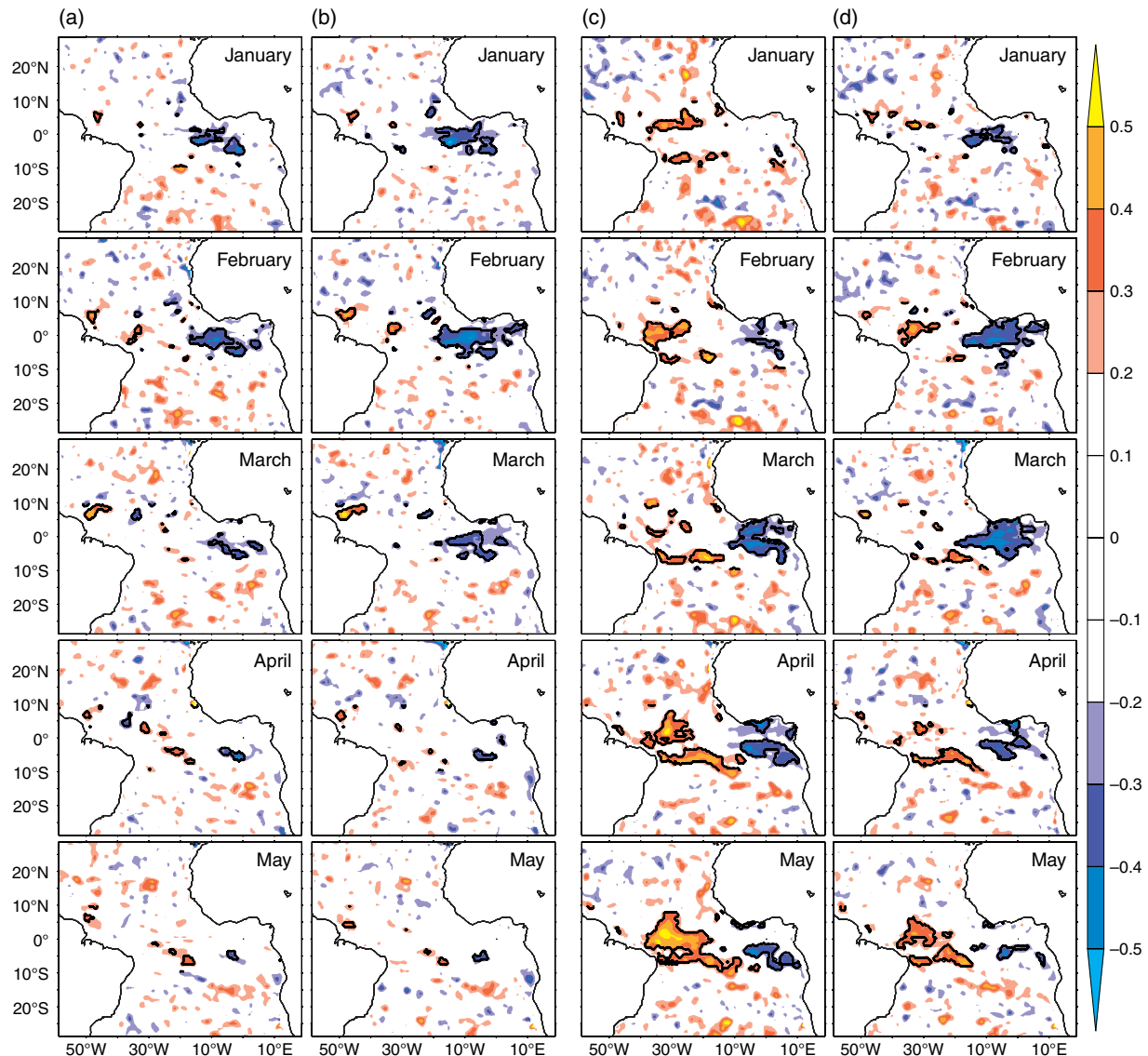


Figure 4. Monthly correlations, during January–May, between anomalies of heat content and JJAS rainfall anomalies over central India (a and b) and the Western Ghats (c and d), before (a and c) and after (b and d) removing the effect of ENSO on the respective regional rainfall during the monsoon season. Correlations above 90% significance level around the equator are shown in black contours.

Our findings are essentially consistent with Ding *et al.* (2010) in that the heat content anomalies in the equatorial Atlantic precede the changes in Atl3 SST associated with the AZM. In addition, the existence of a relationship between the AZM and rainfall over India is reported by some recent studies (e.g., Kucharski *et al.*, 2008; Pottapinjara *et al.*, 2014). Naturally, as one would expect, a predictive value for the Indian monsoon in the heat content in the equatorial Atlantic is of utmost importance, especially for non-ENSO years, and is indeed shown to exist by our analysis. Unfortunately, with our current analysis, why the correlations between the seasonal (JJAS) mean rainfall and the heat content in the EEA drop in May (Figure 4) cannot be explained. These require some sensitivity experiments with models, and we will perform this analysis with forced ocean and coupled climate models

separately. It was suspected that the dip in correlations might be due to a decoupling of the surface and the subsurface in the EEA. However, a study by Keenlyside and Latif (2007) showed that the EEA SSTAs are primarily affected by heat content during late boreal spring and early boreal summer as the thermocline is shallow enough to affect the SST during these months. Moreover, this aspect is depicted in Figure 3 as well. For our purposes, it can be concluded that the supposed decoupling of the thermocline and mixed layer in the EEA in May, which might have explained the falling correlations between ISMR and heat content anomaly in May, is absent. The lead–lag relationship between the heat content and SST in the equatorial Atlantic is critical in this context and is somewhat reminiscent of the spring predictability barrier in the El Niño parlance (Webster and Hoyos, 2010).

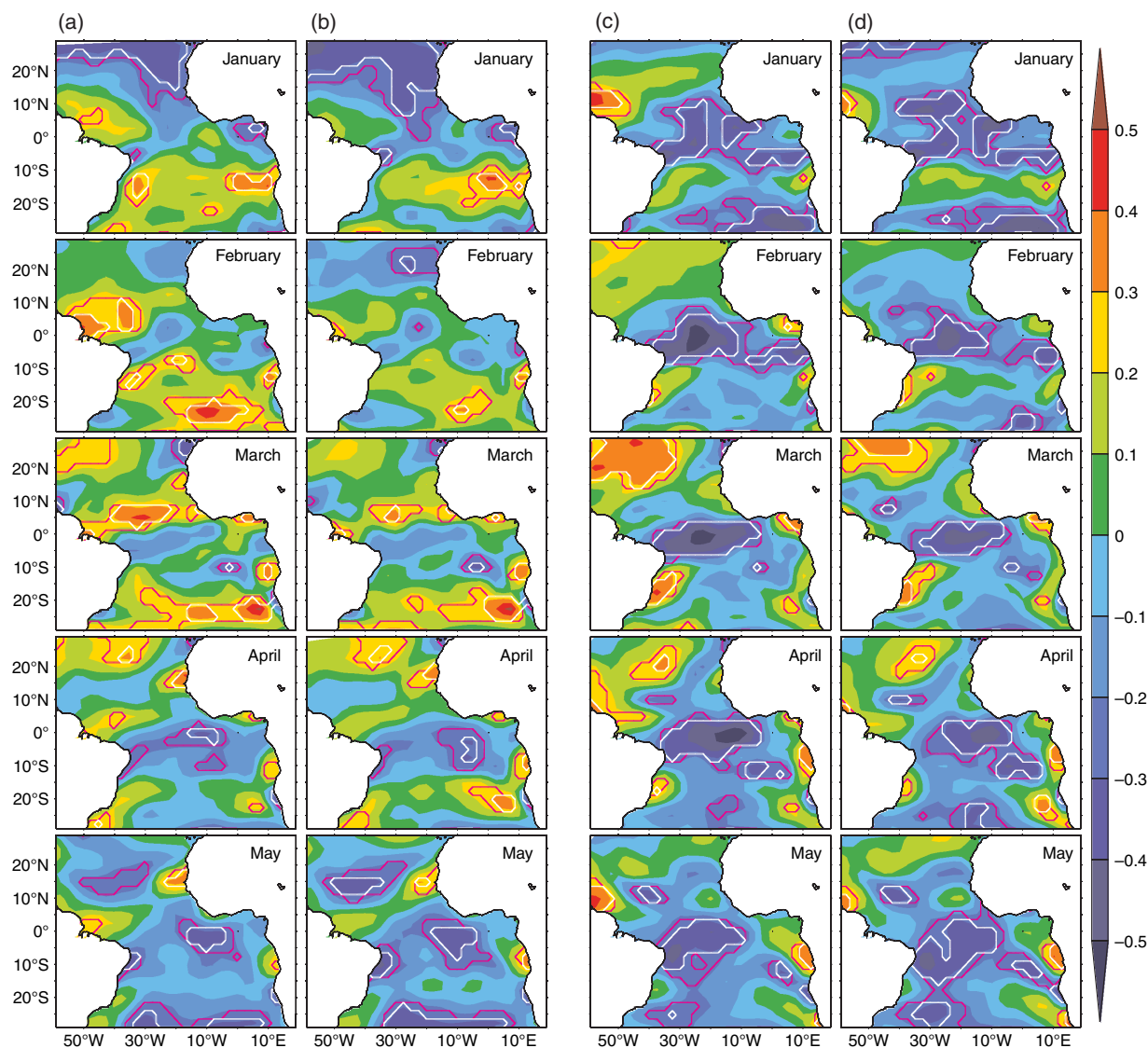


Figure 5. Monthly correlations, during January–May, between anomalies of low level winds, and JJAS rainfall anomalies over central India (a and b) and the Western Ghats (c and d), before (a and b) and after (b and d) removing the effect of the ENSO on the respective regional rainfall during the monsoon season. The contours of 80 and 90% significance levels are indicated in light (pink in online) and white colours, respectively. Correlations over land are masked to highlight the same over the ocean.

The spring warming and the relaxation of the thermocline are seasonal features not only in the equatorial Atlantic but also in the equatorial Pacific. The interaction of the interannual mode with the annual cycle is a subject of extensive studies in the tropical Pacific but apparently should be so in the tropical Atlantic also (e.g., Tziperman *et al.*, 1994). But this is also beyond the scope of this study.

Unlike Ding *et al.* (2010), the local relation we seek between the EEA heat content and SST is driven by maximum correlation specifically for predictive value to ISMR. It should be noted that the local and remote forcing of the thermocline variability in the EEA and the east–west contrast (Busalacchi and Picaut, 1983) is lost in the analysis of Ding *et al.* (2010) due to their averaging of the heat content over the tropical Atlantic, and thus the lead time of their heat content with the Atlantic Niño is

about a season in contrast to the 1-month lead we find here between the EEA heat content and the Atlantic Niño. The role of the Bjerknes feedback and the east–west contrast we report must play a role in determining the anomalous ITCZ position and the strength of the correlation between the meridional and zonal modes and thereby the link between the ITCZ and Indian monsoon. This aspect needs further investigation as well.

The observed asymmetry in different components of the Bjerknes feedback between the cold and warm AZM events (Figure 3) is already reported (e.g., Lübbecke *et al.*, 2014). It may be due to differences in the timing and strength of the associated cold tongue. The possibility of other processes playing a role in generating AZM warm events and the likely absence of Bjerknes feedback in some events might be a reason why composites of winds and

heat content during the warm AZM events do not appear so smooth (Figure 3). However, to look at such a possibility, data covering many more samples of AZM events are needed.

Our understanding of the AZM evolution may not be complete as of now. The close relation between the Atlantic Meridional Mode (AMM), which is usually active in the boreal spring, and AZM has been reported by earlier studies (e.g., Servain *et al.*, 1999; Murtugudde *et al.*, 2001). Foltz and McPhaden (2010) suggested a mechanism where the AMM may drive some AZM events. They showed that the wind anomalies in the WEA associated with AMM can generate westward propagating off-equatorial Rossby waves and eastward propagating Kelvin waves. The Kelvin waves initiate the development of eastern equatorial SST anomalies during boreal spring and summer. They further showed that, the westward propagating Rossby waves reflect off the western boundary as Kelvin waves of opposite sign to the original wind forced Kelvin waves. The arrival of reflected Kelvin waves dampens the evolution of SST anomalies associated with the AZM in the eastern basin. On the other hand, South Atlantic Anticyclone (SAA) sitting in the southern tropical Atlantic can also lead to some AZM events (Lübbecke *et al.*, 2010, 2014). Lübbecke *et al.* (2014) show that the variation in the strength of SAA in boreal spring may cause changes in surface winds in the WEA, thereby leading to the genesis of some AZM events. They also discuss various possible mechanisms by which SAA can affect the AZM, including the ocean adjustment to wind anomalies associated with the SAA. The other mechanism that can influence the AZM evolution is the remote forcing by ENSO (e.g., Enfield and Mayer, 1997; Latif and Grötzner, 2000; Huang *et al.*, 2002; Lübbecke and McPhaden, 2012). These earlier studies show that, as a typical response to El Niño, warming in the northern tropical Atlantic can occur (Enfield and Mayer, 1997; Chiang and Sobel, 2002; Huang *et al.*, 2002; Lübbecke and McPhaden, 2012) which may set up a strong meridional SST gradient. This meridional gradient or the AMM can influence the AZM as shown by Foltz and McPhaden (2010). However, the influence of ENSO on AZM is still under debate (Lübbecke and McPhaden, 2012; see their Introduction). In addition to the different physical mechanisms discussed above, there may be further unknown processes leading to AZM events (Lübbecke, 2013). Hence, it might be concluded that the different phenomena affecting the development of AZM (AMM, SAA, and ENSO) may influence the Indian monsoon via the AZM. The connections between such phenomena and the monsoon either directly or via the AZM are the subject of further studies.

It may be noted from the above discussion that none of the mechanisms can explain the occurrence of all AZM events. Hence, the total interannual variability of the equatorial Atlantic can be achieved only through the synthesis of different mechanisms. However, at the heart of all of these mechanisms lies the Bjerknes feedback, which is initiated by wind anomaly in the WEA and is found to explain most of the variability associated with AZM. In this study,

we are primarily interested only in the coherent changes in different components of the Bjerknes feedback that may foretell the occurrence of AZM events and thereby the ISMR, specifically during non-ENSO years.

Furthermore, the EEA is not quite identical to the eastern equatorial Pacific (Busalacchi and Picaut, 1983). The thermocline-mixed layer interactions in the equatorial Atlantic are also not as strong as in the Pacific in addition to the fact that the relatively narrow zonal extent of the Atlantic renders the background east–west contrast rather weak at all timescales. Thus, the weak Bjerknes feedback and the evolution of the AZM appear somewhat less robust compared to ENSO while still offering a robust path for exploring the causal links from the tropical Atlantic to the ISMR.

Analysing the coupled models in the Coupled Model Intercomparison Project Phase 5 (CMIP 5), Richter *et al.* (2012) note that the ITCZ may play an important role in initiating the AZM events by influencing equatorial surface winds. That is consistent with Servain *et al.* (1999) and Murtugudde *et al.* (2001). They further note that most models in this project have serious biases in surface winds in the equatorial Atlantic. Such biases may initiate false AZM events which in turn may affect monsoon predictions via the mechanism outlined in Pottapinjara *et al.* (2014). Those biases in the models used for the monsoon forecasts need further study. It is also not clear whether these teleconnections are manifest through perturbations to the monsoon onset and withdrawal and the length of the rainy season or simply in the monsoon depressions and other mechanisms discussed above. Clearly, further investigations are needed to fully realize any additional predictability that may arise of these causal links.

Acknowledgements

We thank Director, INCOIS, for encouraging us carry out this work and facilitating the same. We also thank two anonymous reviewers for their insightful comments. RM gratefully acknowledges the National Monsoon Mission funding for partial support. This is ESSO-INCOIS contribution number 230.

References

- Annamalai H, Murtugudde R, Potemra J, Xie SP, Liu P, Wang B. 2003. Coupled dynamics over the Indian Ocean: spring initiation of the zonal mode. *Deep Sea Res. II: Top. Stud. Oceanogr.* **50**(12–13): 2305–2330, doi: 10.1016/S0967-0645(03)00058-4.
- Annamalai H, Xie SP, McCreary JP, Murtugudde R. 2005. Impact of Indian Ocean sea surface temperature on developing El Niño. *J. Clim.* **18**(2): 302–319, doi: 10.1175/JCLI-3268.1.
- Ashok K, Saji NH. 2007. On the impacts of ENSO and Indian Ocean dipole events on sub-regional Indian summer monsoon rainfall. *Nat. Hazards* **42**(2): 273–285, doi: 10.1007/s11069-006-9091-0.
- Ashok K, Guan Z, Yamagata T. 2001. Impact of the Indian Ocean dipole on the relationship between the Indian monsoon rainfall and ENSO. *Geophys. Res. Lett.* **28**(23): 4499–4502.
- Ashok K, Behera SK, Rao SA, Weng H, Yamagata T. 2007. El Niño Modoki and its possible teleconnection. *J. Geophys. Res.* **112**(C11): C11007, doi: 10.1029/2006JC003798.
- Barimalala R, Bracco A, Kucharski F. 2011. The representation of the South Tropical Atlantic teleconnection to the Indian Ocean in

- the AR4 coupled models. *Clim. Dyn.* **38**(5–6): 1147–1166, doi: 10.1007/s00382-011-1082-5.
- Bjerknes J. 1969. Atmospheric teleconnections from the equatorial Pacific. *Mon. Weather Rev.* **97**(3): 163–172, doi: 10.1175/1520-0493(1969)097<0163:ATFTEP>2.3.CO;2.
- Burls NJ, Reason CJC, Penven P, Philander SG. 2012. Energetics of the tropical Atlantic zonal mode. *J. Clim.* **25**(21): 7442–7466, doi: 10.1175/JCLI-D-11-00602.1.
- Busalacchi AJ, Picaut J. 1983. Seasonal variability from a model of the tropical Atlantic Ocean. *J. Phys. Oceanogr.* **13**(9): 1564–1588, doi: 10.1175/1520-0485(1983)013<1564:SVFAMO>2.0.CO;2.
- Carton JA, Giese BS. 2008. A reanalysis of ocean climate using Simple Ocean Data Assimilation (SODA). *Mon. Weather Rev.* **136**(8): 2999–3017, doi: 10.1175/2007MWR1978.1.
- Cherchi A, Gualdi S, Behera S, Luo JJ, Masson S, Yamagata T, Navarra A. 2007. The influence of tropical Indian Ocean SST on the Indian summer monsoon. *J. Clim.* **20**(13): 3083–3105, doi: 10.1175/JCLI4161.1.
- Chiang J, Sobel A. 2002. Tropical tropospheric temperature variations caused by ENSO and their influence on the remote tropical climate. *J. Clim.* **15**: 2616–2631, doi: 10.1175/1520-0442(2002)015<2616:TTTTVCB>2.0.CO;2.
- Clark C, Cole J, Webster P. 2000. Indian Ocean SST and Indian summer rainfall: predictive relationships and their decadal variability. *J. Clim.* **13**: 2503–2519, doi: 10.1175/1520-0442(2000)013<2503:IOSAIS>2.0.CO;2.
- Ding H, Keenlyside NS, Latif M. 2010. Equatorial Atlantic interannual variability: role of heat content. *J. Geophys. Res.* **115**(C9): C09020, doi: 10.1029/2010JC006304.
- Enfield DB, Mayer DA. 1997. Tropical Atlantic sea surface temperature variability and its relation to El Niño–Southern Oscillation. *J. Geophys. Res.* **102**(C1): 929–945.
- Foltz GR, McPhaden MJ. 2010. Interaction between the Atlantic meridional and Niño modes. *Geophys. Res. Lett.* **37**(18): L18604, doi: 10.1029/2010GL044001.
- Gadgil S. 2003. The Indian monsoon and its variability. *Annu. Rev. Earth Planet. Sci.* **31**(1): 429–467, doi: 10.1146/annurev.earth.31.100901.141251.
- Gadgil S. 2014. El Niño and the summer monsoon of 2014. *Curr. Sci.* **106**(10): 1335–1336.
- Gadgil S, Srinivasan J. 2011. Seasonal prediction of the Indian monsoon. *Curr. Sci.* **100**(3): 343–353.
- Huang B, Schopf PS, Pan Z. 2002. The ENSO effect on the tropical Atlantic variability: a regionally coupled model study. *Geophys. Res. Lett.* **29**(21): 2039, doi: 10.1029/2002GL014872.
- Jin F-F. 1997. An equatorial ocean recharge paradigm for ENSO. Part I: conceptual model. *J. Atmos. Sci.* **54**: 811–829, doi: 10.1175/1520-0469(1997)054<0811:AEORPF>2.0.CO;2.
- Kanamitsu M, Ebisuzaki W, Woollen J, Yang S-K, Hnilo JJ, Fiorino M, Potter GL. 2002. NCEP–DOE AMIP-II reanalysis (R-2). *Bull. Am. Meteorol. Soc.* **83**(11): 1631–1643, doi: 10.1175/BAMS-83-11-1631.
- Keenlyside NS, Latif M. 2007. Understanding equatorial Atlantic interannual variability. *J. Clim.* **20**(1): 131–142, doi: 10.1175/JCLI3992.1.
- Kim H-M, Webster PJ, Curry JA, Toma VE. 2012. Asian summer monsoon prediction in ECMWF System 4 and NCEP CFSv2 retrospective seasonal forecasts. *Clim. Dyn.* **39**(12): 2975–2991, doi: 10.1007/s00382-012-1470-5.
- Krishnamurthy V, Shukla J. 2000. Intraseasonal and interannual variability of rainfall over India. *J. Clim.* **13**(24): 4366–4377, doi: 10.1175/1520-0442(2000)013<0001:IAIVOR>2.0.CO;2.
- Krishnan R, Ramesh KV, Samala BK, Meyers G, Slingo JM, Fennesy MJ. 2006. Indian Ocean–monsoon coupled interactions and impending monsoon droughts. *Geophys. Res. Lett.* **33**: L08711, doi: 10.1029/2006GL025811.
- Kucharski F, Bracco A, Yoo JH, Molteni F. 2007. Low-frequency variability of the Indian monsoon–ENSO relationship and the tropical Atlantic: the “weakening” of the 1980s and 1990s. *J. Clim.* **20**(16): 4255–4266, doi: 10.1175/JCLI4254.1.
- Kucharski F, Bracco A, Yoo JH, Molteni F. 2008. Atlantic forced component of the Indian monsoon interannual variability. *Geophys. Res. Lett.* **35**(4): L04706, doi: 10.1029/2007GL033037.
- Kucharski F, Bracco A, Yoo JH, Tompkins AM, Feudale L, Rutigliano P. 2009. A Gill–Matsuno-type mechanism explains the tropical Atlantic influence on African and Indian monsoon rainfall. *Q. J. R. Meteorol. Soc.* **579**(April): 569–579, doi: 10.1002/qj.
- Kumar KK, Rajagopalan B, Cane MA. 1999. On the weakening relationship between the Indian monsoon and ENSO. *Science* **284**(5423): 2156–2159, doi: 10.1126/science.284.5423.2156.
- Latif M, Grötzner A. 2000. The equatorial Atlantic oscillation and its response to ENSO. *Clim. Dyn.* **16**(2–3): 213–218, doi: 10.1007/s003820050014.
- Lübbecke JF. 2013. Tropical Atlantic warm events. *Nat. Geosci.* **6**(1): 22–23, doi: 10.1038/ngeo1685.
- Lübbecke J, McPhaden M. 2012. On the inconsistent relationship between Pacific and Atlantic Niños. *J. Clim.* **25**: 4294–4303, doi: 10.1175/JCLI-D-11-00553.1.
- Lübbecke JF, Böning CW, Keenlyside NS, Xie S-P. 2010. On the connection between Benguela and equatorial Atlantic Niños and the role of the South Atlantic anticyclone. *J. Geophys. Res.* **115**(C9): C09015, doi: 10.1029/2009JC005964.
- Lübbecke JF, Burls NJ, Reason CJC, McPhaden MJ. 2014. Variability in the South Atlantic anticyclone and the Atlantic Niño Mode. *J. Clim.* **27**(21): 8135–8150, doi: 10.1175/JCLI-D-14-00202.1.
- McPhaden MJ, Nagura M. 2013. Indian Ocean dipole interpreted in terms of recharge oscillator theory. *Clim. Dyn.* **42**(5–6): 1569–1586, doi: 10.1007/s00382-013-1765-1.
- Monger B, McClain C, Murtugudde R. 1997. Seasonal phytoplankton dynamics in the eastern tropical Atlantic. *J. Geophys. Res.* **102**(C6): 12389, doi: 10.1029/96JC03982.
- Murtugudde R, McCreary JP, Busalacchi AJ. 2000. Oceanic processes associated with anomalous events in the Indian Ocean with relevance to 1997–1998. *J. Geophys. Res.* **105**(C2): 3295, doi: 10.1029/1999JC900294.
- Murtugudde RG, Ballabrera-Poy J, Beauchamp J, Busalacchi AJ. 2001. Relationship between zonal and meridional modes in the tropical Atlantic. *Geophys. Res. Lett.* **28**(23): 4463–4466, doi: 10.1029/2001GL013407.
- Nanjundiah R. 2009. *A Quick Look into Assessment of Forecasts for the Indian Summer Monsoon Rainfall in 2009*. Indian Institute of Science: Bangalore, India, 33 pp.
- Neelin JD, Battisti DS, Hirst AC, Jin F-F, Wakata Y, Yamagata T, Zebiak SE. 1998. ENSO theory. *J. Geophys. Res.* **103**(C7): 14261, doi: 10.1029/97JC03424.
- Okumura Y, Xie S-P. 2006. Some overlooked features of tropical Atlantic climate leading to a new Niño-like phenomenon. *J. Clim.* **19**(22): 5859–5874, doi: 10.1175/JCLI3928.1.
- Pai DS, Sridhar L, Rajeevan M, Sreejith OP, Satbhai NS, Mukhopadhyay B. 2014. Development of a new high spatial resolution (0.25° × 0.25°) long period (1901–2010) daily gridded rainfall data set over India and its comparison with existing data sets over the region. *Mausam* **65**(1): 1–18.
- Pant GB, Rupakumar K. 1997. *Climates of South Asia*. Wiley, 344 pp: Hoboken, NJ. ISBN: 9780471949480.
- Parthasarathy B, Munot AA, Kothawale DR. 1994. All-India monthly and seasonal rainfall series: 1871–1993. *Theor. Appl. Climatol.* **224**(49): 217–224.
- Philander SGH, Holton J, Dmowska R. 1989. *El Niño, La Niña, and the Southern Oscillation*, 1st edn. Philander S, Holton J, Dmowska R (eds). Elsevier and Academic Press, 293 pp: Waltham, MA. ISBN: 9780125532358.
- Pottapinjara V, Girishkumar MS, Ravichandran M, Murtugudde R. 2014. Influence of the Atlantic zonal mode on monsoon depressions in the Bay of Bengal during boreal summer. *J. Geophys. Res. Atmos.* **119**(11): 6456–6469, doi: 10.1002/2014JD021494.
- Rajeevan M, McPhaden MJ. 2004. Tropical Pacific upper ocean heat content variations and Indian summer monsoon rainfall. *Geophys. Res. Lett.* **31**(18): L18203, doi: 10.1029/2004GL020631.
- Rajeevan M, Nanjundiah RS. 2009. Coupled model simulations of twentieth century climate of the Indian summer monsoon. In *Current Trends in Science: Platinum Jubilee Special*, Mukunda N (ed). Indian Academy of Sciences: Bangalore, India, 537–567.
- Rayner NA, Parker DE, Horton EB, Folland CK, Alexander LV, Rowell DP, Kent EC, Kaplan A. 2003. Global analyses of sea surface temperature, sea ice, and night marine air temperature since the late nineteenth century. *J. Geophys. Res.* **108**(D14): 4407, doi: 10.1029/2002JD002670.
- Richter I, Xie S-P, Behera SK, Doi T, Masumoto Y. 2012. Equatorial Atlantic variability and its relation to mean state biases in CMIP5. *Clim. Dyn.* **42**(1–2): 171–188, doi: 10.1007/s00382-012-1624-5.
- Saji NH, Goswami BN, Vinayachandran PN, Yamagata T. 1999. A dipole mode in the tropical Indian Ocean. *Nature* **401**(6751): 360–363, doi: 10.1038/43854.
- Servain J, Wainer I, McCreary JP, Dessier A. 1999. Relationship between the equatorial and meridional modes of climatic variability in the tropical Atlantic. *Geophys. Res. Lett.* **26**(4): 485–488, doi: 10.1029/1999GL900014.

- Tziperman E, Stone L, Cane MA, Jarosh H. 1994. El nino chaos: overlapping of resonances between the seasonal cycle and the Pacific Ocean-atmosphere oscillator. *Science* **264**(5155): 72–74, doi: 10.1126/science.264.5155.72.
- Varikoden H, Preethi B. 2013. Wet and dry years of Indian summer monsoon and its relation with Indo-Pacific sea surface temperatures. *Int. J. Climatol.* **33**(7): 1761–1771, doi: 10.1002/joc.3547.
- Vecchi G, Harrison D. 2004. Interannual Indian rainfall variability and Indian Ocean sea surface temperature anomalies. In *Earth's Climate: The Ocean-Atmosphere Interaction*, Wang C, Xie SP, Carton JA (eds). American Geophysical Union: Washington, DC, doi: 10.1029/147GM14.
- Wang C, Picaut J. 2004. Understanding ENSO physics – a review. In *Earth's Climate: The Ocean-Atmosphere Interaction*, Wang C, Xie S-P, Carton JA (eds). American Geophysical Union: Washington, DC, doi: 10.1029/GM147.
- Wang C, Kucharski F, Barimalala R, Bracco A. 2009. Teleconnections of the tropical Atlantic to the tropical Indian and Pacific Oceans: a review of recent findings. *Meteorol. Z.* **18**(4): 445–454, doi: 10.1127/0941-2948/2009/0394.
- Webster PJ, Hoyos CD. 2010. Beyond the spring barrier? *Nat. Geosci.* **3**(3): 152–153, doi: 10.1038/ngeo800.
- Webster PJ, Yang S. 1992. Monsoon and ENSO: selectively interactive systems. *Q. J. R. Meteorol. Soc.* **118**(507): 877–926, doi: 10.1002/qj.49711850705.
- Webster P, Magana V, Palmer T, Shukla J, Tomas R, Yanai Y, Yasunari T. 1998. Monsoons: processes, predictability, and the prospects for prediction. *J. Geophys. Res.* **103**(C7): 14451–14510, doi: 10.1029/97JC02719.
- Webster PJ, Moore AM, Loschnigg JP, Leben RR. 1999. Coupled ocean-atmosphere dynamics in the Indian Ocean during 1997–98. *Nature* **401**(6751): 356–360, doi: 10.1038/43848.
- Xie S-P, Carton JA. 2004. Tropical Atlantic variability: patterns, mechanisms, and impacts. In *Earth's Climate: The Ocean-Atmosphere Interaction*, Wang C, Xie SP, Carton JA (eds). American Geophysical Union: Washington, DC, doi: 10.1029/147GM07.
- Zebiak SE. 1993. Air-sea interaction in the equatorial Atlantic region. *J. Clim.* **6**(8): 1567–1586, doi: 10.1175/1520-0442(1993)006<1567:AIITEA>2.0.CO;2.
- Zhao Y, Nigam S. 2015. The Indian Ocean dipole: a monopole in SST. *J. Clim.* **28**(1): 3–20, doi: 10.1175/JCLI-D-14-00047.1.

On the Relation between the Boreal Spring Position of the Atlantic Intertropical Convergence Zone and Atlantic Zonal Mode[Ⓞ]

VIJAY POTTAPINJARA^a AND M. S. GIRISHKUMAR

Indian National Centre for Ocean Information Services, Hyderabad, India

R. MURTUGUDDE

Earth System Science Interdisciplinary Centre, University of Maryland, College Park, College Park, Maryland

K. ASHOK

Centre for Earth, Ocean and Atmospheric Sciences, University of Hyderabad, Hyderabad, India

M. RAVICHANDRAN

Indian National Centre for Ocean Information Services, Hyderabad, and National Centre for Polar and Ocean Research, Goa, India

(Manuscript received 19 September 2018, in final form 4 April 2019)

ABSTRACT

Previous studies have talked about the existence of a relation between the Atlantic meridional mode (AMM) and Atlantic zonal mode (AZM) via the meridional displacement of the intertropical convergence zone (ITCZ) in the Atlantic during boreal spring and the resulting cross-equatorial zonal winds. However, why the strong relation between the ITCZ (or AMM) and zonal winds does not translate into a strong relation between the ITCZ and AZM has not been explained. This question is addressed here, and it is found that there is a skewness in the relation between ITCZ and AZM: while a northward migration of ITCZ during spring in general leads to a cold AZM event in the ensuing summer, the southward migration of the ITCZ is less likely to lead to a warm event. This is contrary to what the previous studies imply. The skewness is attributed to the Atlantic seasonal cycle and to the strong seasonality of the AZM. All those cold AZM events preceded by a northward ITCZ movement during spring are found to strictly adhere to typical timings and evolution of the different Bjerknes feedback components involved. It is also observed that the causative mechanisms of warm events are more diverse than those of the cold events. These results can be expected to enhance our understanding of the AZM as well as that of chronic model biases and contribute to the predictability of the Indian summer monsoon through the links between the two as shown in our earlier studies.

1. Introduction

It is well known that the interannual variability of the Indian summer monsoon rainfall (ISMR) is governed

[Ⓞ] Supplemental information related to this paper is available at the Journals Online website: <https://doi.org/10.1175/JCLI-D-18-0614.s1>.

^a Additional affiliation: Centre for Earth, Ocean and Atmospheric Sciences, University of Hyderabad, Hyderabad, India.

Corresponding author: Vijay Pottapinjara, vijay.p@incois.gov.in

by both internal dynamics and external factors such as El Niño–Southern Oscillation (ENSO) (Sikka 1980; Keshavamurty 1982; Mooley and Parthasarathy 1984; Philander et al. 1989; Webster et al. 1998) and the Indian Ocean dipole (IOD)/zonal mode (IODZM; Behera et al. 1999; Ashok et al. 2001; Slingo and Annamalai 2000), the dominant interannual modes in the tropical climate. The Atlantic zonal mode (AZM), akin to but weaker than ENSO (Zebiak 1993), is active during boreal summer (June–August) and contemporaneous with the Indian summer monsoon (ISM). It has been shown to influence the ISMR by recent studies (Kucharski et al. 2008, 2009; Wang et al. 2009; Pottapinjara et al. 2014;

DOI: 10.1175/JCLI-D-18-0614.1

© 2019 American Meteorological Society. For information regarding reuse of this content and general copyright information, consult the AMS Copyright Policy (www.ametsoc.org/PUBSReuseLicenses).

Richter et al. 2014; Pottapinjara et al. 2016; Kucharski et al. 2016; Yadav 2017). The warm (cold) phase of AZM tends to reduce (enhance) rainfall over India with its effect being especially significant when there is no co-occurring ENSO event (Wang et al. 2009; Pottapinjara et al. 2014). On the other hand, the AZM can sow the seeds for the development of an ENSO event (Rodríguez-Fonseca et al. 2009; Ham et al. 2013; Martin et al. 2014; Kucharski et al. 2016). Therefore, an enhanced understanding of different causative mechanisms of AZM will aid in better prediction of the ISM as well as a better understanding of ENSO dynamics, among other things.

In addition to the AZM, the interannual variability in the tropical Atlantic is dominated by the Atlantic meridional mode (AMM; Nobre and Shukla 1996; Chiang and Vimont 2004; Xie and Carton 2004). AMM, another interannual mode in the tropical Atlantic, is active during boreal spring. It is characterized by SST anomalies of opposite sign on either side of the equator (see data and methods section for the definition). The two modes, AMM (active in boreal spring) and AZM (active in boreal summer), are related via the meridional displacement of the intertropical convergence zone (ITCZ) in boreal spring (Servain et al. 1999; Murtugudde et al. 2001). These early studies indicate that the anomalous meridional movement of ITCZ during spring is an important precursor to the AZM. Chiang et al. (2002) attribute the variability of the ITCZ position in the Atlantic to two factors, namely, the cross-equatorial SST gradient (or AMM) and the remote forcing from the equatorial Pacific through ENSO. The AMM is likely not a completely independent mode. SSTs in the tropical North Atlantic (TNA), the northern lobe of AMM, can be influenced by the North Atlantic Oscillation (e.g., Czaja et al. 2002; Yang et al. 2018) and ENSO (e.g., Huang 2004; Amaya and Foltz 2014). The TNA SST warming occurs a season after the mature phase of ENSO warm events (Enfield and Mayer 1997; Giannini et al. 2000; Yang et al. 2018). The role of AMM in the meridional movement of the ITCZ during spring has already been discussed in previous studies (Servain et al. 1999; Murtugudde et al. 2001). Apart from reiterating the importance of AMM, Chiang et al. (2002) suggest that ENSO can also modulate the meridional position of the ITCZ during spring in the Atlantic through Walker circulation. An El Niño peaking in boreal winter suppresses convection over equatorial Atlantic in the following spring via the descending branch of anomalous Walker circulation. Without presenting the details, they note that as a secondary effect of the suppression of rainfall over the equatorial Atlantic, the ITCZ moves north. Lee et al. (2008) stress the importance of

persistence of the tropical Pacific forcing into boreal spring in determining TNA SST and thus the ITCZ movement. García-Serrano et al. (2017) suggest that ENSO influences TNA SST through a remote secondary Gill-type mechanism. In this mechanism, for example, a decaying El Niño that persists into boreal spring can suppress the convection over the deep tropical Atlantic and generate two upper-level cyclonic circulations as though a heat sink is located over the same region. So, the Atlantic ITCZ during spring can be affected directly (without much time lag) by AMM and directly via convective processes by a decaying ENSO (Neelin and Su 2005), or indirectly (with a time lag of few months) via TNA variability (Czaja et al. 2002; Czaja and Frankignoul 2002; Yang et al. 2018; Wu and Liu 2002).

As mentioned earlier, the meridional movement of the Atlantic ITCZ during spring is an important precursor to the AZM. The relation between the two concisely is that the spring ITCZ migration, through the resulting spring zonal wind anomalies over the equator, triggers the Bjerknes feedback and leads to an AZM event in the following summer. Bjerknes feedback involves western equatorial Atlantic zonal wind anomalies forcing thermocline depth variations in the eastern equatorial Atlantic, which then influence the SST anomalies in the east, which in turn positively feedback to the wind anomalies (Keenlyside and Latif 2007). The correlation between the ITCZ position during spring and concurrent western equatorial Atlantic zonal winds is -0.82 , significant at the 5% level (see Table 1 and data and methods section for details). Given the apparent criticality of the spring western equatorial Atlantic zonal winds in the formation of an AZM event, it may appear that the relation between the spring ITCZ and AZM is quite robust. However, the correlation between the spring ITCZ and Atlantic 3 (ATL3) SST index (see data and methods section for definition) that characterizes the AZM reduces to a moderate -0.34 , still significant at the 5% level but just above the threshold of significance (Table 1). This raises an interesting set of questions: What causes the drop in correlations? Is there a limiting factor in the Bjerknes feedback chain that may explain the drop? Does the relation hold equally well for both cold and warm AZM events? In other words, is the ITCZ–AZM relation symmetric? The question of symmetry is motivated by a result from ENSO diversity studies that highlight that there is more diversity in the warm events in the tropical Pacific (El Niño), and differences between the cold events (La Niña) are subtle (Kug and Ham 2011; Ren and Jin 2011; Capotondi et al. 2015; Chen et al. 2015; Ashok et al. 2017; Timmermann et al. 2018). A few recent reports make a passing mention of this knowledge gap, as discussed below.

TABLE 1. Correlations between different parameters averaged over different months (MAM: March–May; AMJ: April–June; MJJ: May–July; JJA: June–August). AMM: Atlantic meridional mode; AZM: Atlantic zonal mode; zonal wind: central to western equatorial Atlantic zonal winds; EEA HC: eastern equatorial Atlantic heat content; WEA HC: western equatorial Atlantic heat content; ITCZ: intertropical convergence zone. See text (section 3a) and Fig. 2 for the regions over which different parameters are averaged.

	Correlation coefficient		Correlation coefficient
MAM AMM vs MAM ITCZ	0.81	MAM AMM vs JJA ATL3	−0.31
MAM ITCZ vs MAM zonal wind	−0.82	MAM ITCZ vs JJA ATL3	−0.34
MAM zonal wind vs AMJ EEA HC	0.65	MAM zonal wind vs JJA ATL3	0.54
AMJ EEA HC vs MJJ WEA HC	−0.69	AMJ EEAHC vs JJA ATL3	0.50
		MJJ WEAHC vs JJA ATL3	−0.43

Notably, extending the earlier studies (Servain et al. 1999; Murtugudde et al. 2001), a recent study by Foltz and McPhaden (2010) shows that the equatorial zonal winds caused by positive AMM (anomalously warm north and/or cold south), force off-equatorial oceanic Rossby waves that are reflected as downwelling Kelvin waves from the western equatorial Atlantic opposite in sign to the directly forced Kelvin waves. The reflected downwelling Kelvin waves in turn terminate the AZM warm event toward the end of summer. The conclusion of Foltz and McPhaden (2010) that AMM and AZM are related is from a correlation analysis that is insensitive to the asymmetry, if any, in the relation. With regard to differences between cold and warm AZM events during their lifetime, Lübbecke and McPhaden (2017) show, based on a composite analysis, that the Bjerknes feedback components for the cold events are mirror images of those of warm events, that is, AZM is essentially symmetric. However, Lübbecke and McPhaden (2017) do not rule out the possibility of existence of an asymmetry in forcing of cold and warm events. While the former study did not raise the existence of any asymmetry between the ITCZ (or AMM) and AZM, the latter did not rule out such a possibility. Putting these in context, almost all of these previous studies imply that the anomalous northward (southward) shift of the ITCZ in spring can lead to a cold (warm) AZM event, which implicitly implies a symmetric relation between the ITCZ in spring and AZM. Hence, despite the above-mentioned studies, the questions we raised remain unanswered to the best of our knowledge and we attempt to address them in this study. These answers should contribute to the predictability of the monsoon (ISM), especially during non-ENSO AZM years by improving our understanding of the AZM that is shown to influence the ISM (Pottapinjara et al. 2014, 2016).

Pottapinjara et al. (2016) show that from the early signs in the zonal wind and heat content in the equatorial Atlantic in boreal spring, an oncoming AZM event may be foretold that might in turn give us clues about the ISMR one season in advance. However, the causative mechanisms that trigger wind anomaly in the equatorial

Atlantic that is a necessary factor for the development of AZM are not yet fully understood. Understanding different causative mechanisms of AZM events may contribute to the predictability of the ISMR by providing any signals that stretch further back in time giving an advanced warning of a forthcoming AZM event and thus of the impact on ISMR. It may also contribute to the knowledge of different biases that can arise in the coupled models especially those that are used to forecast the monsoon and thereby provide process understanding for the improvement of such models.

2. Data and methods

The Hadley Centre Sea Ice and Sea Surface Temperature dataset (HadISST; Rayner et al. 2003) is used in this study. The AZM is characterized by the ATL3 index that is the average of SST anomalies over ATL3 region (3°S–3°N and 20°–0°W). A warm (cold) AZM is considered to occur in any year when the June–August average of ATL3 index exceeds (falls below) +1 (−1) standard deviation (Zebiak 1993; Burls et al. 2012). Following this definition, during the study period (1979–2013), we identify nine warm AZM events that occurred in 1984, 1987, 1988, 1995, 1996, 1998, 1999, 2008, and 2010 and six cold AZM events in years 1982, 1983, 1992, 1994, 1997, and 2005. This list is consistent with our earlier studies (Pottapinjara et al. 2014, 2016). Further, following Foltz and McPhaden (2010), AMM is defined as the difference between SST anomalies averaged over the northern (5°–28°N and 60°–20°W) and southern (20°S–5°N and 30°W–10°E) tropical Atlantic.

In this study, we focus on the ITCZ movement rather than on AMM as the ITCZ captures different remote influences in addition to that of AMM and its relation to the AZM. The meridional movement of ITCZ is tracked using the latitude of the zero meridional surface wind speed along the longitude of 28°W in the latitudinal range of 5°S–20°N (Servain et al. 1999). The wind data used are taken from the European Centre for Medium Range Weather Forecasts (ECMWF) interim reanalysis (ERA-Interim) (Dee et al. 2011). The fact that the

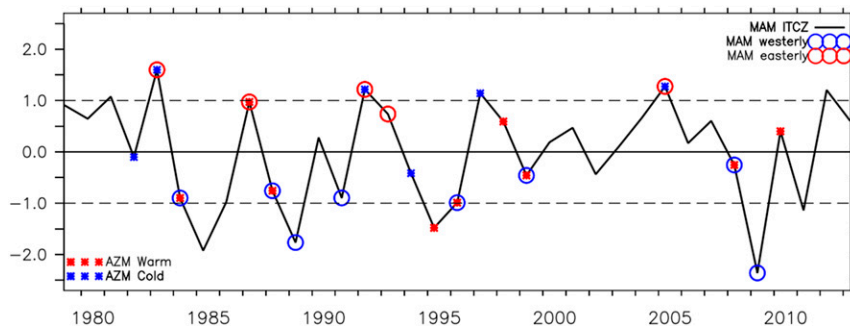


FIG. 1. Interannual variations of anomalous meridional position of ITCZ in March–May (black). The time series is normalized by its standard deviation and ± 1 standard deviation is indicated by a black dashed line. Whenever the central to western equatorial zonal wind in March–May is sufficiently strong crossing $+0.9$ (-0.9) of its respective standard deviation, i.e., westerly (easterly), it is indicated by blue (red) circles. Whenever the ATL3 SST in June–August crosses $+1$ (-1) of its respective standard deviation, i.e., when there is a warm (cold) AZM event, it is indicated by red (blue) stars.

correlation between ATL3 index and March–May (MAM) ITCZ (-0.34) is marginally higher than that with AMM (-0.31), and the correlation between MAM zonal wind and MAM ITCZ (-0.82) is also larger than that with zonal wind and AMM (-0.73), support our choice to focus on ITCZ instead of AMM (Table 1) to address the questions we have raised earlier. In addition, these significant correlations suggest that understanding the ITCZ movement will give a fresher and potentially a different perspective on the asymmetry in its relation with AZM. The upper-ocean heat content (per unit area) above the 20°C isotherm is calculated using ocean temperature data from the EN4 analysis of the Met Office Hadley Centre (Good et al. 2013). Different Bjerknes feedback components are computed and normalized by their respective standard deviations. A two-tailed Student's t test is used to determine the statistical significance of the correlation coefficients. In the following, all the seasons used are from the perspective of the Northern Hemisphere, unless mentioned otherwise.

3. Results

As mentioned in the introduction, studies such as Servain et al. (1999), Murtugudde et al. (2001), and Foltz and McPhaden (2010) demonstrate the existence of a relationship between the ITCZ (or AMM) and AZM. Indeed, Table 1 shows that during the study period, the correlation between the spring ITCZ position and spring zonal winds is -0.82 , but the correlation between ITCZ and June–August (JJA) ATL3 index is -0.34 (0.33 is the threshold correlation at the 5% significance level for a sample size of 35). The reduction in correlation implies that not all the meridional excursions of the spring ITCZ lead to AZM events in the following summer despite the

variations in the position of ITCZ strongly affecting the spring equatorial zonal winds, a prerequisite for an AZM event.

a. Skewness in the relation between the Atlantic spring ITCZ position and AZM

To see how many meridional excursions of ITCZ ultimately lead to the AZM events, the interannual variations of spring ITCZ position along with the indicator of the AZM occurrence (listed in the data and methods section) are plotted in Fig. 1. Whenever the spring ITCZ position exceeds its $+1$ (-1) standard deviation, the ITCZ is considered to be located anomalously north (south) from its mean position. From the figure, it can be seen that the ITCZ in spring is anomalously north in six years (1981, 1983, 1992, 1997, 2005, and 2012) and in four of these years (1983, 1992, 1997, and 2005), the AZM cold events occurred in the following summer. On the other hand, while the ITCZ is anomalously south in six years (1985, 1986, 1989, 1995, 2009, and 2011), an AZM warm event occurred in the subsequent summer in only one of these years (1995). It is worth mentioning that two AZM warm events that occurred in 1984 and 1996 have a spring ITCZ position just short of the threshold of anomalous southward position, that is, -1 standard deviation. The ratio of AZM cold (warm) events that are preceded by anomalous northward (southward) ITCZ in spring is 4:6 (1:9), that is, 66% (11%). Even if we include the two just-below-the-threshold warm events of 1984 and 1996, the ratio of warm AZM events preceded by southward migration of ITCZ in spring is 3:9 (33%), which is still significantly less than its counterpart for the cold AZM. Therefore, while an anomalous northward ITCZ in spring tends to give rise to an AZM cold event in the following summer, an anomalous southward

position of the same is less likely to lead to an AZM warm event. Clearly, there is a skewness in the relation between the position of ITCZ in spring and AZM in the ensuing summer, an important result that has not been reported thus far.

Since the relation between ITCZ and AZM is skewed toward the cold events, to understand different processes involved when the northward displacement of ITCZ in spring leads to an AZM cold event in the following summer, we show the monthly evolution of composite anomalies of different fields in Fig. 2. A positive AMM type of SST configuration (relatively warm in the north and/or cold in the south) during February–May moves the ITCZ anomalously north in spring (MAM). The resultant cross-equatorial winds strengthen the concurrent southeast trades and weaken the northeast trades around the equator in spring. The net result is an enhancement in the strength of easterlies over the equatorial band, a prerequisite for the development of a cold AZM event. The strengthened equatorial easterlies, in turn, result in the increased heat content in the western equatorial Atlantic by deepening the thermocline. An upwelling Kelvin wave propagates to the east to shoal the thermocline and leads to cooler SSTs in the following summer, thus leading to a cold AZM event. As already mentioned in the introduction, the AMM is not the only factor influencing the spring Atlantic ITCZ position but the other factors are not discussed here in Fig. 2 for the sake of simplicity.

It is interesting to inquire as to what gives rise to the skewness in the relation between the position of the ITCZ in spring and AZM. We pose a question as to whether the skewness can be explained by the findings of Richter et al. (2014). Taking monthly means of ITCZ position and equatorial zonal winds, and compositing the winds over each unique ITCZ position during the entire study period, Richter et al. (2014) show that as the ITCZ moves from its southernmost to its northernmost position, equatorial zonal winds remain easterly and grow stronger almost linearly. Given that anomalous equatorial easterlies in spring are a precondition to a cold AZM, if a relation between anomalous spring ITCZ and contemporaneous anomalous equatorial zonal winds holds as presented in Richter et al. (2014); that is, if any anomalous meridional movement of spring ITCZ produces concurrent anomalous equatorial easterlies, it would explain the skewness between spring ITCZ and AZM. But does such a relation exist in reality? The high negative and significant correlation in spring between the ITCZ and central to western equatorial Atlantic zonal winds of -0.82 (Table 1) tells us that the anomalous northward migration of ITCZ in spring is indeed associated with anomalous easterly

winds over the central to western equatorial Atlantic. However, a southward migration of the ITCZ in spring is associated with westerly anomalies. A scatterplot between these two quantities (Fig. S1 in the online supplemental material) underscores the same. Therefore, considering the importance of spring wind anomalies for AZMs, the reason for the skewness must lie elsewhere and the interaction of the seasonal cycle and the interannual anomalies may be crucial. The supposed contradiction between the result of Richter et al. (2014) and ours is discussed later in the discussion and conclusions section. The seemingly counterintuitive westerlies associated with the anomalous southward movement of ITCZ in spring can be explained by a careful observation of a spatial map of wind anomalies in the equatorial Atlantic in individual years (figures not shown). In almost all the years when the ITCZ is anomalously south in spring, wind anomalies that are northerly or northeasterly just north of the equator turn and develop a westerly component as they cross the equator. The westerly component just south of the equator is stronger than the easterly component just north of the equator, giving rise to net westerly winds upon averaging in the equatorial band. The mechanisms for these westerly anomalies need further investigation and are beyond the scope of the current study.

The reason for the skewness in fact lies in the peculiar features of climatological movement of the ITCZ in the Atlantic (Fig. 3). From the figure, it may be noted that during January–April the mean position of the ITCZ is relatively close to the equator and the variability of the position of ITCZ is at its highest. The drastic change both in the mean position and the variability occurs during May–June, with the position of the mean ITCZ moving north by about 6° and the standard deviation falling to about $1/3$ of that in April (standard deviation is 1.743° and 0.576° latitude in April and June, respectively). During the study period, that is, 1979–2013, the position of ITCZ in spring is anomalously southward in 6 years and in four of those years, winds that are northerly or northeasterly just north of equator develop a strong westerly component upon crossing the equator in spring, as noted above. The maximum of this wind anomaly is centered around 7°S with weaker westerlies over the western equatorial Atlantic (WEA) compared to easterlies in spring in the same region when the ITCZ is anomalously north. The westerlies can drive an equatorial downwelling Kelvin wave and remotely deepen the thermocline in the east, if they are sufficiently strong. Nonetheless, the westerlies weaken further in May–June as the climatological ITCZ moves into the Northern Hemisphere and the inherent variability of the ITCZ itself reduces as shown in Fig. 3. This leads to a

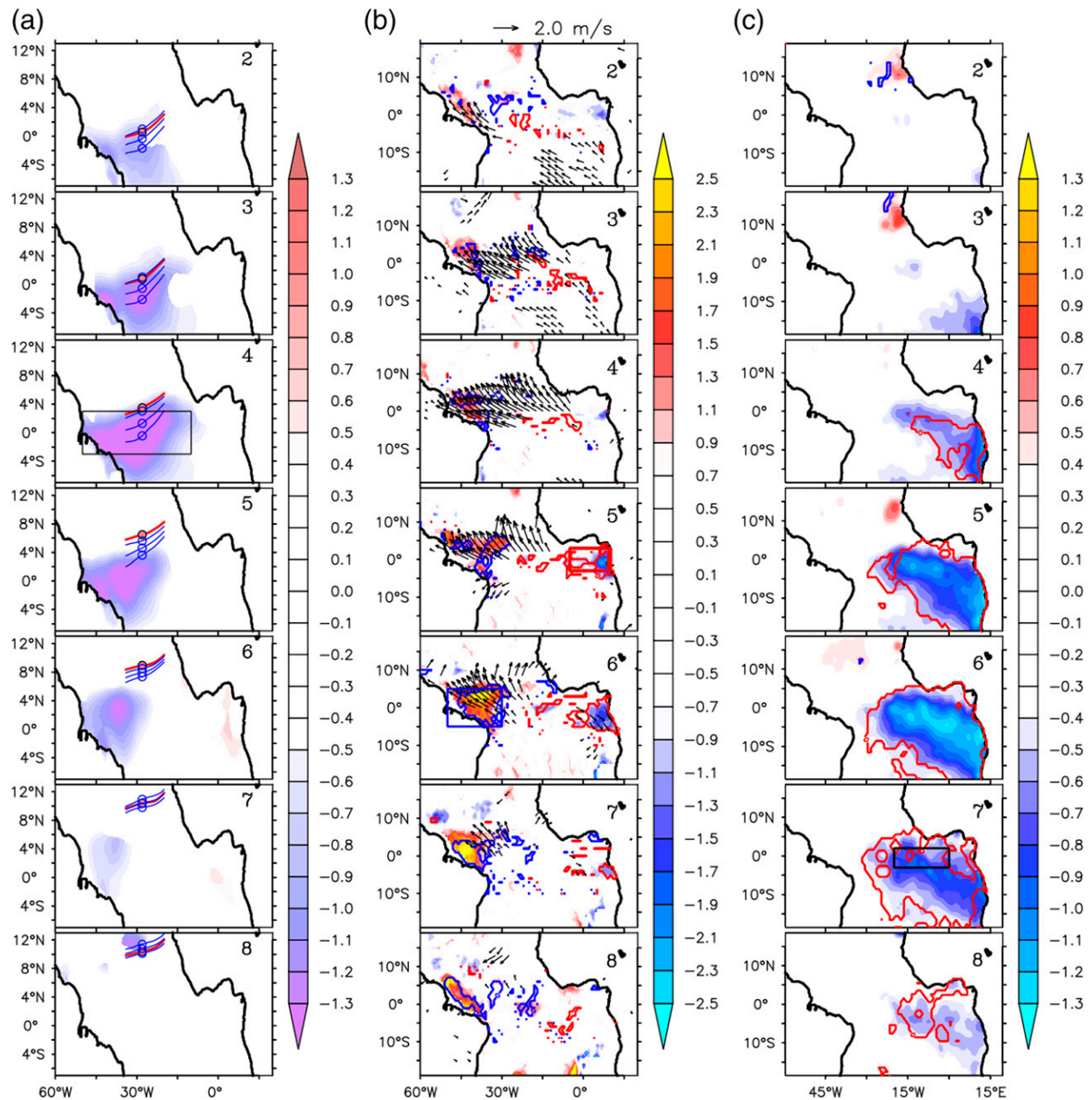


FIG. 2. Monthly (February–August) evolution of composites of (a) ITCZ position (lines) and zonal wind anomalies (shading; m s^{-1}); (b) anomalies of winds (vectors) and heat content (shading; 10^{10} J m^{-2}); and (c) SST anomalies (shading; $^{\circ}\text{C}$) when the spring Atlantic ITCZ is anomalously northward and gives rise to a cold AZM event. In (a), the red line (dot inside a black circle) indicates the ITCZ position at respective longitudes (along 28°W) whereas the blue lines (circle) indicate the envelope of ITCZ variability, i.e., the middle blue line (circle) indicates the climatological ITCZ position in that month, and the top and bottom blue lines (circles) indicate ± 1 standard deviation of the position from the mean in the same month. The number of calendar month is indicated in each subpanel. Only those zonal winds in (a) and vectors in (b) that are significant at the 5% level are shown. The significance of heat content anomalies in (b) and SST anomalies in (c) are indicated by line contours. The rectangular boxes in black [in (a); April], red [in (b); May], blue [in (b); June], and thick black [in (c); July] indicate the regions over which anomalies of winds, eastern equatorial Atlantic heat content, western equatorial Atlantic heat content, and SST are averaged, respectively, for use in other analyses.

premature death of a weak incipient warm event resulting ultimately in a very low proportion of AZM warm events surviving into the summer. Figure 4 shows that in the years when spring ITCZ position is anomalously south

and winds are westerly over the WEA, the westerlies are not as strong and are less persistent in contrast to those years when the position of ITCZ in spring is anomalously north and winds over WEA are easterly.

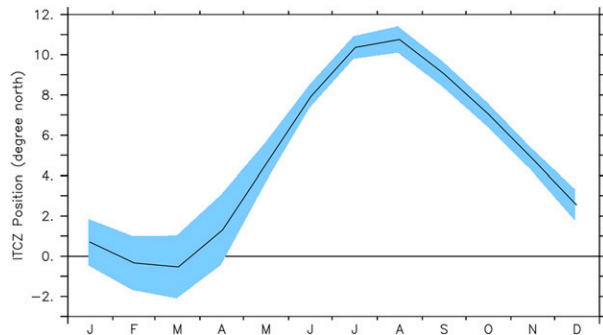


FIG. 3. Monthly evolution of the mean position of the ITCZ in the Atlantic (black line; along 28°W; °N) with the shading indicating the ± 1 standard deviation about the mean in the respective months.

In light of the above explanation, a reconsideration of why an anomalous northward movement of ITCZ in spring is highly likely to lead to a cold AZM event is necessary. The fact that the mean position of the ITCZ in February–March is south of the equator implies that even when the ITCZ is anomalously north, the center of maximum easterly wind anomalies is closer to the equator and thus the magnitude of the easterlies over the WEA is stronger than that of the westerly wind anomalies associated with anomalous southward position of the ITCZ (Fig. 4). The strong

spring easterlies shoal the thermocline in the east, preparing the ground for an oncoming AZM cold event but weaken in early summer as the mean ITCZ itself moves farther north. Nevertheless, the easterlies persist albeit restricted to an area to the west of 30°W, helping the cold event survive into the summer. In a nutshell, the skewness in the relation between the position of Atlantic ITCZ in spring and AZM is inherent in the seasonal cycle itself.

From earlier studies (Murtugudde et al. 2001; Pottapinjara et al. 2016; Lübbecke and McPhaden 2017), and our analysis presented in Fig. 2 and Table S1, we identify different factors involved in the mechanism where the anomalous spring migration of ITCZ leads to an AZM in the following summer to be (i) the position of ITCZ in spring (MAM ITCZ), (ii) the concurrent zonal winds averaged over the central to western equatorial Atlantic (3°S–3°N and 50°–10°W), (iii) heat content (HC) averaged over the eastern equatorial Atlantic (EEA) in midspring to early summer [April–June (AMJ) EEA HC; 3°S–3°N and 5°W–15°E], (iv) heat content averaged over the western equatorial Atlantic in late spring to midsummer [May–July (MJJ) WEA HC; 5°S–5°N and 50°–30°W], and (v) SST averaged over the ATL3 region in summer (JJA ATL3; 3°S–2°N and 20°–0°W). Monthly evolutions of composites of these different factors

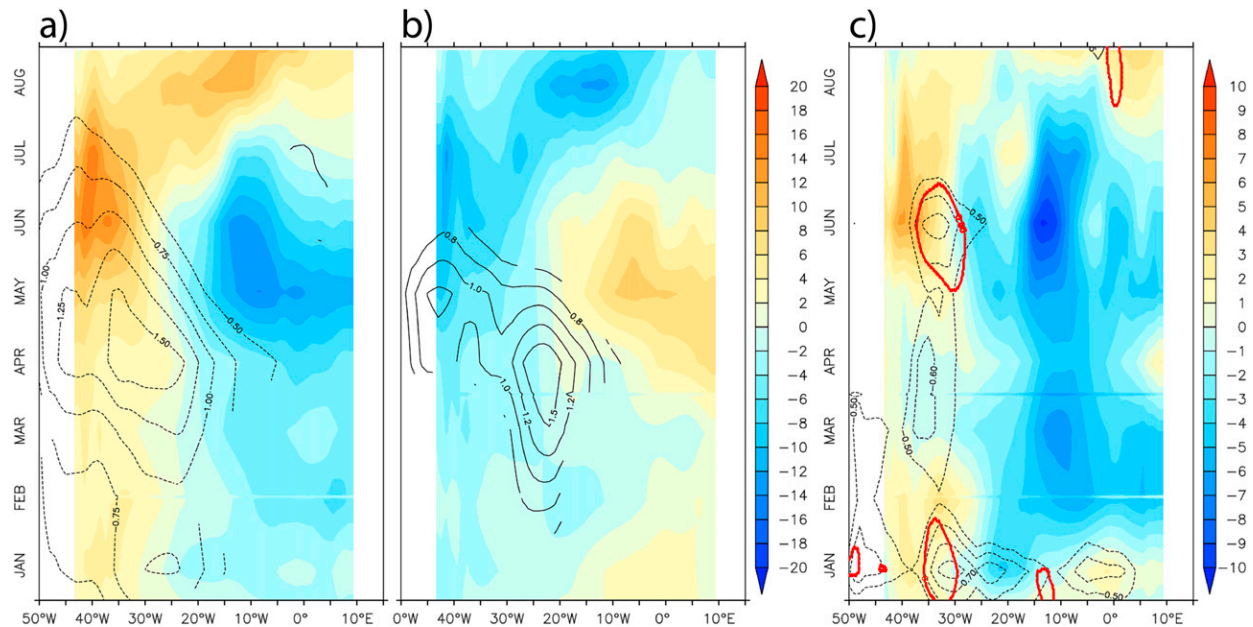


FIG. 4. (a),(b) Hovmöller diagram of the composite of anomalies of thermocline depth (shading) overlaid by zonal winds (contours) over the equator in the Atlantic when the MAM ITCZ is anomalously north (south) and zonal wind anomalies over WEA are easterly (westerly). (c) Hovmöller diagram obtained by adding the anomalies shown in (a) and (b) [= anomalies in (a) – negative of anomalies in (b)], intended to show the dominance of the anomalies in (a) over that in (b). In (a) and (b), only the wind anomalies that are significant at the 5% level are shown. In (c), the significant wind anomalies are indicated by the contour lines in red. Significance contour lines become discontinuous if the zonal winds between the two ends of a contour are not significant.

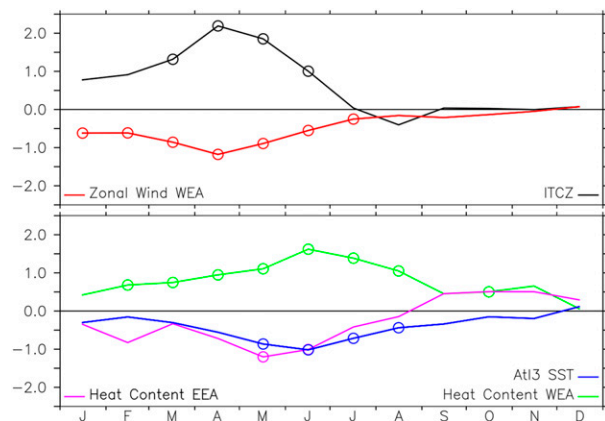


FIG. 5. Monthly evolution of composites of anomalies of (top) zonal winds (m s^{-1}) in the western equatorial Atlantic and position of ITCZ ($^{\circ}$ latitude) and (bottom) SST averaged over ATL3 region ($^{\circ}\text{C}$) and heat content (10^{10} J m^{-2}) averaged in the western equatorial Atlantic and eastern equatorial Atlantic, composited in the years when the MAM ITCZ is north and leads to the development of a cold AZM event in the subsequent summer. The circles on each line indicate when the respective composite means become significant at the 5% level.

averaged in their respective regions are presented in Fig. 5 to identify any distinct signatures associated with the cold AZM events that are preceded by northward spring ITCZ. From the figure, it can be seen that the maximum northward displacement of the ITCZ occurs during MAM with the central to western equatorial easterlies peaking simultaneously. The heat content in the eastern equatorial Atlantic reaches its minimum during AMJ while the heat content in the western equatorial Atlantic attains its maximum during MJJ. The SST anomalies in the ATL3 region are at their coldest during JJA. The timings of these different factors agree with the previous studies (Keenlyside and Latif 2007; Pottapinjara et al. 2016) and also yield the highest correlations with the links above and below in the chain of processes (Table S1). These seasonal timings of when different factors become important will be used later to show the distinction of the cold AZM events preceded by northward ITCZ in spring. For the sake of completeness, the counterpart of Fig. 2, that is, the evolution of monthly composites of different fields of all those AZM events that were preceded by an anomalously south ITCZ in spring is shown in Fig. S2.

b. Meridional movement of ITCZ in spring explains strong canonical AZM events

The Bjerknes feedback is a dominant mechanism that explains AZMs (Keenlyside and Latif 2007) although there are several other mechanisms contributing (Foltz

and McPhaden 2010; Zhu et al. 2012; Lübbecke 2013; Lübbecke et al. 2018; Richter et al. 2013). Richter et al. (2013) classify AZM events into those that can and cannot be explained by ENSO-like dynamics. The distinctive criterion that Richter et al. (2013) adopt for the classification is that if a warm (cold) AZM event in summer is preceded by westerly (easterly) winds in the central to western equatorial Atlantic in spring, then it is referred to as a canonical warm (cold) event. On the other hand, if it is preceded by winds of opposite sign, it is called a noncanonical event. It is worth noting that oceanic subsurface changes, which are an important part of the Bjerknes feedback, are not taken into account in this classification. Also, those events that have near neutral winds cannot be covered by their classification. Modifying their definition to account for the above events as well, we classify a “strong canonical” warm (cold) event to be one that is preceded by westerly winds in March–May, positive (negative) heat content in the eastern equatorial Atlantic in April–June and negative (positive) heat content in the western equatorial Atlantic in May–July. All those events that do not meet this criterion are classified as “non-strong-canonical” warm (cold) events. Note that the respective timings when different Bjerknes components become important are only for a typical AZM event (Keenlyside and Latif 2007). Interannual variations of these different factors are normalized by their respective standard deviations and plotted in Fig. 6. To categorize an AZM event as strong canonical, the amplitude of these factors (with the exception of winds) is required to exceed one respective standard deviation. This condition is relaxed in the case of winds as they tend to be noisy. The threshold of amplitude is lowered to 0.9 times their standard deviation. In addition, the relaxation accommodates several events for which the amplitude of winds falls short of the threshold imposed on all other factors, that is, one standard deviation.

Going by this definition, it can be seen from Fig. 6 that the strong canonical (non-strong-canonical) cold AZM events are 1983, 1992, 1997, and 2005 (1981 and 1994). For every strong canonical cold event, normalized factors clearly exceed one respective standard deviation along with the spring ITCZ position in Fig. 1. The strong canonical (non-strong-canonical) warm events are 1984, 1996, and 2008 (1987, 1988, 1995, 1998, 1999, and 2010). None of the strong canonical warm events have ITCZ in spring located farther southward than the threshold position although the ITCZ was appreciably southward in 1984 and 2008. The proportion of strong canonical cold (warm) AZM events is 4:6 (3:9), that is, 66% (33%). In other words, the proportion of strong canonical events is larger in case of cold events than that of warm events. It is interesting to note that all strong canonical

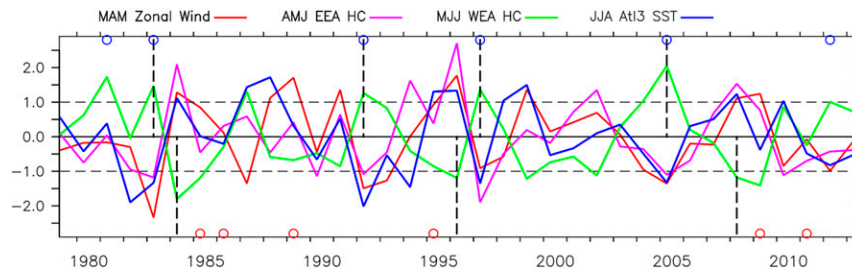


FIG. 6. Interannual variations of anomalies of western equatorial Atlantic zonal winds in March–May (red; m s^{-1}), eastern equatorial Atlantic heat content in April–June (purple; 10^{10} J m^{-2}), western equatorial Atlantic heat content in May–July (green; 10^{10} J m^{-2}) and SST in the characteristic ATL3 region in June–August (blue; $^{\circ}\text{C}$). Strong canonical cold (warm) events are indicated with black dashed line in upper (lower) portion. All the time series are normalized by their respective standard deviation. Whenever the spring ITCZ crosses +1 (−1) standard deviation, i.e., north (south), it is indicated with blue (red) thick circles.

cold AZM events are preceded by northward movement of ITCZ in spring whereas only two out of three strong canonical warm events are preceded by southward movement of ITCZ in spring. The proportion of strong canonical events, either warm or cold, that can be explained by the spring movement of ITCZ is 86%. From this, we may conclude that most of the strong canonical AZM events can be explained by anomalous spring position of ITCZ and this relation is stronger in the case of cold events compared to that of the warm events. This point is also demonstrated by the drop in correlation between anomalous ITCZ position in MAM and JJA ATL3 index. The correlation when the cold events preceded by ITCZ northward movement in spring are included is -0.34 and is significant at the 5% level (Table 1). The correlation drops to a statistically insignificant -0.13 , when those events are removed. A major reason for the reduction in the correlation may be attributed to changes in the heat content in the western equatorial Atlantic (MJJ WEA HC) as it is the only component whose correlation falls below significance after removing the strong canonical cold AZM events (not shown). It must be clarified that we separate AZM events into strong canonical and non-strong-canonical as opposed to the separation of “canonical” and “non-canonical” of Richter et al. (2013) that is based on Bjerknes feedback mechanism and our classification of non-strong-canonical does not imply that those events cannot be explained by the said mechanism. On a related note, it should also be mentioned that our classification of AZM events into strong canonical and non-strong-canonical events is sensitive to the data product used and the classification of a few events may change. However, it does not alter our result that almost all the strong canonical AZM events can be explained by the spring Atlantic ITCZ movement and that this relation is stronger for the cold AZM events.

It may be noted that not all anomalous northward excursions of ITCZ in spring lead to AZM cold events in summer. There are 2 years (1981 and 2012) in which despite the ITCZ being anomalously north in spring, a cold AZM event did not follow (see supplemental material for details). Although the northward excursion of ITCZ in spring is a necessary condition for the development of a cold event, it is not sufficient unless its position and resulting easterlies over the equatorial Atlantic are sustained throughout spring. In addition, decadal variability of the ITCZ position and oceanic factors may also be important for the ITCZ–AZM relationship. This may potentially explain the decadal changes in the AZM–AMM correlation reported by Murtugudde et al. (2001). However, further investigations will be needed to quantify the low-frequency variability of this asymmetry between ITCZ and AZM interactions.

c. Asymmetry in diversity of causative mechanisms of cold and warm AZM events

In the previous section, we have shown that most of the strong canonical AZM events are explained by the ITCZ movement in spring and subsequent Bjerknes feedback. It is interesting to explore what other mechanisms may explain the AZM events apart from the ITCZ movement and/or the dominant Bjerknes feedback. As it is difficult to show spatial evolution of each and every event, we present a novel pictorial representation of the evolution of the Bjerknes components of all the AZM events during the study period in Fig. 7. This representation serves multiple purposes: (i) whether a particular event can be explained by the Bjerknes feedback can be conveniently determined; (ii) evolution of multiple events can be summarized in one frame. For an easy interpretation of the figure, tracking of the cold event in 1983 is explained. While

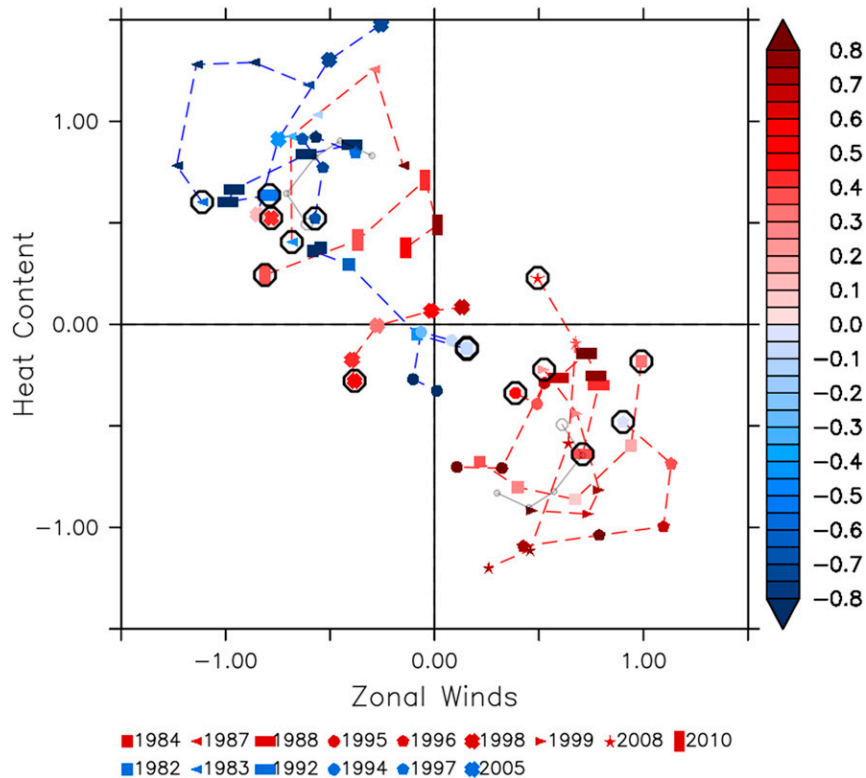


FIG. 7. Evolution of different Bjerknes components during March–July of each AZM event in the phase space of zonal winds averaged over the central to western equatorial Atlantic (abscissa; m s^{-1}) and heat content in the western equatorial Atlantic (ordinate; 10^{10} J m^{-2}) with the color of each point/symbol representing the SST in the ATL3 region ($^{\circ}\text{C}$). Different symbols are used to mark different AZM events and the red (blue) dashed lines connecting them indicate a warm (cold) AZM event. The starting point of each year, i.e., March, is indicated by a black circle. The gray line connects the one standard deviation points in the phase space during March–July, and the March point is indicated with a bigger gray circle. This line serves as a reference against which the strength of a particular event can be compared. All the Bjerknes components plotted are smoothed by a 3-month running mean for a better appearance. For the Bjerknes feedback to be considered active all three elements of Keenlyside and Latif (2007) have to be present. While the heat content and zonal wind anomalies are used as the axes, SST in the ATL3 region is shown filling different symbols used to differentiate between the events and is easy to miss. Since only the AZM events that we already know have an SST response (AZM definition is based on ATL3 SST index) are plotted, this representation is adequate to tell us whether or not an AZM event can be explained by the Bjerknes feedback.

the equatorial zonal winds remain almost steady during March–May, the heat content in the western equatorial Atlantic increases. Both the winds and heat content decrease in strength after May. The SST in the ATL3 region reaches its peak in May–June. The movement along the trajectory in a clockwise direction indicates that the changes in the zonal winds precede those in the heat content. From Fig. 7, it can be noted that normally the trajectories of cold (warm) events are in the top-left (bottom right) quadrant. All such events can be explained by Bjerknes mechanism to one degree or another whether preceded by an appropriate ITCZ movement in spring or not. However, there are

exceptions: the cold event of 1994 and warm events of 1987, 1998, and 2010. The cold event of 1982 is a slight exception in that its track is close to the origin because of weak Bjerknes components but ultimately moves to the top-left quadrant when the components become strong enough. Apparently, the two exceptions among cold events (1982 and 1994) are also the events that are not preceded by a spring northward movement of ITCZ. This figure is clearly reminiscent of Kessler (2002) and captures similar aspects of the recharge–discharge processes involved in AZM, although the focus there was on whether ENSO is an oscillation or a series of events. A similar question is relevant

for AZM as well, and we will present that analysis elsewhere.

What are the mechanisms by which cold AZM events form without a northward movement of ITCZ and/or the Bjerknes feedback? As mentioned earlier, the AZM cold events that are not preceded by northward ITCZ in spring occurred in 1982 and 1994. In both of these events, a negative SST anomaly forms because of winds off the equator (either southerly alongshore or easterlies parallel to the equator) and spreads over to the equator to eventually become a cold event (see supplemental material for detailed discussion of the events). Thus, during the study period, most of the cold AZM events are explained by Bjerknes feedback associated with the spring movement of ITCZ and the rest by the wave activity induced by alongshore winds off Angola and/or off-equatorial winds.

The causative mechanisms and timing of the triggers of a warm event appear to be more diverse than that of a cold event. As mentioned earlier, only two out of nine warm events are explained by ITCZ movement in spring and subsequent Bjerknes feedback. The remaining warm events are: 1987, 1988, 1995, 1999, 2008, and 2010. Most of them can be broadly explained by the Bjerknes feedback mechanism if we do not adhere strictly to the requirement of a strong subsurface response (1988, 1995, 1999, and 2008; Figs. 1 and 6). The exceptions are the warm events of 1998, 1987, and 2010 (see supplemental material for details). Although the Bjerknes feedback mechanism seems to be at the center of most of the warm events, only a few events are triggered by a southward spring transition of ITCZ. On a side note, it is interesting to see that after accounting for the change of center of action as in the case of the cold event of 1994 and the warm event of 1998, trajectories of all the cold events move in a clockwise direction, which means that the changes in the zonal winds precede the changes in heat content (Fig. S3). However, the trajectories of warm events of 1988 and 1998 move in an anticlockwise direction.

Several previous studies have discussed different mechanisms by which a warm AZM event can occur. Richter et al. (2013) show that AZM warm events that cannot be explained by ENSO-like dynamics are driven by a mechanism in which surface wind anomalies just north of the equator induce warm heat content anomalies that are advected toward the equator and propagate to the east. They argue that such warm events are caused by AMM with warm SST anomalies in the TNA. This is different in details compared to the mechanism suggested by Foltz and McPhaden (2010), which involves waves described earlier in the introduction. Zhu et al. (2012) show an interesting relation between the AMM and AZM on a 3–4-yr time scale. The positive heat

content anomalies in northern tropical Atlantic resulting from positive AMM, can discharge into the equatorial waveguide when the AMM weakens, and stimulate a warm AZM event about 12–15 months later (the warm event of 1987 is an example of this mechanism but on shorter time scales). Lübbecke (2013) summarizes different mechanisms causing a warm event. Lübbecke et al. (2018) review the important results, mechanisms and viewpoints related to the AZM. From all these previous studies mentioned above and our analysis, it may be concluded that the causative mechanisms of a warm AZM event are more diverse compared to that of a cold event. Our findings here add a finer point via the asymmetry in the ITCZ–AZM interactions. In this study, we are more specifically focused on the asymmetry of cold and warm events related to ITCZ variability and not on proposing any new mechanism for the AZM itself.

4. Discussion and conclusions

Several earlier studies have discussed the existence of a relation between the ITCZ position in spring (or AMM) in the tropical Atlantic and the AZM in summer, using correlation analyses. However, to the best of our knowledge, none of these studies addressed why the high correlation between the anomalous position of ITCZ and equatorial zonal winds in spring, a prerequisite for the development of an AZM event, does not translate into strong association between the ITCZ position in spring and AZM in summer. By starting from an initial hypothesis that the ITCZ–AZM relation may have a skewness with regard to cold and warm AZM events, we show that the relation between the ITCZ in spring and AZM is stronger for cold AZMs than warm AZMs, with a skew toward cold events (Fig. 8). We further show that the skewness is inherent in the seasonal cycle itself. The weakened and less persistent westerly winds in the western equatorial Atlantic during warm events and the resultant lack of support from the subsurface ocean response, an important factor in the Bjerknes feedback, are argued to result in a weak association between the ITCZ and warm AZM. We also show that the AZM events caused by ITCZ movement are “strongly canonical,” that is, associated not only with zonal surface winds in spring but also an oceanic subsurface response in late spring to midsummer.

Further, we observe that the timing and causative mechanisms of a cold AZM event are less diverse than that of a warm event. We infer that the asymmetry in the diversity may be explained by the fact the AZM is phase locked to the seasonal cycle (Keenlyside and Latif 2007; Burls et al. 2012), which is due to the seasonal ITCZ movement (Richter et al. 2014, 2017). Further, the cold

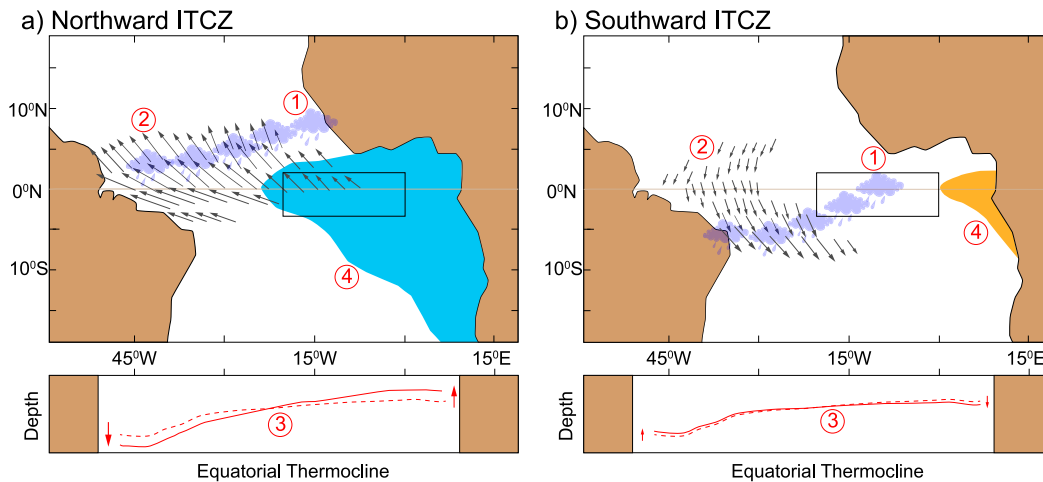


FIG. 8. A schematic diagram summarizing the most likely scenario when the Atlantic ITCZ in spring is anomalously (a) north and (b) south. When the Atlantic ITCZ in spring is anomalously north as shown in (a) at point 1, it leads to concurrent anomalous winds that have strong easterly component over the WEA (point 2), which in turn shoals the equatorial thermocline in the east and deepens the same in the west with a delay of 1 or 2 months (point 3; dashed line: mean thermocline; thick line: shifted thermocline), finally resulting in a cold AZM event in the following summer (point 4). On the contrary, when the ITCZ in spring is anomalously south as shown in (b) at point 1, it leads to concurrent anomalous winds that are predominantly northerly in the vicinity of the equator but develop a strong westerly component upon crossing into the south but away from the equator (point 2). The westerly component of the winds in the WEA is so weak that they cause insufficient deepening of equatorial thermocline in the east (point 3) inducing weak warm SST anomalies and thus no warm AZM event (point 4). In summary, while the anomalous northward spring ITCZ leads to a cold AZM event in the following summer most of the times, the converse is less likely and hence the skewness in the relation between spring ITCZ position and AZM. The ATL3 region is marked with a rectangular box. This schematic is only for representative purposes and not to scale.

AZM being simply an enhancement of the climatological condition and the warm AZM being an anomaly in its true sense, may also be important to consider. It should be noted that there are more warm events in the study period than cold events, and thus inadequate sampling may be an issue. However, it must be observed that almost all the studies that propose a different mechanism other than the straightforward Bjerknes feedback do it only for a warm AZM case. We opine that the asymmetry is inherent in the strong association of the AZM with the seasonal cycle. While we have discussed the asymmetry in causative mechanisms of cold and warm AZM events, Lutz et al. (2015) discuss the asymmetry of rainfall response to the cold and warm tropical Atlantic SSTs, they show that the effect of the cold and warm events on the rainfall in different regions in Africa is asymmetric in season and magnitude.

Our set goal was to understand the causes for the drop in correlation between the ITCZ in spring and AZM despite a high correlation between ITCZ and equatorial zonal winds in spring, and apparent criticality of these winds for the development of an AZM. However, a related question of why the relation between wind anomalies in spring and SST anomalies in summer is

weaker than the correlation between equatorial trades and ITCZ latitude (Table 1) can be also posed. This has been addressed by several studies either overtly or implicitly. Foltz and McPhaden (2010), Lübbecke and McPhaden (2012), and Richter et al. (2013) talk about how spring warm SST anomalies in the TNA can sometimes cause a warm AZM event in the following summer instead of the usual cold AZM event. The positive meridional mode is associated with equatorial easterly winds in boreal spring, which normally is a precondition for a cold AZM. However, in some special cases, via the mechanisms discussed in earlier studies (Foltz and McPhaden 2010; Lübbecke and McPhaden 2012; Richter et al. 2013), warm AZM events can occur, which weakens the relation between the spring equatorial winds and the summer SSTs. On a related note, Chang et al. (2006) talk about how the tropospheric warming over the tropical Atlantic induced by an El Niño destructively interferes with the spring equatorial easterly winds, which leads to a summer SST cooling in the STA. This can contribute to reducing the association between the spring winds and summer SST anomalies. Nonetheless, as shown in Table 1, the correlation between the spring ITCZ position and summer ATL3 index is lower than that between spring WEA zonal winds and summer ATL3 index making our set goal worthwhile.

A close relation between equatorial zonal winds and position of the ITCZ has been noted in an earlier study by Richter et al. (2014), who show that the equatorial easterlies grow strong almost linearly when the ITCZ is to the north of equator but they are uniformly weak when the ITCZ is in the south; nevertheless, the winds remain easterly throughout. Although their result appears to be at odds with our observation that anomalous northward (southward) movement of ITCZ during spring is associated with concurrent anomalous easterlies (westerlies), it is not in reality, owing to differences in methodology and time period of the two studies. While Richter et al. (2014) average the monthly mean absolute equatorial zonal wind stress over each unique absolute ITCZ position during their entire study period, which represents the mean picture and removes some of the seasonal preferences, we focused on the relation between anomalies of ITCZ and equatorial zonal winds only during spring. Therefore, we posit that our findings are novel in eliciting the asymmetric relation between the spring position of the ITCZ and AZM and its explanation through interaction between the seasonal cycle and interannual anomalies.

We have described different processes involved when an anomalous northward spring ITCZ, which can be influenced by AMM among other things, leads to a cold AZM in the following summer in Fig. 2. Contrary to our intention, the figure might give an impression that a northward ITCZ shift and easterly wind anomalies occur before the development of significant cool SST anomalies in the southeast Atlantic in the late spring to summer, leading to the question of causality: is the AMM a result of anomalous spring ITCZ position rather than a cause? We clarify this apparent contradiction here. Note that Fig. 2 shows the composite of anomalies of different fields including SST and winds for all those cold AZM events preceded by the ITCZ displaced anomalously north in spring. A positive AMM type of SST structure (warm north and/or cool south) during spring is not present in all the composite years, but whenever it is present (in 1997 and 2005) it persists from February followed by a northward displacement of ITCZ in spring and the associated equatorial easterlies (figure not shown). In the composite picture (Fig. 2), the AMM pattern appears weak in the north but strong in the south because AZM has early SST anomalies of the same sign in the south overlapping with that of AMM there but no signal in the north, which adds to the fact that the AMM SST pattern is not present in all the constituent years. The question of causality is also not supported by earlier studies (e.g., Hu and Huang 2006) that show that the development of an AMM event can span from boreal fall to boreal spring preceding the

anomalous meridional displacement of ITCZ in spring with the associated equatorial easterlies.

Although AMM is not central to our study, since it is invoked as one of the factors influencing the spring ITCZ position, it must be pointed out that some studies suggest that AMM may not be a coupled mode and its southern and northern lobes may evolve independently (e.g., Yang et al. 2018). The relative importance of the northern and southern flanks of the AMM for the spring ITCZ position may need to be investigated but that is beyond the scope of our present study.

Our observation that causative mechanisms of the cold AZM (counterpart of La Niña in the tropical Atlantic) are less diverse than that of the warm AZM (counterpart of El Niño) is supported by studies about ENSO diversity reporting similar results (Kug and Ham 2011; Ren and Jin 2011; Chen et al. 2015; Ashok et al. 2017). Chen et al. (2015) attribute the cause of asymmetry, irregularity, and extremes of El Niño to westerly wind bursts and also point out that the wind bursts strongly affect El Niño but not La Niña. Capotondi et al. (2015) and Ashok et al. (2017) suggest that while different types of El Niño are distinguishable, the La Niña events are not. Timmermann et al. (2018) also note that La Niña events exhibit less diversity in their spatial patterns compared to El Niño events pointing to an asymmetry in the dynamical processes involved. These results lend a hand to our speculation that cold AZMs have less diversity compared to warm AZMs. We intend to verify the validity of this hypothesis in a future study.

Given that ITCZ movement is also affected by a decaying ENSO, our result together with the relevant previous studies (Kucharski et al. 2008; Pottapinjara et al. 2014; García-Serrano et al. 2017) hint at an interesting linkage between the tropical Pacific and the ISM in a novel way. Previous studies show that a persistent (into spring) yet decaying El Niño can suppress rainfall over the deep tropical Atlantic and move the ITCZ north in spring. The northward (southward) spring ITCZ can cause a cold (warm) AZM event in the following summer, which in turn can enhance (reduce) the rainfall over India. Normally, an El Niño that is active in summer tends to reduce the ISMR. However, an El Niño peaking in the preceding winter and decaying thereafter can enhance the ISMR through the cold AZM, El Niño's reincarnation. This should at least motivate more focused model sensitivity studies to better understand the ITCZ–AZM interaction and its asymmetries.

Acknowledgments. This is a part of the Ph.D. thesis of V.P. We acknowledge two anonymous reviewers whose insightful comments helped improve this paper. The

encouragement and support of the Director of INCOIS is gratefully acknowledged. R.M. thanks IIT, Bombay, for the position of Visiting Professor, which facilitated discussions on this work. The graphics are generated using PyFerret of PMEL, NOAA. This is INCOIS contribution number 337 and NCPOR contribution number J-04/2019-20.

REFERENCES

- Amaya, D. J., and G. R. Foltz, 2014: Impacts of canonical and Modoki El Niño on tropical Atlantic SST. *J. Geophys. Res. Oceans*, **119**, 777–789, <https://doi.org/10.1002/2013JC009476>.
- Ashok, K., Z. Guan, and T. Yamagata, 2001: Impact of the Indian Ocean dipole on the relationship between the Indian monsoon rainfall and ENSO. *Geophys. Res. Lett.*, **28**, 4499–4502, <https://doi.org/10.1029/2001GL013294>.
- , M. Shama, A. K. Sahai, and P. Swapna, 2017: Nonlinearities in the evolutionary distinctions between El Niño and La Niña types. *J. Geophys. Res. Oceans*, **122**, 9649–9662, <https://doi.org/10.1002/2017JC013129>.
- Behera, S. K., R. Krishnan, and T. Yamagata, 1999: Unusual ocean–atmosphere conditions in the tropical Indian Ocean during 1994. *Geophys. Res. Lett.*, **26**, 3001–3004, <https://doi.org/10.1029/1999GL010434>.
- Burls, N., C. Reason, P. Penven, and S. G. Philander, 2012: Energetics of the tropical Atlantic zonal mode. *J. Climate*, **25**, 7442–7466, <https://doi.org/10.1175/JCLI-D-11-00602.1>.
- Capotondi, A., and Coauthors, 2015: Understanding ENSO diversity. *Bull. Amer. Meteor. Soc.*, **96**, 921–938, <https://doi.org/10.1175/BAMS-D-13-00117.1>.
- Chang, P., Y. Fang, R. Saravanan, L. Ji, and H. Seidel, 2006: The cause of the fragile relationship between the Pacific El Niño and the Atlantic Niño. *Nature*, **443**, 324–328, <https://doi.org/10.1038/nature05053>.
- Chen, D., and Coauthors, 2015: Strong influence of westerly wind bursts on El Niño diversity. *Nat. Geosci.*, **8**, 339–345, <https://doi.org/10.1038/ngeo2399>.
- Chiang, J. C. H., and D. J. Vimont, 2004: Analogous Pacific and Atlantic meridional modes of tropical atmosphere–ocean variability. *J. Climate*, **17**, 4143–4158, <https://doi.org/10.1175/JCLI4953.1>.
- , Y. Kushnir, and A. Giannini, 2002: Deconstructing Atlantic intertropical convergence zone variability: Influence of the local cross-equatorial sea surface temperature gradient and remote forcing from the eastern equatorial Pacific. *J. Geophys. Res.*, **107**, 4004, <https://doi.org/10.1029/2000JD000307>.
- Czaja, A., and C. Frankignoul, 2002: Observed impact of Atlantic SST anomalies on the North Atlantic oscillation. *J. Climate*, **15**, 606–623, [https://doi.org/10.1175/1520-0442\(2002\)015<0606:OIOASA>2.0.CO;2](https://doi.org/10.1175/1520-0442(2002)015<0606:OIOASA>2.0.CO;2).
- , P. Van der Vaart, and J. Marshall, 2002: A diagnostic study of the role of remote forcing in tropical Atlantic variability. *J. Climate*, **15**, 3280–3290, [https://doi.org/10.1175/1520-0442\(2002\)015<3280:ADSOTR>2.0.CO;2](https://doi.org/10.1175/1520-0442(2002)015<3280:ADSOTR>2.0.CO;2).
- Dee, D. P., and Coauthors, 2011: The ERA-Interim reanalysis: Configuration and performance of the data assimilation system. *Quart. J. Roy. Meteor. Soc.*, **137**, 553–597, <https://doi.org/10.1002/qj.828>.
- Enfield, D. B., and D. A. Mayer, 1997: Tropical Atlantic sea surface temperature variability and its relation to El Niño–Southern Oscillation. *J. Geophys. Res.*, **102**, 929–945, <https://doi.org/10.1029/96JC03296>.
- Foltz, G. R., and M. J. McPhaden, 2010: Interaction between the Atlantic meridional and Niño modes. *Geophys. Res. Lett.*, **37**, L18604, <https://doi.org/10.1029/2010GL044001>.
- García-Serrano, J., C. Cassou, H. Douville, A. Giannini, and F. J. Doblas-Reyes, 2017: Revisiting the ENSO teleconnection to the tropical North Atlantic. *J. Climate*, **30**, 6945–6957, <https://doi.org/10.1175/JCLI-D-16-0641.1>.
- Giannini, A., Y. Kushnir, M. A. Cane, A. Giannini, Y. Kushnir, and M. A. Cane, 2000: Interannual variability of Caribbean rainfall, ENSO, and the Atlantic Ocean. *J. Climate*, **13**, 297–311, [https://doi.org/10.1175/1520-0442\(2000\)013<0297:IVOCRE>2.0.CO;2](https://doi.org/10.1175/1520-0442(2000)013<0297:IVOCRE>2.0.CO;2).
- Good, S. A., M. J. Martin, and N. A. Rayner, 2013: EN4: Quality controlled ocean temperature and salinity profiles and monthly objective analyses with uncertainty estimates. *J. Geophys. Res. Oceans*, **118**, 6704–6716, <https://doi.org/10.1002/2013JC009067>.
- Ham, Y.-G., J.-S. Kug, and J.-Y. Park, 2013: Two distinct roles of Atlantic SSTs in ENSO variability: North tropical Atlantic SST and Atlantic Niño. *Geophys. Res. Lett.*, **40**, 4012–4017, <https://doi.org/10.1002/grl.50729>.
- Hu, Z.-Z., and B. Huang, 2006: Physical processes associated with the tropical Atlantic SST meridional gradient. *J. Climate*, **19**, 5500–5517, <https://doi.org/10.1175/JCLI3923.1>.
- Huang, B., 2004: Remotely forced variability in the tropical Atlantic Ocean. *Climate Dyn.*, **23**, 133–152, <https://doi.org/10.1007/s00382-004-0443-8>.
- Keenlyside, N. S., and M. Latif, 2007: Understanding equatorial Atlantic interannual variability. *J. Climate*, **20**, 131–142, <https://doi.org/10.1175/JCLI3992.1>.
- Keshavamurthy, R., 1982: Response of the atmosphere to sea surface temperature anomalies over the equatorial Pacific and the teleconnections of the Southern Oscillation. *J. Atmos. Sci.*, **39**, 1241–1259, [https://doi.org/10.1175/1520-0469\(1982\)039<1241:ROTATS>2.0.CO;2](https://doi.org/10.1175/1520-0469(1982)039<1241:ROTATS>2.0.CO;2).
- Kessler, W. S., 2002: Is ENSO a cycle or a series of events? *Geophys. Res. Lett.*, **29**, 2125, <https://doi.org/10.1029/2002GL015924>.
- Kucharski, F., A. Bracco, J. H. Yoo, and F. Molteni, 2008: Atlantic forced component of the Indian monsoon interannual variability. *Geophys. Res. Lett.*, **35**, L04706, <https://doi.org/10.1029/2007GL033037>.
- , —, —, A. M. Tompkins, L. Feudale, and P. Ruti, 2009: A Gill–Matsuno-type mechanism explains the tropical Atlantic influence on African and Indian monsoon rainfall. *Quart. J. Roy. Meteor. Soc.*, **135**, 569–579, <https://doi.org/10.1002/qj.406>.
- , and Coauthors, 2016: The teleconnection of the tropical Atlantic to Indo-Pacific sea surface temperatures on interannual to centennial time scales: A review of recent findings. *Atmosphere*, **7**, 29, <https://doi.org/10.3390/atmos7020029>.
- Kug, J. S., and Y. G. Ham, 2011: Are there two types of La Niña? *Geophys. Res. Lett.*, **38**, L16704, <https://doi.org/10.1029/2011GL048237>.
- Lee, S. K., D. B. Enfield, and C. Wang, 2008: Why do some El Niños have no impact on tropical North Atlantic SST? *Geophys. Res. Lett.*, **35**, 1968–1969, <https://doi.org/10.1029/2008GL034734>.
- Lübbecke, J. F., 2013: Tropical Atlantic warm events. *Nat. Geosci.*, **6**, 22–23, <https://doi.org/10.1038/ngeo1685>.
- , and M. J. McPhaden, 2012: On the inconsistent relationship between Pacific and Atlantic Niños. *J. Climate*, **25**, 4294–4303, <https://doi.org/10.1175/JCLI-D-11-00553.1>.

- , and —, 2017: Symmetry of the Atlantic Niño mode. *Geophys. Res. Lett.*, **44**, 965–973, <https://doi.org/10.1002/2016GL071829>.
- , B. Rodríguez-Fonseca, I. Richter, M. Martín-Rey, T. Losada, I. Polo, and N. S. Keenlyside, 2018: Equatorial Atlantic variability—Modes, mechanisms, and global teleconnections. *Wiley Interdiscip. Rev.: Climate Change*, **9**, e527, <https://doi.org/10.1002/wcc.527>.
- Lutz, K., J. Jacobeit, and J. Rathmann, 2015: Atlantic warm and cold water events and impact on African west coast precipitation. *Int. J. Climatol.*, **35**, 128–141, <https://doi.org/10.1002/joc.3969>.
- Martin, M., B. Rodriguez-Fonseca, and I. Polo, 2014: Atlantic opportunities for ENSO prediction. *Geophys. Res. Lett.*, **42**, 6802–6810, <https://doi.org/10.1002/2015GL065062>.
- Mooley, D. A., and B. Parthasarathy, 1984: Indian summer monsoon and the east equatorial Pacific sea surface temperature. *Atmos.–Ocean*, **22**, 23–35, <https://doi.org/10.1080/07055900.1984.9649182>.
- Murtugudde, R. G., J. Ballabrera-Poy, J. Beauchamp, and A. J. Busalacchi, 2001: Relationship between zonal and meridional modes in the tropical Atlantic. *Geophys. Res. Lett.*, **28**, 4463–4466, <https://doi.org/10.1029/2001GL013407>.
- Neelin, J. D., and H. Su, 2005: Moist teleconnection mechanisms for the tropical South American and Atlantic sector. *J. Climate*, **18**, 3928–3950, <https://doi.org/10.1175/JCLI3517.1>.
- Nobre, P., and J. Shukla, 1996: Variations of sea surface temperature, wind stress, and rainfall over the tropical Atlantic and South America. *J. Climate*, **9**, 2464–2479, [https://doi.org/10.1175/1520-0442\(1996\)009<2464:VOSSTW>2.0.CO;2](https://doi.org/10.1175/1520-0442(1996)009<2464:VOSSTW>2.0.CO;2).
- Philander, S. G. H., J. Holton, and R. Dmowska, 1989: *El Niño, La Niña, and the Southern Oscillation*. 1st ed. Academic Press, 293 pp.
- Pottapinjara, V., M. S. Girishkumar, M. Ravichandran, and R. Murtugudde, 2014: Influence of the Atlantic zonal mode on monsoon depressions in the Bay of Bengal during boreal summer. *J. Geophys. Res. Atmos.*, **119**, 6456–6469, <https://doi.org/10.1002/2014JD021494>.
- , —, S. Sivareddy, M. Ravichandran, and R. Murtugudde, 2016: Relation between the upper ocean heat content in the equatorial Atlantic during boreal spring and the Indian monsoon rainfall during June–September. *Int. J. Climatol.*, **36**, 2469–2480, <https://doi.org/10.1002/joc.4506>.
- Rayner, N. A., D. E. Parker, E. B. Horton, C. K. Folland, L. V. Alexander, D. P. Rowell, E. C. Kent, and A. Kaplan, 2003: Global analyses of sea surface temperature, sea ice, and night marine air temperature since the late nineteenth century. *J. Geophys. Res.*, **108**, 4407, <https://doi.org/10.1029/2002JD002670>.
- Ren, H. L., and F. F. Jin, 2011: Niño indices for two types of ENSO. *Geophys. Res. Lett.*, **38**, L04704, <https://doi.org/10.1029/2010GL046031>.
- Richter, I., S. K. Behera, Y. Masumoto, B. Taguchi, H. Sasaki, and T. Yamagata, 2013: Multiple causes of interannual sea surface temperature variability in the equatorial Atlantic Ocean. *Nat. Geosci.*, **6**, 43–47, <https://doi.org/10.1038/ngeo1660>.
- , S.-P. Xie, S. K. Behera, T. Doi, and Y. Masumoto, 2014: Equatorial Atlantic variability and its relation to mean state biases in CMIP5. *Climate Dyn.*, **42**, 171–188, <https://doi.org/10.1007/s00382-012-1624-5>.
- , —, Y. Morioka, T. Doi, B. Taguchi, and S. Behera, 2017: Phase locking of equatorial Atlantic variability through the seasonal migration of the ITCZ. *Climate Dyn.*, **48**, 3615–3629, <https://doi.org/10.1007/s00382-016-3289-y>.
- Rodríguez-Fonseca, B., I. Polo, J. García-Serrano, T. Losada, E. Mohino, C. R. Mechoso, and F. Kucharski, 2009: Are Atlantic Niños enhancing Pacific ENSO events in recent decades? *Geophys. Res. Lett.*, **36**, L20705, <https://doi.org/10.1029/2009GL040048>.
- Servain, J., I. Wainer, J. P. McCreary, and A. Dessier, 1999: Relationship between the equatorial and meridional modes of climatic variability in the tropical Atlantic. *Geophys. Res. Lett.*, **26**, 485–488, <https://doi.org/10.1029/1999GL900014>.
- Sikka, D. R., 1980: Some aspects of the large-scale fluctuations of summer monsoon rainfall over India in relation to fluctuations in the planetary and regional scale circulation parameters. *Proc. Ind. Acad. Sci. Earth Planet. Sci.*, **89**, 179–195, <https://doi.org/10.1007/BF02913749>.
- Slingo, J. M., and H. Annamalai, 2000: The El Niño of the century and the response of the Indian summer monsoon. *Mon. Wea. Rev.*, **128**, 1778–1797, [https://doi.org/10.1175/1520-0493\(2000\)128<1778:TENOOT>2.0.CO;2](https://doi.org/10.1175/1520-0493(2000)128<1778:TENOOT>2.0.CO;2).
- Timmermann, A., and Coauthors, 2018: El Niño–Southern Oscillation complexity. *Nature*, **559**, 535–545, <https://doi.org/10.1038/s41586-018-0252-6>.
- Wang, C., F. Kucharski, R. Barimalala, and A. Bracco, 2009: Teleconnections of the tropical Atlantic to the tropical Indian and Pacific Oceans: A review of recent findings. *Meteor. Z.*, **18**, 445–454, <https://doi.org/10.1127/0941-2948/2009/0394>.
- Webster, P., V. Magana, T. Palmer, J. Shukla, R. Tomas, Y. Yanai, and T. Yasunari, 1998: Monsoons: Processes, predictability, and the prospects for prediction. *J. Geophys. Res.*, **103**, 14 451–14 510, <https://doi.org/10.1029/97JC02719>.
- Wu, L., and Z. Liu, 2002: Is tropical Atlantic variability driven by the North Atlantic oscillation? *Geophys. Res. Lett.*, **29**, 29–32, <https://doi.org/10.1029/2002GL014939>.
- Xie, S.-P., and J. A. Carton, 2004: Tropical Atlantic variability: Patterns, mechanisms, and impacts. *Earth's Climate: The Ocean–Atmosphere Interaction*, *Geophys. Monogr.*, Vol. 147, Amer. Geophys. Union, <https://doi.org/10.1029/147GM07>.
- Yadav, R. K., 2017: On the relationship between east equatorial Atlantic SST and ISM through Eurasian wave. *Climate Dyn.*, **48**, 281–295, <https://doi.org/10.1007/s00382-016-3074-y>.
- Yang, Y., S.-P. Xie, L. Wu, Y. Kosaka, and J. Li, 2018: ENSO forced and local variability of North tropical Atlantic SST: Model simulations and biases. *Climate Dyn.*, **51**, 4511–4524, <https://doi.org/10.1007/s00382-017-3679-9>.
- Zebiak, S. E., 1993: Air–sea interaction in the equatorial Atlantic region. *J. Climate*, **6**, 1567–1586, [https://doi.org/10.1175/1520-0442\(1993\)006<1567:AIITEA>2.0.CO;2](https://doi.org/10.1175/1520-0442(1993)006<1567:AIITEA>2.0.CO;2).
- Zhu, J., B. Huang, and Z. Wu, 2012: The role of ocean dynamics in the interaction between the Atlantic meridional and equatorial modes. *J. Climate*, **25**, 3583–3598, <https://doi.org/10.1175/JCLI-D-11-00364.1>.

Similarity Report

A study on links between the tropical Atlantic and Indian summer monsoon on interannual timescales

by Pottapinjara Vijay

Submission date: 11-Mar-2020 05:13PM (UTC+0530)

Submission ID: 1273580039

File name: thesis_vijay_main_10mar2020_plag_check_library.pdf (21.62M)

Word count: 39225

Character count: 191248

A study on links between the tropical Atlantic and Indian summer monsoon on interannual timescales

ORIGINALITY REPORT

44%

SIMILARITY INDEX

39%

INTERNET SOURCES

42%

PUBLICATIONS

7%

STUDENT PAPERS

PRIMARY SOURCES

1

journals.ametsoc.org

Internet Source

22%

2

rmets.onlinelibrary.wiley.com

Internet Source

12%

3

Pottapinjara, Vijay, M. S. Girishkumar, S. Sivareddy, M. Ravichandran, and R. Murtugudde. "Relation between the upper ocean heat content in the equatorial Atlantic during boreal spring and the Indian monsoon rainfall during June-September : RELATION BETWEEN ATLANTIC AND INDIAN SUMMER MONSOON RAINFALL", International Journal of Climatology, 2015.

Publication

1%

4

agupubs.onlinelibrary.wiley.com

Internet Source

1%

5

link.springer.com

Internet Source

1%